Supplementary Information for

Abnormal Sergeants-and-Soldiers Effect of Poly(quinoxaline-2,3-diyl)s Enabling Discrimination of One-Carbon Homologous *n*-Alkanes through a Highly Sensitive Solvent-dependent Helix Inversion

Yuuya Nagata,* Tsuyoshi Nishikawa, and Michinori Suginome*

Department of Synthetic Chemistry and Biological Chemistry, Graduate School of Engineering, Kyoto University, Kyoto 606-8501, Japan

615-8510, Japan

*To whom correspondence should be addressed.

E-mail: nagata@sbchem.kyoto-u.ac.jp, suginome@sbchem.kyoto-u.ac.jp

Contents

1 General

All reactions were carried out under an atmosphere of nitrogen with magnetic stirring. ^{1}H NMR spectra were recorded on a Varian 400-MR spectrometer at ambient temperature. ^{1}H NMR data are reported as follows: chemical shift in ppm downfield from tetramethylsilane (δ scale), multiplicity (s = singlet, d = doublet, t = triplet, q = quartet, quint = quintet, sex = sextet, m = multiplet and br = broad), coupling constant (Hz), and integration. The GPC analysis was carried out with TSKgel GMH_{XL} ($CHCl_3$, polystyrene standards). Preparative GPC was performed on JAI LC-908 equipped with JAIGEL-1H and -2H columns in a series ($CHCl_3$). UV-vis absorption spectra were recorded on a JASCO V-770 spectrometer equipped with a JASCO ETC-505T temperature/stirring controller at 20 °C. Circular dichroism (CD) spectra were recorded on a JASCO J-1500 spectrometer equipped with a JASCO PTC-510 temperature/stirring controller at 20 °C. Fluorescence spectra were recorded on a JASCO FP-6300 spectrofluorometer. Absolute quantum yields were measured by a Hamamatsu absolute PL quantum yield spectrometer C11347. Circularly polarized luminescence (CPL) spectra were recorded on a JASCO CPL-200S at room temperature. Tetrahydrofurane (THF) was dried and deoxygenized using an alumina/catalyst column system (Glass Contour Co.). *o*-TolNiCl(PMe_3)$_2$,[1] 1,2-dibutoxy-4,5-diisocyano-3,6-dimethylbenzene (**Q1**),[2] 1,2-diisocyano-3,6-dimethyl-4,5-bis(propoxymethyl)benzene (**Q2**),[3] 1,2-diisocyano-3,6-dimethyl-4,5-bis((((*S*)-octan-2-yl)oxy)methyl)benzene (**Qa**),[4] 1,2-diisocyano-3,6-dimethyl-4,5-bis((((*S*)-octan-3-yl)oxy)methyl)benzene (**Qb**),[4] **1a(100)**,[5] **1b(100)**,[5] **2b(40/60)**,[6] **3b(40/60)**,[6] **3b(2.5/97.5)**,[6] **3b(5/95)**,[6] **3b(7.5/92.5)**,[6] **3b(10/90)**,[6] **3b(15/85)**,[6] **3b(20/80)**,[6] **3b(30/70)**,[6] **3b(40/60)**,[6] **3b(60/40)**,[6] **3b(80/20)**,[6] 2',3'-diisocyano-4,4"-dimethoxy-1,1':4',1"-terphenyl (**Qlum**),[7,8,9] were prepared according to the reported procedures. Other chemical reagents were purchased from the commercial sources and were used without further purification.

2 Experimental Procedures and Spectral Data for New Compounds

Synthesis of 2a(40/60): Qa (10.6 mg, 24.0 μmol) and **Q1** (10.8 mg, 36.0 μmol) were dissolved in THF (3 mL). A THF solution of *o*-TolNiCl(PMe_3)$_2$ (14.24 mM, 42.1 μL, 0.600 μmol) was added to the monomer solution with vigorous stirring. After 14 h, $NaBH_4$ (4.77 mg, 126 μmol) was added to the reaction mixture and stirred for 1 h. Water (20 mL) was added to the solution and extracted with CH_2Cl_2 (20 ml). The organic extract was washed with brine (20 mL), dried over Na_2SO_4, and the solvent was evaporated. The residue was subjected to preparative GPC to give **2a(40/60)** as a beige solid (16.5 mg, 77%). ^{1}H NMR ($CDCl_3$) δ 4.59 ($H_{a\text{-}B}$, 40×4H, br s), 3.95 ($H_{2\text{-}B}$, 60×2H, br s), 3.84 ($H_{2\text{-}B}$, 60×2H, br s), 3.48 ($H_{a\text{-}C}$, 40×2H, br s), 2.17 ($H_{a\text{-}A}$, $H_{2\text{-}A}$ and $H_{t\text{-}B}$, (40×6+60×6+3)H, br s), 1.72 ($H_{a\text{-}D}$ and $H_{2\text{-}C}$ (40×2+60×4)H, br s), 1.47 ($H_{a\text{-}E}$, $H_{a\text{-}F}$, and $H_{a\text{-}G}$, 40×16H, br s), 1.26 ($H_{a\text{-}J}$ and $H_{2\text{-}D}$ (40×6+60×4)H), 0.95 ($H_{2\text{-}E}$, 60×6H, br s), 0.84 ($H_{a\text{-}I}$, 40×6H, br s), small peaks originated from end-group were observed in 10.04 ($H_{t\text{-}A}$, 1H, s) and 7.09 ppm ($H_{t\text{-}C}$, 4H, br s); GPC ($CHCl_3$, g/mol): $M_n = 2.69 \times 10^4$, $M_w/M_n = 1.11$.

Scheme S1. Synthesis of **2a(40/60)**.

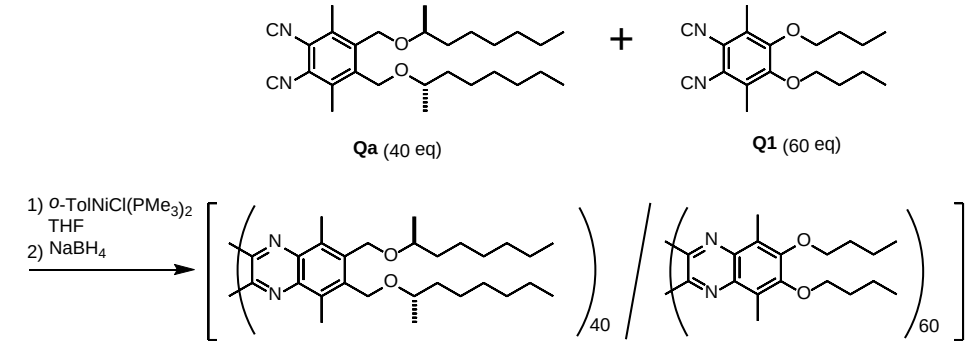

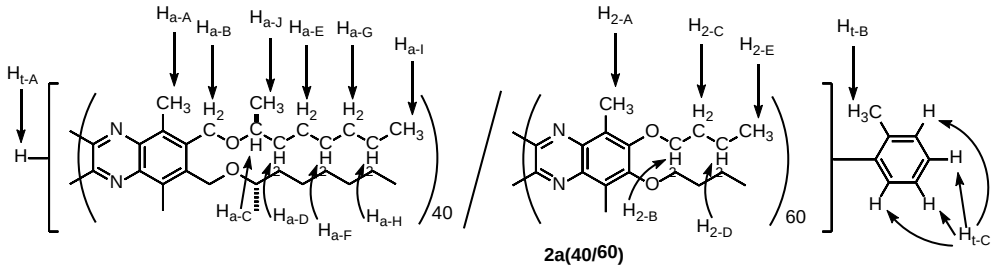

Figure S1. Structure of **2a(40/60)** with ^{1}H NMR assignment.

Synthesis of 3a(40/60): Qa (10.6 mg, 24.0 μmol) and **Q2** (10.8 mg, 36.0 μmol) were dissolved in THF (3 mL). A THF solution of *o*-TolNiCl(PMe_3)$_2$ (14.24 mM, 42.1 μL, 0.600 μmol) was added to the monomer solution with vigorous stirring. After 11 h, $NaBH_4$ (4.77 mg, 126 μmol) was added to the reaction mixture and stirred for 1 h. Water (20 mL) was added to the solution and extracted with CH_2Cl_2 (20 ml). The organic extract was washed with brine (20 mL), dried over Na_2SO_4, and the solvent was evaporated. The residue was subjected to preparative GPC to give **3a(40/60)** as a beige solid (19.4 mg, 91%). ^{1}H NMR ($CDCl_3$) δ 4.64 ($H_{a\text{-}B}$ and $H_{3\text{-}B}$, (40×4+60×4)H, br s), 3.46 ($H_{l\text{-}C}$ and $H_{3\text{-}C}$, (40×2+60×4)H, br s), 2.33 ($H_{l\text{-}A}$, $H_{3\text{-}A}$ and $H_{t\text{-}B}$, (40×6+60×6+3)H, br s), 1.59 ($H_{a\text{-}D}$, and $H_{3\text{-}D}$, (40×4+60×4)H, br s), 1.41 ($H_{a\text{-}E}$, 40×4H, br s), 1.26 ($H_{a\text{-}F}$, $H_{a\text{-}G}$ and $H_{a\text{-}H}$, 40×12H, br s), 1.07–0.66 ($H_{l\text{-}J}$, $H_{l\text{-}I}$ and $H_{3\text{-}E}$, (40×12+60×6)H, br s), small peaks originated from end-group were observed in 10.04 ($H_{t\text{-}A}$, 1H, s) and 7.09 ppm ($H_{t\text{-}C}$, 4H, br s); GPC ($CHCl_3$, g/mol): M_n = 3.60 × 10^4, M_w/M_n = 1.10.

Scheme S2. Synthesis of **3a(40/60)**.

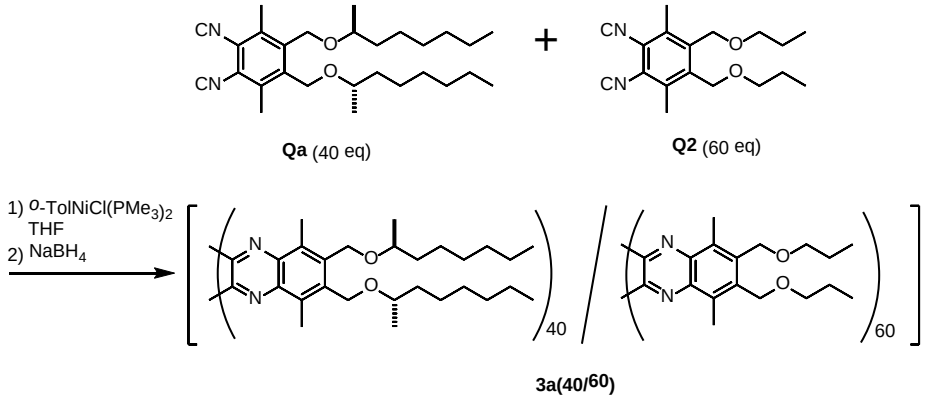

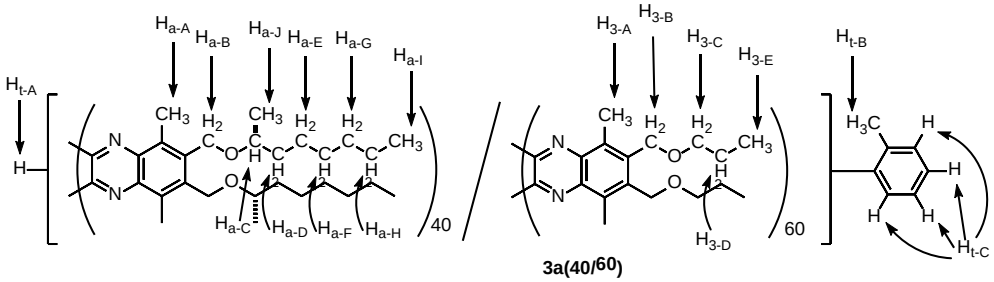

Figure S2. Structure of **3a(40/60)** with ^{1}H NMR assignment.

Synthesis of 3b(350/650): Qb (20.1 mg, 45.5 μmol) and **Q2** (25.4 mg, 84.5 μmol) were dissolved in THF (7 mL). A THF solution of *o*-TolNiCl(PMe_3)$_2$ (14.24 mM, 9.13 μL, 0.130 μmol) was added to the monomer solution with vigorous stirring. After 84 h, $NaBH_4$ (1.03 mg, 27.3 μmol) was added to the reaction mixture and stirred for 2 h. Water (40 mL) was added to the solution and extracted with CH_2Cl_2 (40 ml). The organic extract was washed with brine (40 mL), dried over Na_2SO_4, and concentrated under vacuum. The residue was purified by reprecipitation using methanol to give **3b(350/650)** as a beige solid (29.8 mg, 66%). ^{1}H NMR ($CDCl_3$) δ 4.77 ($H_{b\text{-}B}$ and $H_{3\text{-}B}$, (350×4+650×4)H, br s), 3.45 ($H_{3\text{-}C}$, 650×4H, br s), 3.32 ($H_{b\text{-}C}$, 350×2H, br s), 2.34 ($H_{b\text{-}A}$, $H_{3\text{-}A}$ and $H_{t\text{-}B}$, (350×6+650×6+3)H, br s), 1.75–1.12 ($H_{b\text{-}D}$, $H_{b\text{-}E}$, $H_{b\text{-}F}$, $H_{b\text{-}G}$, $H_{b\text{-}I}$ and $H_{3\text{-}D}$, (350×20+650×4)H, br s), 0.86 ($H_{b\text{-}H}$, $H_{b\text{-}J}$ and $H_{3\text{-}E}$, (350×12+650×6)H, br s), the peaks originated from end-group were not observed because of high polymerization degree; GPC ($CHCl_3$, g/mol): $M_n = 5.13 \times 10^5$, $M_w/M_n = 1.69$.

Scheme S3. Synthesis of **3b(350/650)**.

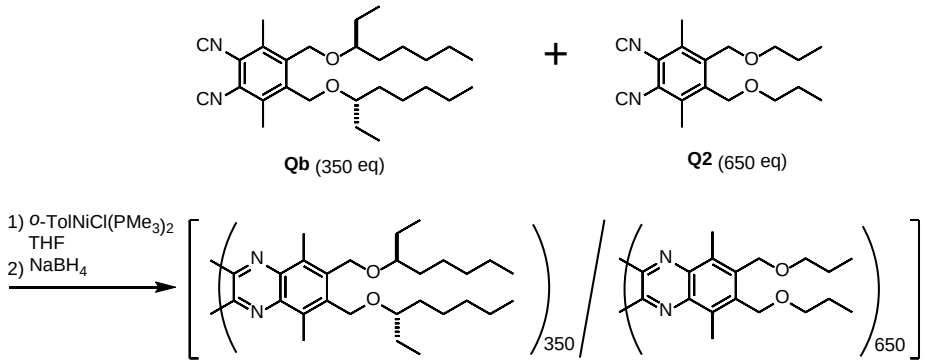

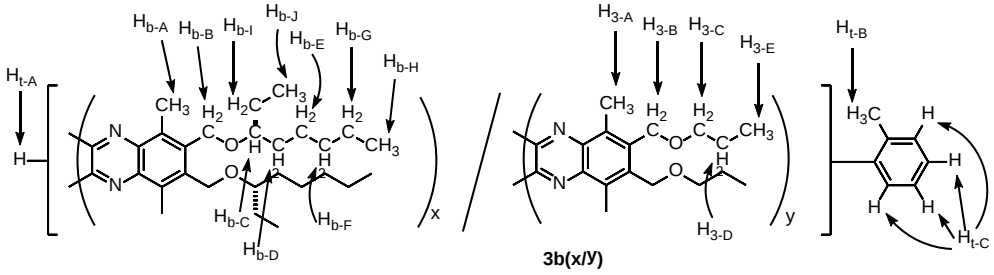

Figure S3. Structure of **3b(x/y)** with ^{1}H NMR assignment.

Synthesis of 3b(400/600): Qb (24.7 mg, 56.0 μmol) and **Q2** (25.2 mg, 84.0 μmol) were dissolved in THF (7 mL). A THF solution of *o*-TolNiCl(PMe_3)$_2$ (14.24 mM, 9.83 μL, 0.140 μmol) was added to the monomer solution with vigorous stirring. After 23 h, $NaBH_4$ (1.11 mg, 29.4 μmol) was added to the reaction mixture and stirred for 2 h. Water (40 mL) was added to the solution and extracted with CH_2Cl_2 (40 ml). The organic extract was washed with brine (40 mL), dried over Na_2SO_4, and concentrated under vacuum. The residue was purified by reprecipitation using methanol to give **3b(400/600)** as a beige solid (44.9 mg, 90%). ^{1}H NMR ($CDCl_3$) δ 4.57 ($H_{b\text{-}B}$ and $H_{3\text{-}B}$, (400×4+600×4)H, br s), 3.45 ($H_{3\text{-}C}$, 600×4H, br s), 3.32 ($H_{b\text{-}C}$, 400×2H, br s), 2.33 ($H_{b\text{-}A}$, $H_{3\text{-}A}$ and $H_{t\text{-}B}$, (400×6+600×6+3)H, br s), 1.69–1.16 ($H_{b\text{-}D}$, $H_{b\text{-}E}$, $H_{b\text{-}F}$, $H_{b\text{-}G}$, $H_{b\text{-}I}$ and $H_{3\text{-}D}$, (400×20+600×4)H, br s), 0.88 ($H_{b\text{-}H}$, $H_{b\text{-}J}$ and $H_{3\text{-}E}$, (400×12+600×6)H, br s), the peaks originated from end-group were not observed because of high polymerization degree; GPC ($CHCl_3$, g/mol): $M_n = 5.18 \times 10^5$, $M_w/M_n = 1.59$.

Scheme S4. Synthesis of **3b(400/600)**.

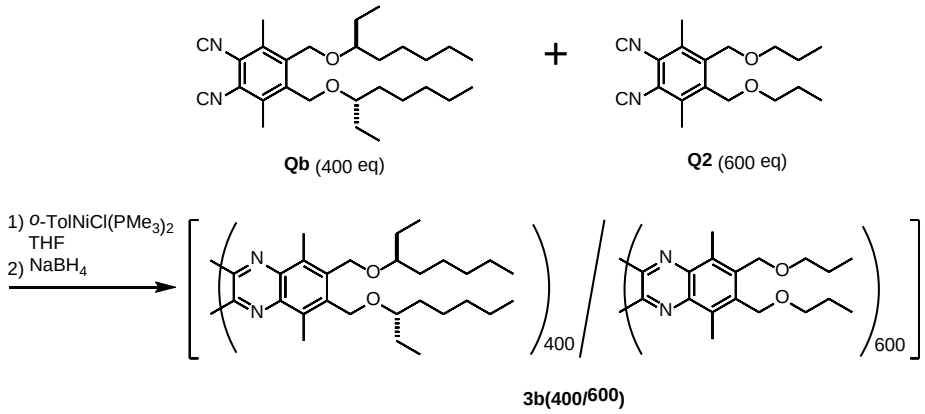

Synthesis of 3b(500/500): Qb (30.8 mg, 70.0 μmol) and **Q2** (21.0 mg, 70.0 μmol) were dissolved in THF (7 mL). A THF solution of *o*-TolNiCl(PMe_3)$_2$ (14.24 mM, 9.83 μL, 0.140 μmol) was added to the monomer solution with vigorous stirring. After 23 h, $NaBH_4$ (1.11 mg, 29.4 μmol) was added to the reaction mixture and stirred for 2 h. Water (40 mL) was added to the solution and extracted with CH_2Cl_2 (40 ml). The organic extract was washed with brine (40 mL), dried over Na_2SO_4, and concentrated under vacuum. The residue was purified by reprecipitation using methanol to give **3b(500/500)** as a beige solid (42.4 mg, 82%). ^{1}H NMR ($CDCl_3$) δ 4.57 ($H_{b\text{-}B}$ and $H_{3\text{-}B}$, (500×4+500×4)H, br s), 3.44 ($H_{3\text{-}C}$, 500×4H, br s), 3.32 ($H_{b\text{-}C}$, 500×2H, br s), 2.34 ($H_{b\text{-}A}$, $H_{3\text{-}A}$ and $H_{t\text{-}B}$,

(500×6+500×6+3)H, br s), 1.75–1.12 ($H_{b\text{-}D}$, $H_{b\text{-}E}$, $H_{b\text{-}F}$, $H_{b\text{-}G}$, $H_{b\text{-}I}$ and $H_{3\text{-}D}$, (500×20+500×4)H, br s), 0.87 ($H_{b\text{-}H}$, $H_{b\text{-}J}$ and $H_{3\text{-}E}$, (500×12+500×6)H, br s), the peaks originated from end-group were not observed because of high polymerization degree; GPC ($CHCl_3$, g/mol): $M_n = 5.08 \times 10^5$, $M_w/M_n = 1.59$.

Scheme S5. Synthesis of **3b(500/500)**.

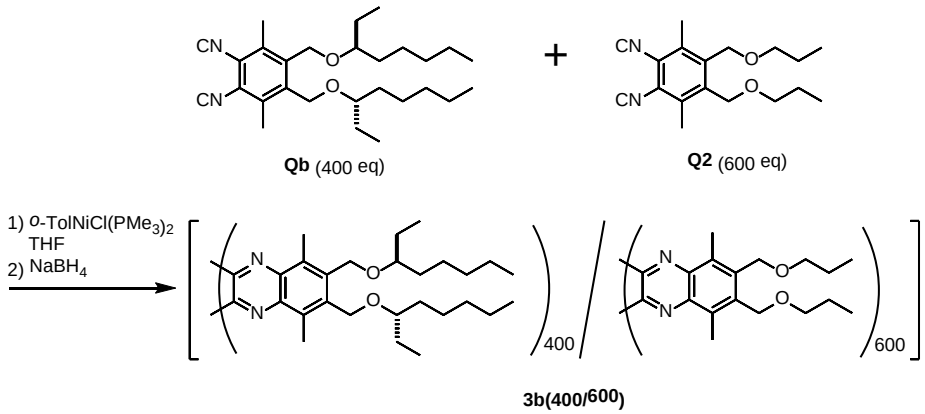

Synthesis of 3b(400/600/2): Qb (24.7 mg, 56.0 μmol), **Q2** (25.2 mg, 84.0 μmol), and **Qlum** (60.11 mM, 4.66 μL, 0.280 mmol) were dissolved in THF (7 mL). A THF solution of *o*-TolNiCl(PMe_3)$_2$ (14.24 mM, 9.83 μL, 0.140 μmol) was added to the monomer solution with vigorous stirring. After 41 h, $NaBH_4$ (1.11 mg, 29.4 μmol) was added to the reaction mixture and stirred for 2 h. Water (40 mL) was added to the solution and extracted with CH_2Cl_2 (40 ml). The organic extract was washed with brine (40 mL), dried over Na_2SO_4, and concentrated under vacuum. The residue was purified by reprecipitation using methanol to give **2b(400/600/2)** as a beige solid (46.9 mg, 94%). ^{1}H NMR ($CDCl_3$) δ 7.97–7.02 ($H_{lum\text{-}B}$, $H_{lum\text{-}A}$, and $H_{lum\text{-}C}$, and $H_{t\text{-}C}$, (2×10+4)H, br m), 4.59 ($H_{b\text{-}B}$ and $H_{3\text{-}B}$, (400×4+600×4)H, br s), 3.65 ($H_{3\text{-}C}$, 600×4H, br s), 3.45 ($H_{b\text{-}C}$, and $H_{lum\text{-}D}$, (400×2+2×6)H, br s), 2.33 ($H_{b\text{-}A}$, $H_{3\text{-}A}$ and $H_{t\text{-}B}$, (400×6+600×6+3)H, br s), 1.79–1.16 ($H_{b\text{-}D}$, $H_{b\text{-}E}$, $H_{b\text{-}F}$, $H_{b\text{-}G}$, $H_{b\text{-}I}$ and $H_{3\text{-}D}$, (400×20+600×4)H, br s), 0.88 ($H_{b\text{-}H}$, $H_{b\text{-}J}$ and $H_{3\text{-}E}$, (400×12+600×6)H, br s), a peak originated from $H_{t\text{-}A}$ was not observed because of high polymerization degree; GPC ($CHCl_3$, g/mol): $M_n = 4.15 \times 10^5$, $M_w/M_n = 1.29$.

Scheme S6. Synthesis of **3b(400/600/2)**.

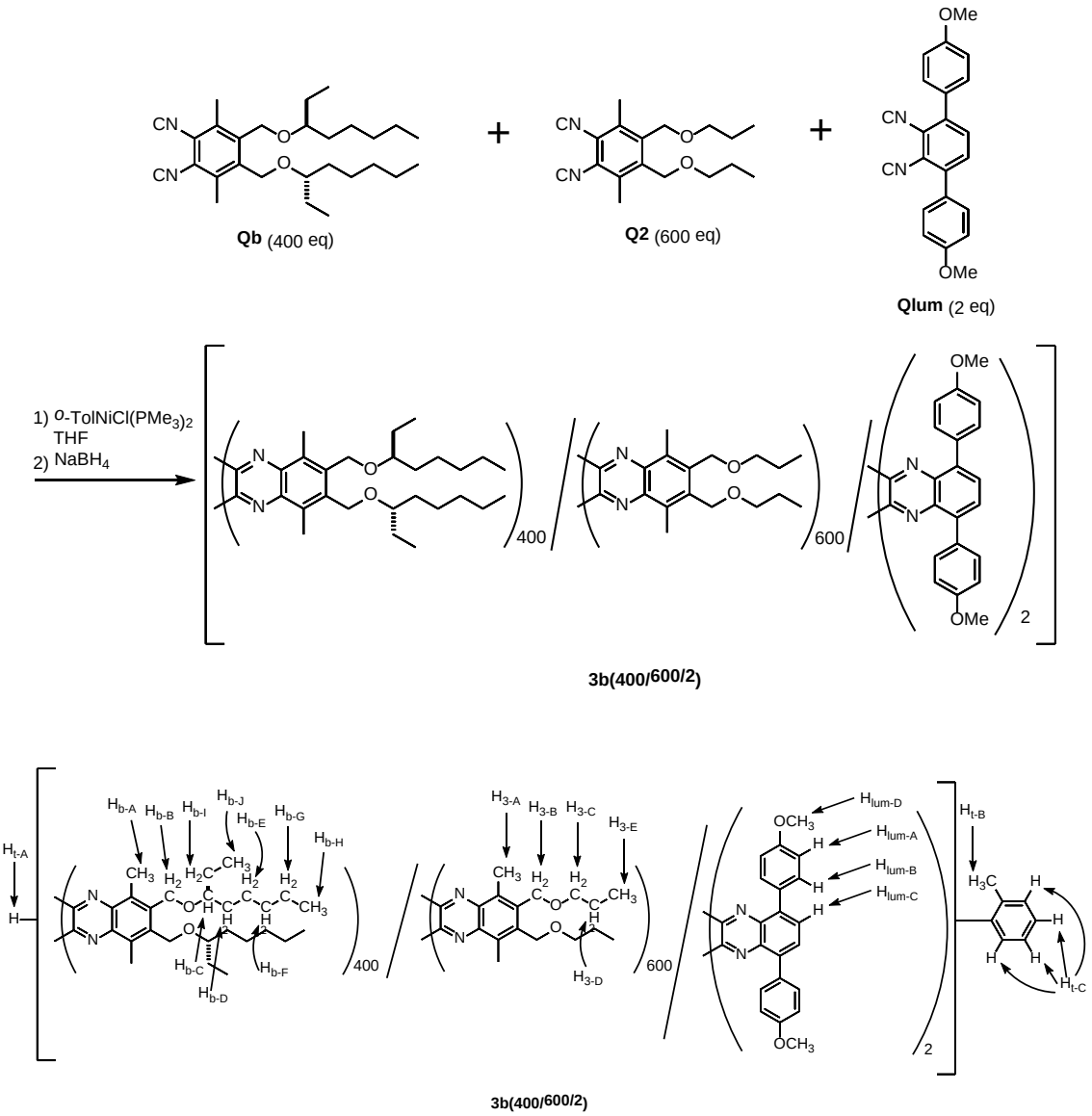

Figure S4. Structure of **3b(400/600/2)** with ^{1}H NMR assignment.

3 Chiroptical Properties of Polymer Solutions

Table S1. Dissymmetry factors g_{abs} of polymers for Figure 2.

	g_{abs} at 366.0 nm /10^{-3}					
	n-pentane	*n*-hexane	*n*-heptane	*n*-octane	*n*-nonane	*n*-decane
2b(2.5/97.5)	+0.173	+0.138	+0.103	+0.126	+0.061	−*
2b(5/95)	+0.226	+0.249	+0.188	+0.170	+0.128	+0.118
2b(7.5/92.5)	+0.312	+0.398	+0.262	+0.275	+0.159	+0.102
2b(10/90)	+0.375	+0.414	+0.323	+0.277	+0.193	+0.093
2b(15/85)	+0.489	+0.570	+0.365	+0.294	+0.221	+0.145
2c(20/80)	+0.636	+0.629	+0.400	+0.311	+0.139	+0.017
2a(30/70)	+0.650	+0.543	+0.286	+0.203	−0.051	−0.240
2b(40/60)	+0.564	+0.379	+0.132	−0.179	−0.375	−0.507
2b(60/40)	−0.209	−0.537	−0.973	−1.212	−1.553	−1.730
2b(80/20)	−1.621	−1.693	−1.875	−2.016	−2.081	−2.219
1b(100)	−2.284	−2.280	−2.238	−2.313	−2.335	−2.406

* A reliable result could not be obtained because of low solubility of the polymer.

4 Circularly Polarized Luminescence (CPL) Measurement

The CPL spectra were recorded at room temperature on a JASCO CPL-200 with an SQ-grade quartz cuvette (a path length of 10 mm). A scanning rate of 50 nm/min, an excitation bandwidth of 3000 μm, a monitoring bandwidth of 3000 μm, a response time of 8 seconds, and 5 times accumulation were employed. The CPL dissymmetry factor g_{lum} is defined as $g_{lum} = 2 \times (I_L - I_R)/(I_L + I_R)$, where I_L and I_R are the fluorescence intensities of the left- and right-handed circularly polarized light, respectively. The value of g_{lum} can be calculated on a JASCO CPL-200 as follows.

$$g_{lum} = [\text{PL ellipticity (mdeg)}] / [\text{PL intensity (V)}] / (1000 \times 180 / 4\pi)$$
$$= [\text{PL ellipticity (mdeg)}] / [\text{PL intensity (V)}] \times (6.98 \times 10^{-5})$$

The validity of the coefficient (6.98×10^{-5}) was also confirmed by the measurement of previously reported CPL materials[11] (europium(III) ions coordinated by chiral *N*,*N*′-bis(1-phenylethyl)-2,6-pyridinedicarboxamide in MeCN). For a curve fitting of observed CPL spectra, following equation was adopted on the basis of the supposition that the CPL signals are expressed as a Gaussian distribution functions of the wavenumber,

$$I_L - I_R = a \times \exp(b \times (1/\lambda - c)^2)$$

where λ is the wavelength (i.e., $1/\lambda$ is the wavenumber), and a, b, and c are variables for the curve fitting. Nonlinear least-squares fitting of $I_L - I_R$ versus λ was performed by using the Solver Function in Microsoft Office Excel 2013. Sums of the squares of the deviation were minimized by varying 3 parameters (a, b, and c).

5 CD Measurement with a Solvent-jump Method

In order to reveal the stability the helicity of the polymers in different solvent, a solvent-jump CD measurement was carried out. Firstly, **3b(400/600)** was dissolved in *n*-heptane (0.39 g/L) and was kept to equilibrate for 24 hours at room temperature. 350 μL of the solution of **3b(400/600)** in *n*-heptane was transferred to a quartz cell (path length = 10 mm), and the solvent was removed under vacuum in the quartz cell. Finally, 3.5 mL of *n*-octane was added to the quartz cell with **3b(400/600)**, and CD measurement was immediately started to observe the time course of the CD signal.

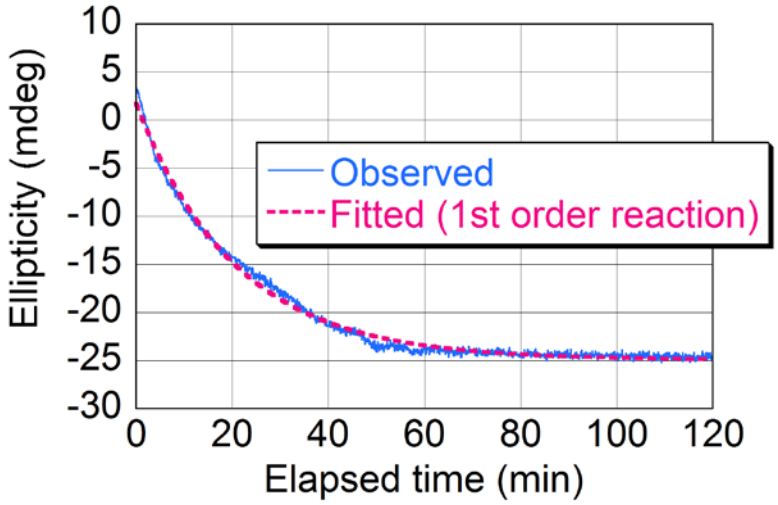

Figure S5. Time-resolved CD intensity change of **3b(400/600)** in *n*-octane. **3b(400/600)** was equilibrated in *n*-heptane and was dried before the measurement.
(3.9×10^{-2} g/L, 366.0 nm, path length = 10 mm, 393 K)

The *P*-helical structure of **3b(400/600)** induced by *n*-heptane was rapidly inverted to *M*-helical structure in *n*-octane. The half-life of the helix inversion was estimated to 14.4 min at 393 K on the supposition that the helix inversion is a first order reaction.

6 Acknowledgements

This work was partly supported by the following grants.

- MEXT KAKENHI, a Grant-in-Aid for Scientific Research on Innovative Areas, “Coordination Asymmetry: Design of Asymmetric Coordination Sphere and Anisotropic Assembly for the Creation of Functional Molecules”, Grant Number 17H05368 (YN)
- MEXT KAKENHI, a Grant-in-Aid for Scientific Research (C), Grant Number 16K05796 (YN)
- CREST, Japan Science and Technology Agency, “Establishment of Molecular Technology towards the Creation of New Function” Area, Grant Number JPMJCR14L1 (MS)

7 References

1. Carmona, E.; Paneque, M.; Poveda, M. L. *Polyhedron* **1989**, *8*, 285−291.
2. Nagata, Y.; Suginome, M. *J. Polym. Sci., Part A: Polym. Chem*. **2011**, *49*, 4275−4282.
3. Ito, Y.; Ihara, E.; Uesaka, T.; Murakami, M. *Macromolecules* **1992**, *25*, 6711−6713.
4. Nagata, Y.; Yamada, T.; Adachi, T.; Akai, Y.; Yamamoto, T.; Suginome, M. *J. Am. Chem. Soc.* **2013**, *135*, 10104−10113.
5. Nagata, Y.; Nishikawa, T.; Suginome, M. *J. Am. Chem. Soc.* **2014**, *136*, 15901−15904.
6. Nagata, Y.; Nishikawa, T.; Suginome, M. *J. Am. Chem. Soc.* **2015**, *137*, 4070−4073.
7. Ito, Y.; Kojima, Y.; Murakami, M.; Suginome, M. *Bull. Chem. Soc. Jpn.* **1997**, *70*, 2801−2806.
8. Ito, Y.; Ihara, E.; Uesaka, T.; Murakami, M. *Macromolecules* **1992**, *25*, 6711−6713.
9. Ito, Y.; Ohnishi, A.; Ohsaki, H.; Murakami, M. *Synthesis* **1988**, *9*, 714−715.
10. Bonsall, S. D.; Houcheime, M.; Straus, D. A.; Muller, G. *Chem. Commun.* **2007**, *35*, 3676−3678.

8 NMR Spectra of New Compounds

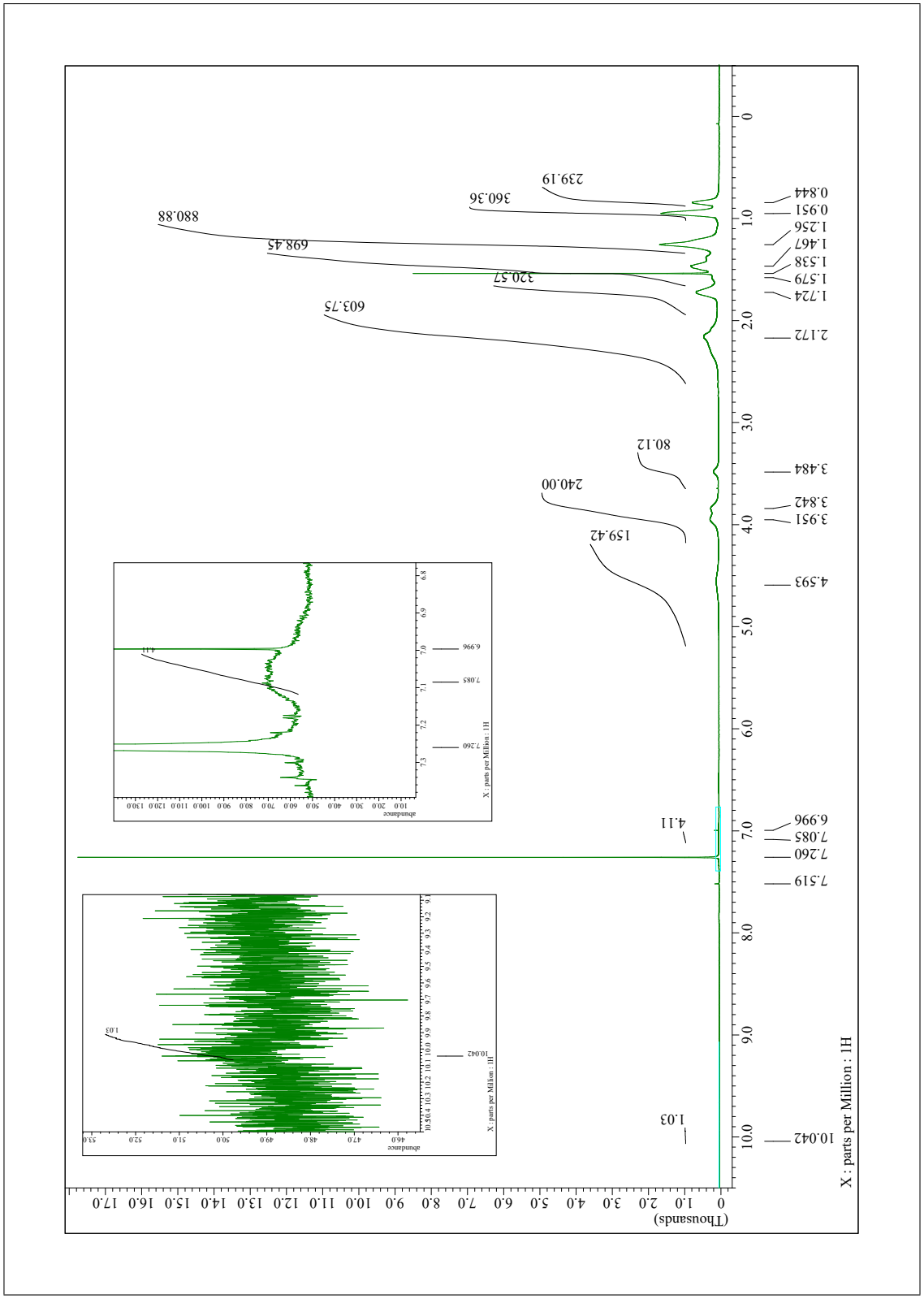

Figure S6. ^{1}H NMR spectrum of **2a(40/60)** in $CDCl_3$.

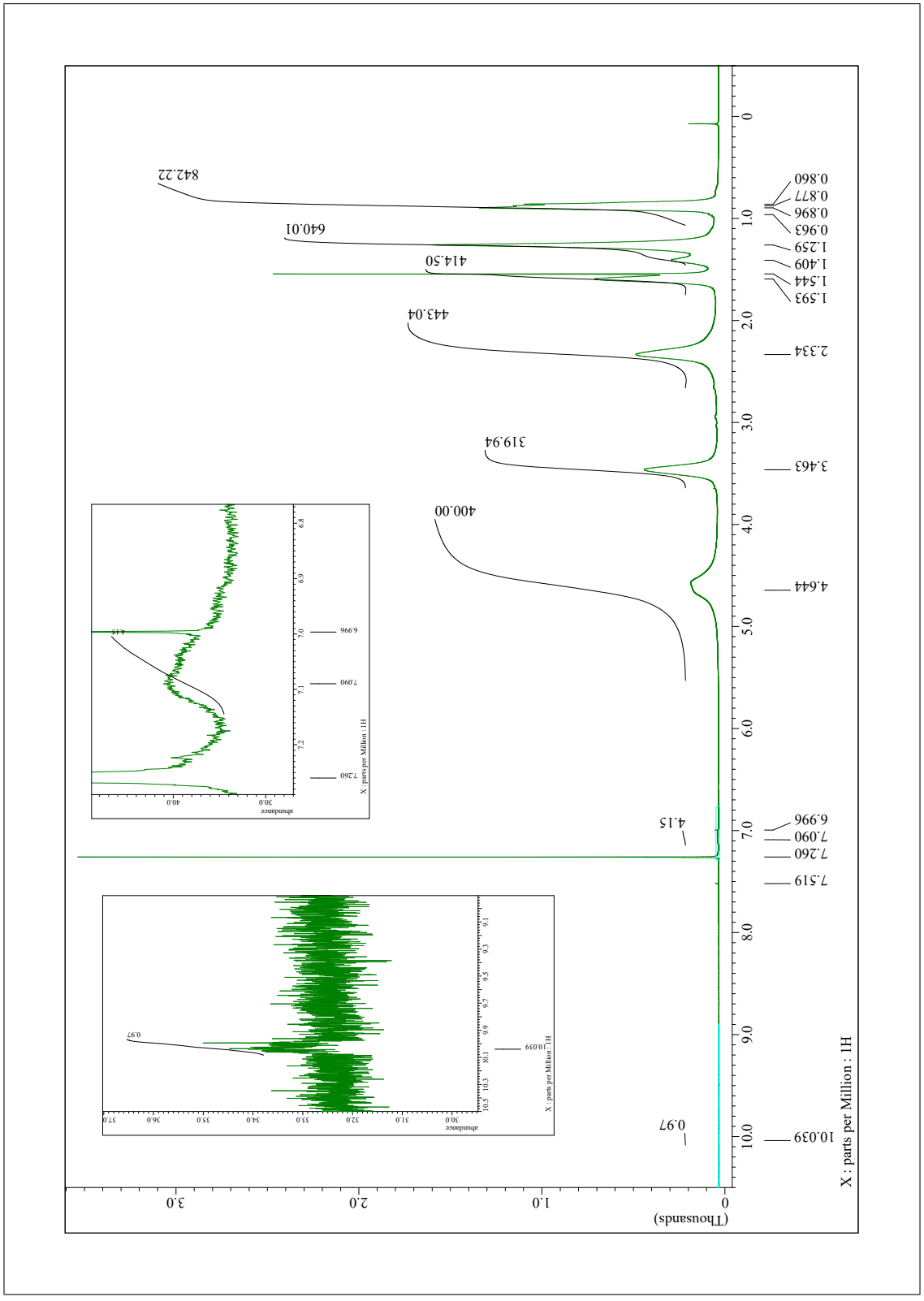

Figure S7. ^{1}H NMR spectrum of **3a(40/60)** in $CDCl_3$.

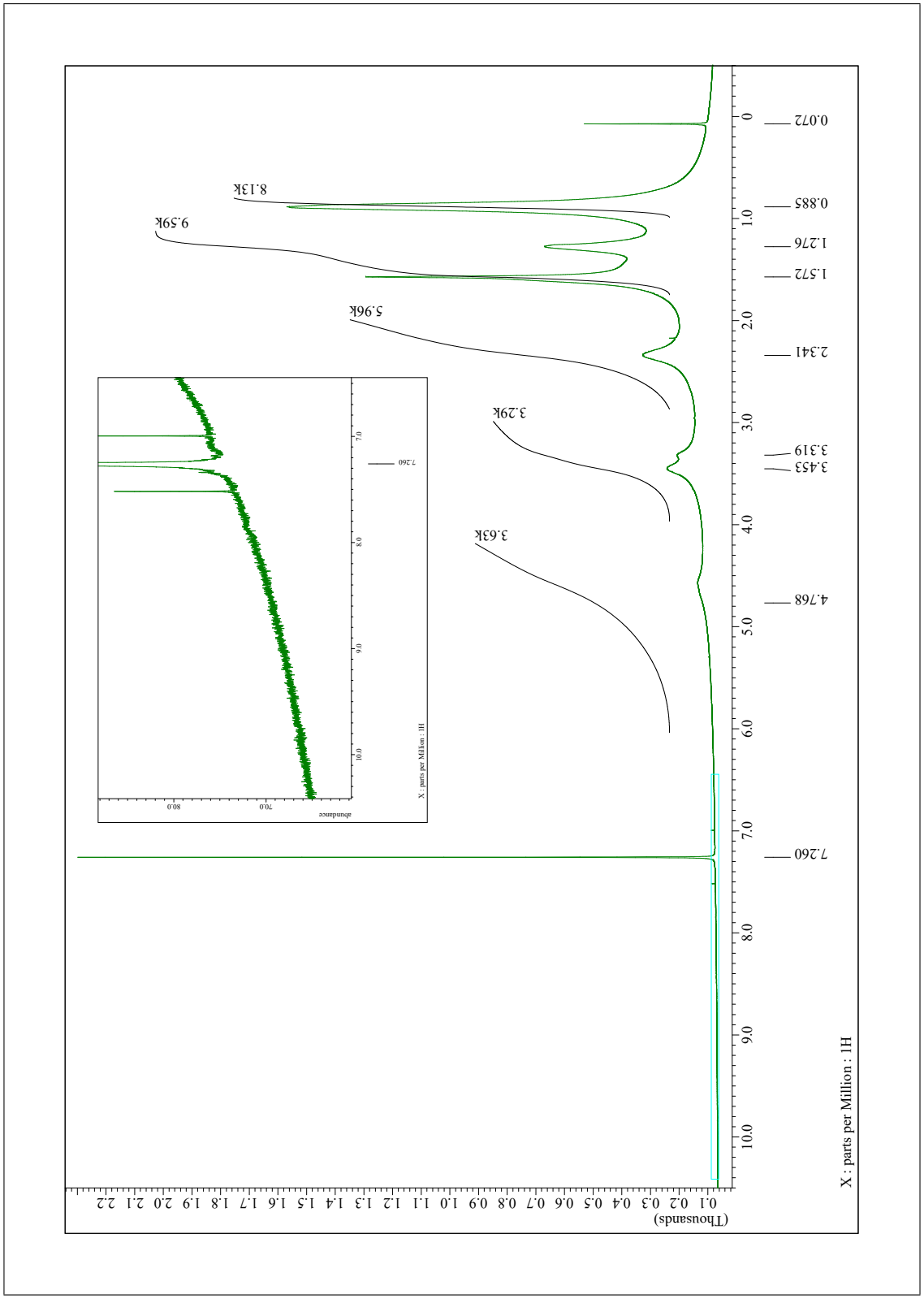

Figure S8. ^{1}H NMR spectrum of **3b(350/650)** in $CDCl_3$.

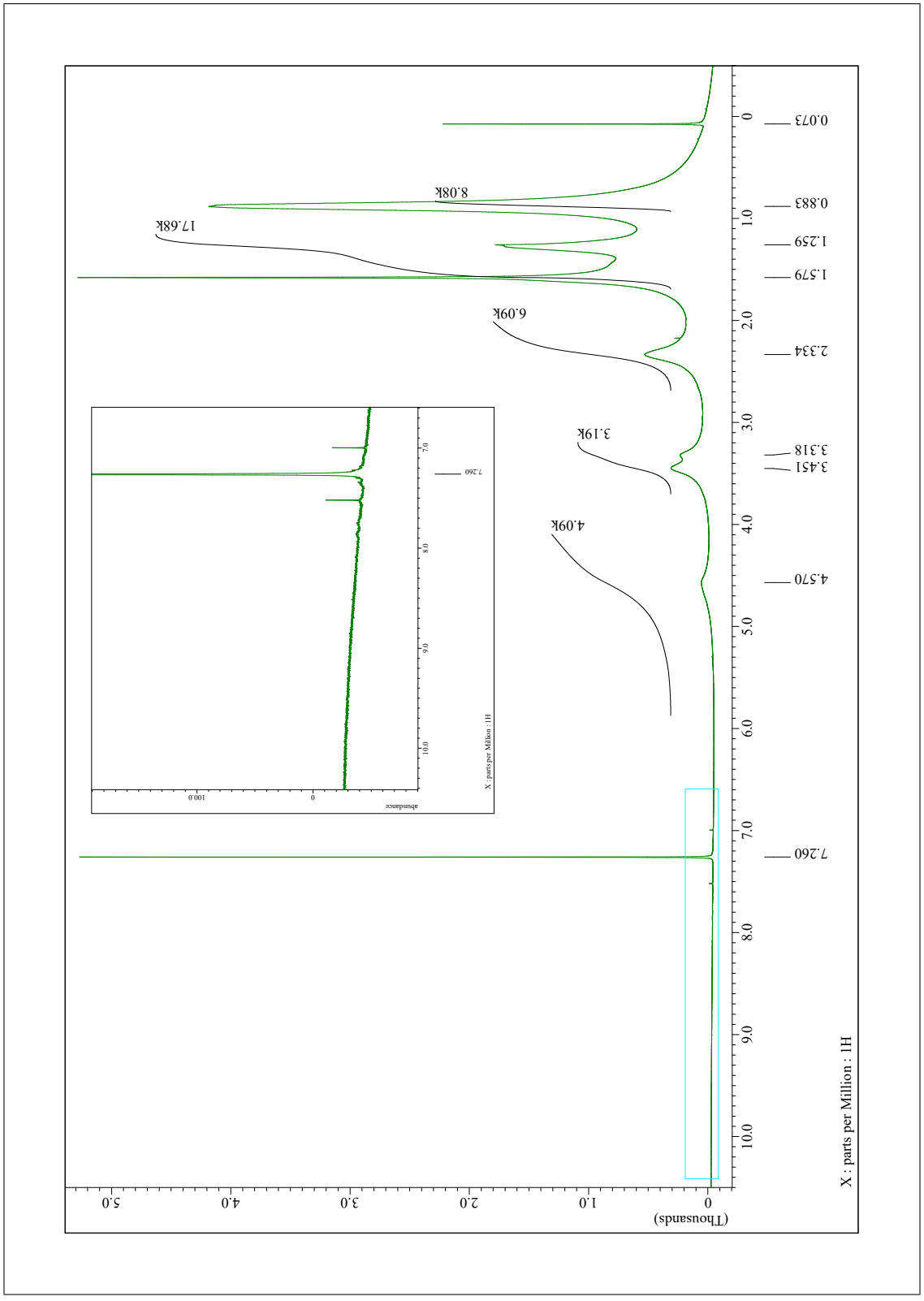

Figure S9. ^{1}H NMR spectrum of **3b(400/600)** in $CDCl_3$.

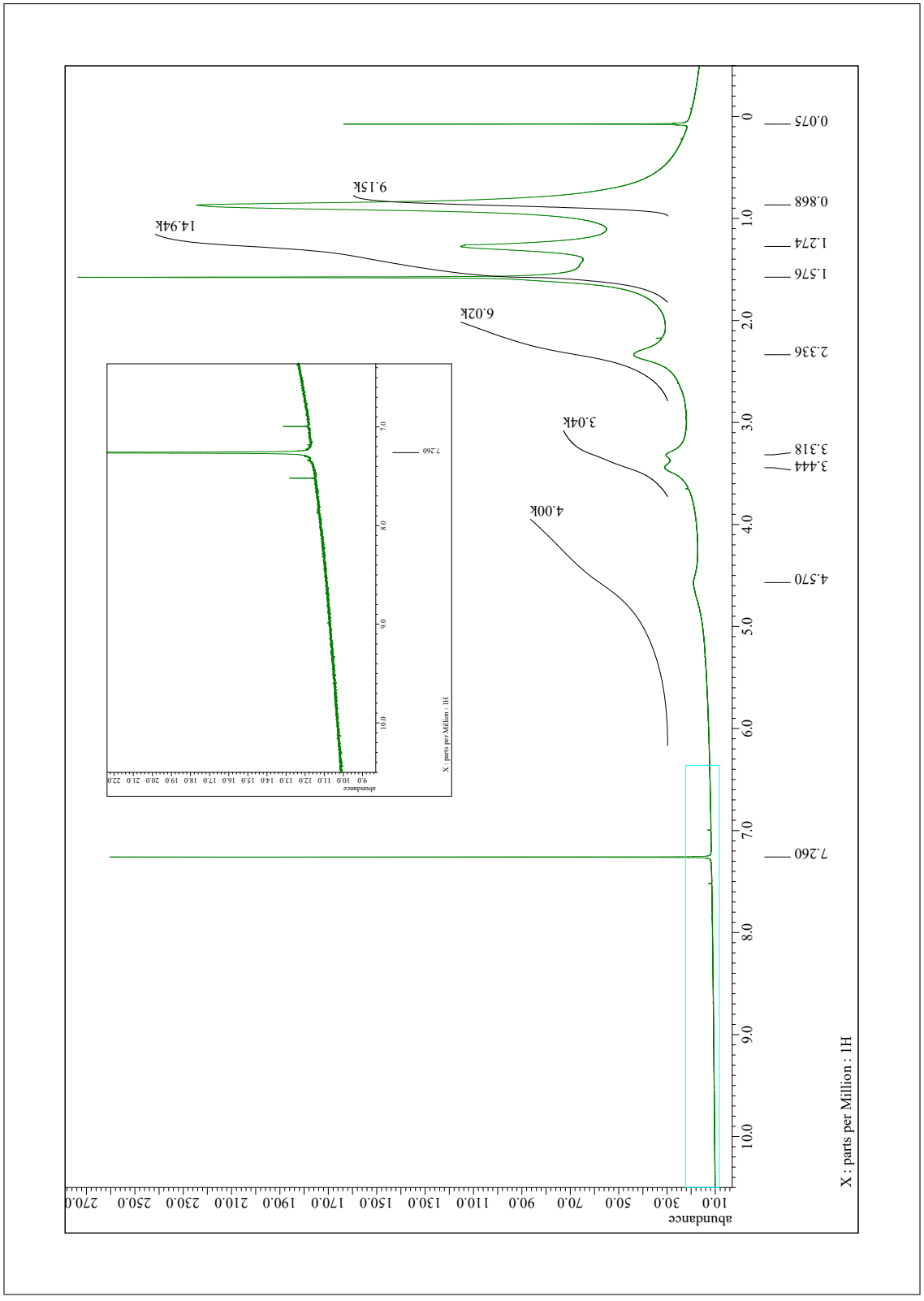

Figure S10. ^{1}H NMR spectrum of **3b(500/500)** in $CDCl_3$.

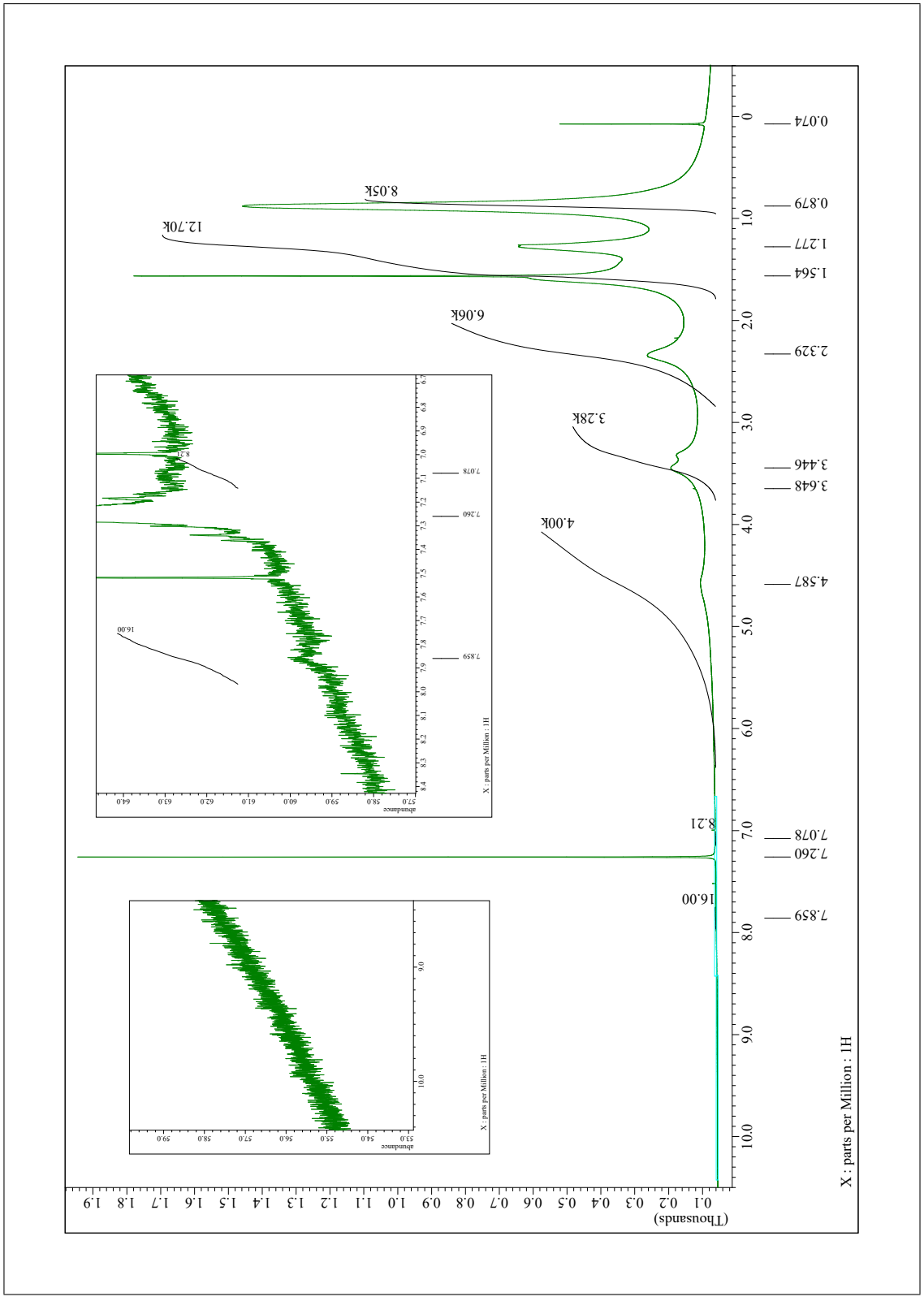

Figure S11. ^{1}H NMR spectrum of **3b(400/600/2)** in $CDCl_3$.

9 UV-vis and CD Spectra of New Compounds

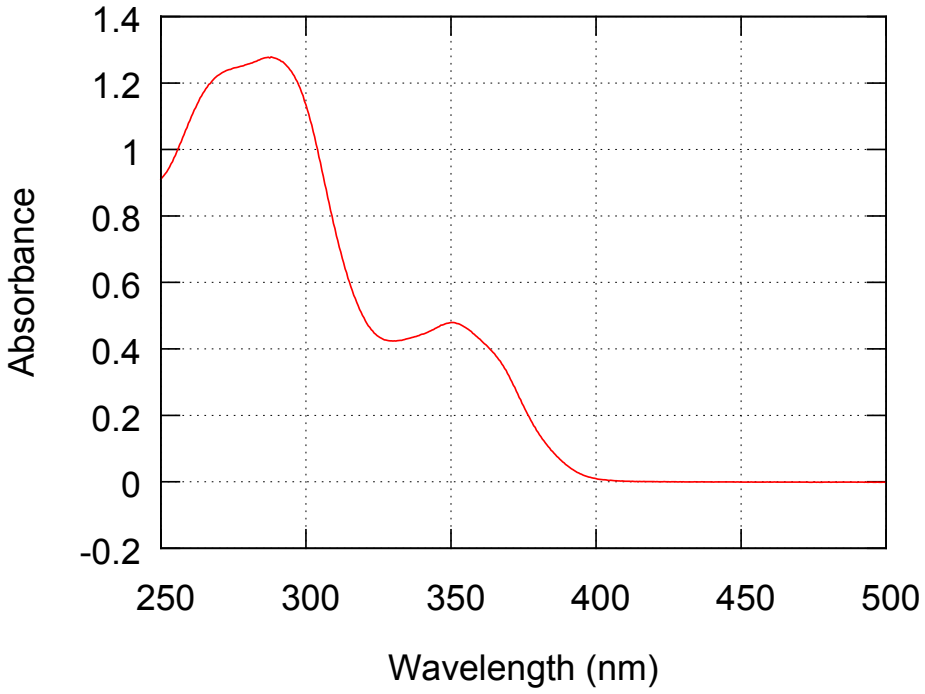

Figure S12. UV-vis absorption spectrum of **1a(100)** in *n*-pentane (3.12×10^{-2} g/L, path length = 10 mm).

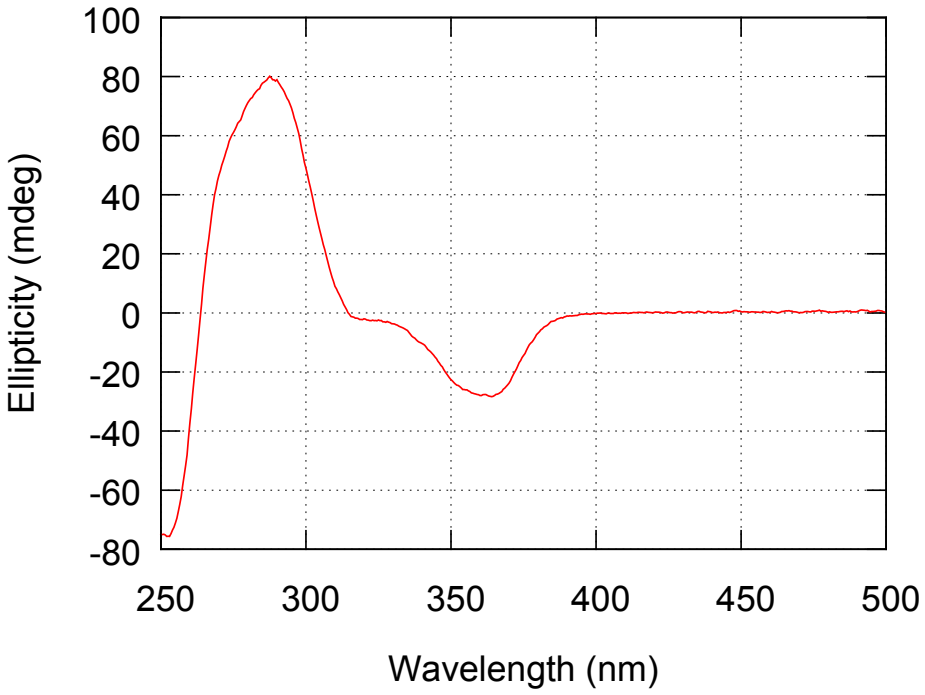

Figure S13. CD spectrum of **1a(100)** in *n*-pentane (3.12×10^{-2} g/L, path length = 10 mm).

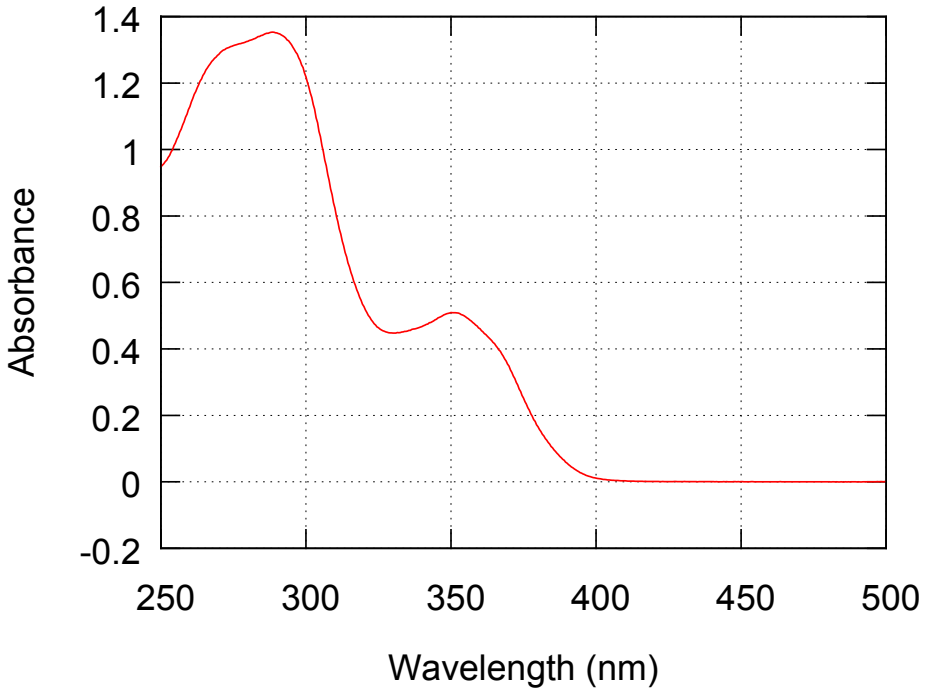

Figure S14. UV-vis absorption spectrum of **1a(100)** in *n*-hexane (3.12×10^{-2} g/L, path length = 10 mm).

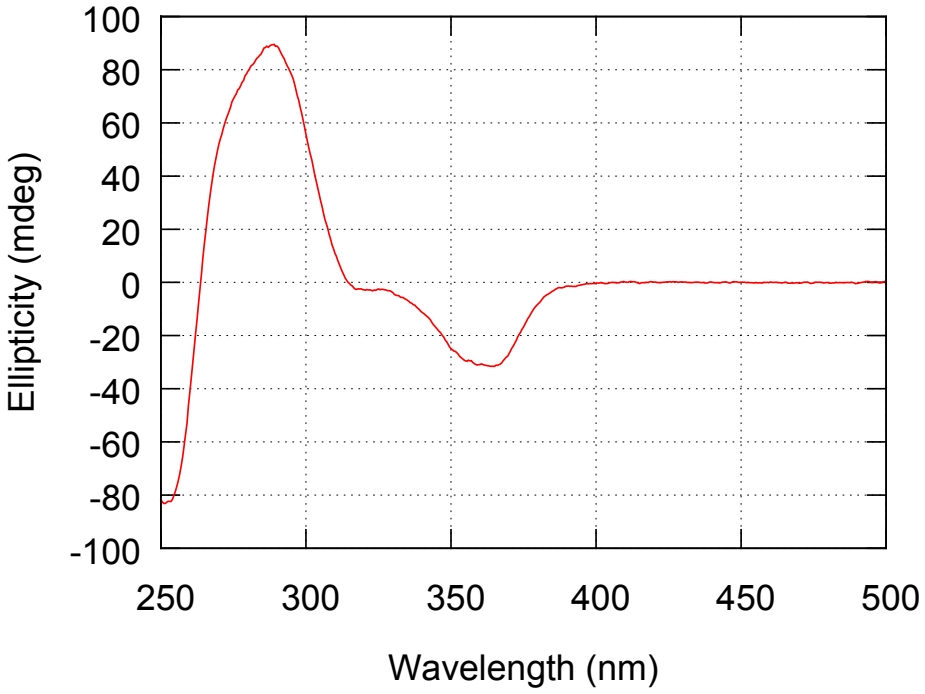

Figure S15. CD spectrum of **1a(100)** in *n*-hexane (3.12×10^{-2} g/L, path length = 10 mm).

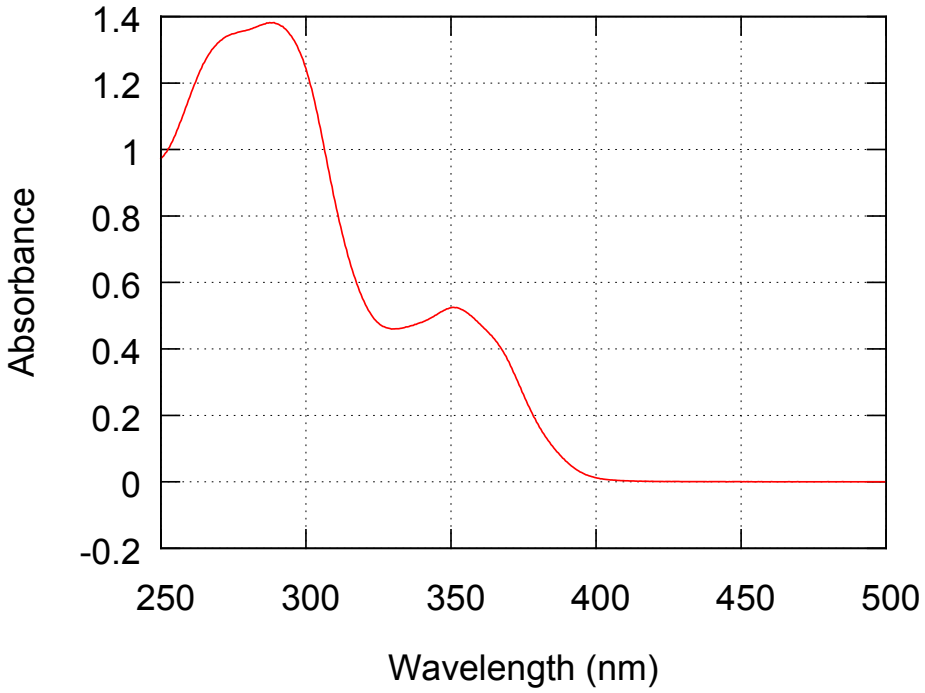

Figure S16. UV-vis absorption spectrum of **1a(100)** in *n*-heptane (3.12×10^{-2} g/L, path length = 10 mm).

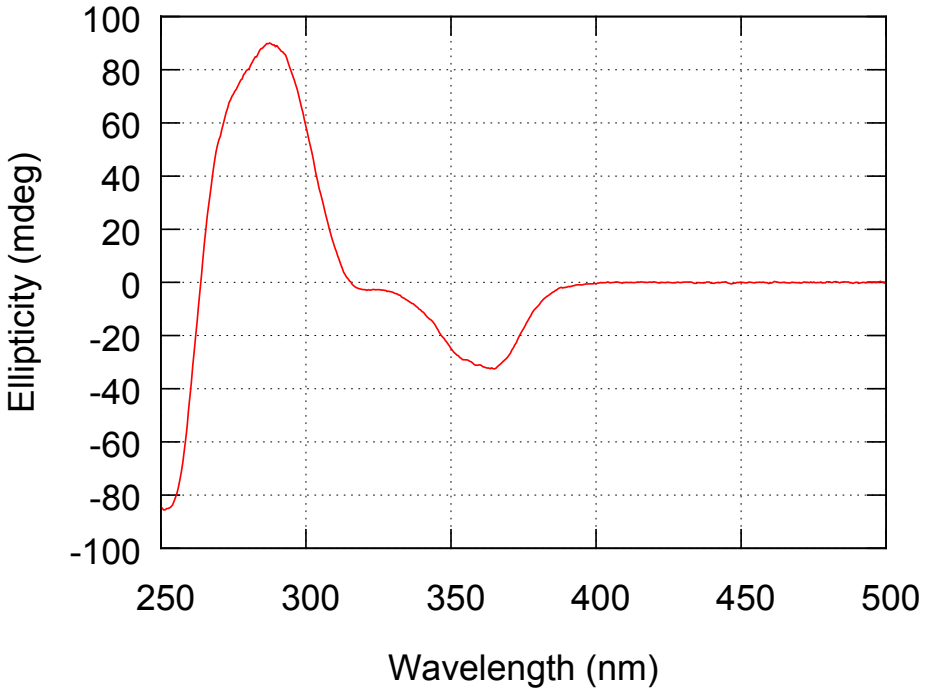

Figure S17. CD spectrum of **1a(100)** in *n*-heptane (3.12×10^{-2} g/L, path length = 10 mm).

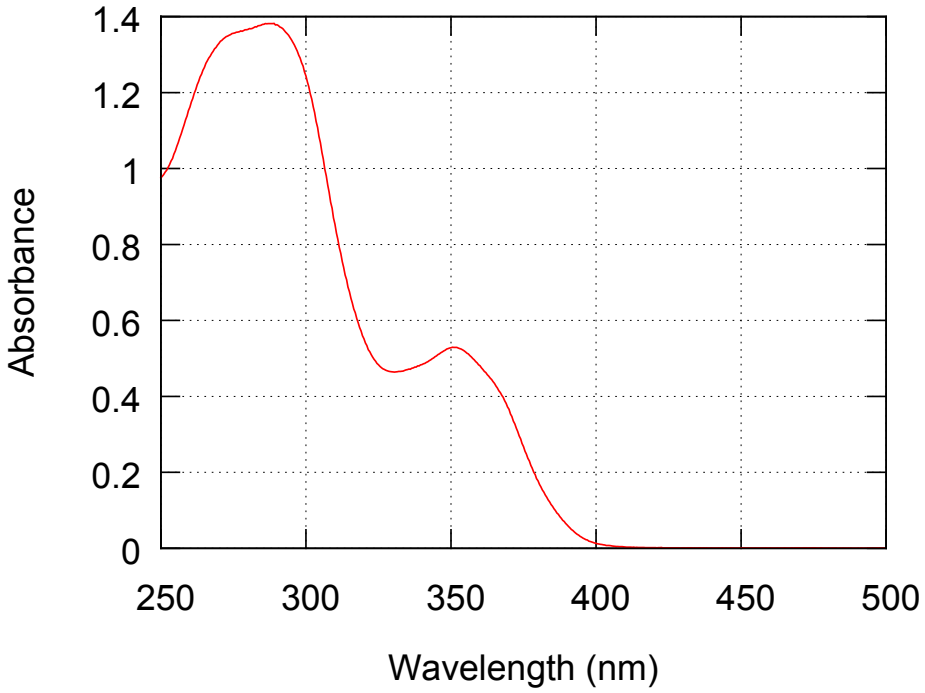

Figure S18. UV-vis absorption spectrum of **1a(100)** in *n*-octane (3.12×10^{-2} g/L, path length = 10 mm).

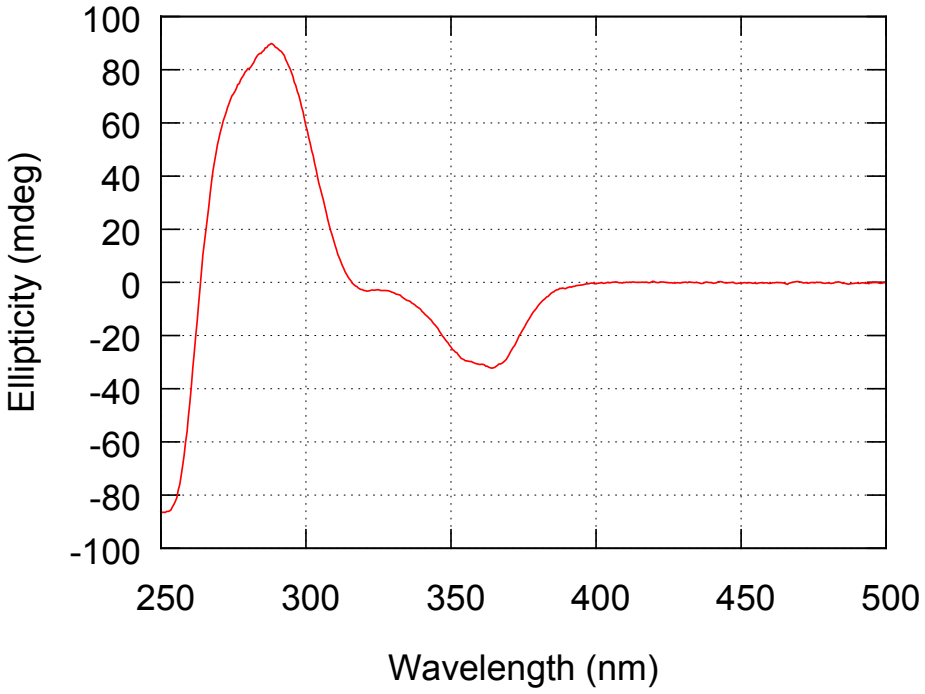

Figure S19. CD spectrum of **1a(100)** in *n*-octane (3.12×10^{-2} g/L, path length = 10 mm).

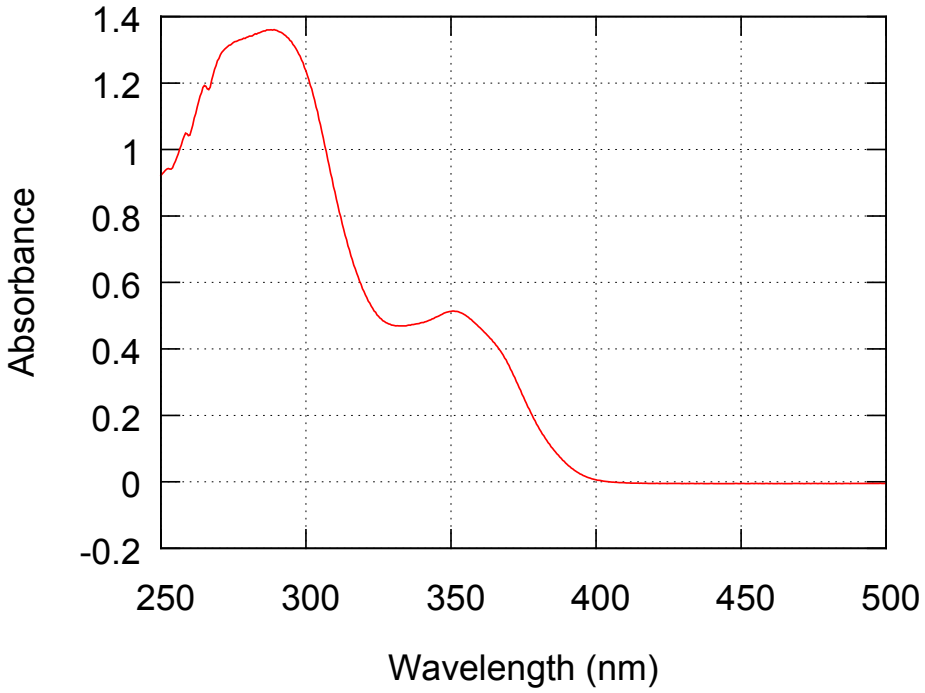

Figure S20. UV-vis absorption spectrum of **1a(100)** in *n*-nonane (3.12×10^{-2} g/L, path length = 10 mm).

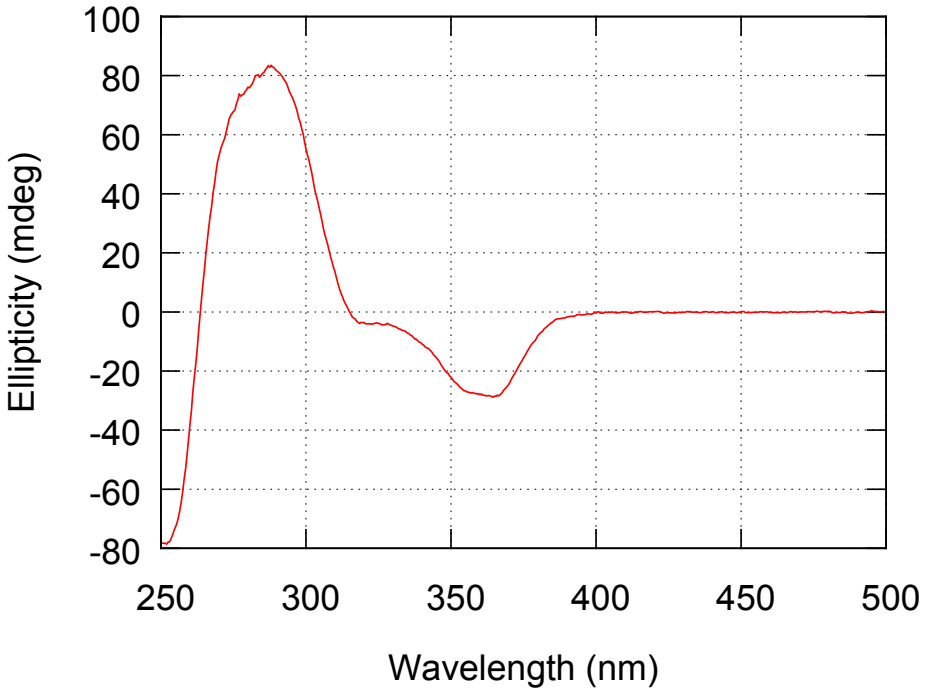

Figure S21. CD spectrum of **1a(100)** in *n*-nonane (3.12×10^{-2} g/L, path length = 10 mm).

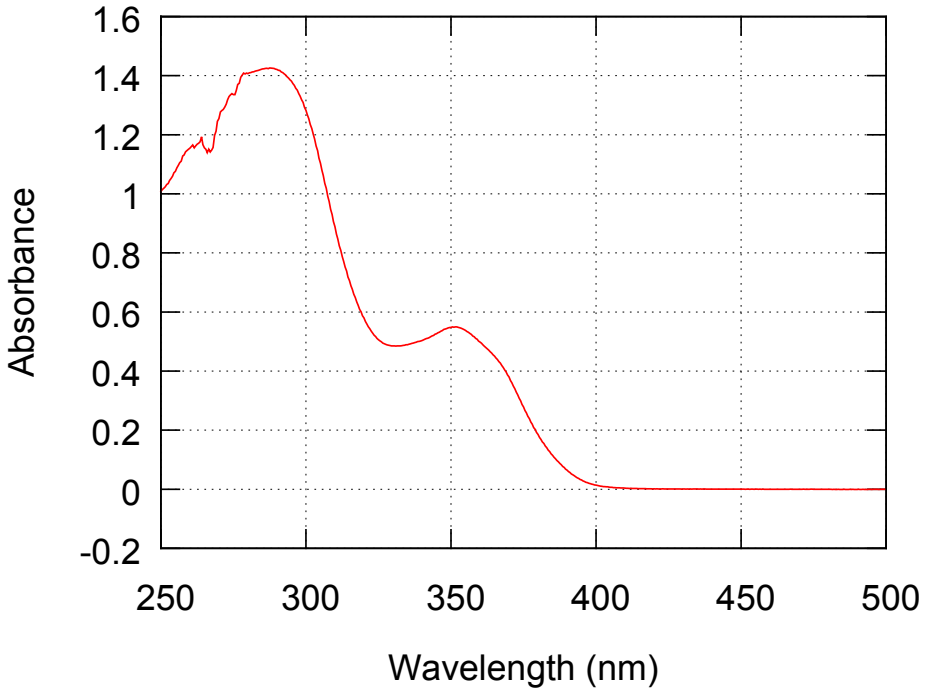

Figure S22. UV-vis absorption spectrum of **1a(100)** in *n*-decane (3.12×10^{-2} g/L, path length = 10 mm).

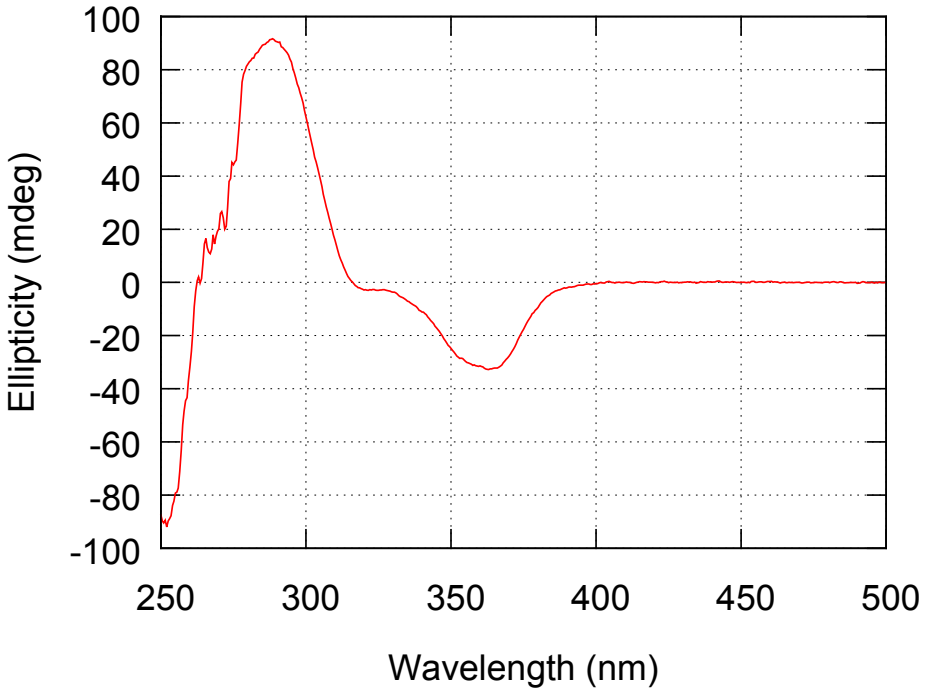

Figure S23. CD spectrum of **1a(100)** in *n*-decane (3.12×10^{-2} g/L, path length = 10 mm).

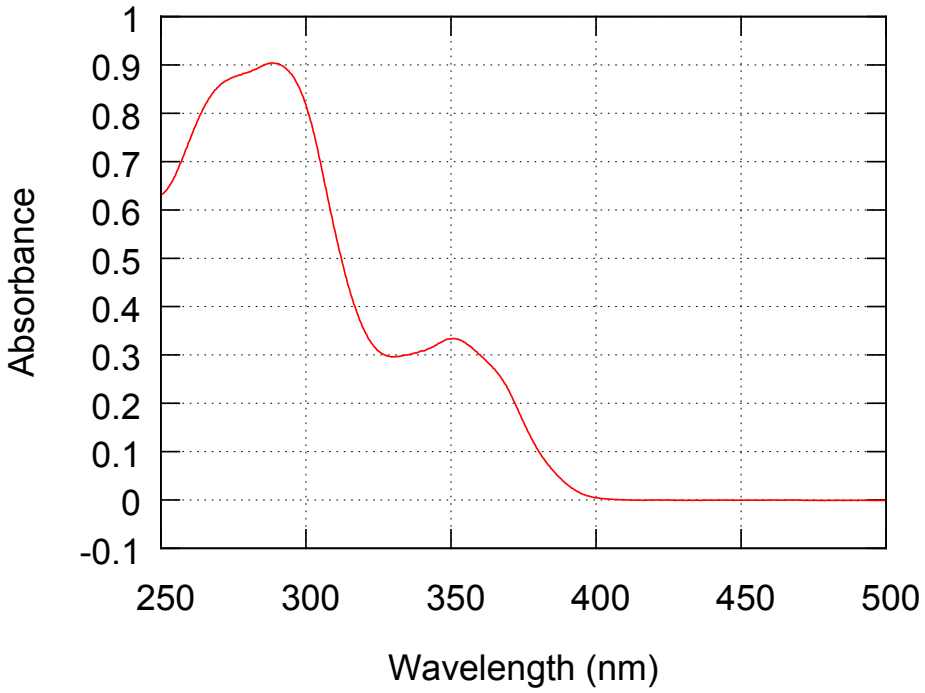

Figure S24. UV-vis absorption spectrum of **1b(100)** in *n*-pentane (1.75×10^{-2} g/L, path length = 10 mm).

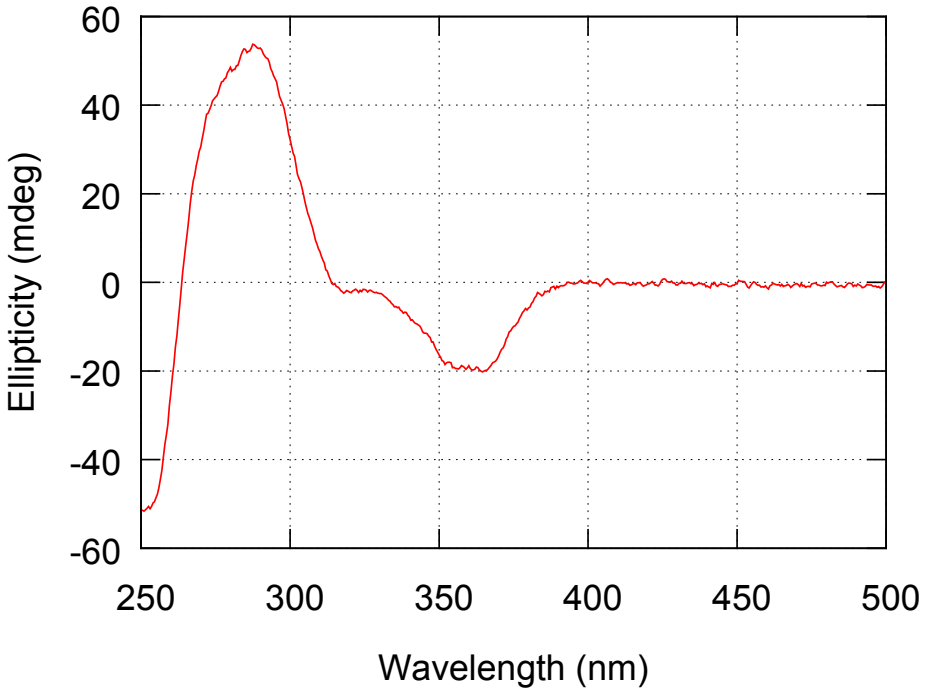

Figure S25. CD spectrum of **1b(100)** in *n*-pentane (1.75×10^{-2} g/L, path length = 10 mm).

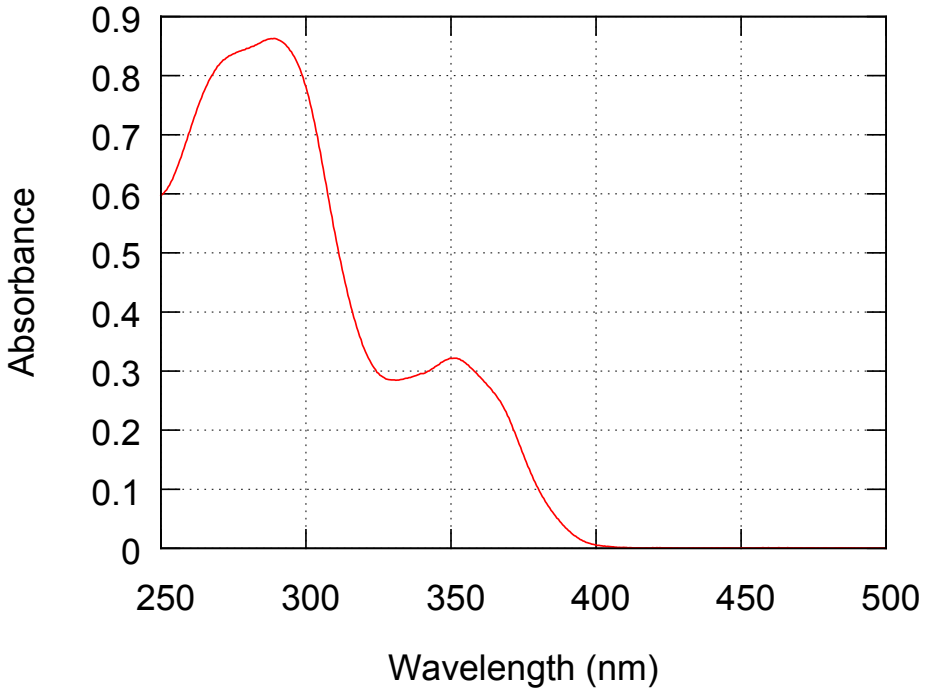

Figure S26. UV-vis absorption spectrum of **1b(100)** in *n*-hexane (1.75×10^{-2} g/L, path length = 10 mm).

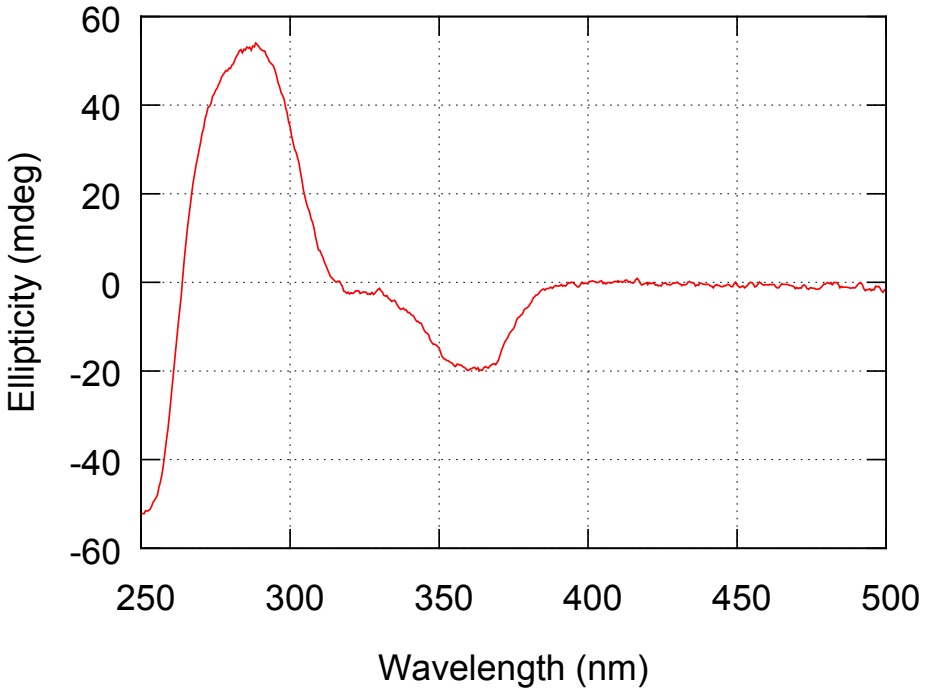

Figure S27. CD spectrum of **1b(100)** in *n*-hexane (1.75×10^{-2} g/L, path length = 10 mm).

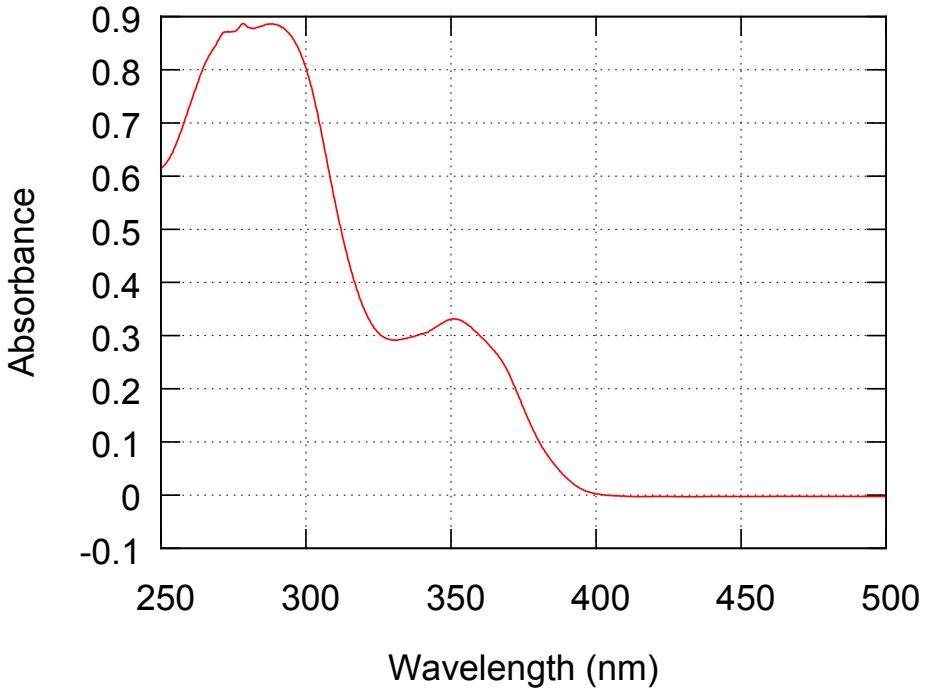

Figure S28. UV-vis absorption spectrum of **1b(100)** in *n*-heptane (1.75×10^{-2} g/L, path length = 10 mm).

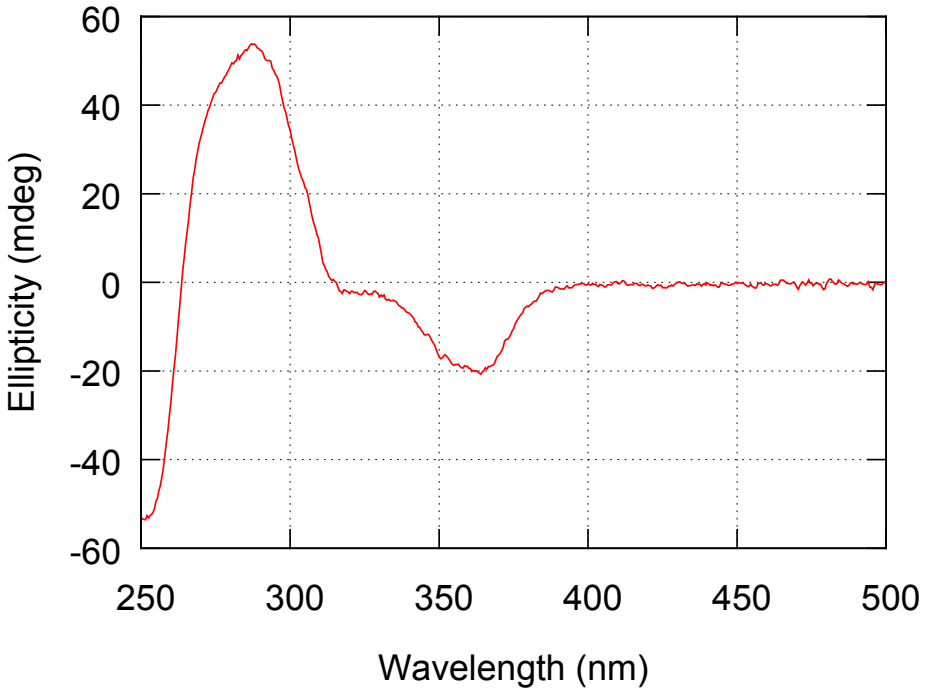

Figure S29. CD spectrum of **1b(100)** in *n*-heptane (1.75×10^{-2} g/L, path length = 10 mm).

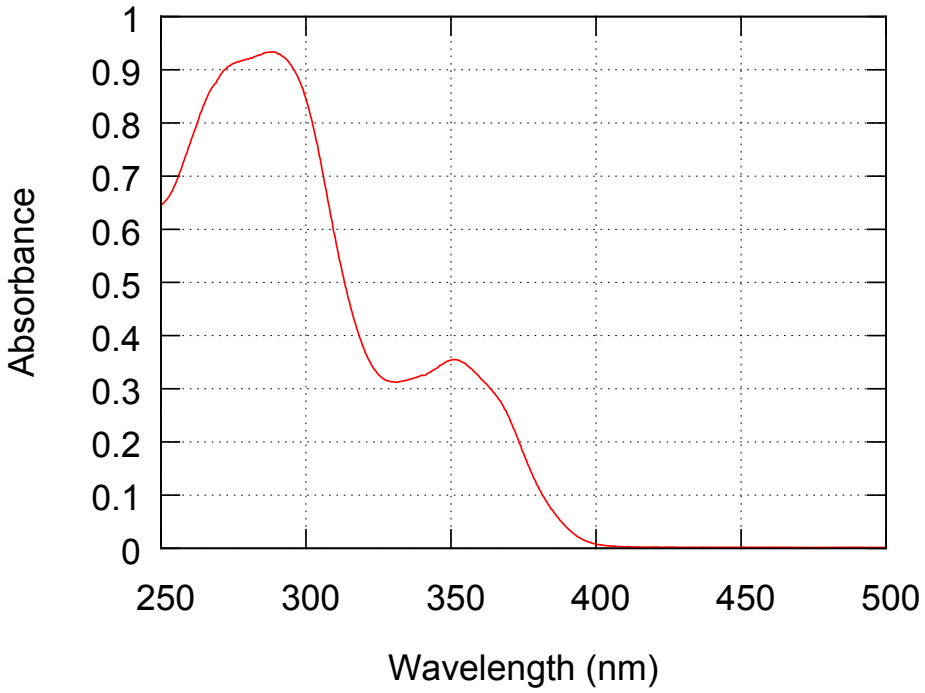

Figure S30. UV-vis absorption spectrum of **1b(100)** in *n*-octane (1.75×10^{-2} g/L, path length = 10 mm).

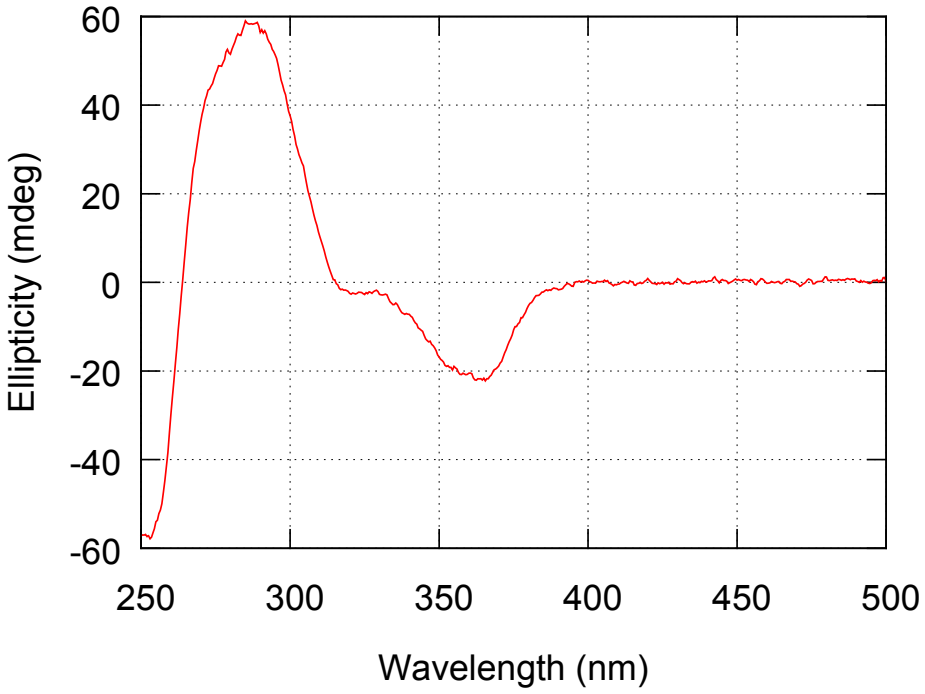

Figure S31. CD spectrum of **1b(100)** in *n*-octane (1.75×10^{-2} g/L, path length = 10 mm).

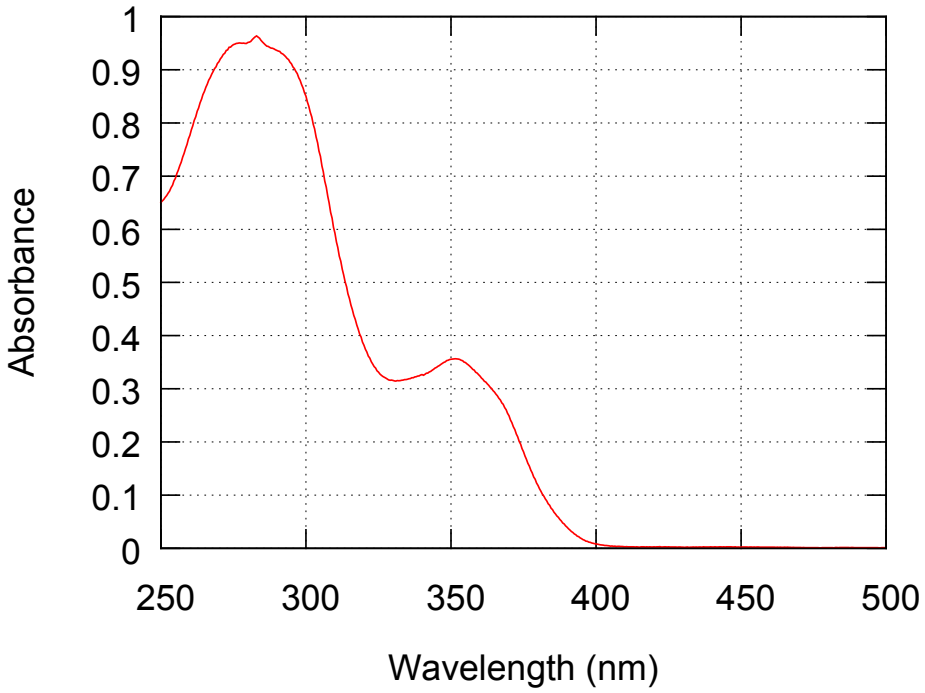

Figure S32. UV-vis absorption spectrum of **1b(100)** in *n*-nonane (1.75×10^{-2} g/L, path length = 10 mm).

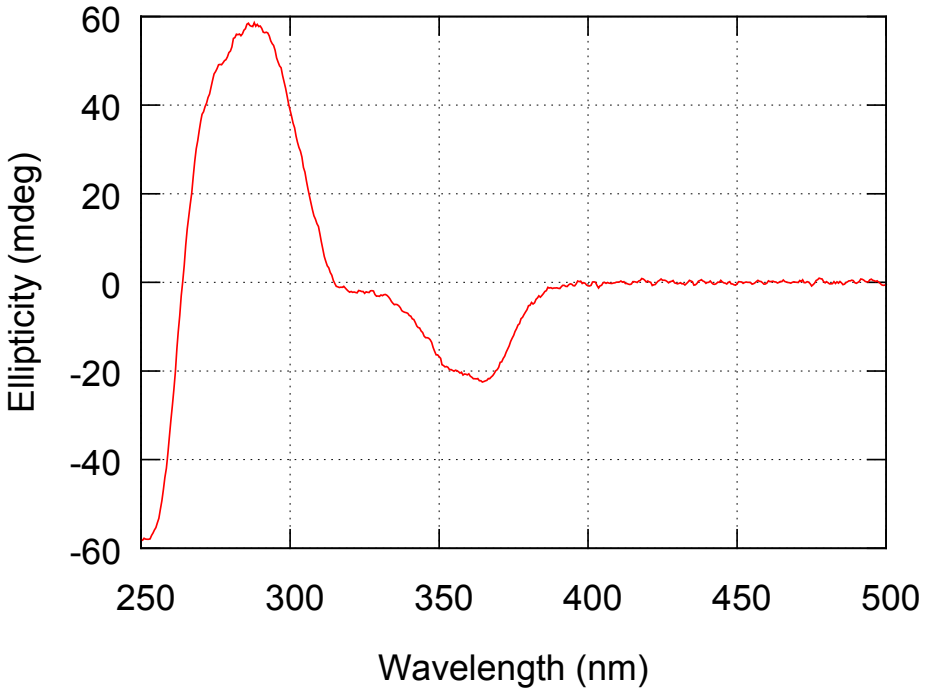

Figure S33. CD spectrum of **1b(100)** in *n*-nonane (1.75×10^{-2} g/L, path length = 10 mm).

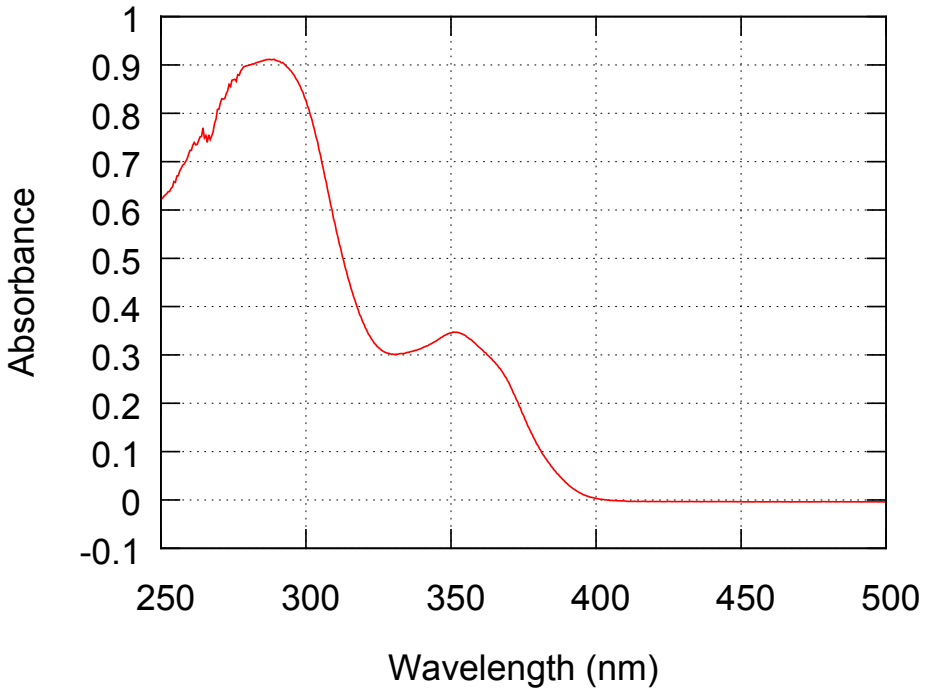

Figure S34. UV-vis absorption spectrum of **1b(100)** in *n*-decane (1.75×10^{-2} g/L, path length = 10 mm).

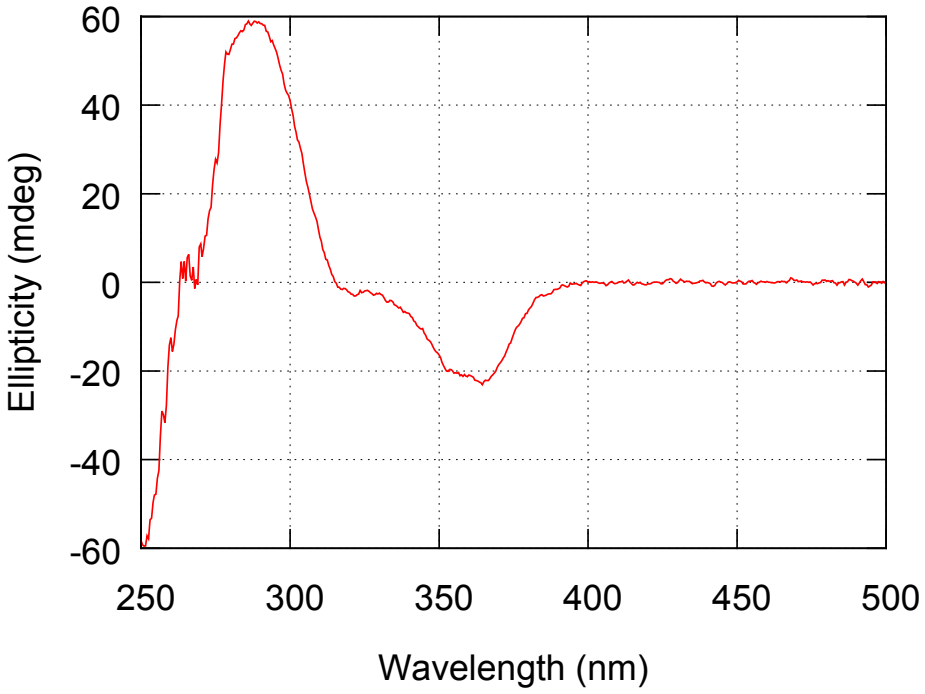

Figure S35. CD spectrum of **1b(100)** in *n*-decane (1.75×10^{-2} g/L, path length = 10 mm).

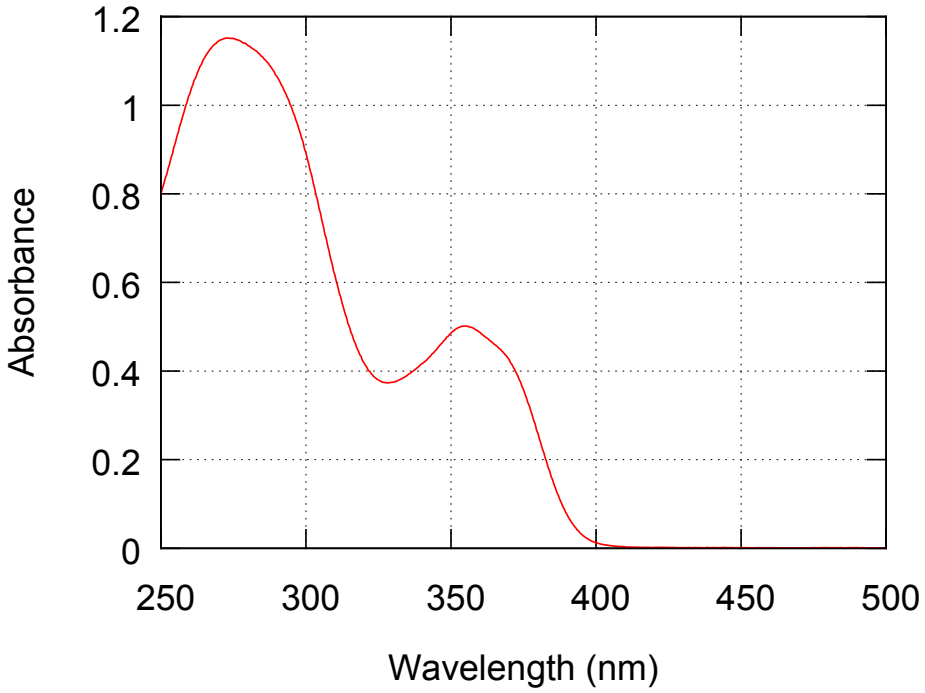

Figure S36. UV-vis absorption spectrum of **2a(40/60)** in *n*-pentane (2.51×10^{-2} g/L, path length = 10 mm).

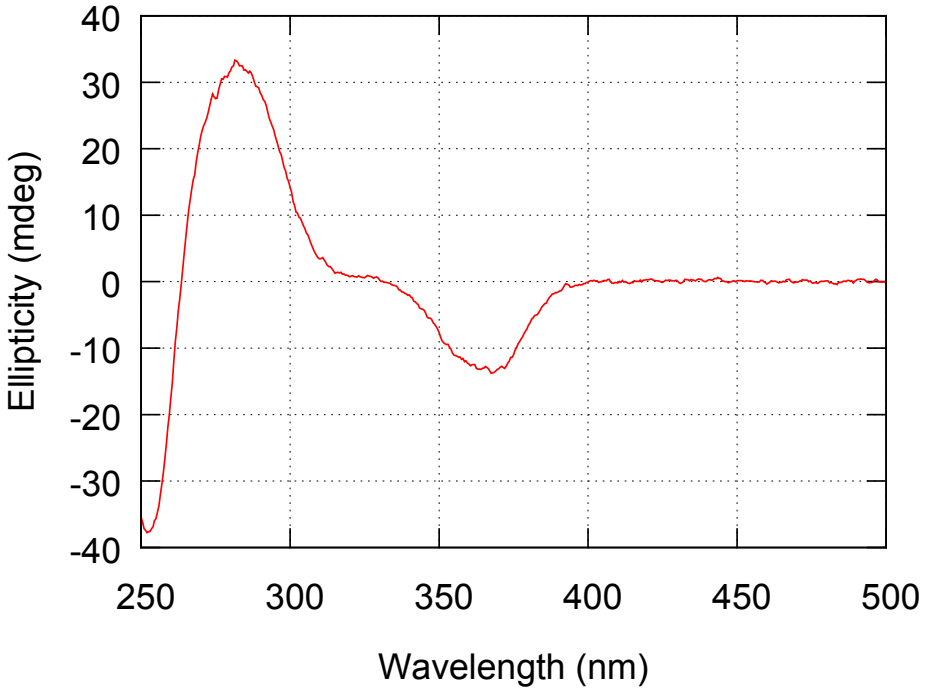

Figure S37. CD spectrum of **2a(40/60)** in *n*-pentane (2.51×10^{-2} g/L, path length = 10 mm).

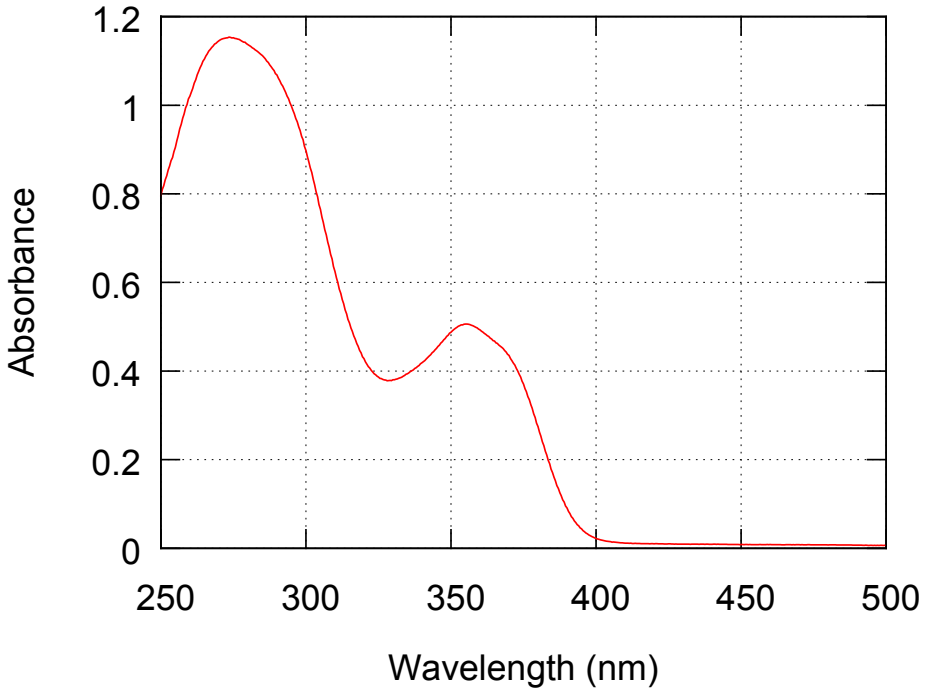

Figure S38. UV-vis absorption spectrum of **2a(40/60)** in *n*-hexane (2.51×10^{-2} g/L, path length = 10 mm).

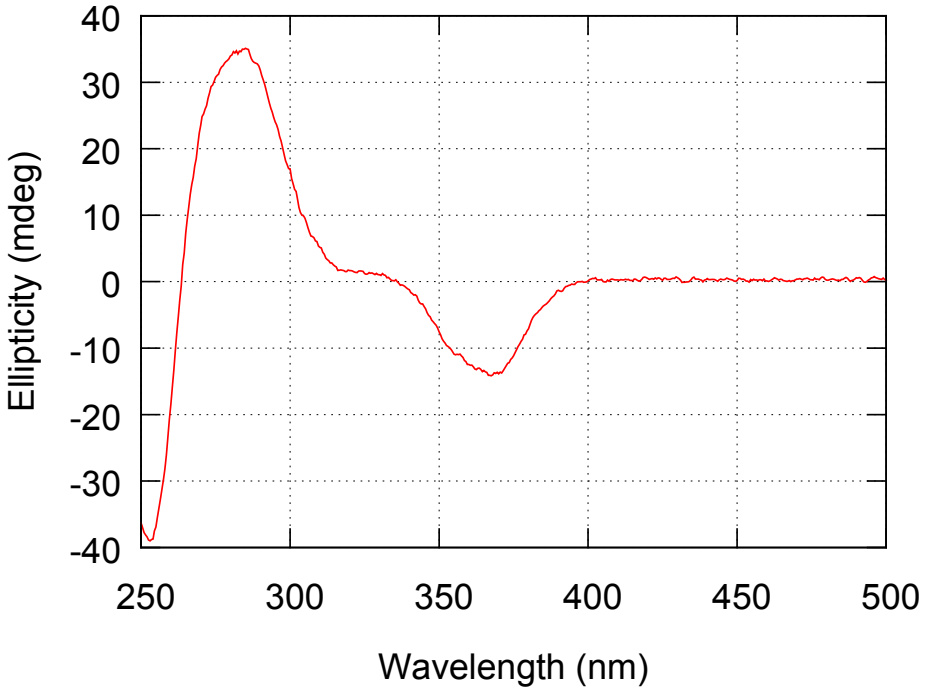

Figure S39. CD spectrum of **2a(40/60)** in *n*-hexane (2.51×10^{-2} g/L, path length = 10 mm).

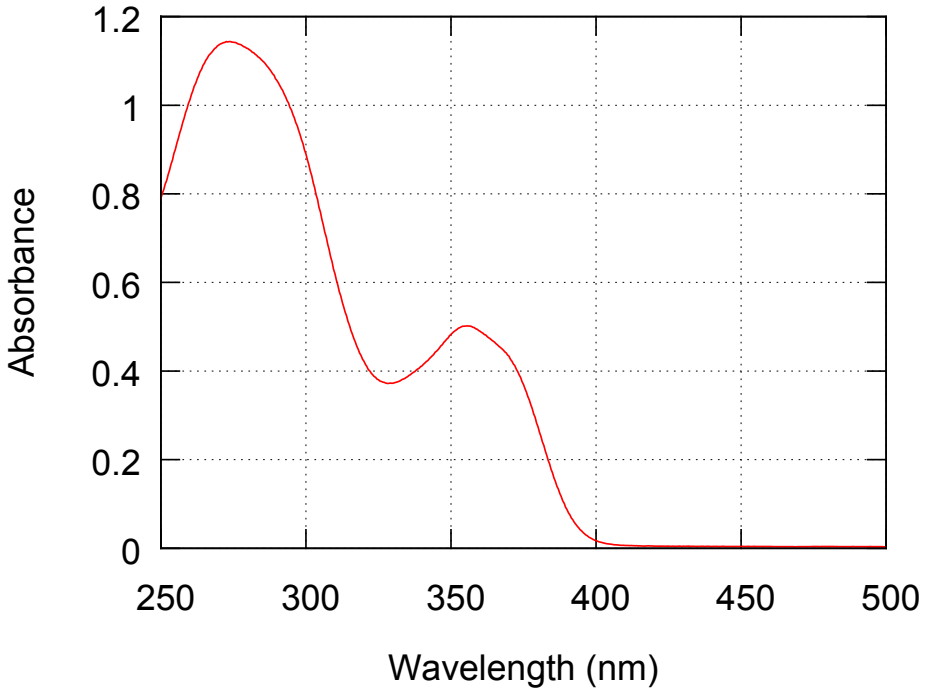

Figure S40. UV-vis absorption spectrum of **2a(40/60)** in *n*-heptane (2.51×10^{-2} g/L, path length = 10 mm).

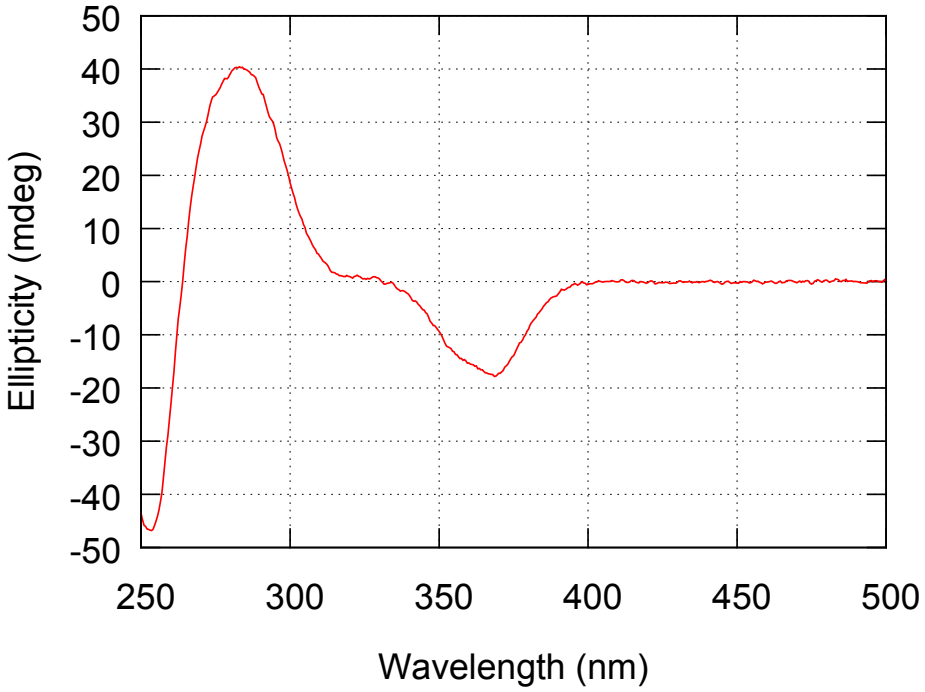

Figure S41. CD spectrum of **2a(40/60)** in *n*-heptane (2.51×10^{-2} g/L, path length = 10 mm).

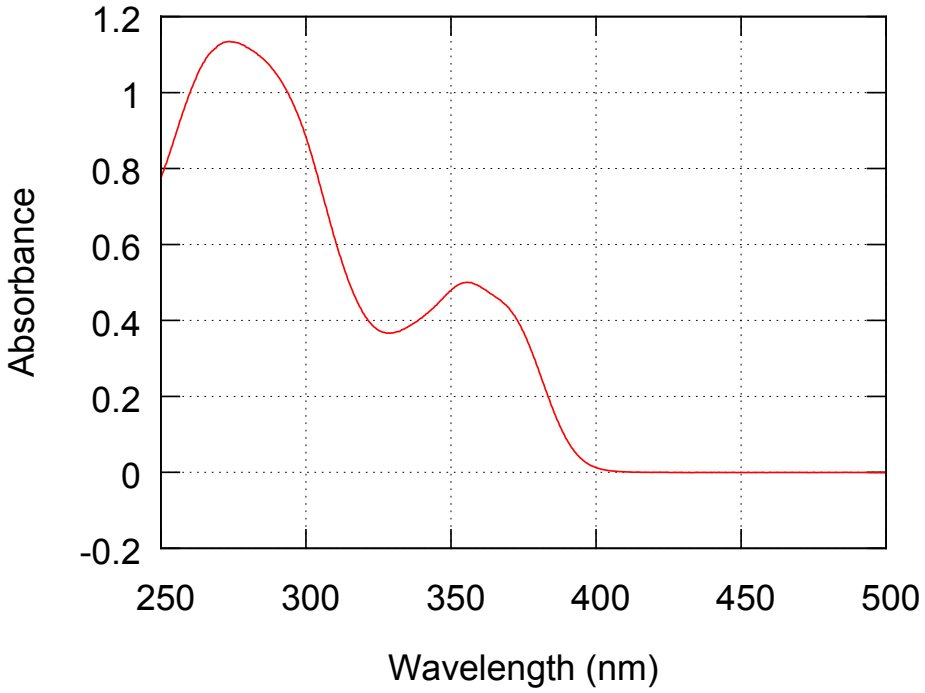

Figure S42. UV-vis absorption spectrum of **2a(40/60)** in *n*-octane (2.51×10^{-2} g/L, path length = 10 mm).

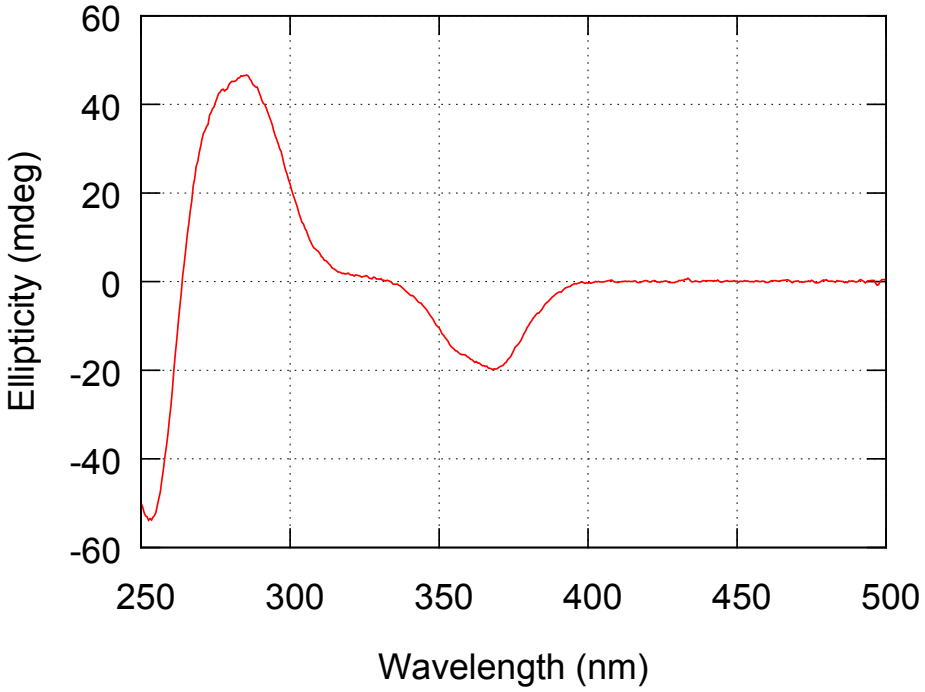

Figure S43. CD spectrum of **2a(40/60)** in *n*-octane (2.51×10^{-2} g/L, path length = 10 mm).

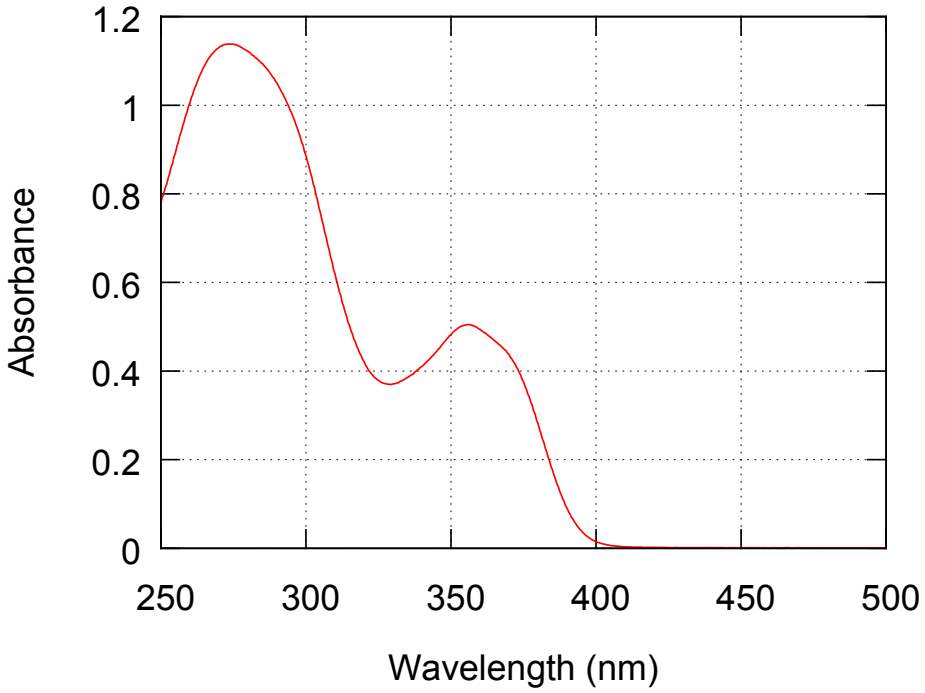

Figure S44. UV-vis absorption spectrum of **2a(40/60)** in *n*-nonane (2.51×10^{-2} g/L, path length = 10 mm).

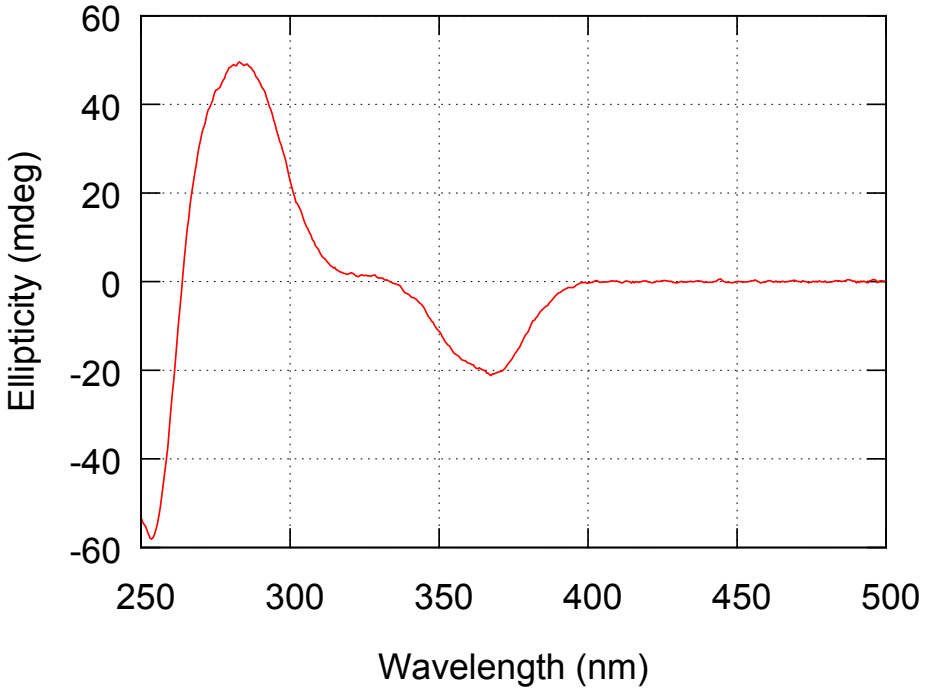

Figure S45. CD spectrum of **2a(40/60)** in *n*-nonane (2.51×10^{-2} g/L, path length = 10 mm).

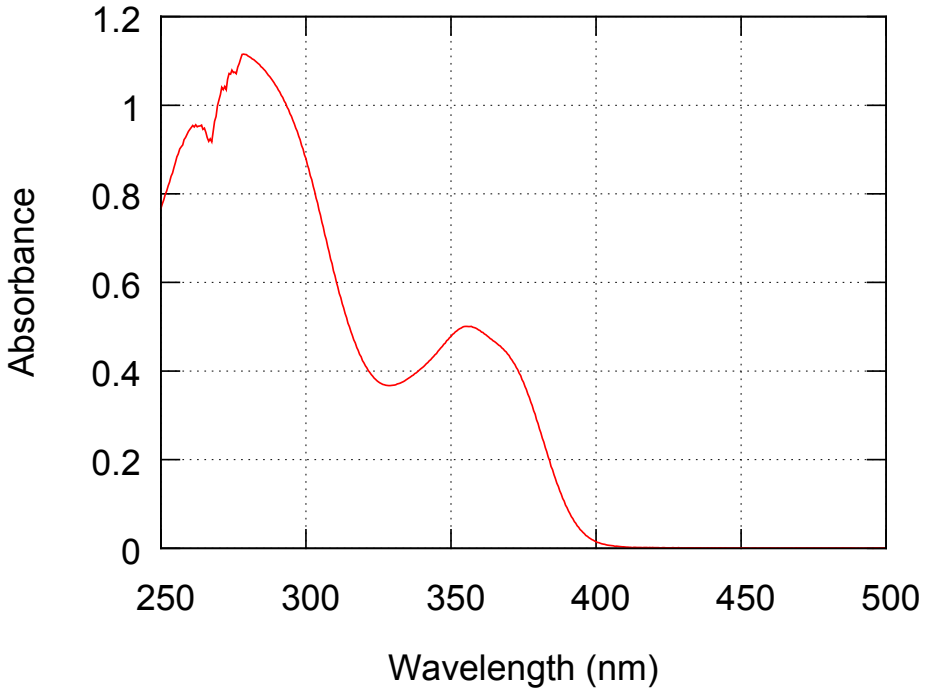

Figure S46. UV-vis absorption spectrum of **2a(40/60)** in *n*-decane (2.51×10^{-2} g/L, path length = 10 mm).

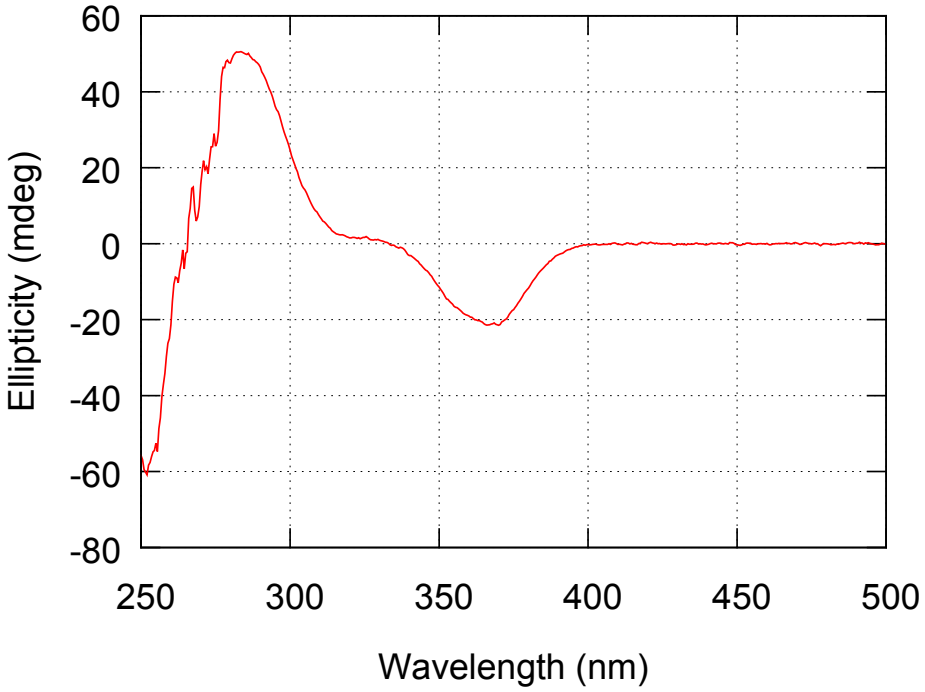

Figure S47. CD spectrum of **2a(40/60)** in *n*-decane (2.51×10^{-2} g/L, path length = 10 mm).

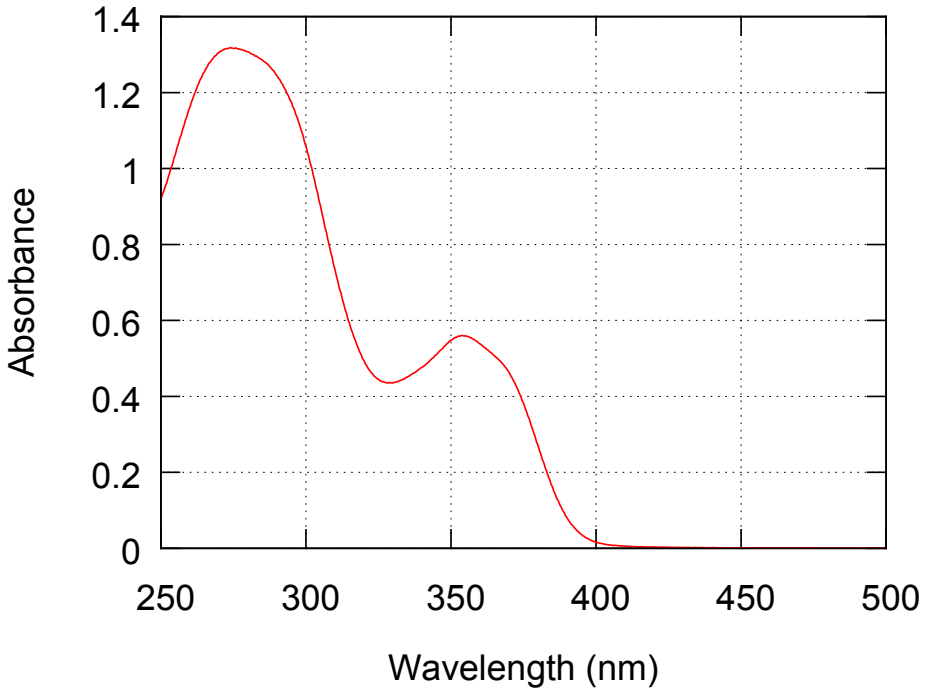

Figure S48. UV-vis absorption spectrum of **2b(40/60)** in *n*-pentane (1.97×10^{-2} g/L, path length = 10 mm).

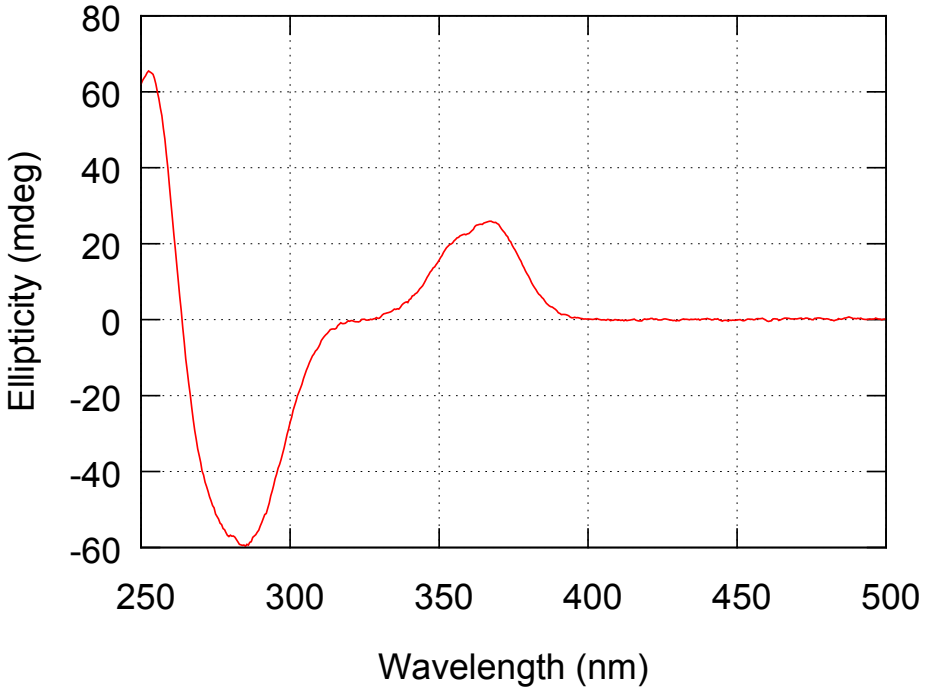

Figure S49. CD spectrum of **2b(40/60)** in *n*-pentane (1.97×10^{-2} g/L, path length = 10 mm).

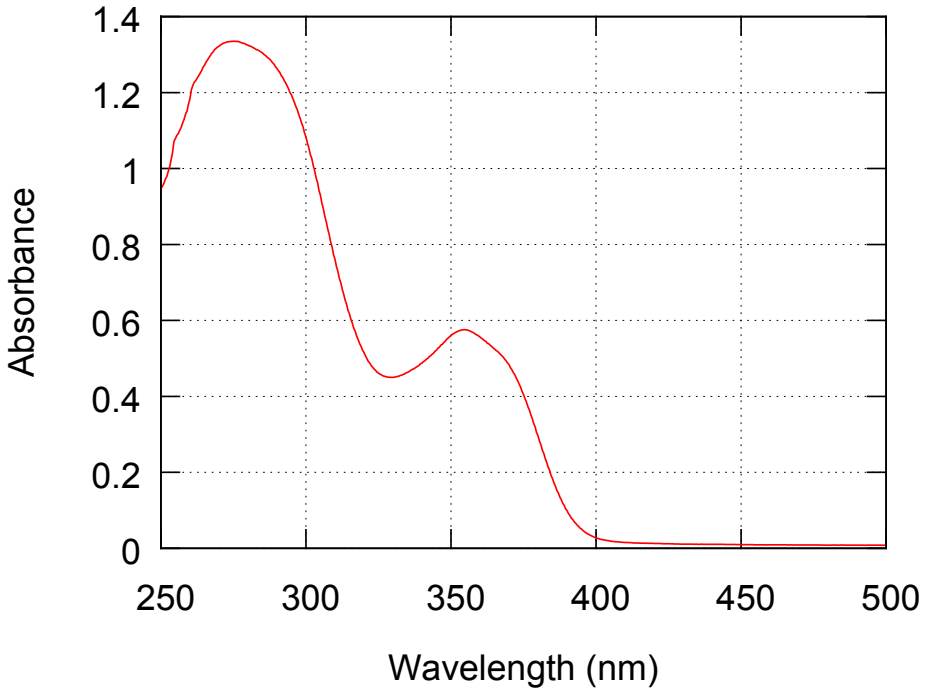

Figure S50. UV-vis absorption spectrum of **2b(40/60)** in *n*-hexane (1.97×10^{-2} g/L, path length = 10 mm).

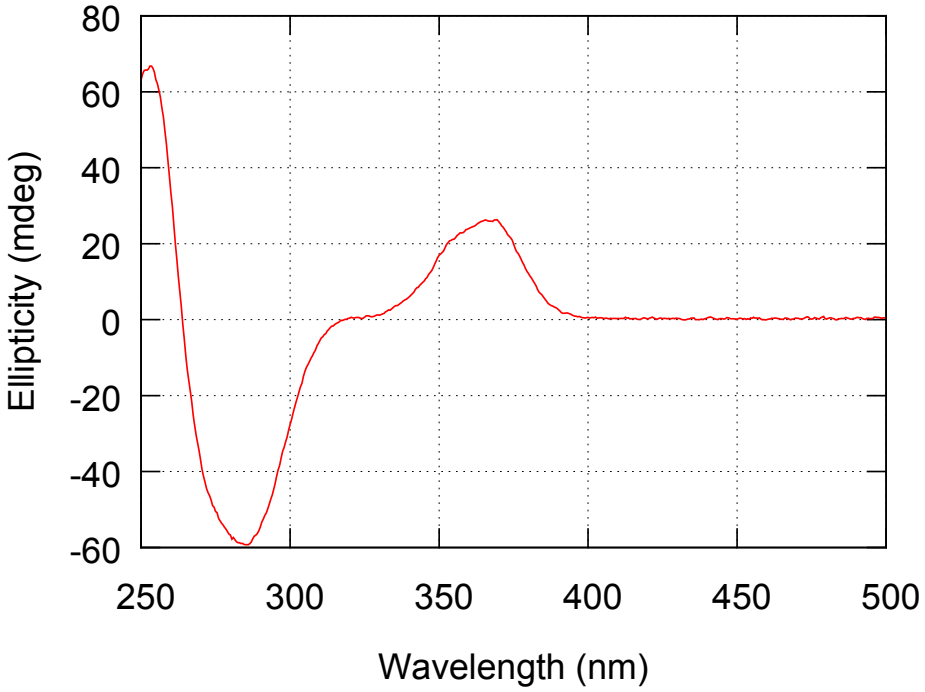

Figure S51. CD spectrum of **2b(40/60)** in *n*-hexane (1.97×10^{-2} g/L, path length = 10 mm).

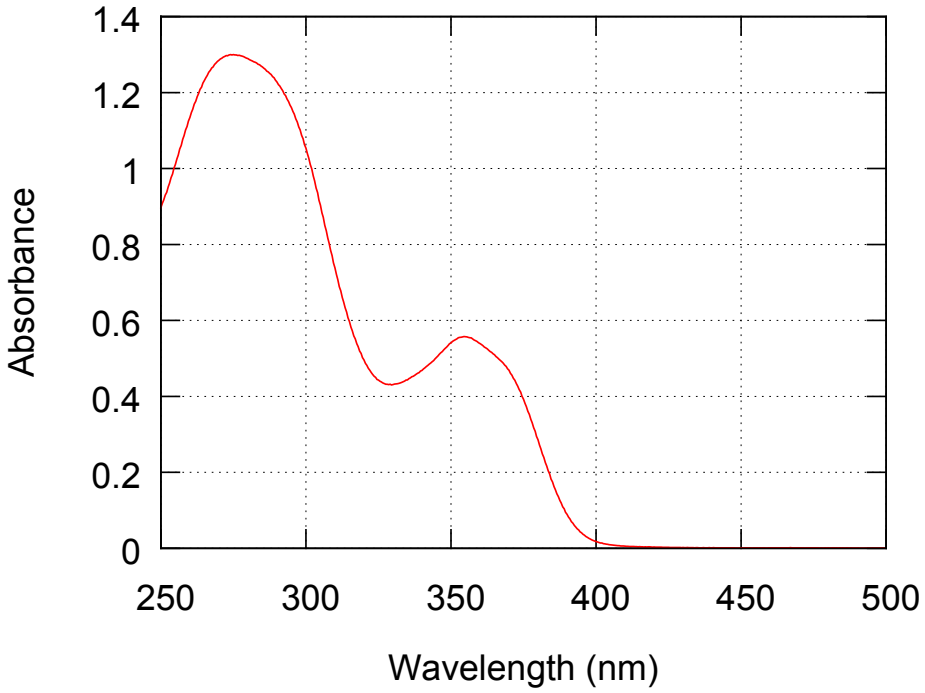

Figure S52. UV-vis absorption spectrum of **2b(40/60)** in *n*-heptane (1.97×10^{-2} g/L, path length = 10 mm).

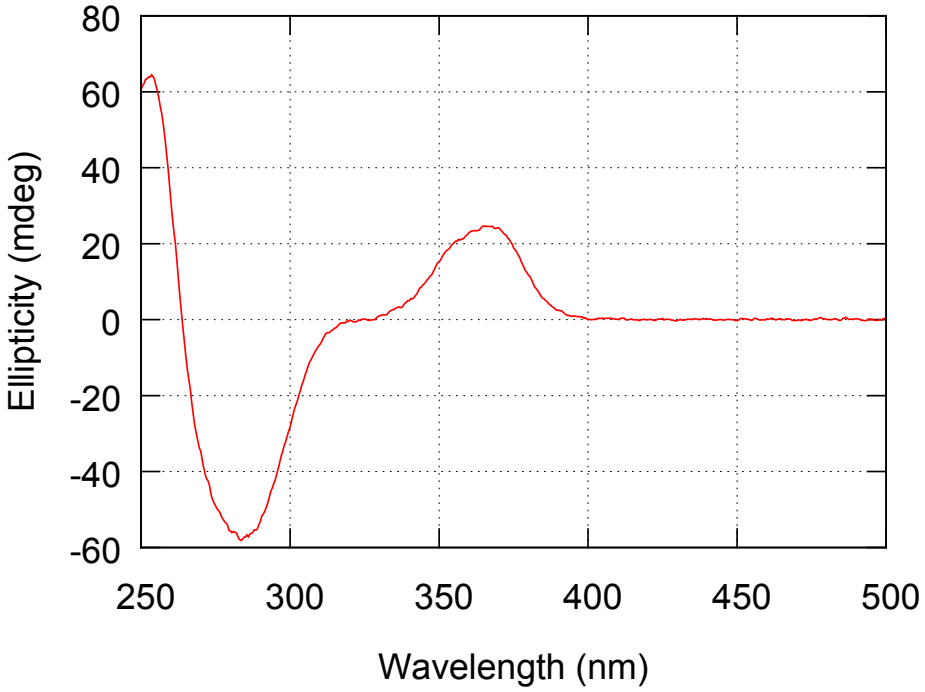

Figure S53. CD spectrum of **2b(40/60)** in *n*-heptane (1.97×10^{-2} g/L, path length = 10 mm).

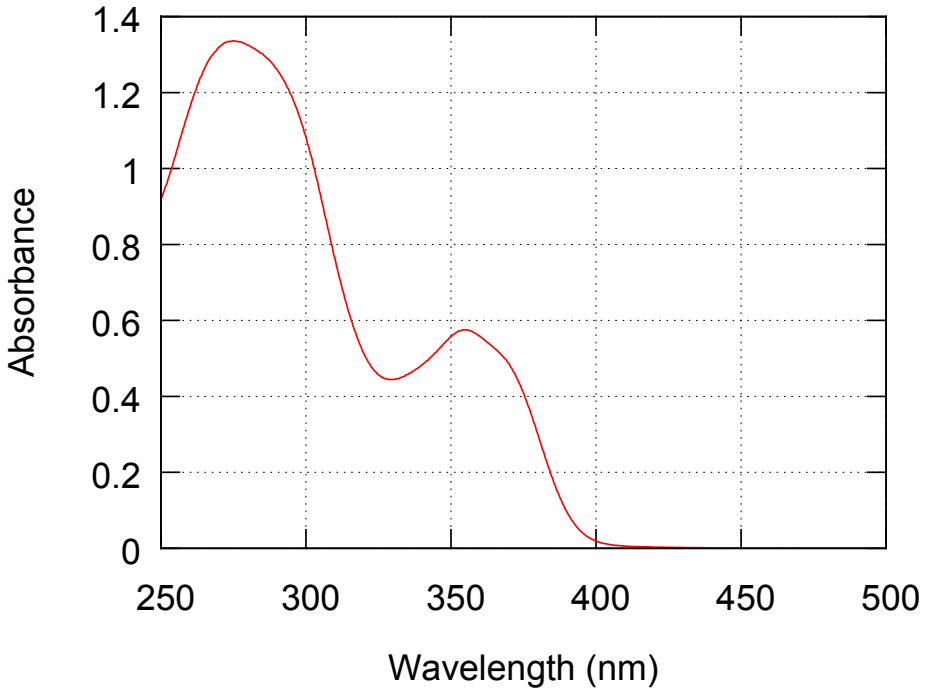

Figure S54. UV-vis absorption spectrum of **2b(40/60)** in *n*-octane (1.97×10^{-2} g/L, path length = 10 mm).

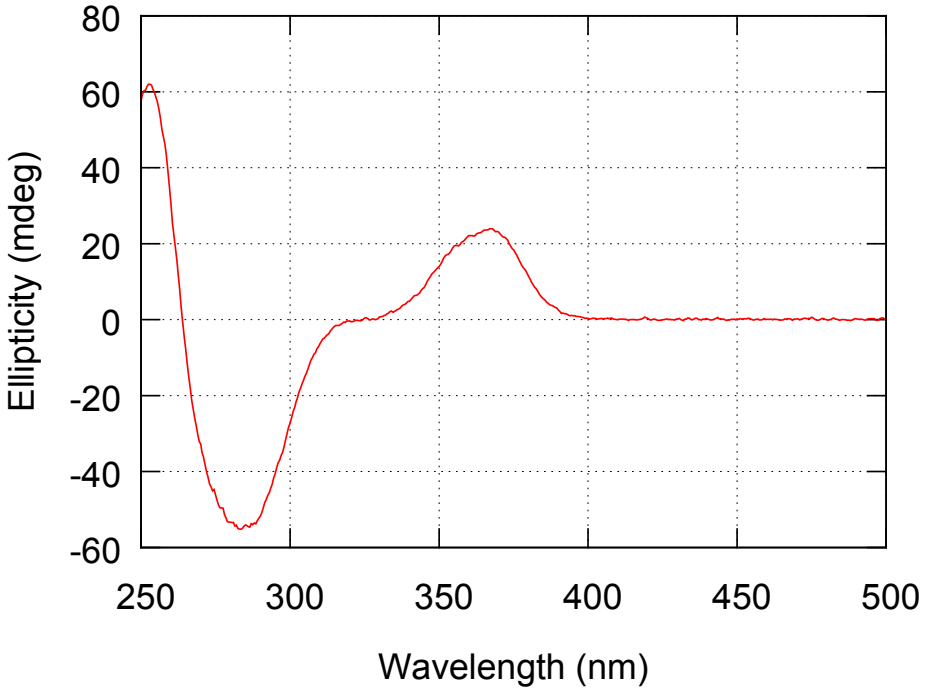

Figure S55. CD spectrum of **2b(40/60)** in *n*-octane (1.97×10^{-2} g/L, path length = 10 mm).

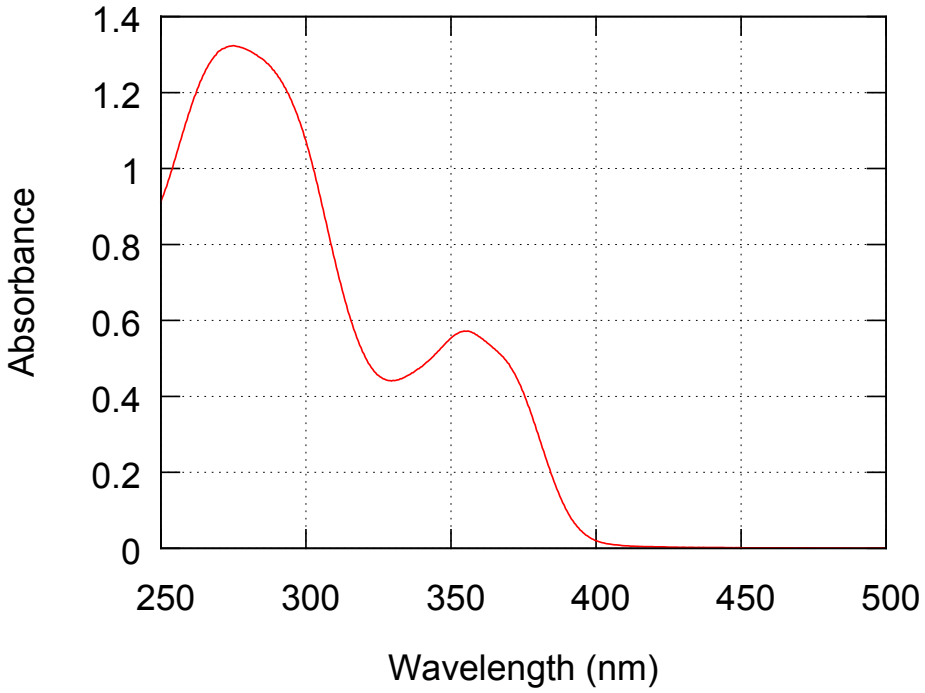

Figure S56. UV-vis absorption spectrum of **2b(40/60)** in *n*-nonane (1.97×10^{-2} g/L, path length = 10 mm).

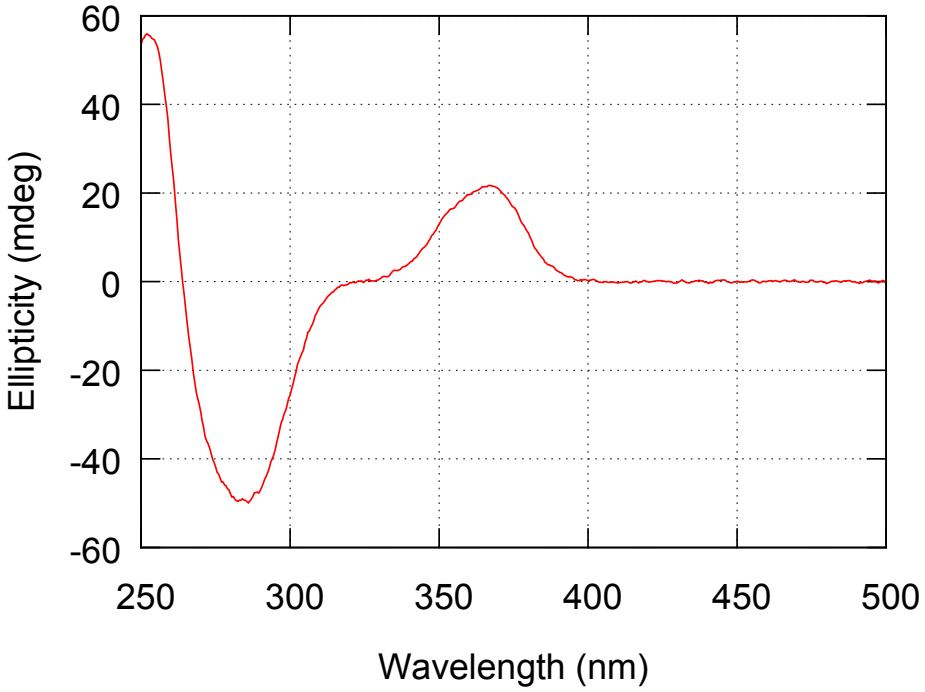

Figure S57. CD spectrum of **2b(40/60)** in *n*-nonane (1.97×10^{-2} g/L, path length = 10 mm).

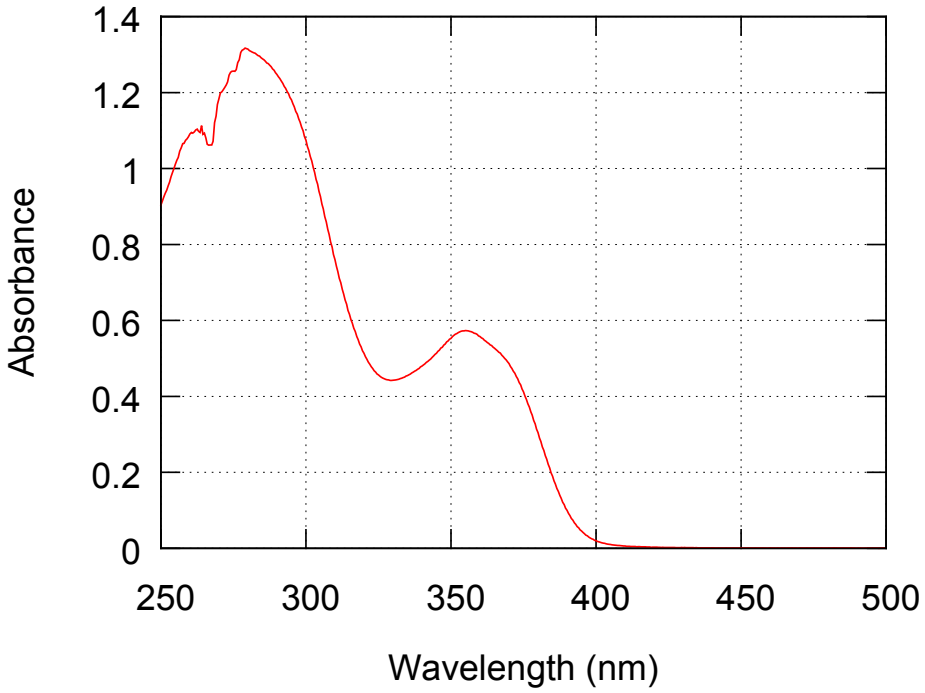

Figure S58. UV-vis absorption spectrum of **2b(40/60)** in *n*-decane (1.97×10^{-2} g/L, path length = 10 mm).

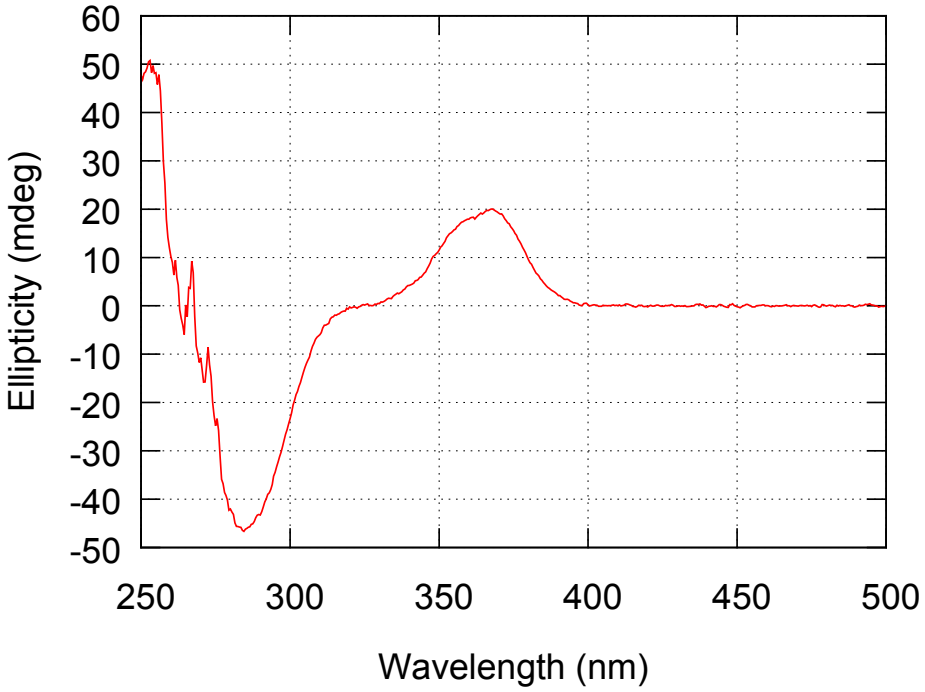

Figure S59. CD spectrum of **2b(40/60)** in *n*-decane (1.97×10^{-2} g/L, path length = 10 mm).

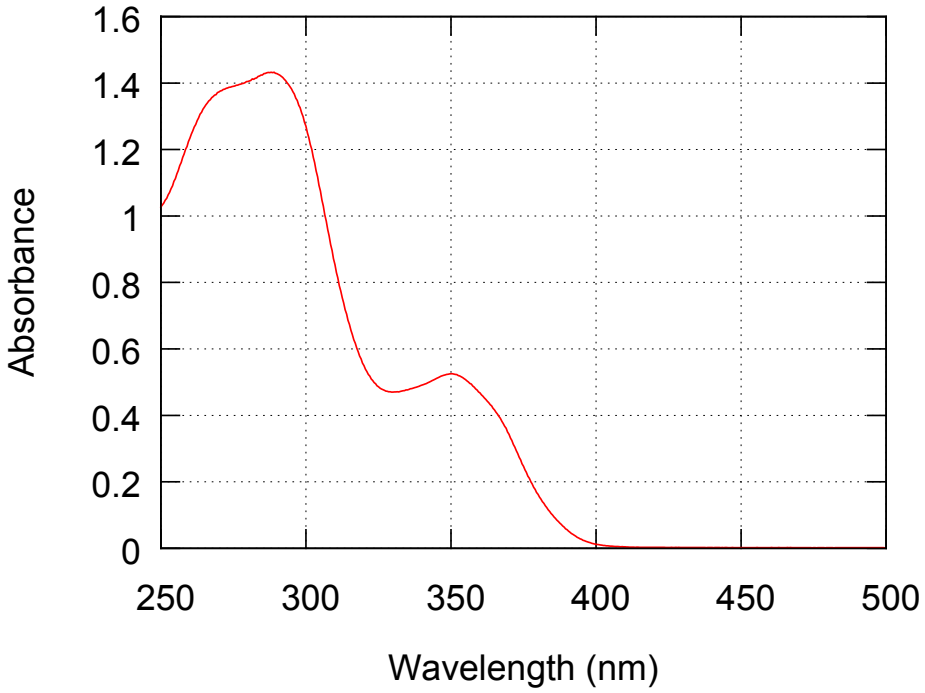

Figure S60. UV-vis absorption spectrum of **3a(40/60)** in *n*-pentane (2.31×10^{-2} g/L, path length = 10 mm).

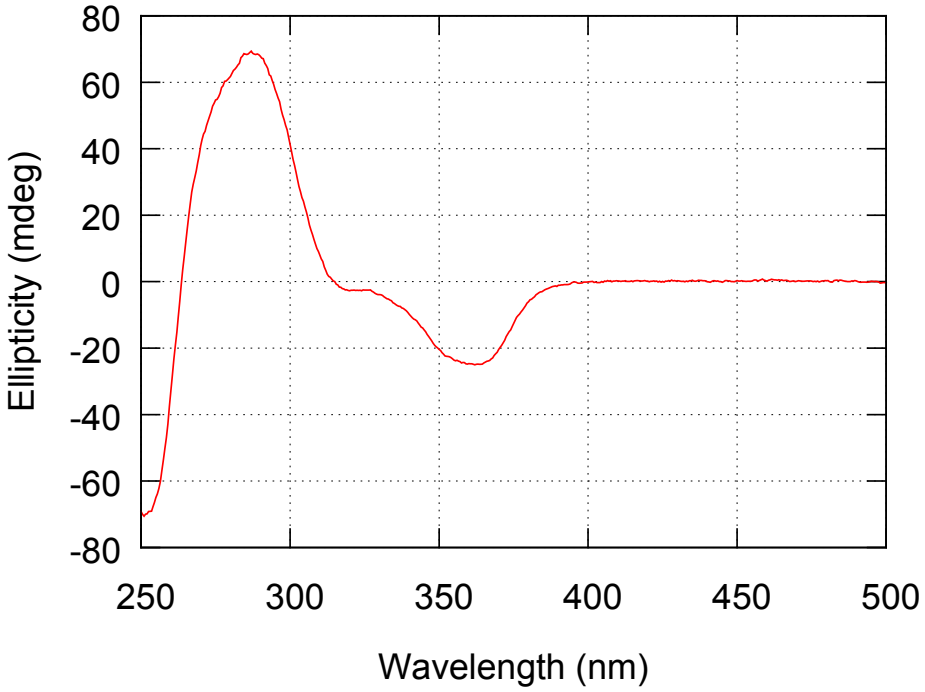

Figure S61. CD spectrum of **3a(40/60)** in *n*-pentane (2.31×10^{-2} g/L, path length = 10 mm).

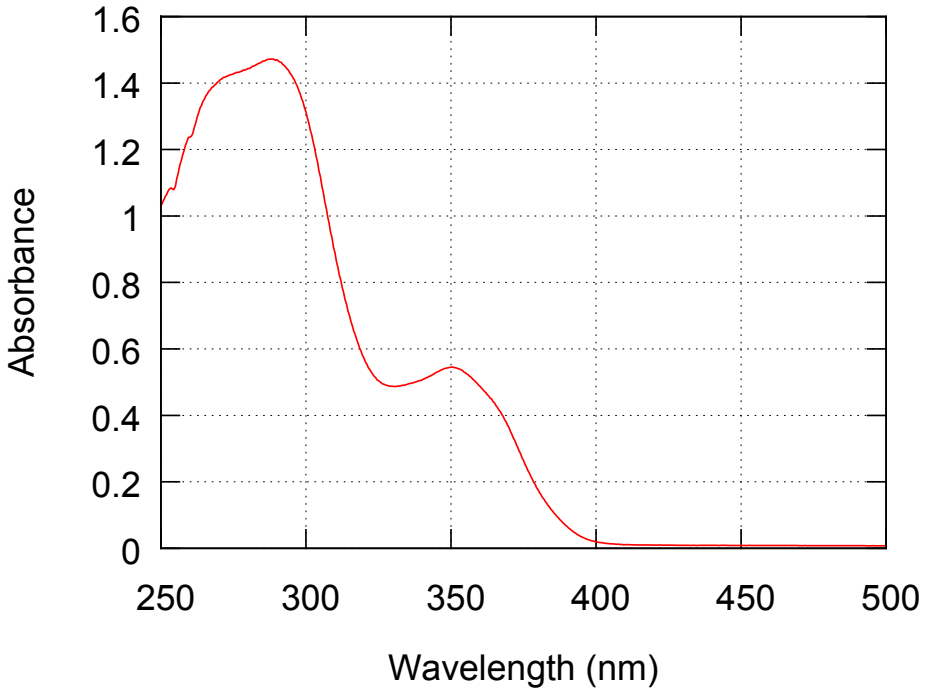

Figure S62. UV-vis absorption spectrum of **3a(40/60)** in *n*-hexane (2.31×10^{-2} g/L, path length = 10 mm).

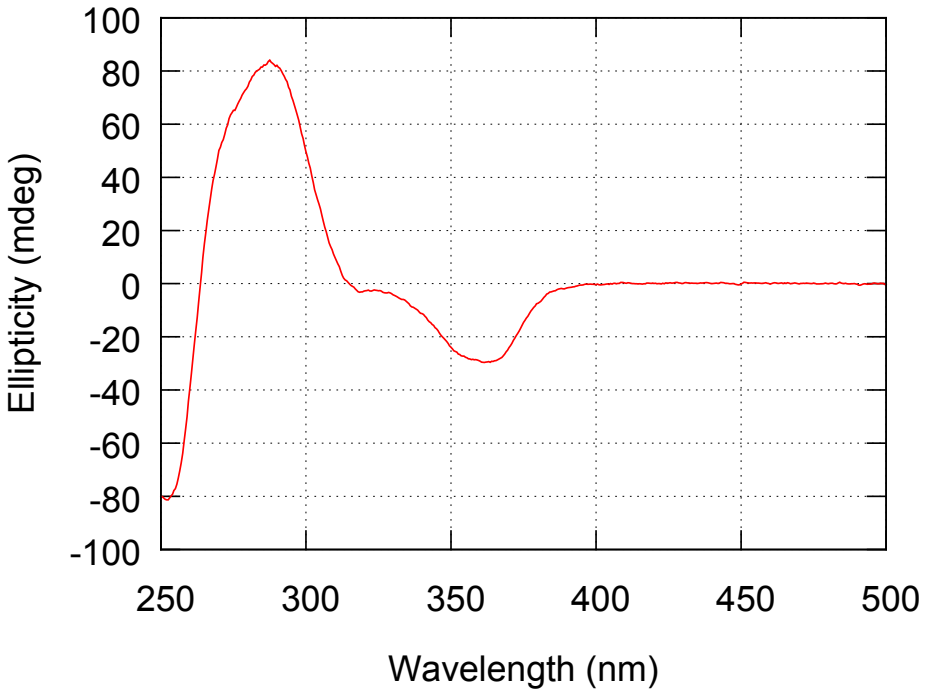

Figure S63. CD spectrum of **3a(40/60)** in *n*-hexane (2.31×10^{-2} g/L, path length = 10 mm).

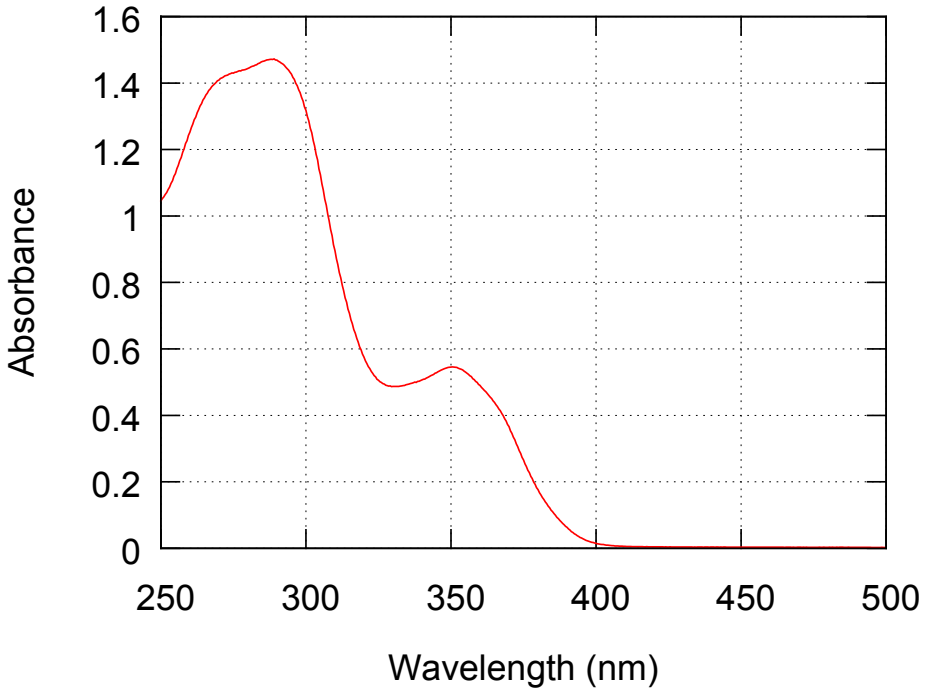

Figure S64. UV-vis absorption spectrum of **3a(40/60)** in *n*-heptane (2.31×10^{-2} g/L, path length = 10 mm).

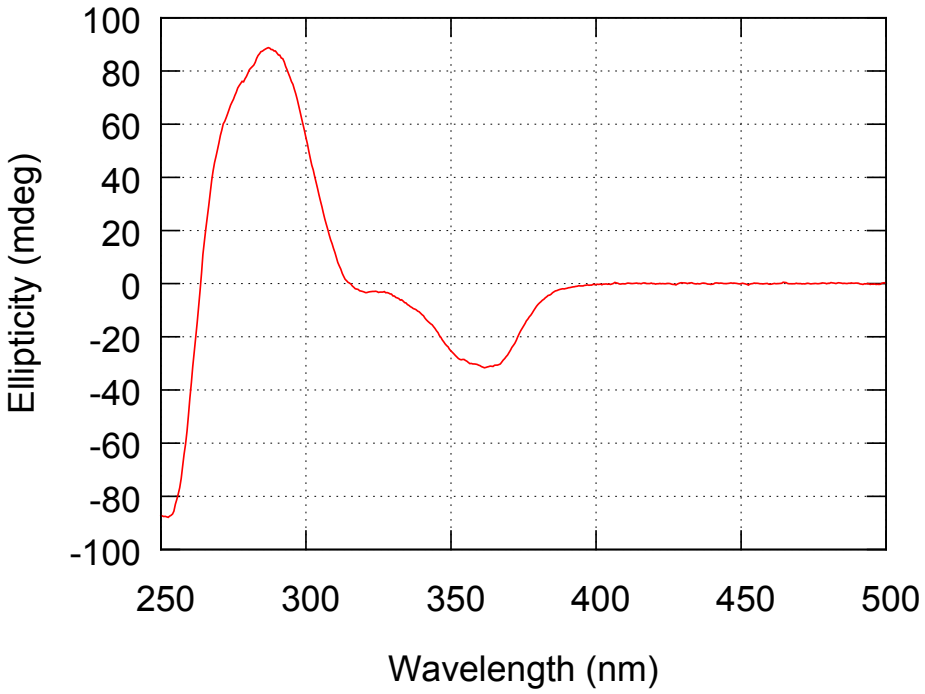

Figure S65. CD spectrum of **3a(40/60)** in *n*-heptane (2.31×10^{-2} g/L, path length = 10 mm).

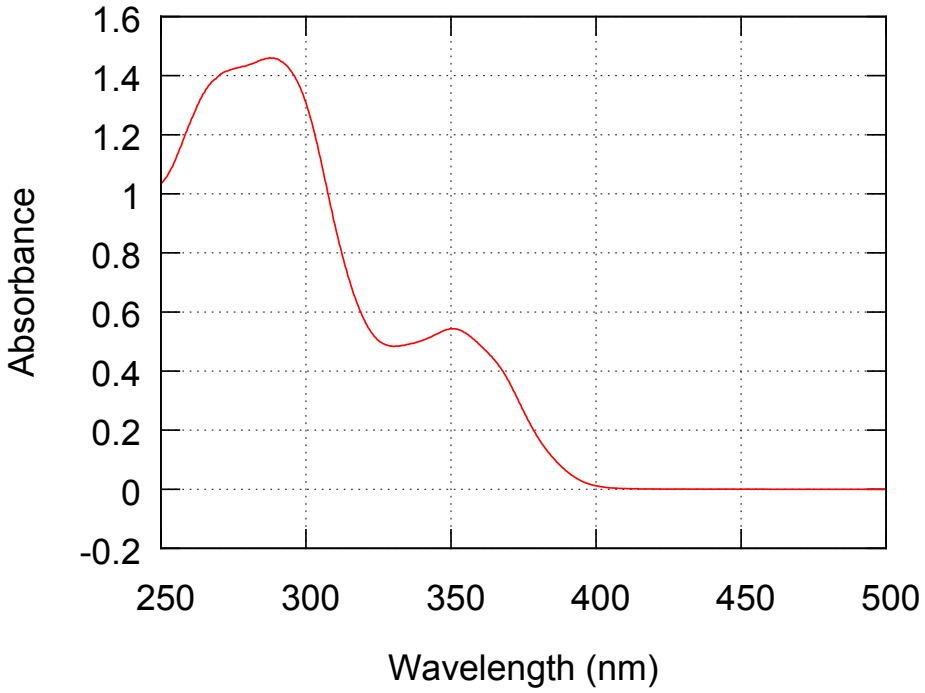

Figure S66. UV-vis absorption spectrum of **3a(40/60)** in *n*-octane (2.31×10^{-2} g/L, path length = 10 mm).

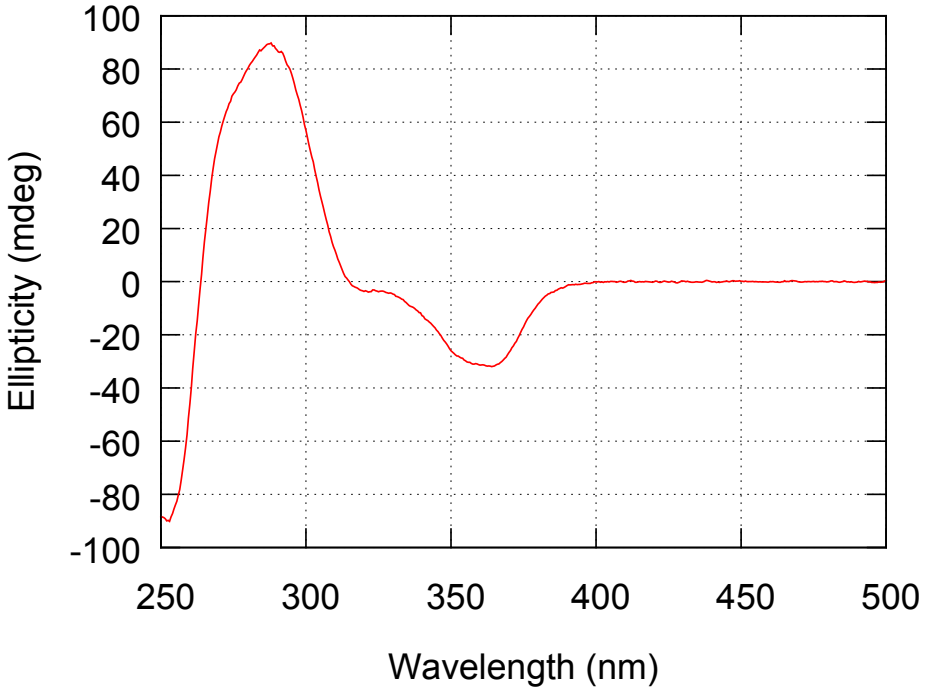

Figure S67. CD spectrum of **3a(40/60)** in *n*-octane (2.31×10^{-2} g/L, path length = 10 mm).

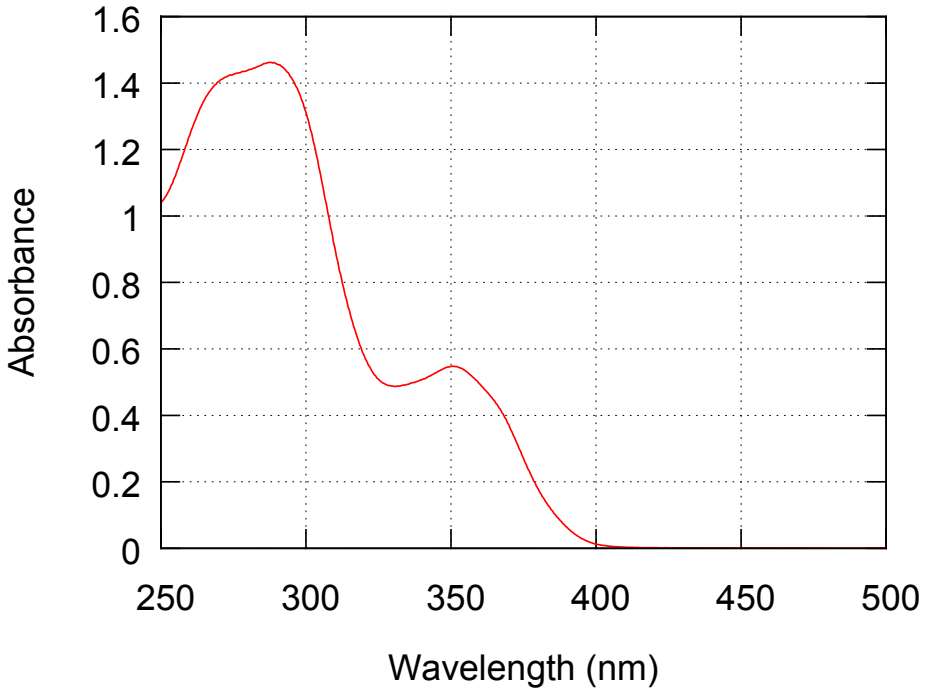

Figure S68. UV-vis absorption spectrum of **3a(40/60)** in *n*-nonane (2.31×10^{-2} g/L, path length = 10 mm).

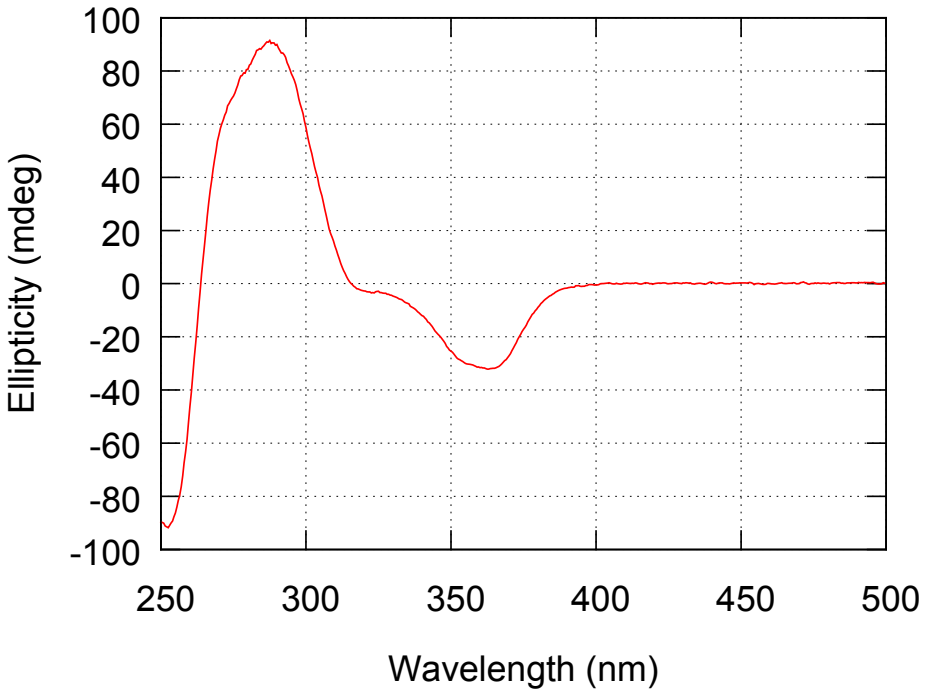

Figure S69. CD spectrum of **3a(40/60)** in *n*-nonane (2.31×10^{-2} g/L, path length = 10 mm).

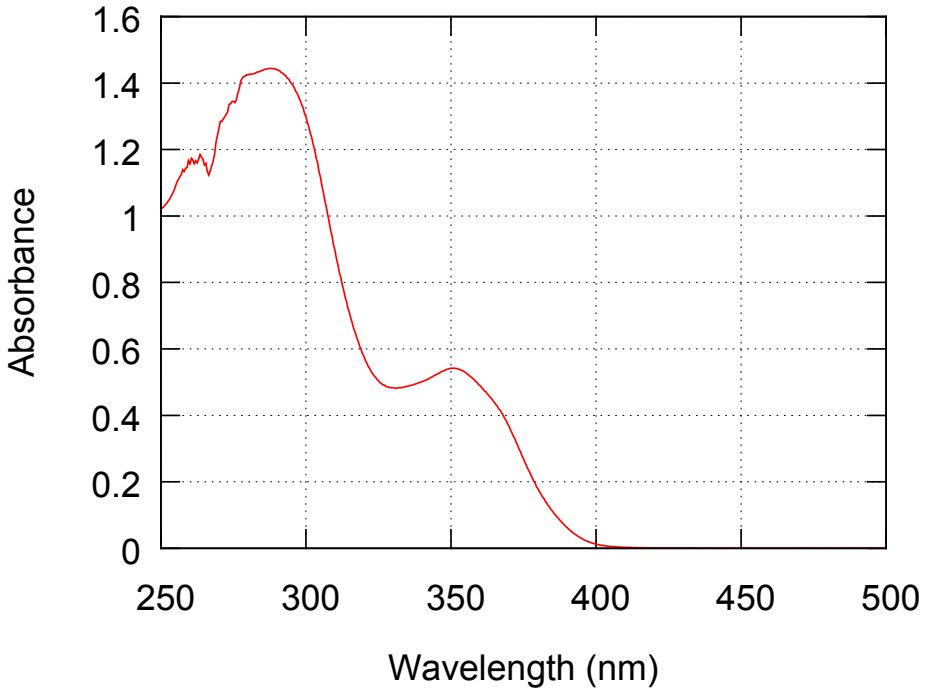

Figure S70. UV-vis absorption spectrum of **3a(40/60)** in *n*-decane (2.31×10^{-2} g/L, path length = 10 mm).

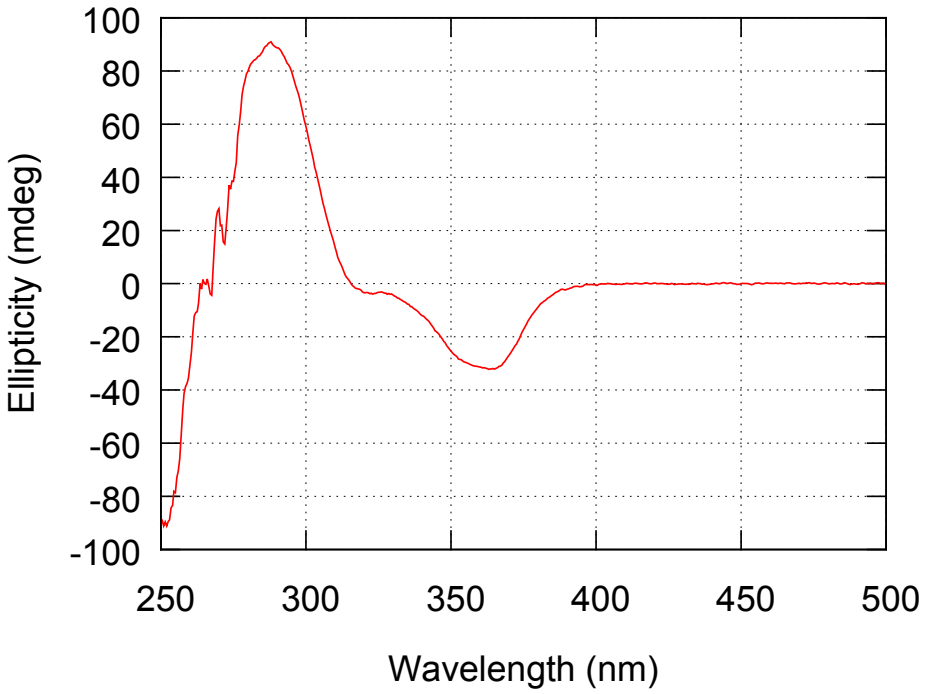

Figure S71. CD spectrum of **3a(40/60)** in *n*-decane (2.31×10^{-2} g/L, path length = 10 mm).

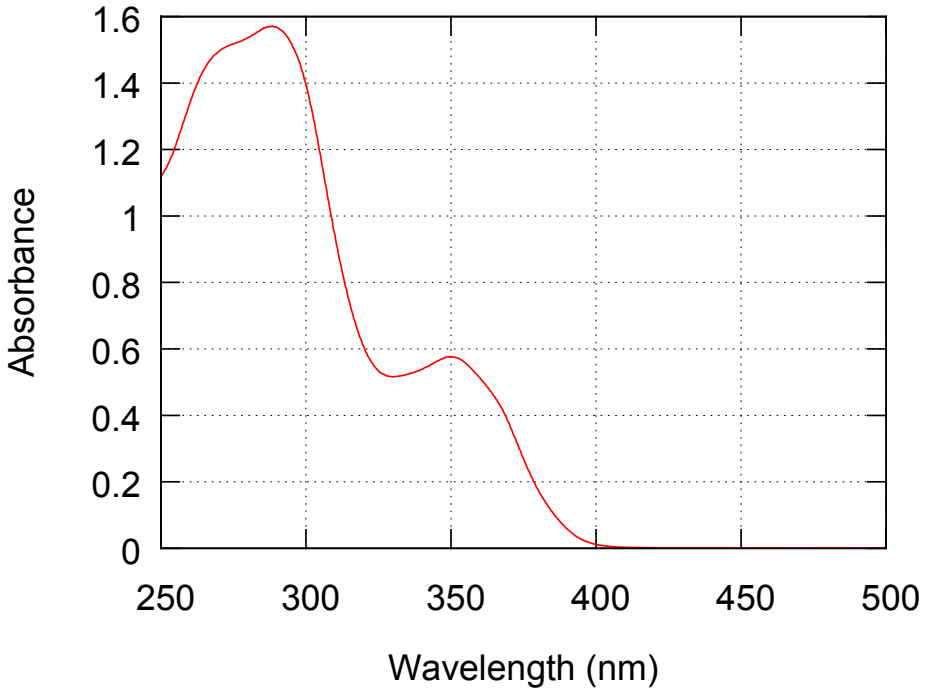

Figure S72. UV-vis absorption spectrum of **3b(40/60)** in *n*-pentane (2.89×10^{-2} g/L, path length = 10 mm).

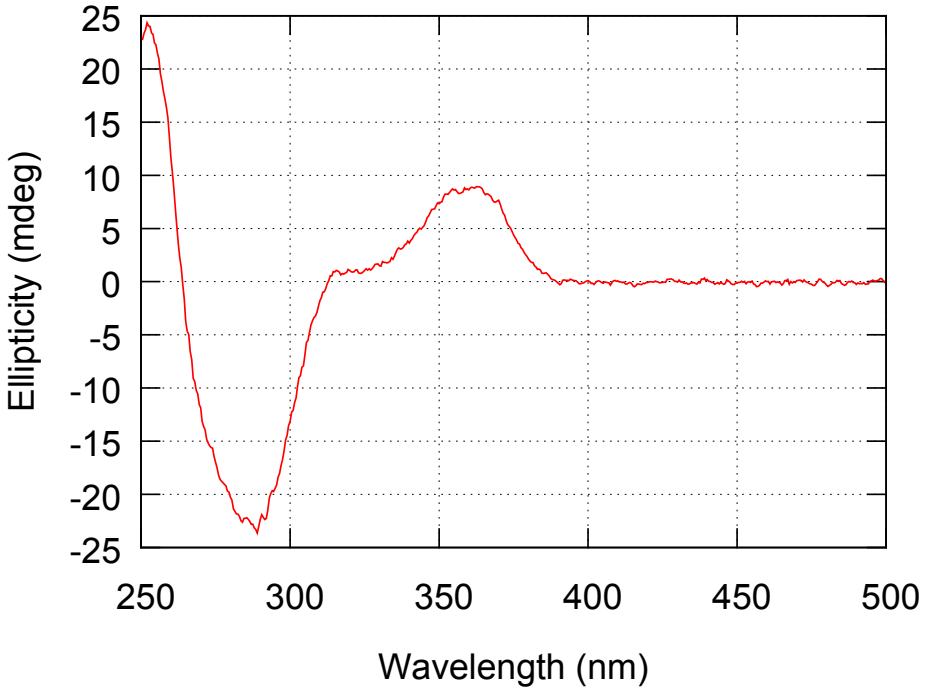

Figure S73. CD spectrum of **3b(40/60)** in *n*-pentane (2.89×10^{-2} g/L, path length = 10 mm).

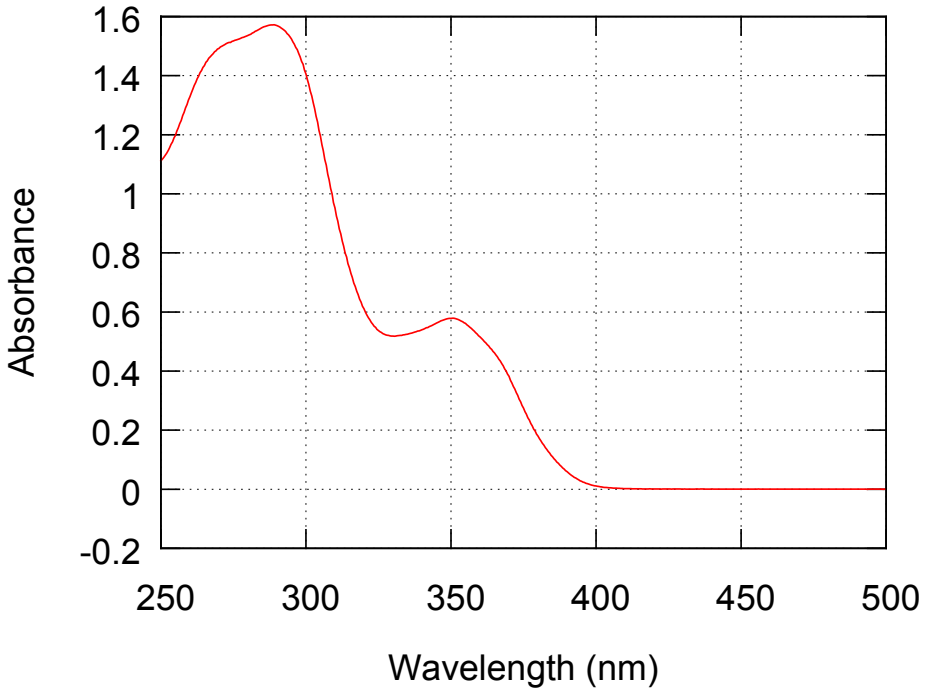

Figure S74. UV-vis absorption spectrum of **3b(40/60)** in *n*-hexane (2.89×10^{-2} g/L, path length = 10 mm).

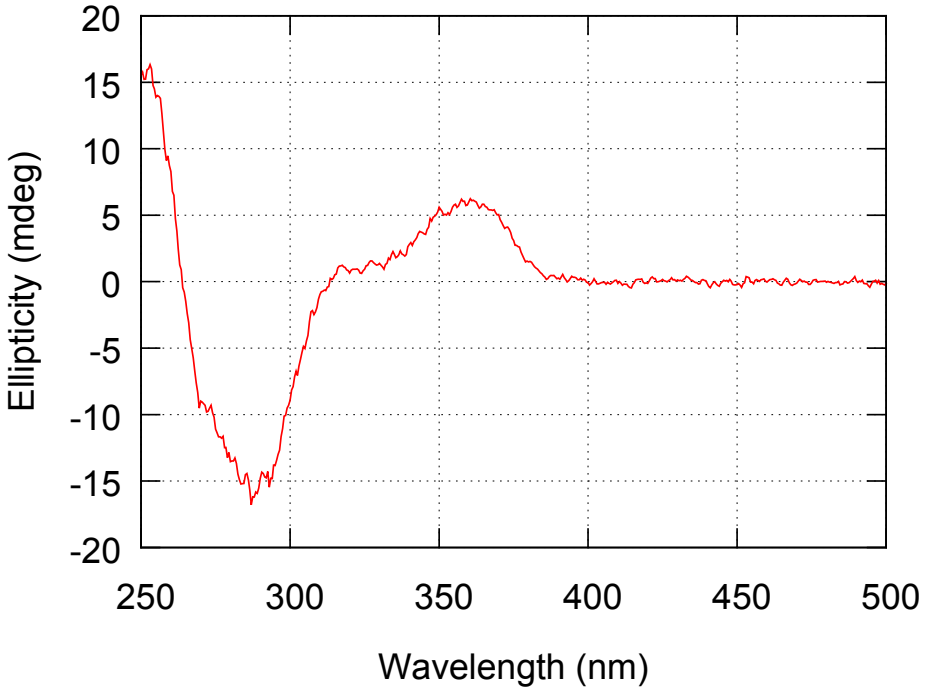

Figure S75. CD spectrum of **3b(40/60)** in *n*-hexane (2.89×10^{-2} g/L, path length = 10 mm).

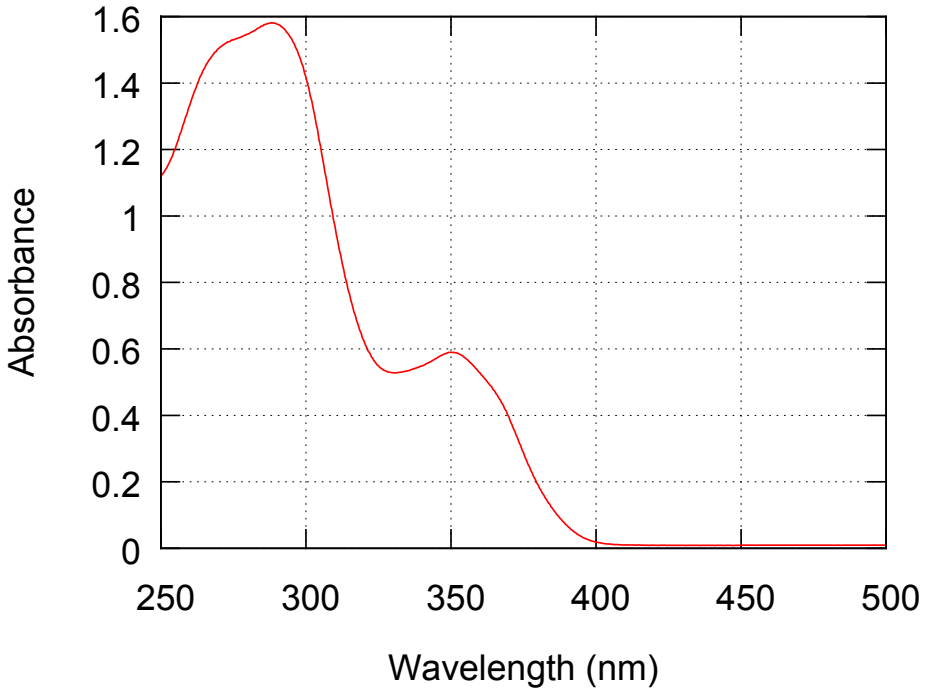

Figure S76. UV-vis absorption spectrum of **3b(40/60)** in *n*-heptane (2.89×10^{-2} g/L, path length = 10 mm).

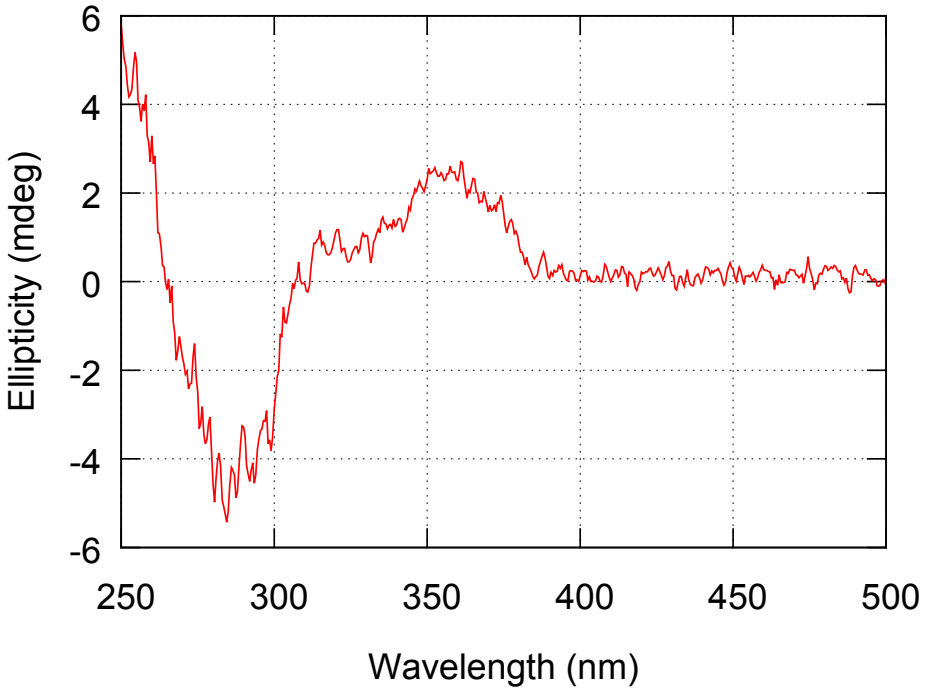

Figure S77. CD spectrum of **3b(40/60)** in *n*-heptane (2.89×10^{-2} g/L, path length = 10 mm).

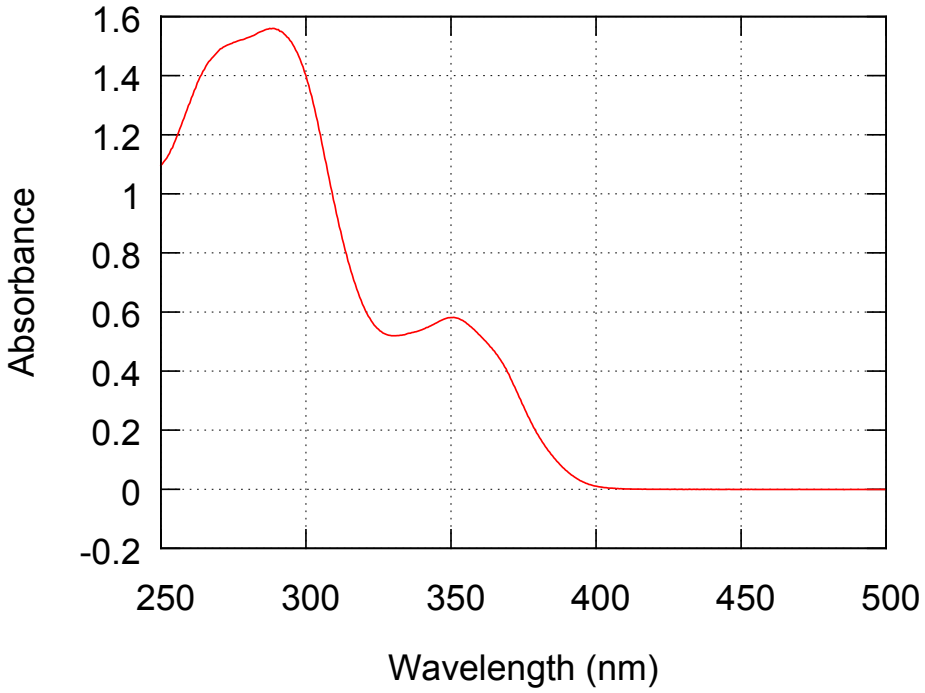

Figure S78. UV-vis absorption spectrum of **3b(40/60)** in *n*-octane (2.89×10^{-2} g/L, path length = 10 mm).

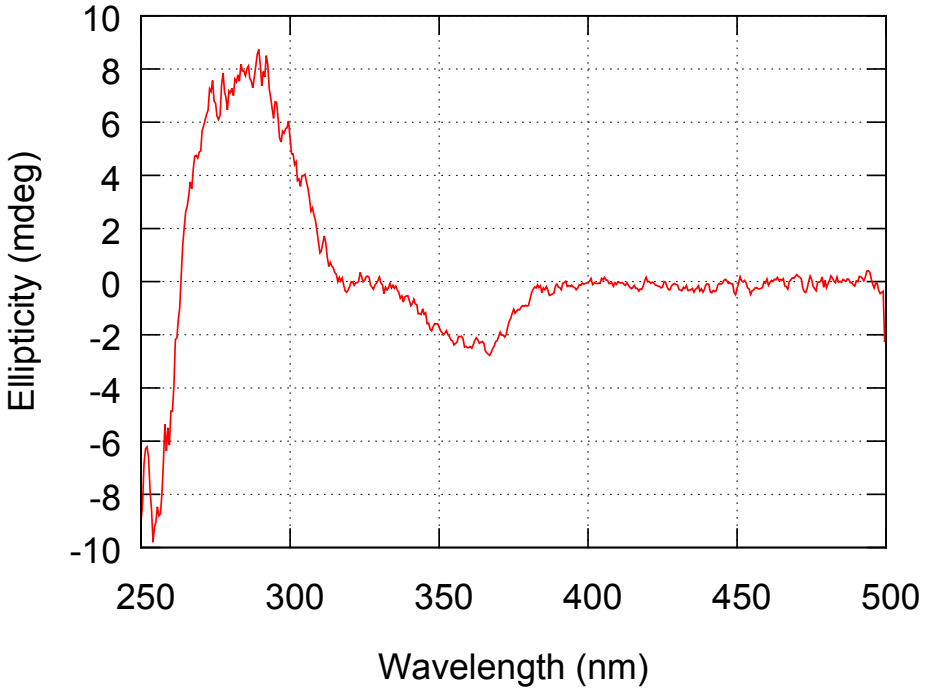

Figure S79. CD spectrum of **3b(40/60)** in *n*-octane (2.89×10^{-2} g/L, path length = 10 mm).

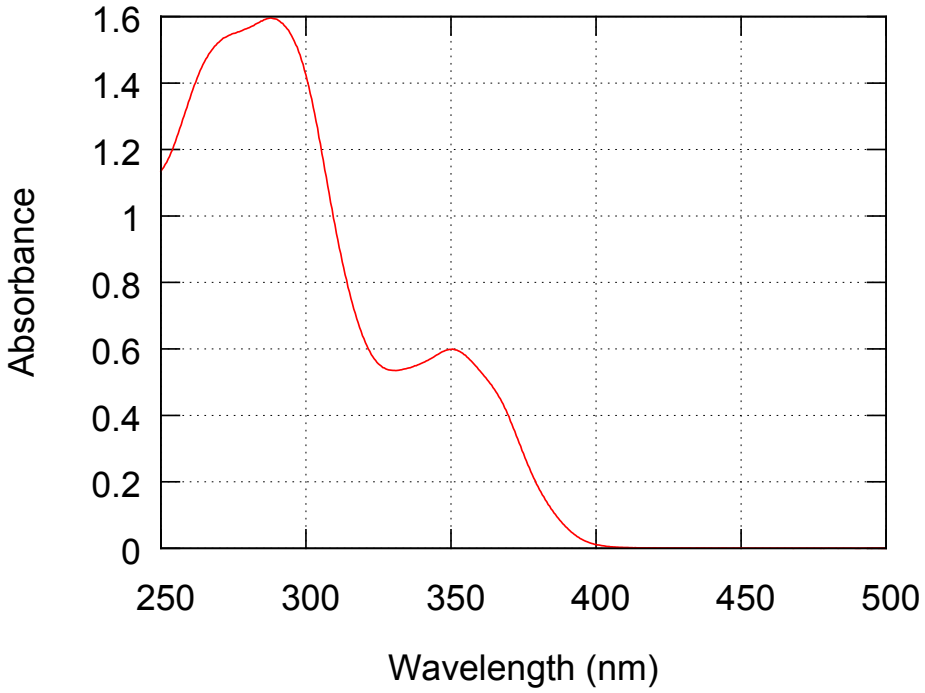

Figure S80. UV-vis absorption spectrum of **3b(40/60)** in *n*-nonane (2.89×10^{-2} g/L, path length = 10 mm).

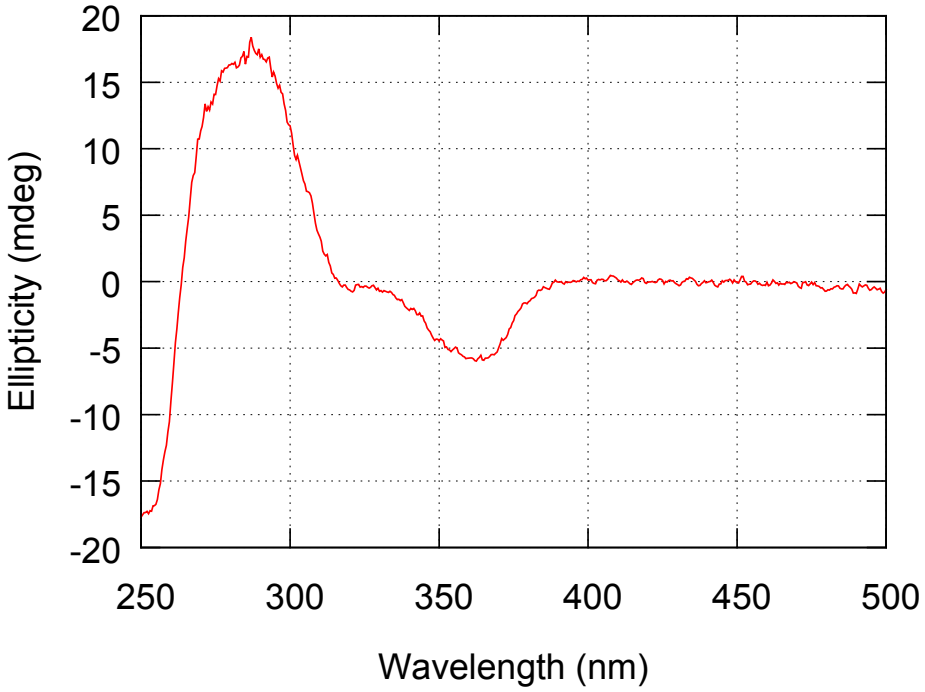

Figure S81. CD spectrum of **3b(40/60)** in *n*-nonane (2.89×10^{-2} g/L, path length = 10 mm).

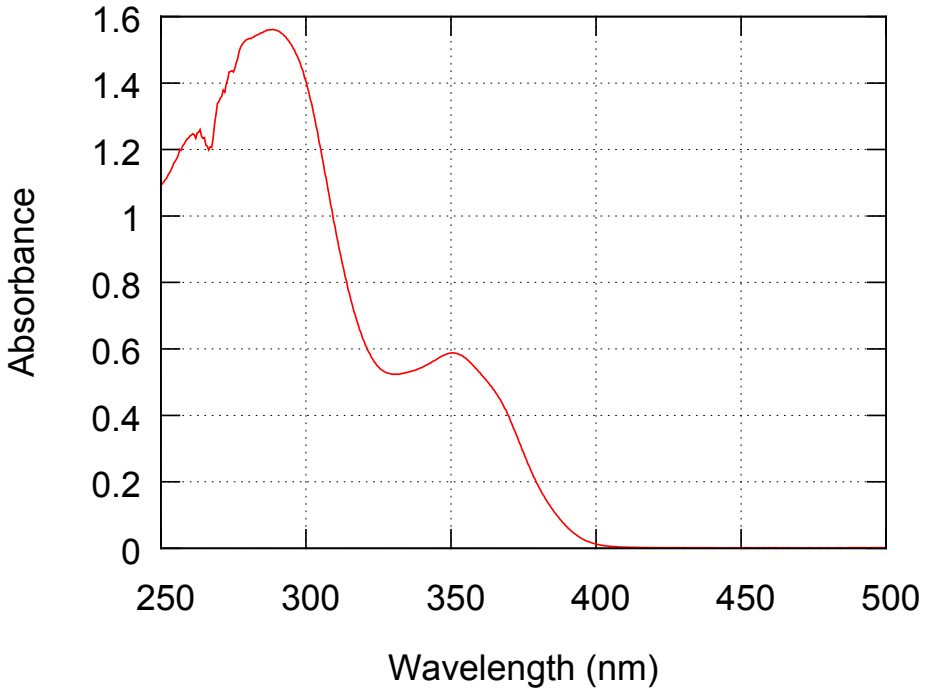

Figure S82. UV-vis absorption spectrum of **3b(40/60)** in *n*-decane (2.89×10^{-2} g/L, path length = 10 mm).

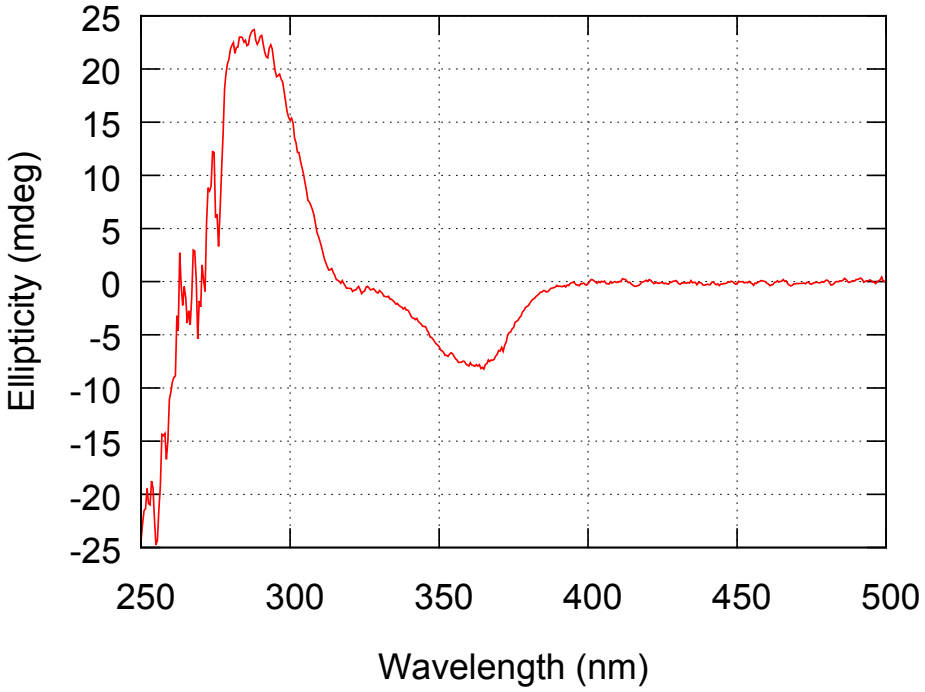

Figure S83. CD spectrum of **3b(40/60)** in *n*-decane (2.89×10^{-2} g/L, path length = 10 mm).

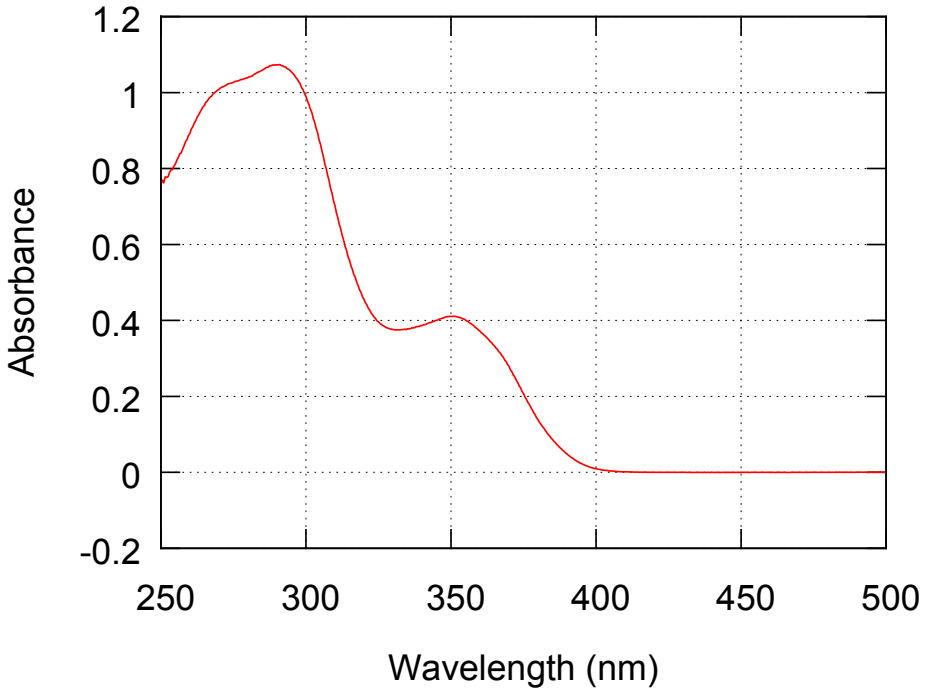

Figure S84. UV-vis absorption spectrum of **3b(40/60)** in *cis*-decaline (2.78×10^{-2} g/L, path length = 10 mm).

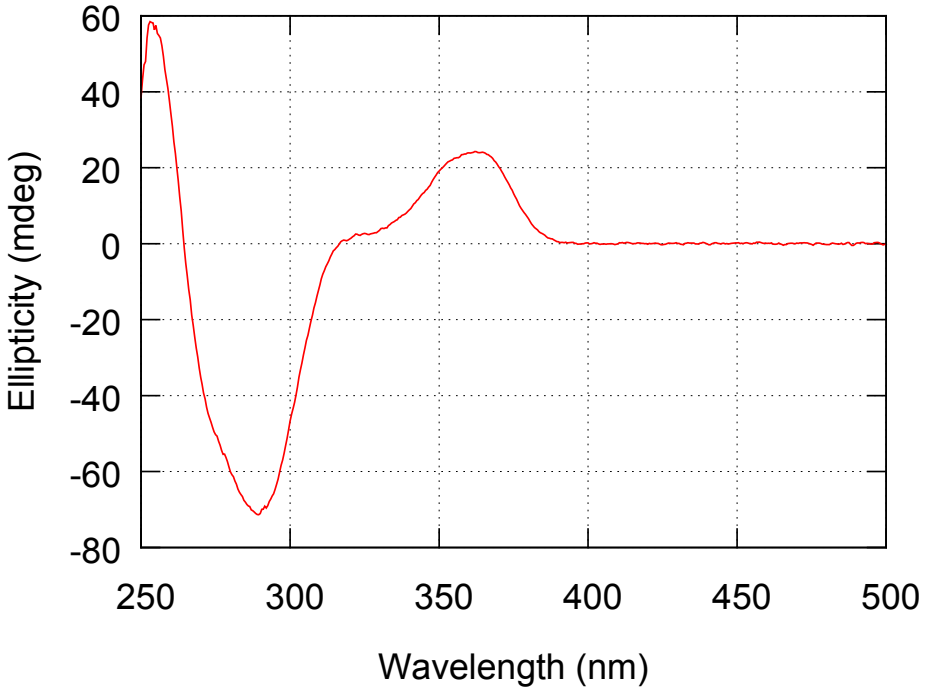

Figure S85. CD spectrum of **3b(40/60)** in *cis*-decaline (2.78×10^{-2} g/L, path length = 10 mm).

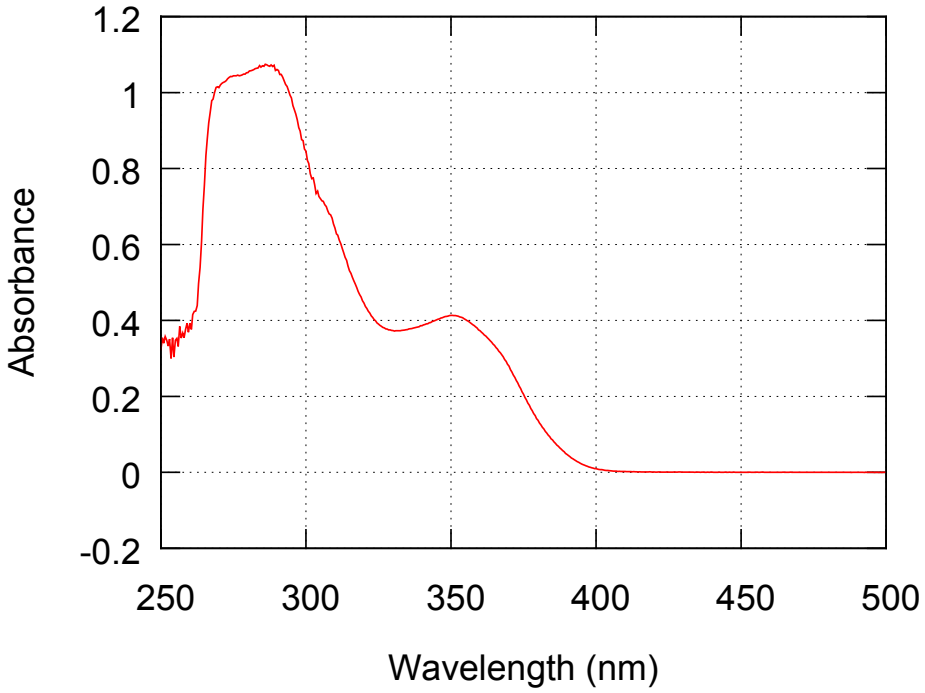

Figure S86. UV-vis absorption spectrum of **3b(40/60)** in *trans*-decaline (2.78×10^{-2} g/L, path length = 10 mm).

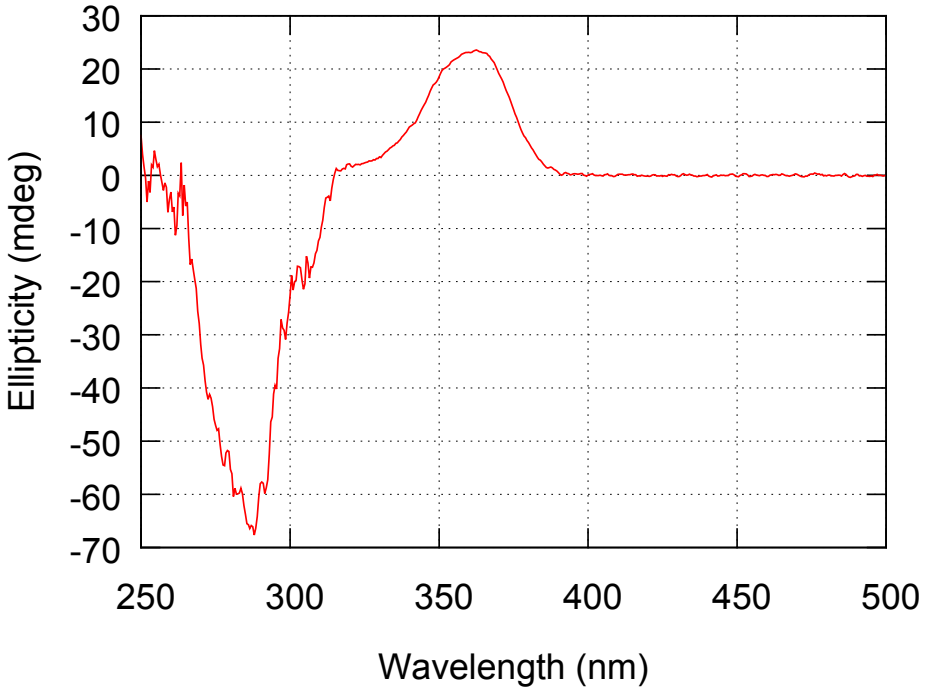

Figure S87. CD spectrum of **3b(40/60)** in *trans*-decaline (2.78×10^{-2} g/L, path length = 10 mm).

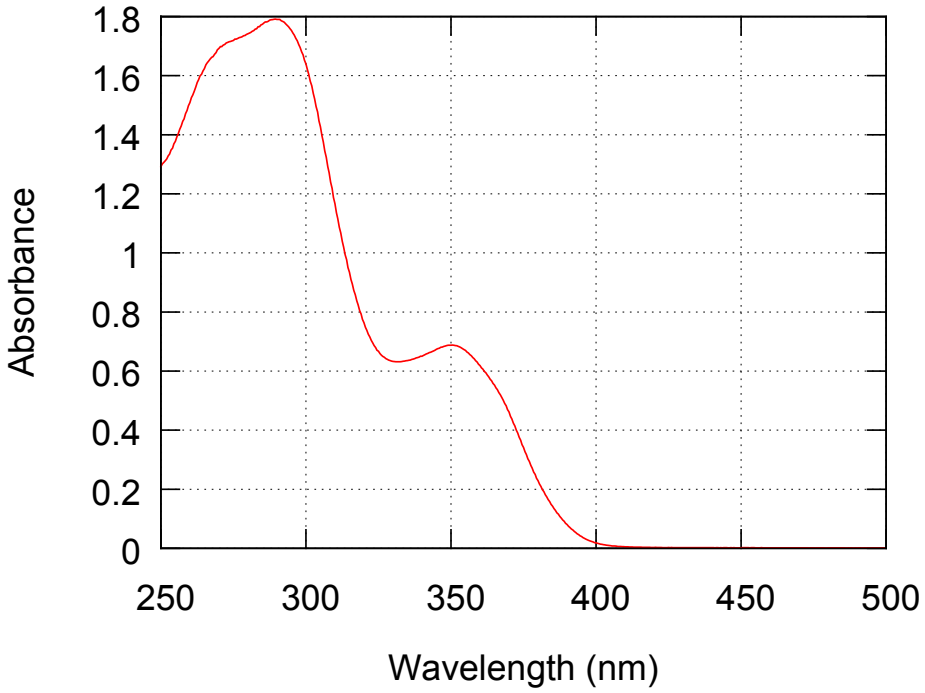

Figure S88. UV-vis absorption spectrum of **3b(40/60)** in cyclooctane (3.00×10^{-2} g/L, path length = 10 mm).

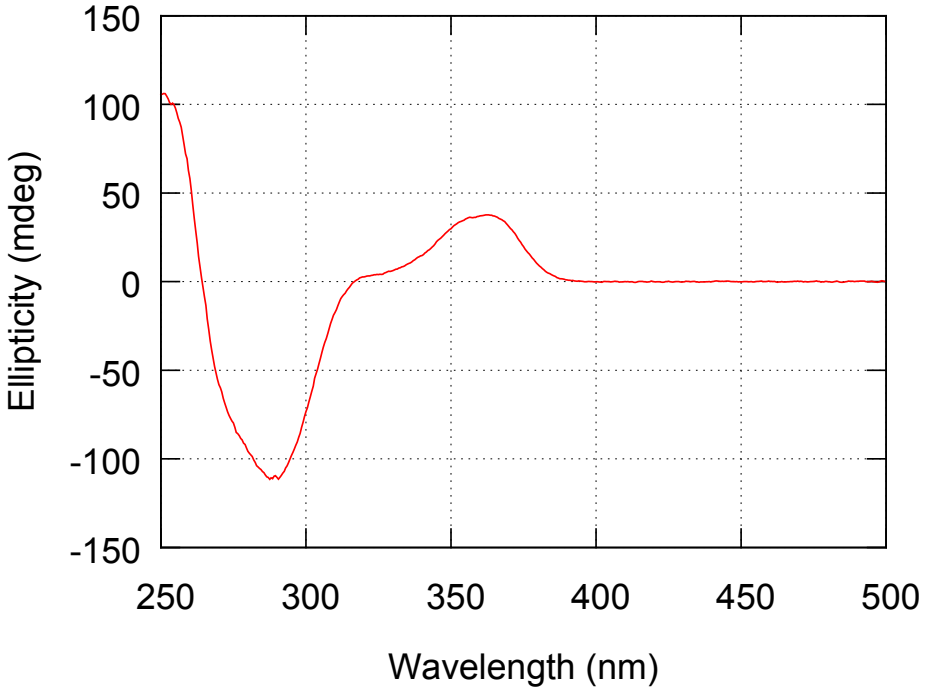

Figure S89. CD spectrum of **3b(40/60)** in cyclooctane (3.00×10^{-2} g/L, path length = 10 mm).

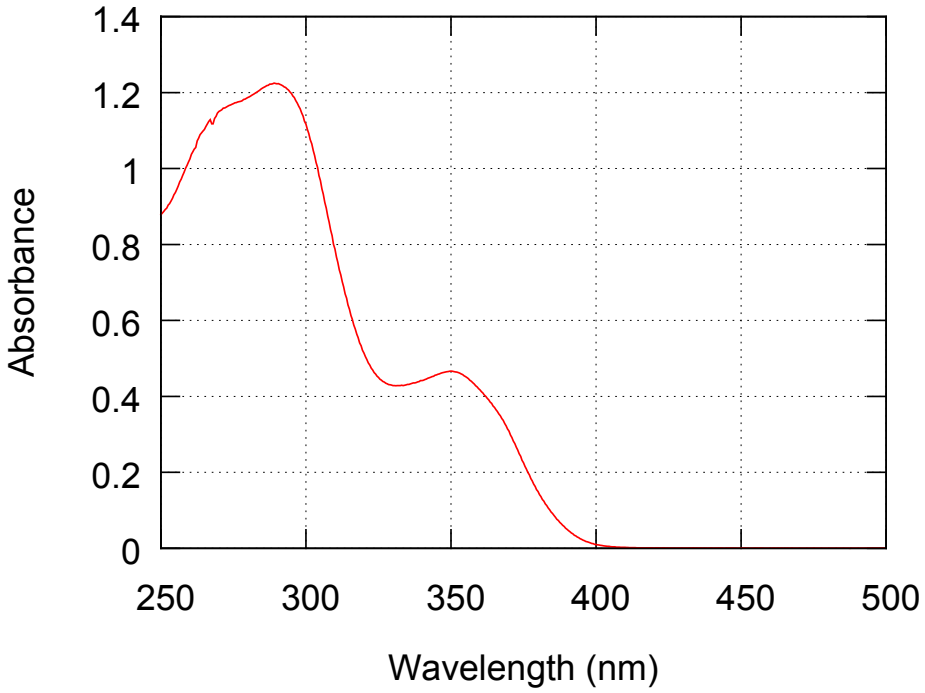

Figure S90. UV-vis absorption spectrum of **3b(40/60)** in cycloheptane (1.75×10^{-2} g/L, path length = 10 mm).

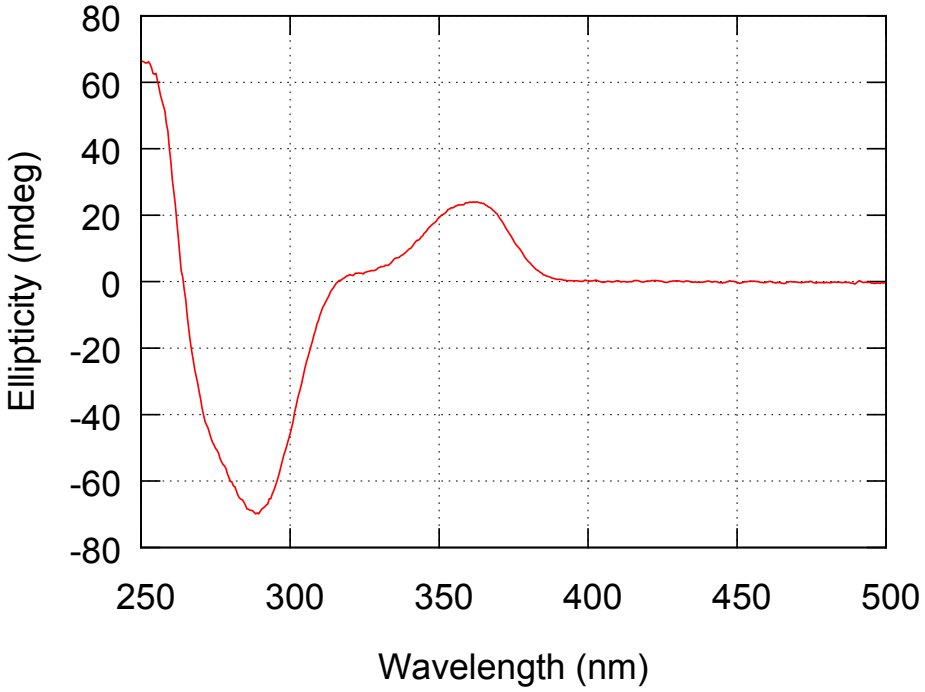

Figure S91. CD spectrum of **3b(40/60)** in cycloheptane (1.75×10^{-2} g/L, path length = 10 mm).

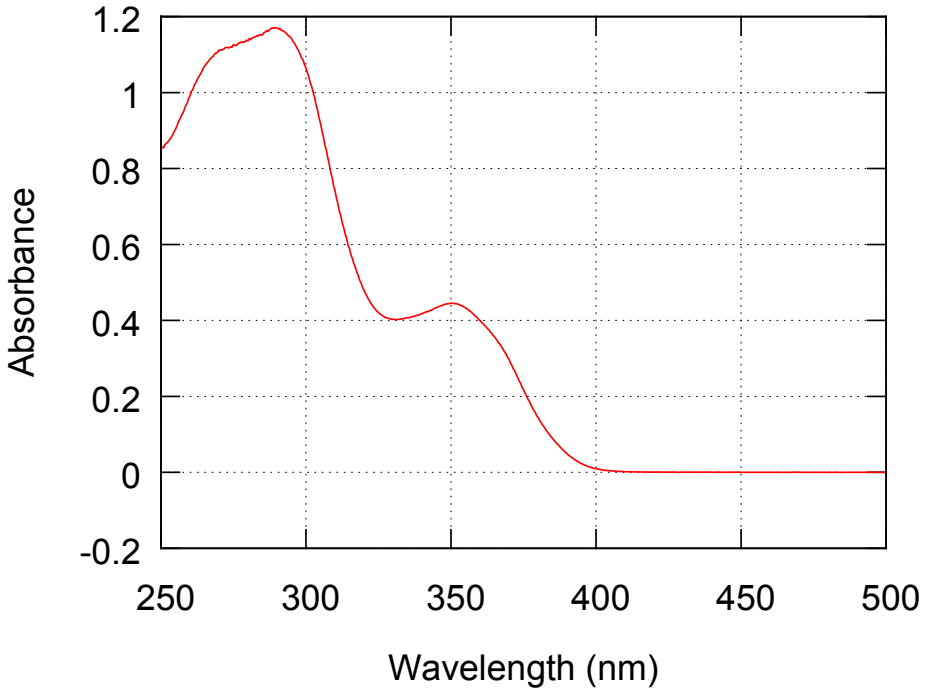

Figure S92. UV-vis absorption spectrum of **3b(40/60)** in isopropylcyclohexane (1.75×10^{-2} g/L, path length = 10 mm).

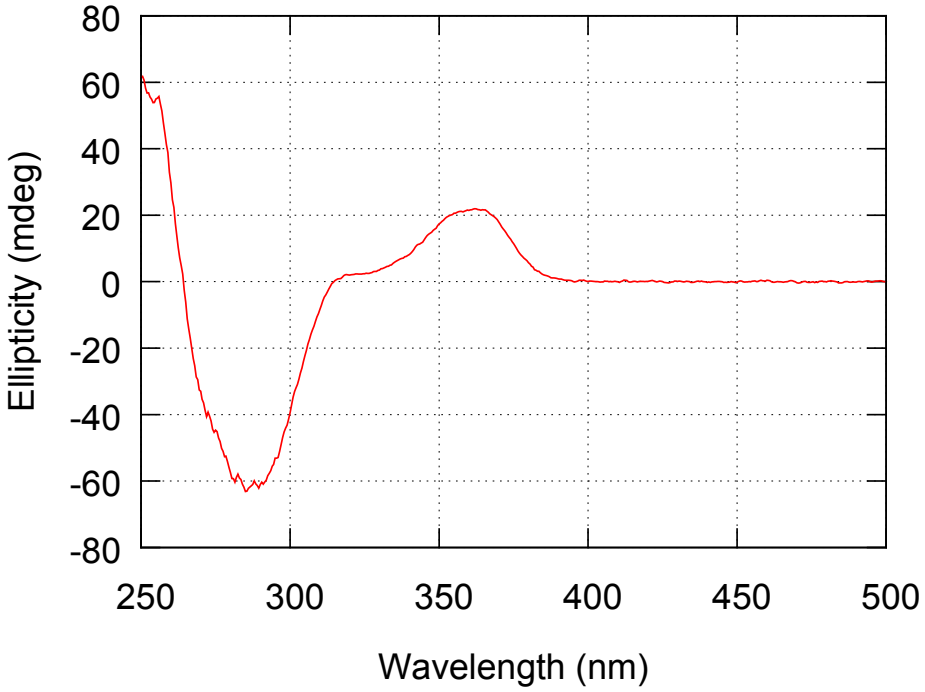

Figure S93. CD spectrum of **3b(40/60)** in isopropylcyclohexane (1.75×10^{-2} g/L, path length = 10 mm).

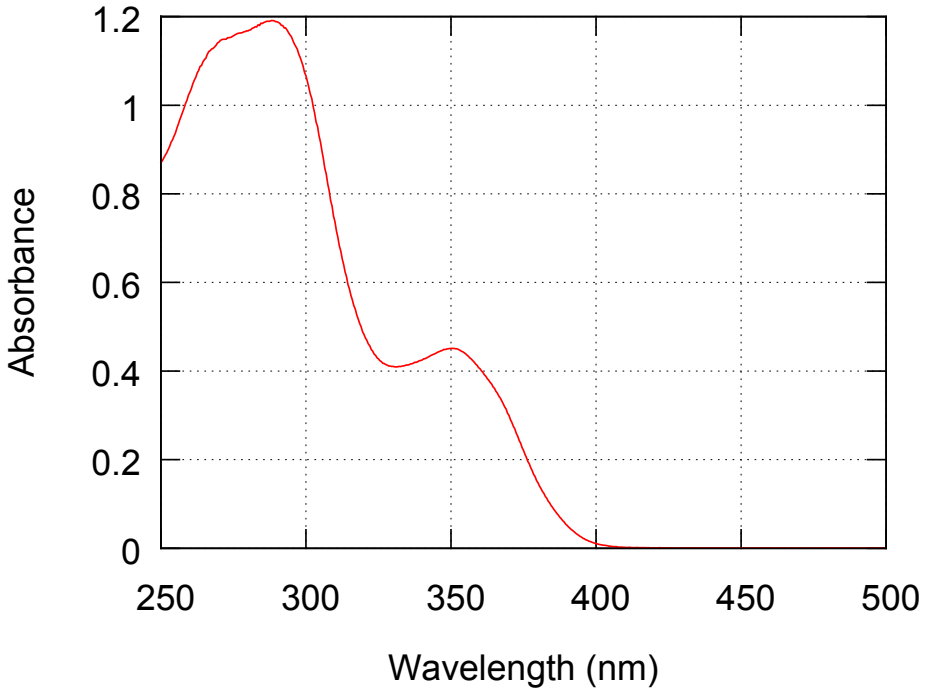

Figure S94. UV-vis absorption spectrum of **3b(40/60)** in 2,3,4-trimethylpentane (1.75×10^{-2} g/L, path length = 10 mm).

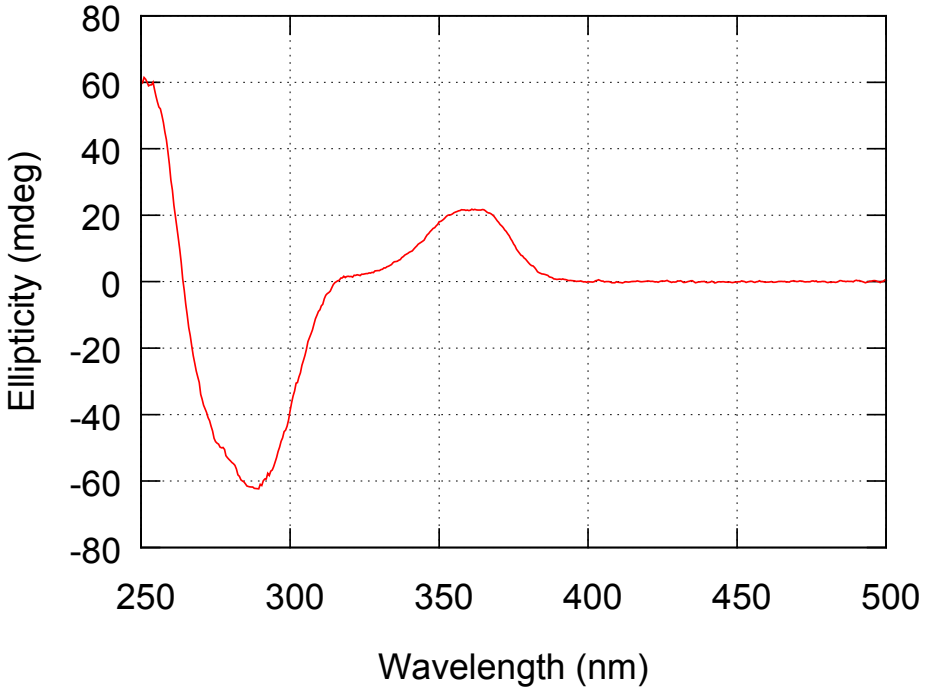

Figure S95. CD spectrum of **3b(40/60)** in 2,3,4-trimethylpentane (1.75×10^{-2} g/L, path length = 10 mm).

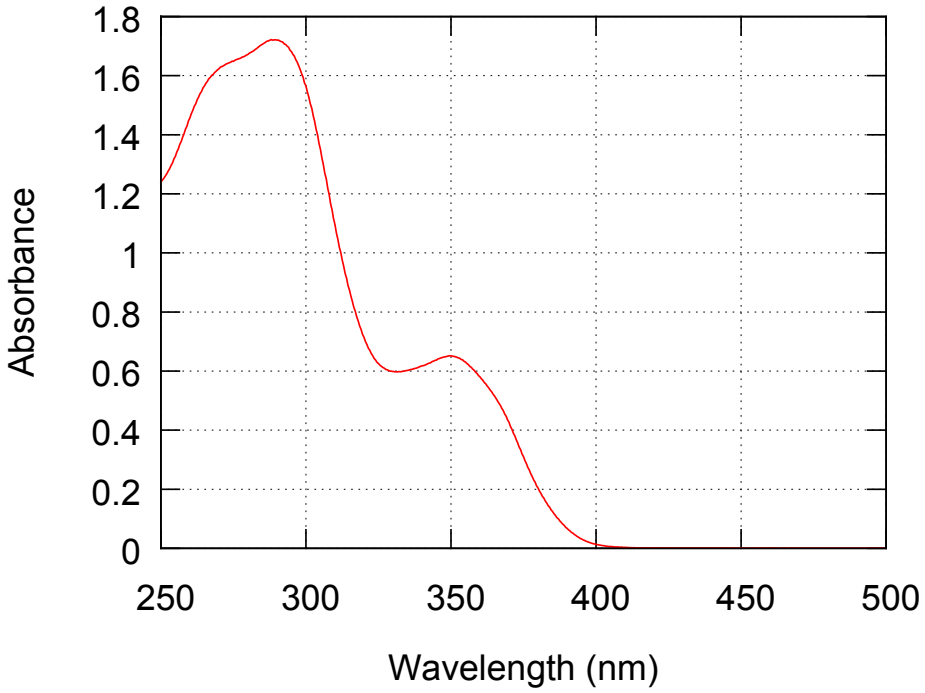

Figure S96. UV-vis absorption spectrum of **3b(40/60)** in cyclohexane (3.00×10^{-2} g/L, path length = 10 mm).

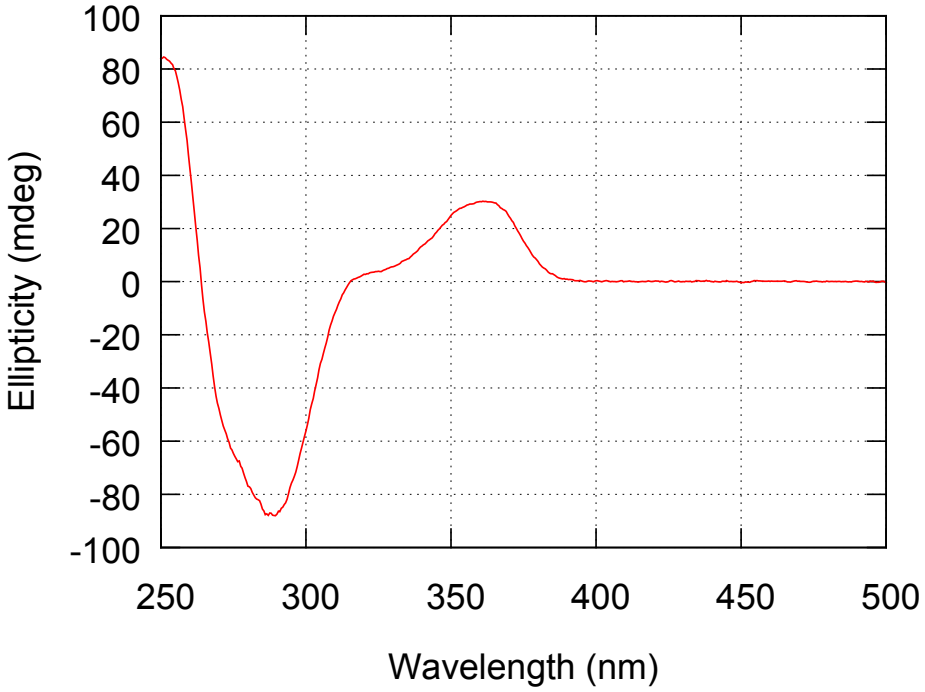

Figure S97. CD spectrum of **3b(40/60)** in cyclohexane (3.00×10^{-2} g/L, path length = 10 mm).

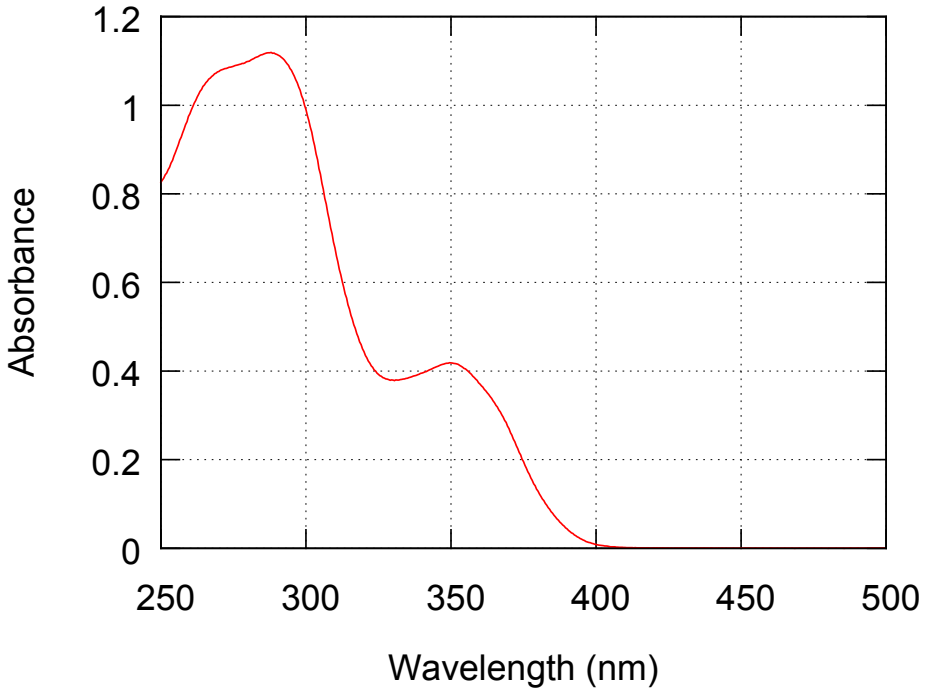

Figure S98. UV-vis absorption spectrum of **3b(40/60)** in 2,3-dimethylbutane (1.75×10^{-2} g/L, path length = 10 mm).

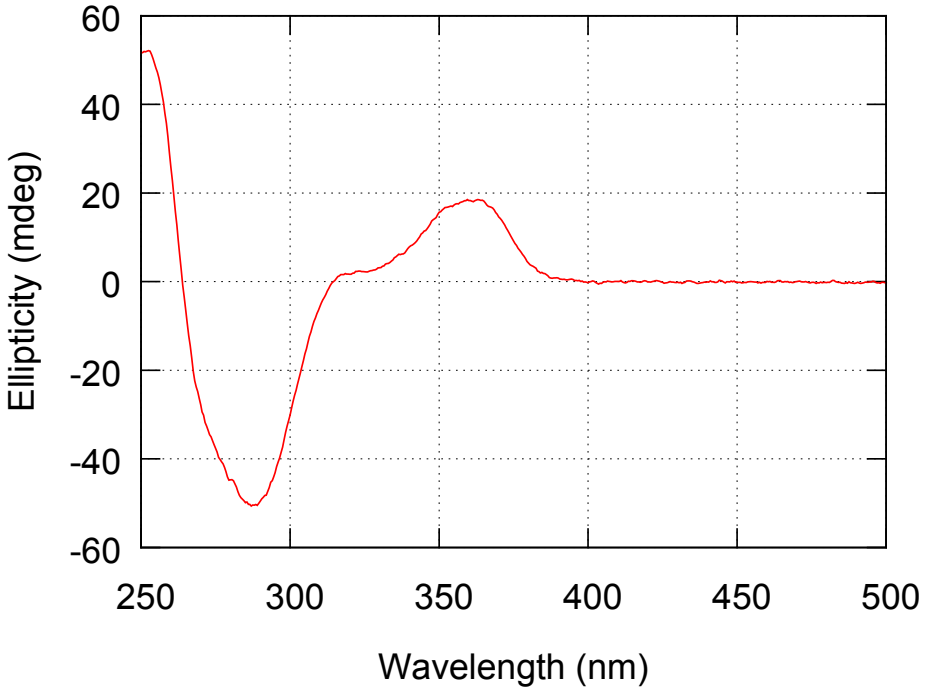

Figure S99. CD spectrum of **3b(40/60)** in 2,3-dimethylbutane (1.75×10^{-2} g/L, path length = 10 mm).

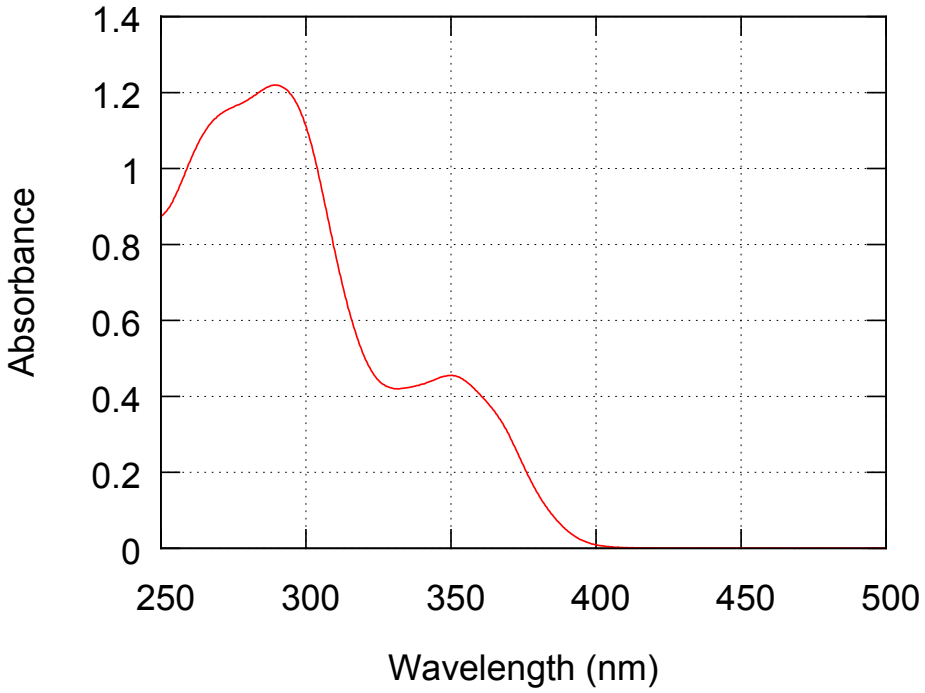

Figure S100. UV-vis absorption spectrum of **3b(40/60)** in cyclopentane (1.75×10^{-2} g/L, path length = 10 mm).

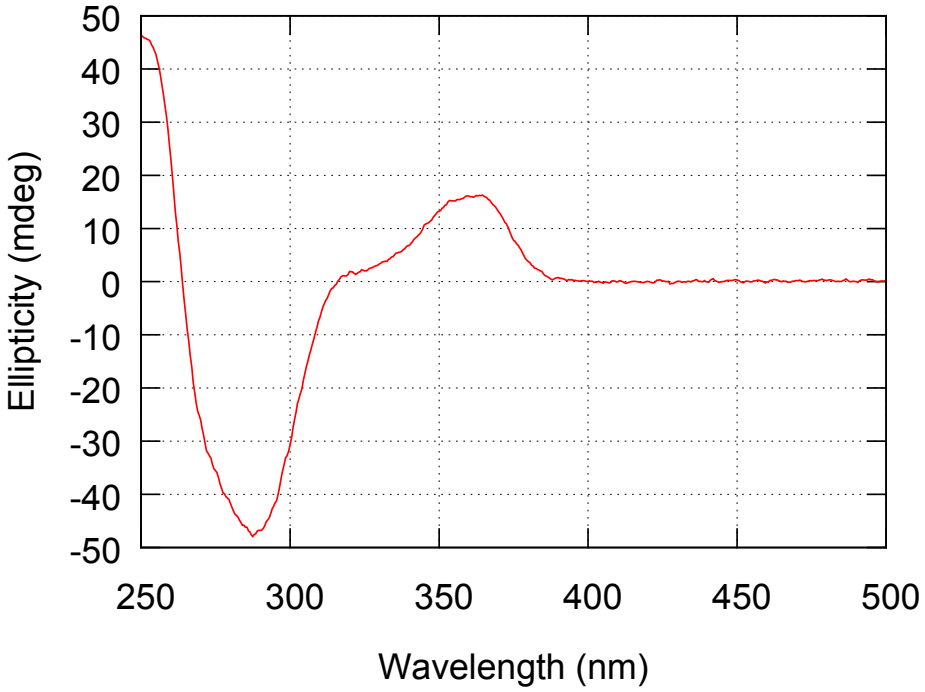

Figure S101. CD spectrum of **3b(40/60)** in cyclopentane (1.75×10^{-2} g/L, path length = 10 mm).

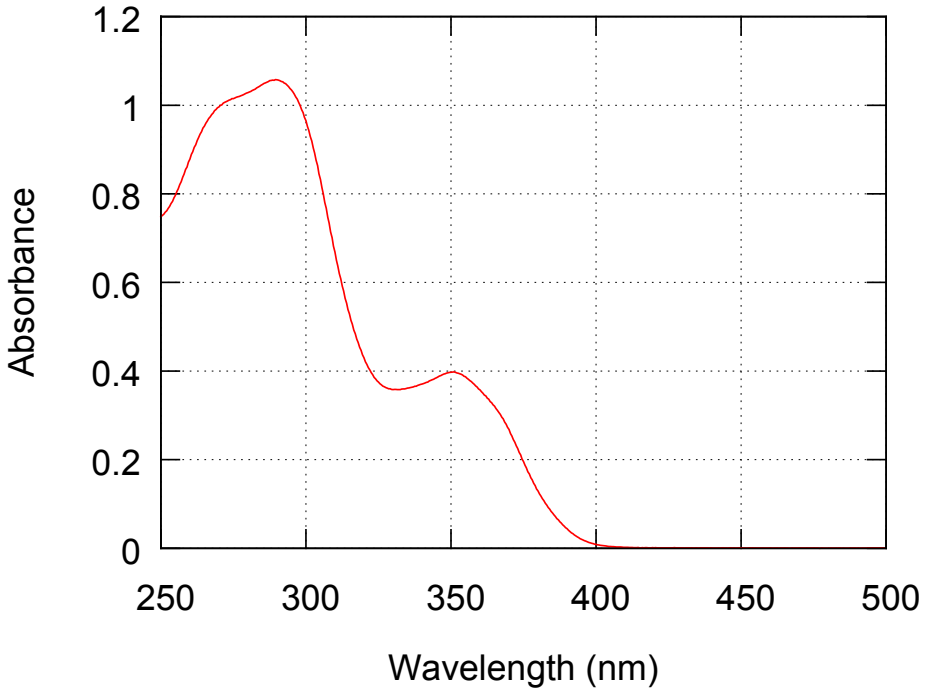

Figure S102. UV-vis absorption spectrum of **3b(40/60)** in propylcyclohexane (2.78×10^{-2} g/L, path length = 10 mm).

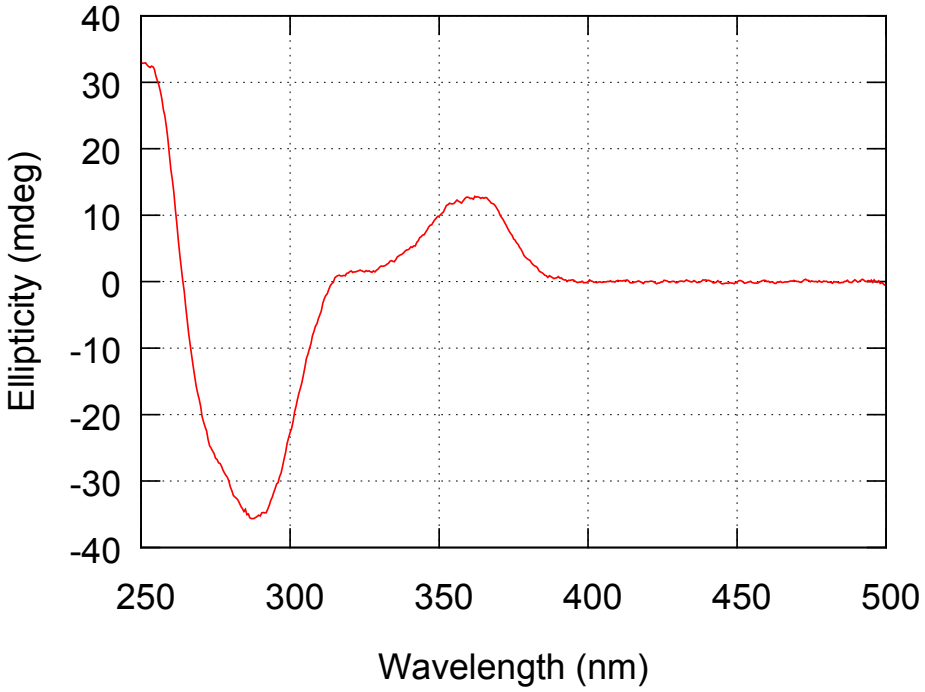

Figure S103. CD spectrum of **3b(40/60)** in propylcyclohexane (2.78×10^{-2} g/L, path length = 10 mm).

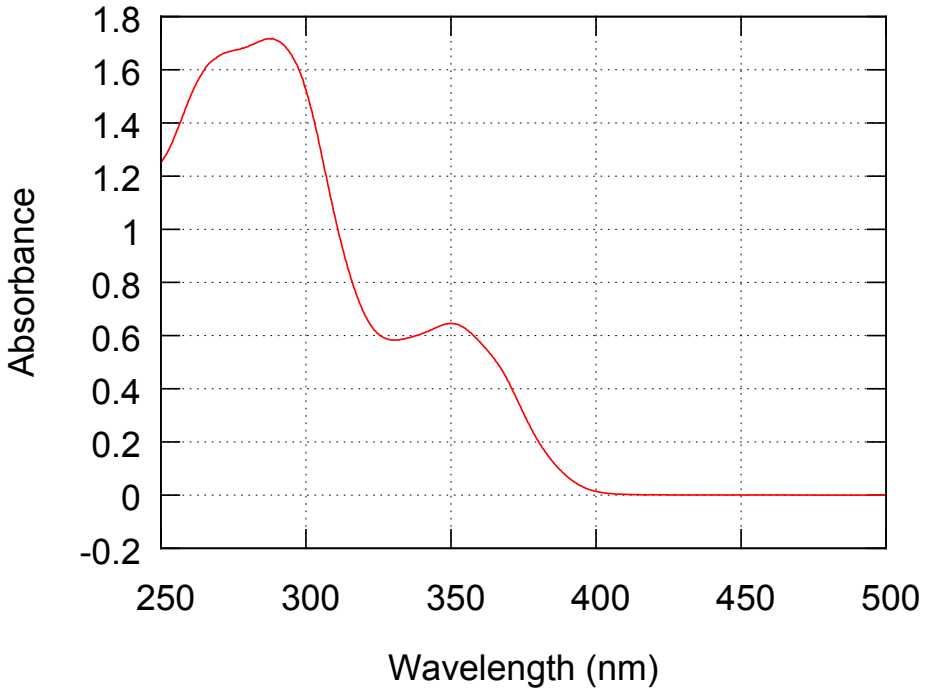

Figure S104. UV-vis absorption spectrum of **3b(40/60)** in 2,2,4-trimethylpentane (3.00×10^{-2} g/L, path length = 10 mm).

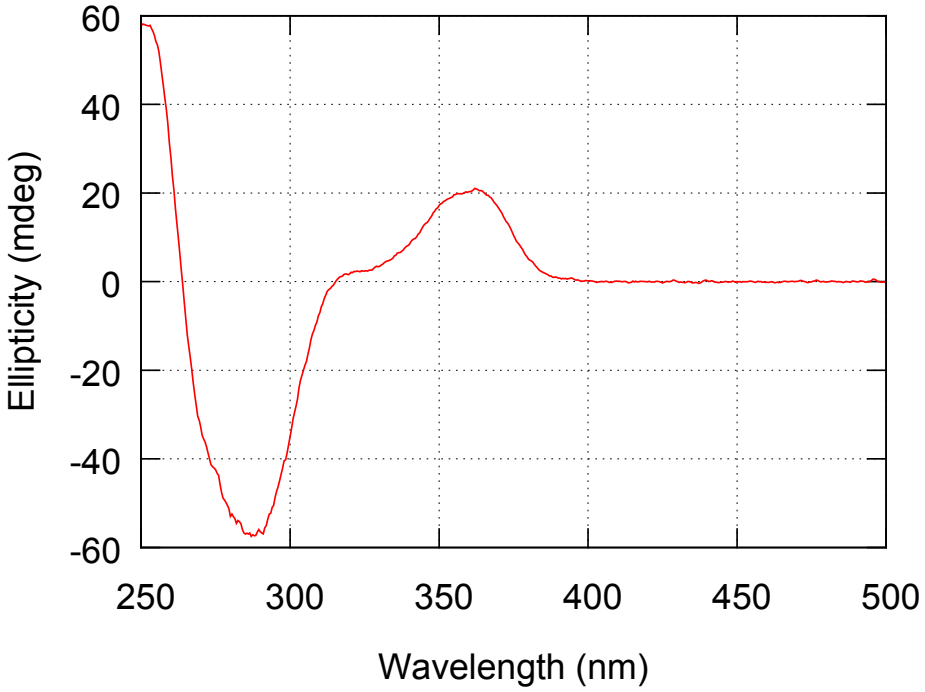

Figure S105. CD spectrum of **3b(40/60)** in 2,2,4-trimethylpentane (3.00×10^{-2} g/L, path length = 10 mm).

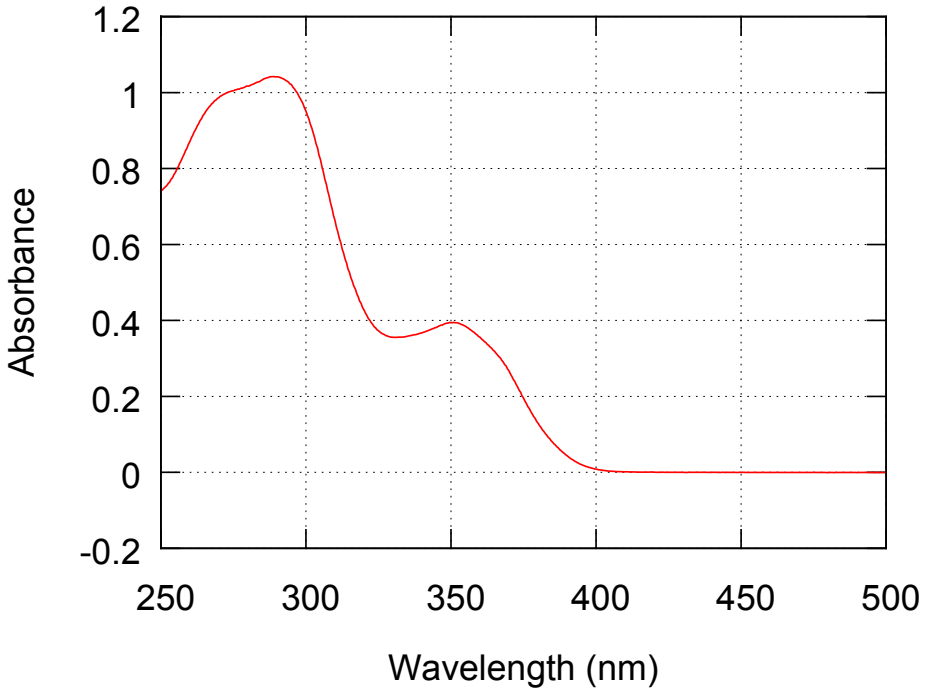

Figure S106. UV-vis absorption spectrum of **3b(40/60)** in butylcyclohexane (2.78×10^{-2} g/L, path length = 10 mm).

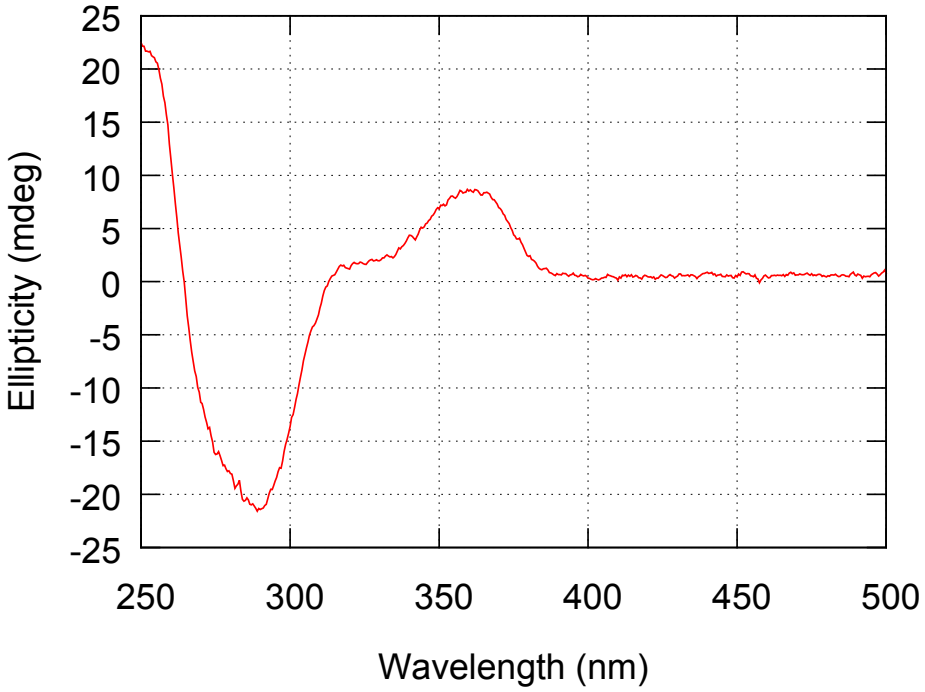

Figure S107. CD spectrum of **3b(40/60)** in butylcyclohexane (2.78×10^{-2} g/L, path length = 10 mm).

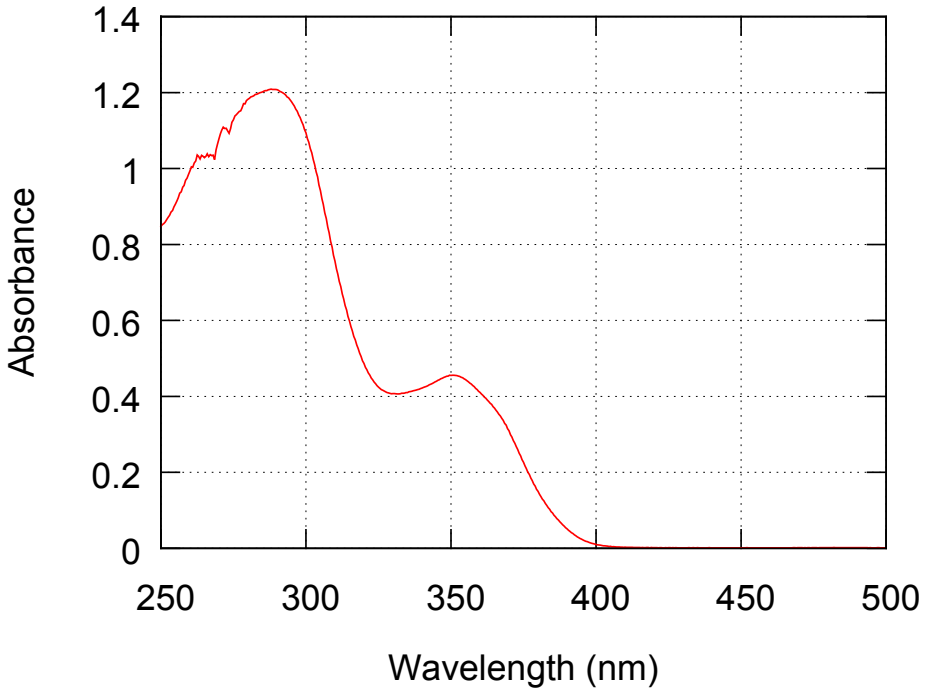

Figure S108. UV-vis absorption spectrum of **3b(40/60)** in *n*-undecane (1.75×10^{-2} g/L, path length = 10 mm).

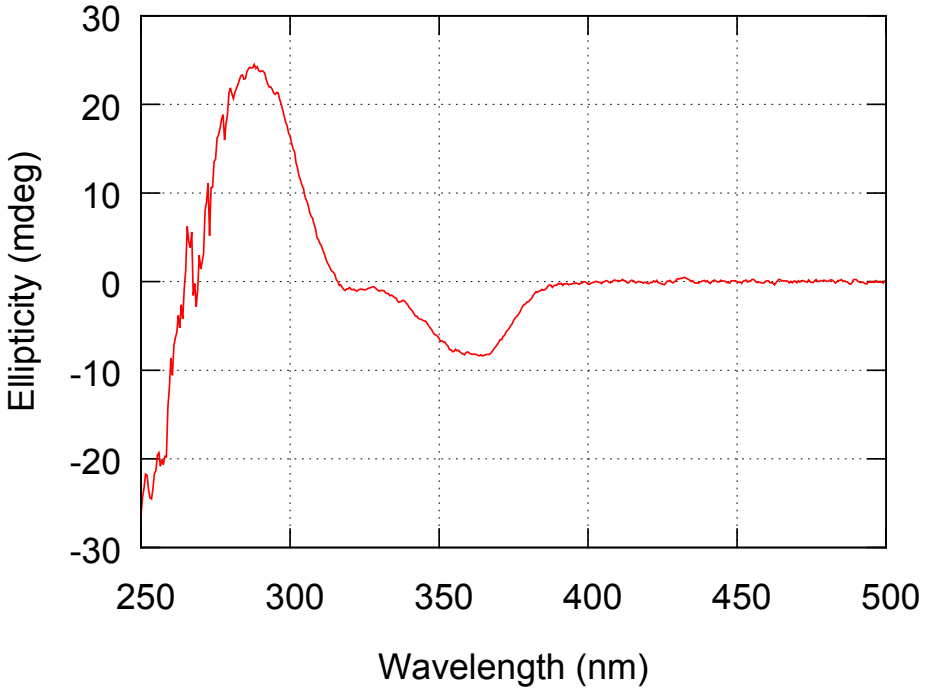

Figure S109. CD spectrum of **3b(40/60)** in *n*-undecane (1.75×10^{-2} g/L, path length = 10 mm).

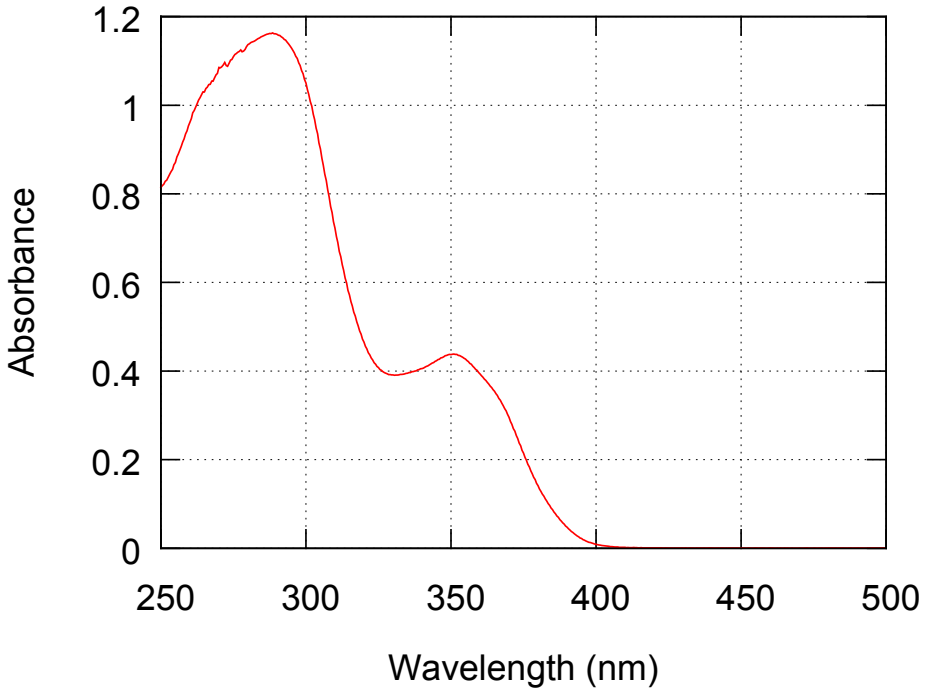

Figure S110. UV-vis absorption spectrum of **3b(40/60)** in *n*-dodecane (1.75×10^{-2} g/L, path length = 10 mm).

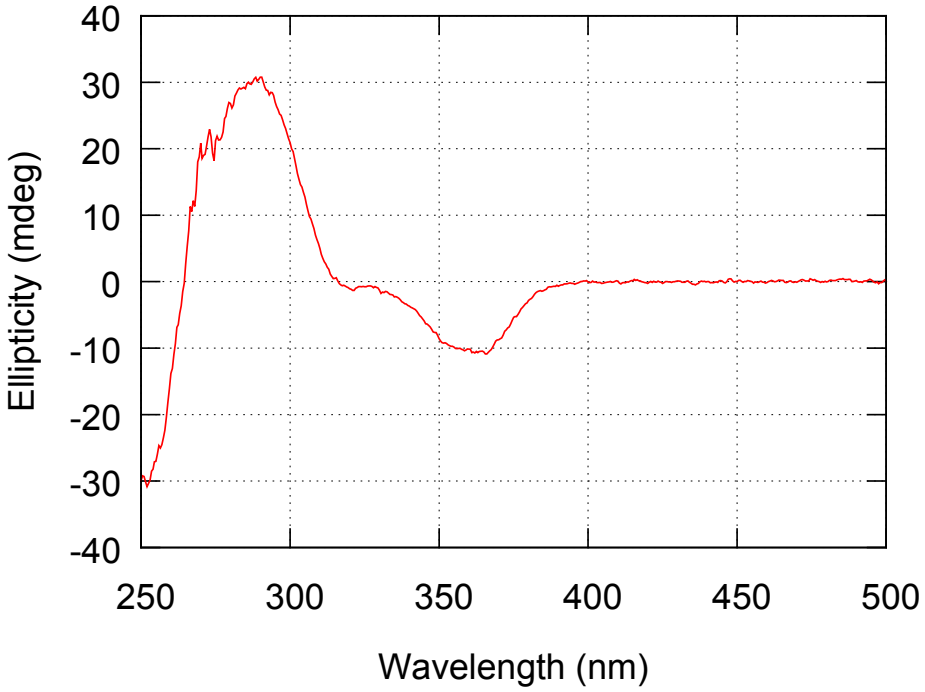

Figure S111. CD spectrum of **3b(40/60)** in *n*-dodecane (1.75×10^{-2} g/L, path length = 10 mm).

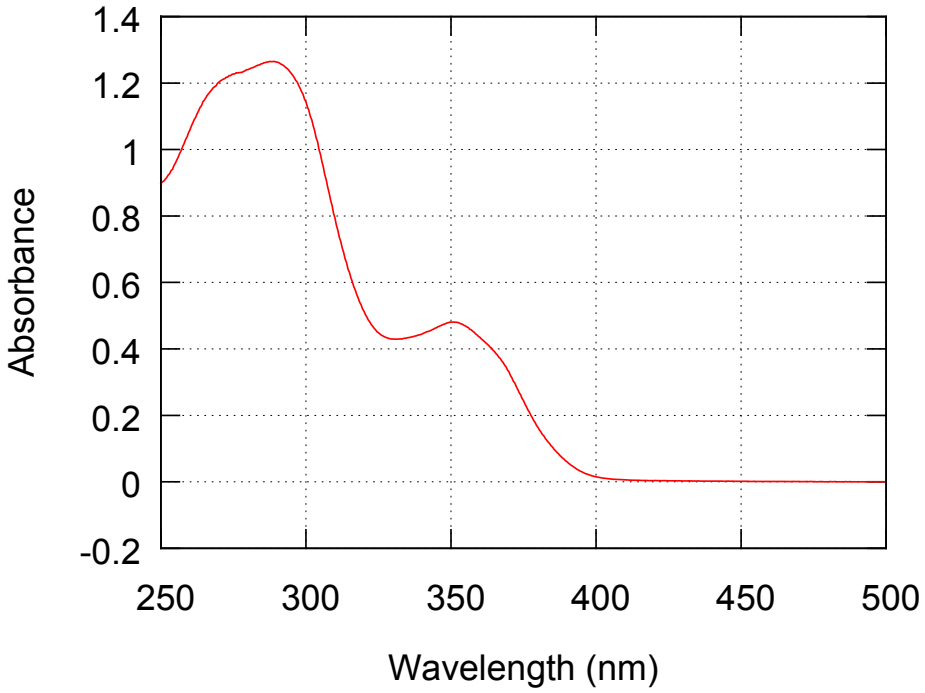

Figure S112. UV-vis absorption spectrum of **3b(40/60)** in *n*-tridecane (1.75×10^{-2} g/L, path length = 10 mm).

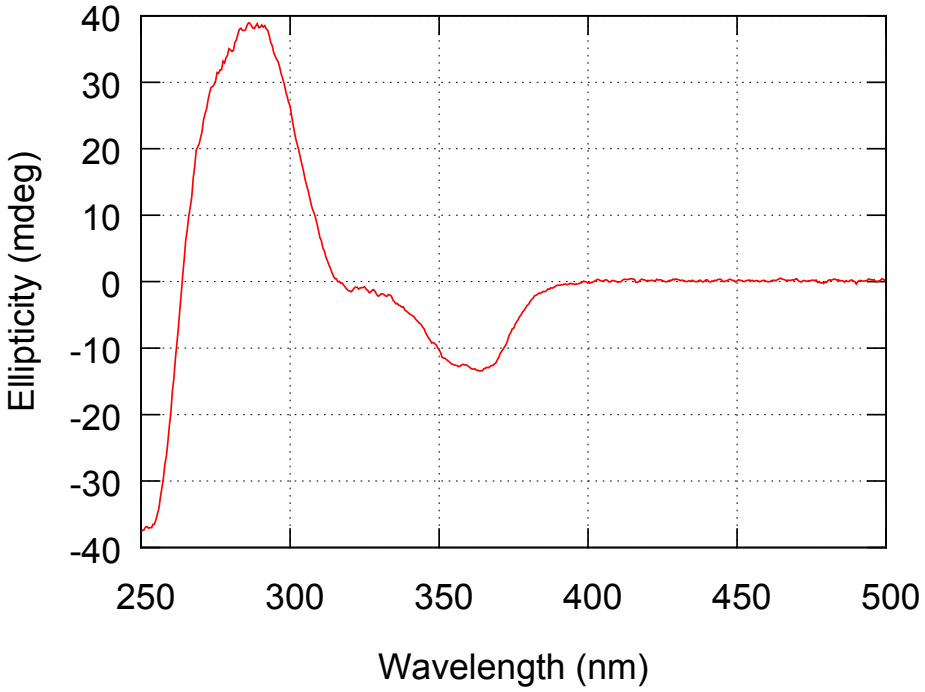

Figure S113. CD spectrum of **3b(40/60)** in *n*-tridecane (1.75×10^{-2} g/L, path length = 10 mm).

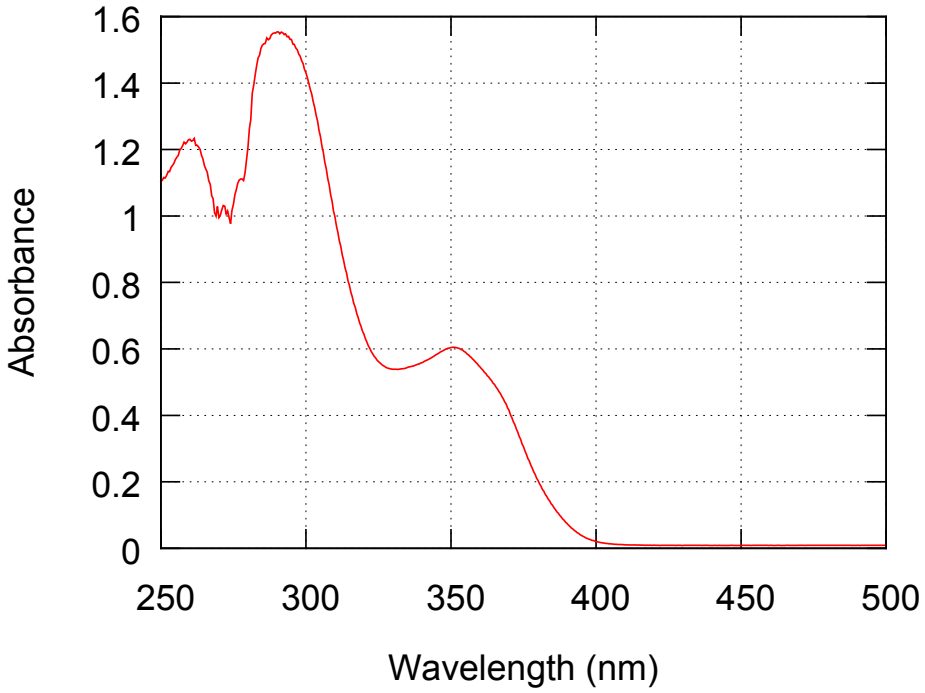

Figure S114. UV-vis absorption spectrum of **3b(40/60)** in *n*-tetradecane (2.98×10^{-2} g/L, path length = 10 mm).

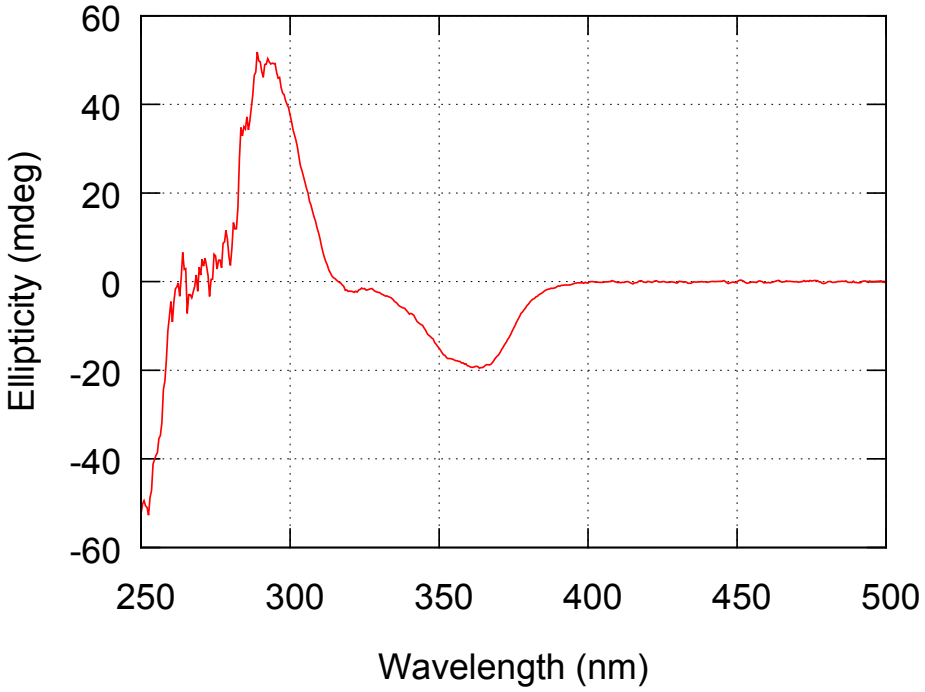

Figure S115. CD spectrum of **3b(40/60)** in *n*-tetradecane (2.98×10^{-2} g/L, path length = 10 mm).

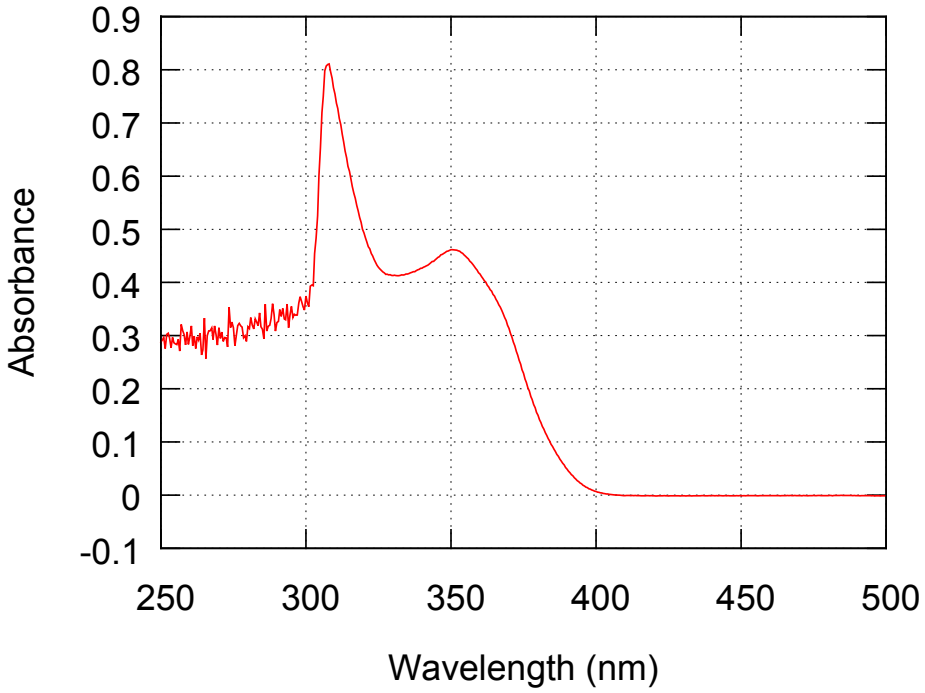

Figure S116. UV-vis absorption spectrum of **3b(40/60)** in *n*-pentadecane (1.75×10^{-2} g/L, path length = 10 mm).

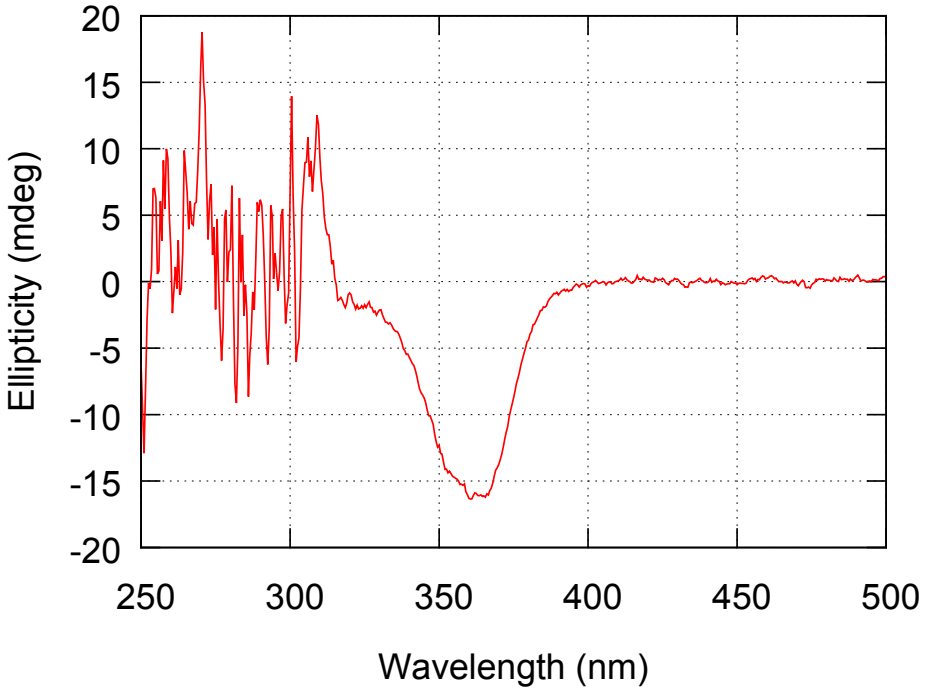

Figure S117. CD spectrum of **3b(40/60)** in *n*-pentadecane (1.75×10^{-2} g/L, path length = 10 mm).

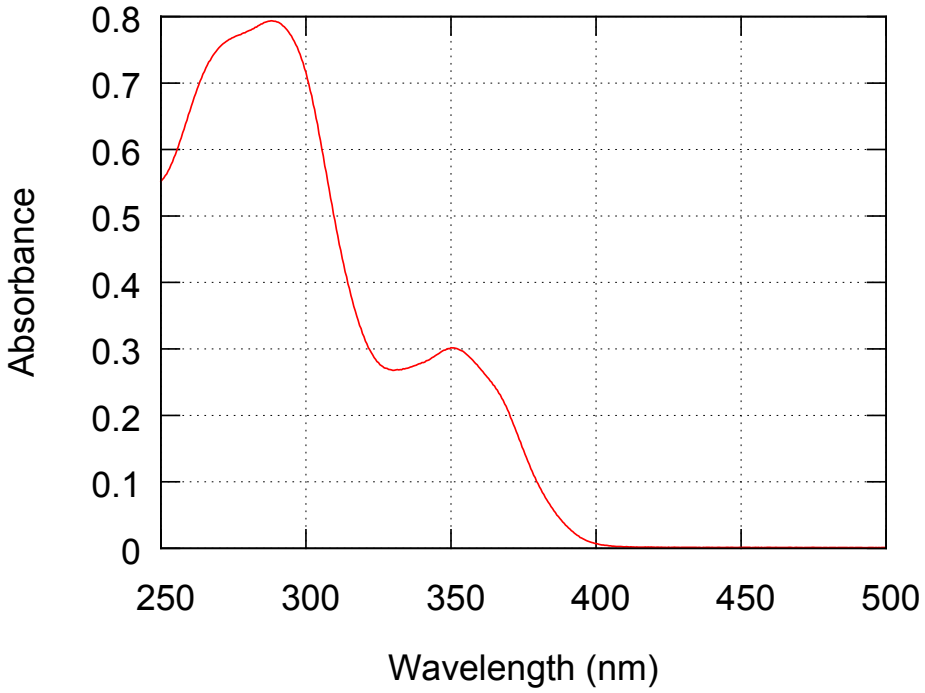

Figure S118. UV-vis absorption spectrum of **3b(40/60)** in *n*-hexadecane (3.00×10^{-2} g/L, path length = 10 mm).

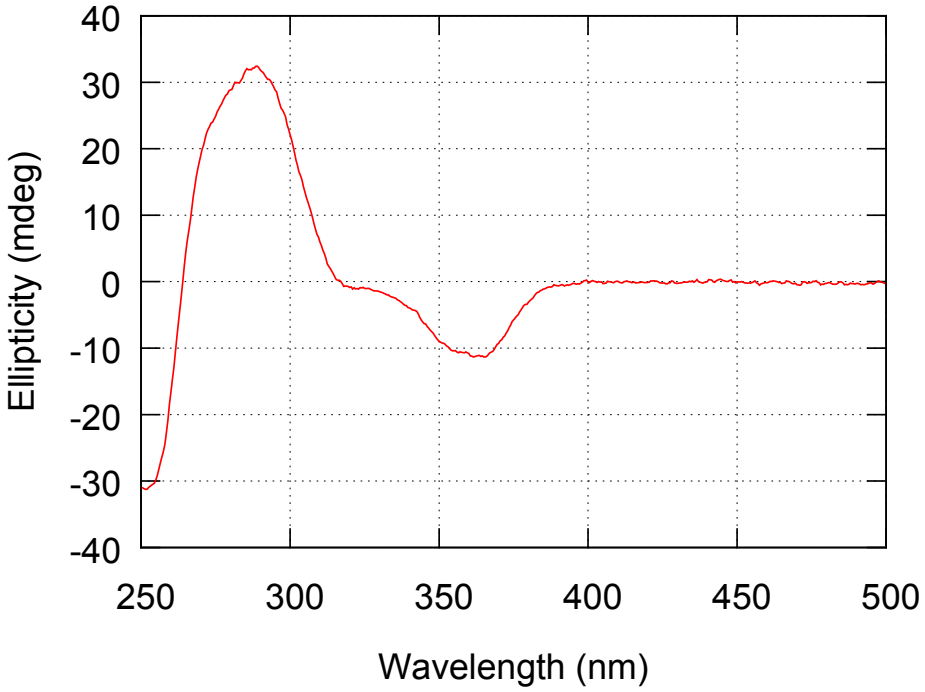

Figure S119. CD spectrum of **3b(40/60)** in *n*-hexadecane (3.00×10^{-2} g/L, path length = 10 mm).

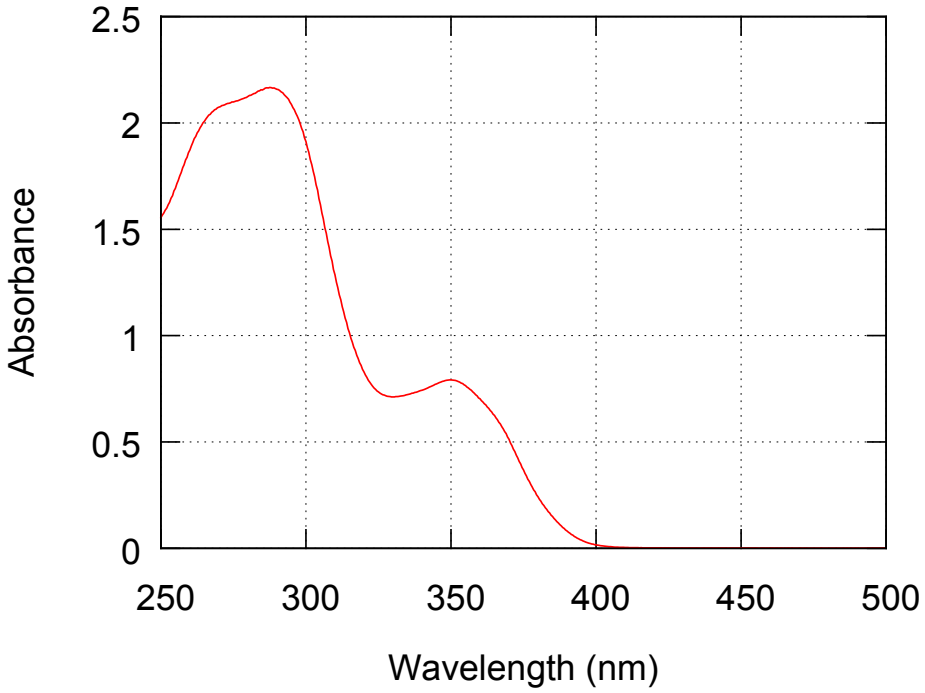

Figure S120. UV-vis absorption spectrum of **3b(2.5/97.5)** in *n*-pentane (3.34×10^{-2} g/L, path length = 10 mm).

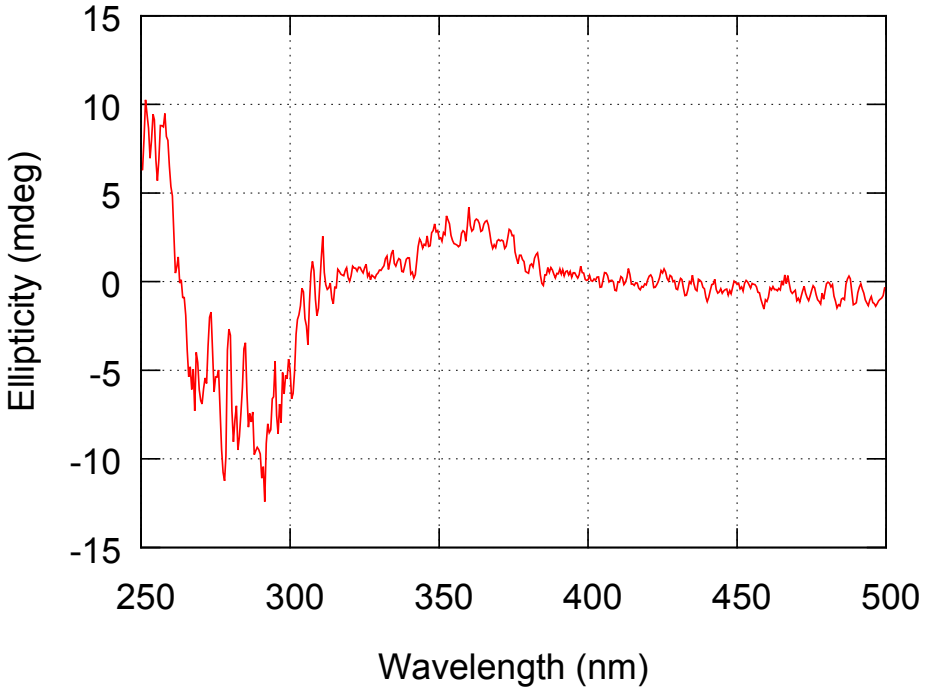

Figure S121. CD spectrum of **3b(2.5/97.5)** in *n*-pentane (3.34×10^{-2} g/L, path length = 10 mm).

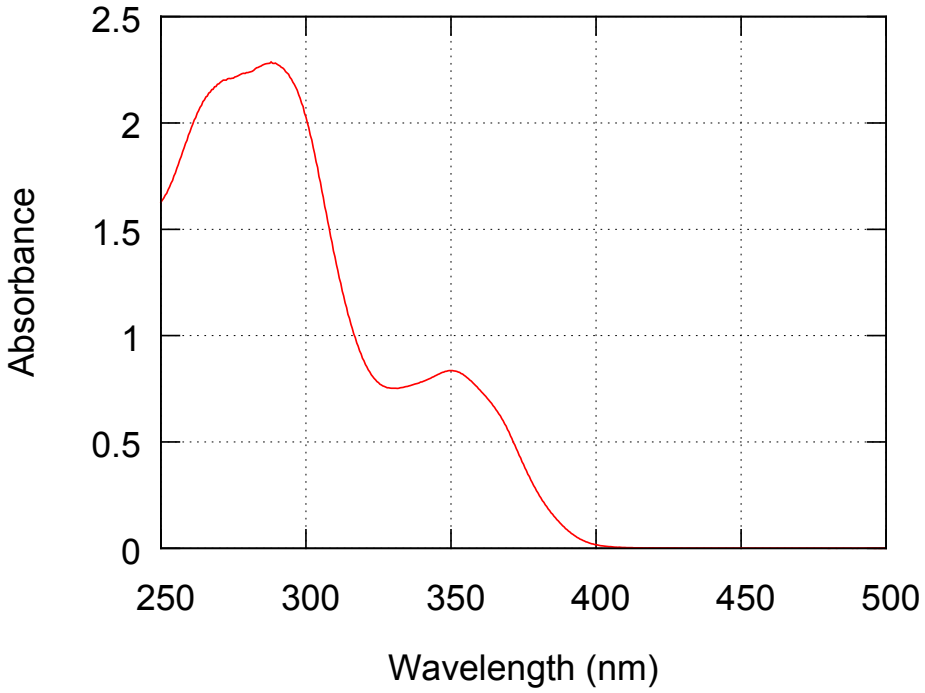

Figure S122. UV-vis absorption spectrum of **3b(2.5/97.5)** in *n*-hexane (3.34×10^{-2} g/L, path length = 10 mm).

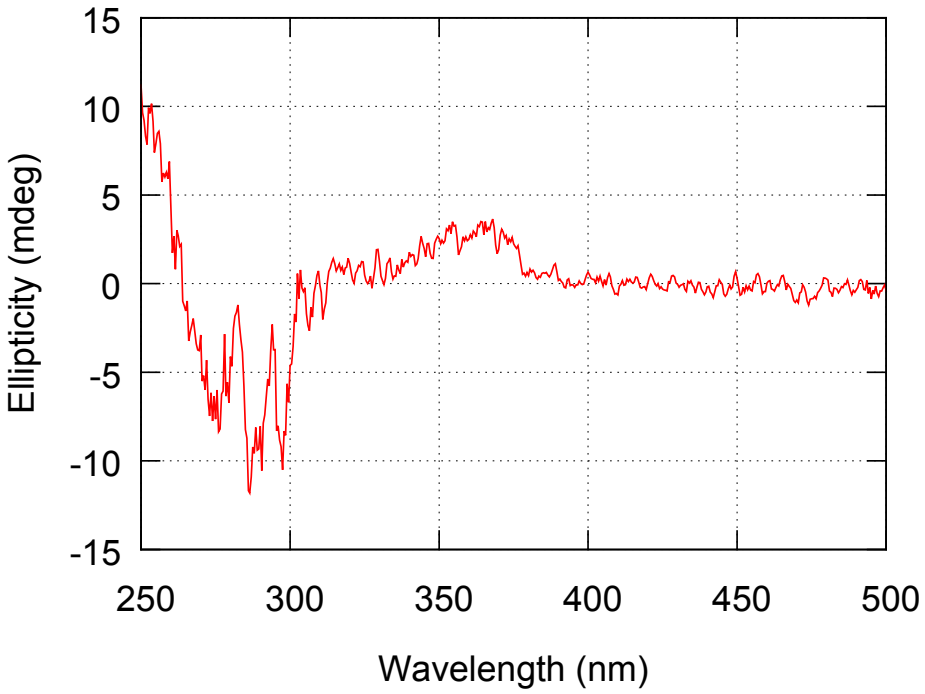

Figure S123. CD spectrum of **3b(2.5/97.5)** in *n*-hexane (3.34×10^{-2} g/L, path length = 10 mm).

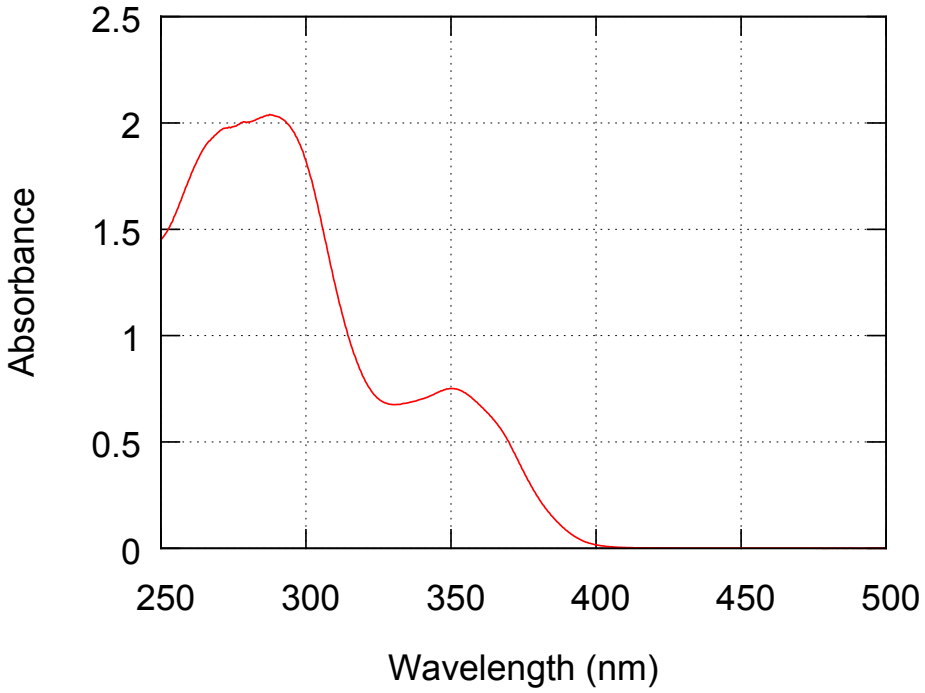

Figure S124. UV-vis absorption spectrum of **3b(2.5/97.5)** in *n*-heptane (3.34×10^{-2} g/L, path length = 10 mm).

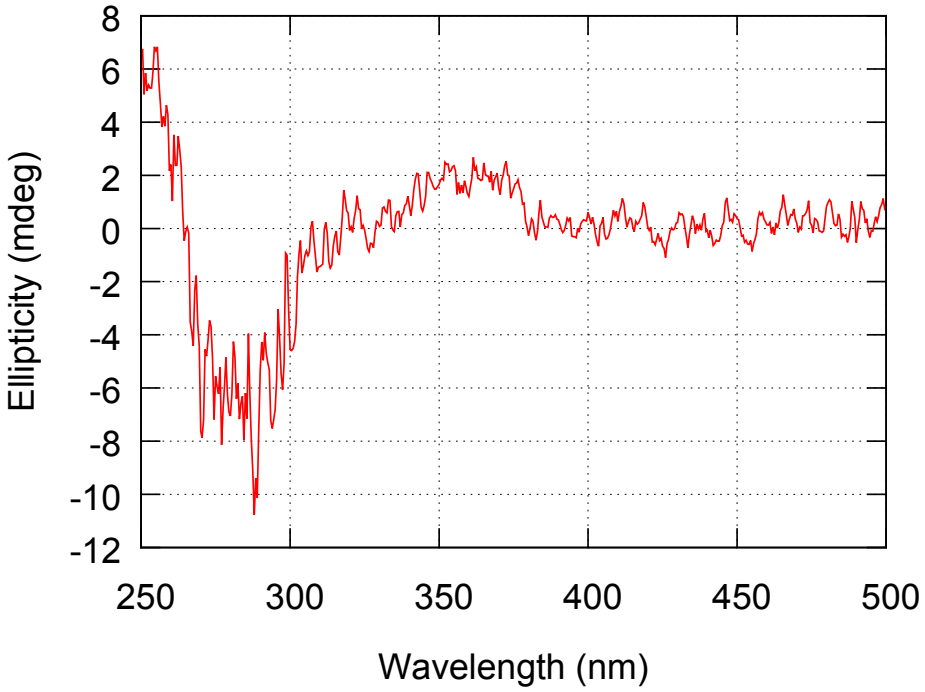

Figure S125. CD spectrum of **3b(2.5/97.5)** in *n*-heptane (3.34×10^{-2} g/L, path length = 10 mm).

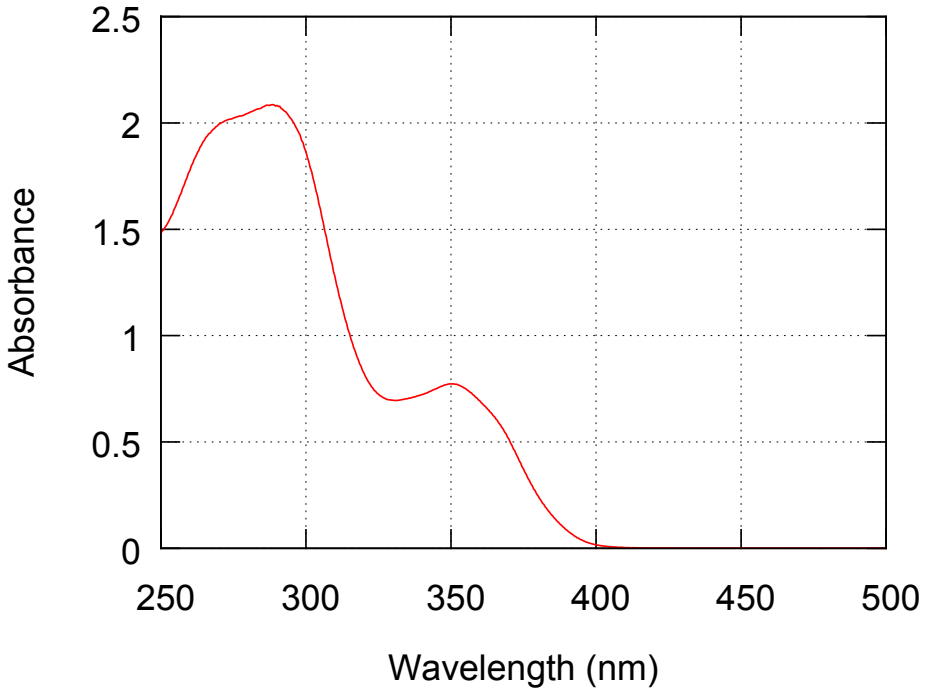

Figure S126. UV-vis absorption spectrum of **3b(2.5/97.5)** in *n*-octane (3.34×10^{-2} g/L, path length = 10 mm).

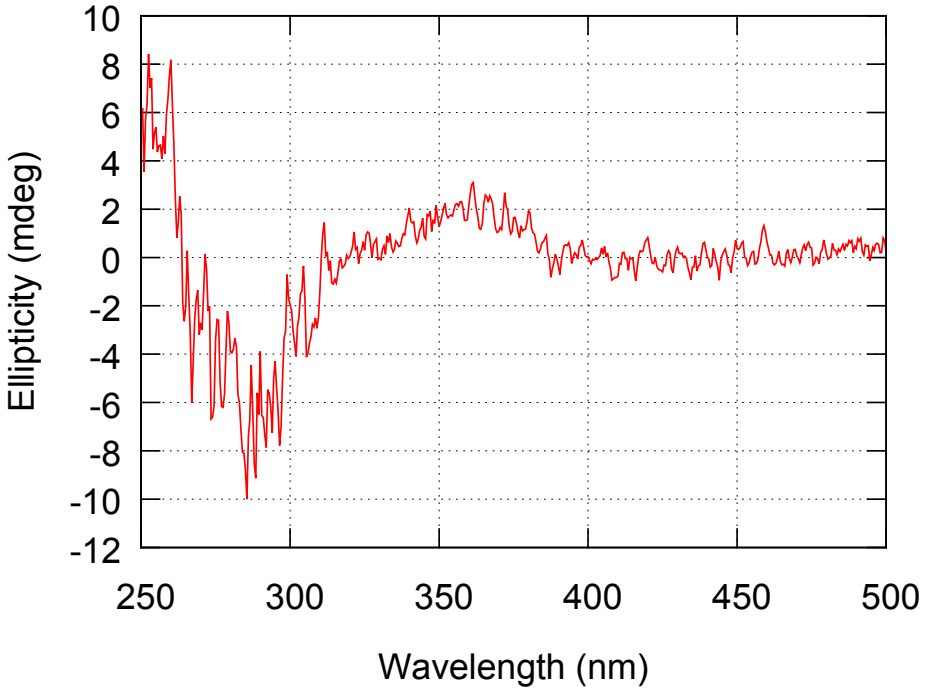

Figure S127. CD spectrum of **3b(2.5/97.5)** in *n*-octane (3.34×10^{-2} g/L, path length = 10 mm).

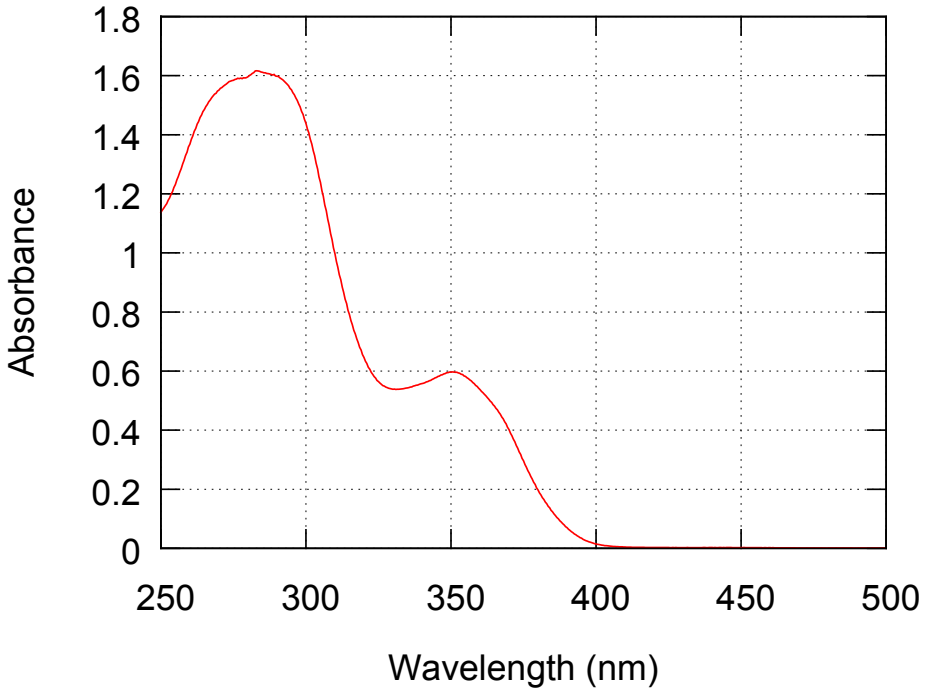

Figure S128. UV-vis absorption spectrum of **3b(2.5/97.5)** in *n*-nonane (3.34×10^{-2} g/L, path length = 10 mm).

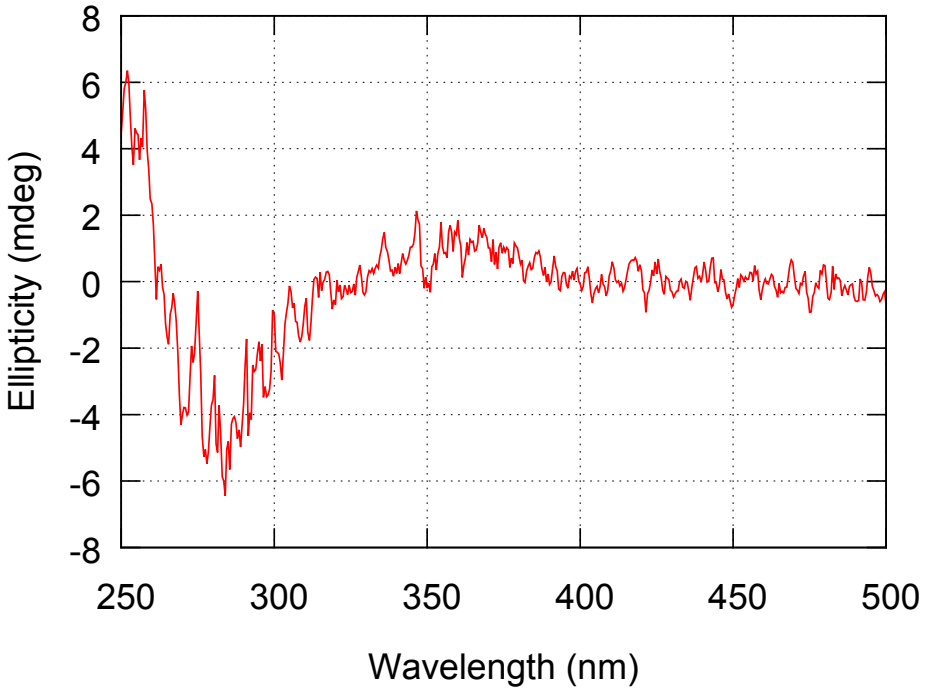

Figure S129. CD spectrum of **3b(2.5/97.5)** in *n*-nonane (3.34×10^{-2} g/L, path length = 10 mm).

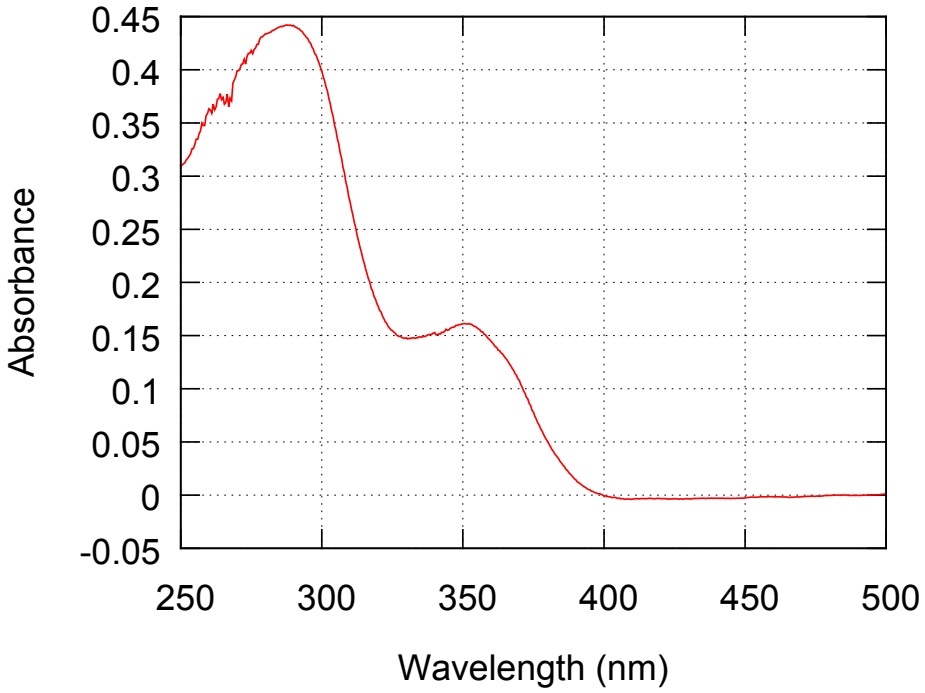

Figure S130. UV-vis absorption spectrum of **3b(2.5/97.5)** in *n*-decane (3.34×10^{-2} g/L, path length = 10 mm).

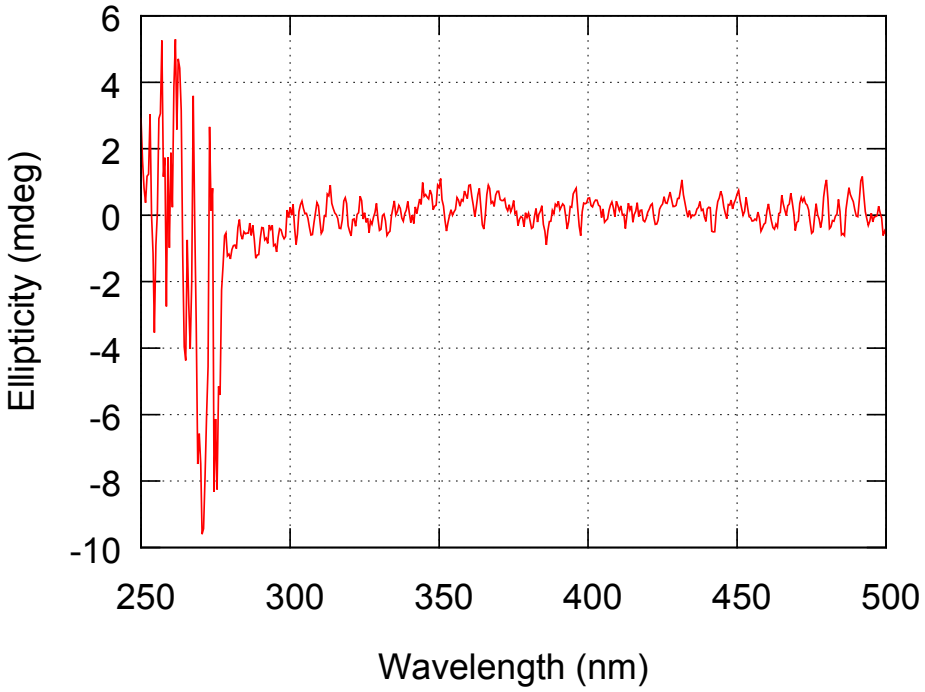

Figure S131. CD spectrum of **3b(2.5/97.5)** in *n*-decane (3.34×10^{-2} g/L, path length = 10 mm).

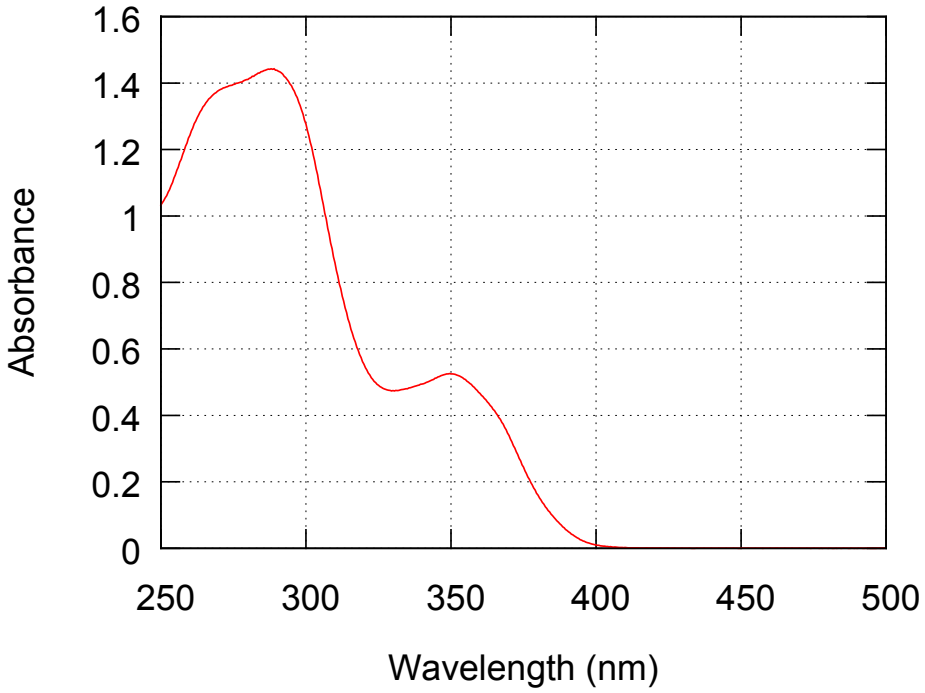

Figure S132. UV-vis absorption spectrum of **3b(5/95)** in *n*-pentane (2.12×10^{-2} g/L, path length = 10 mm).

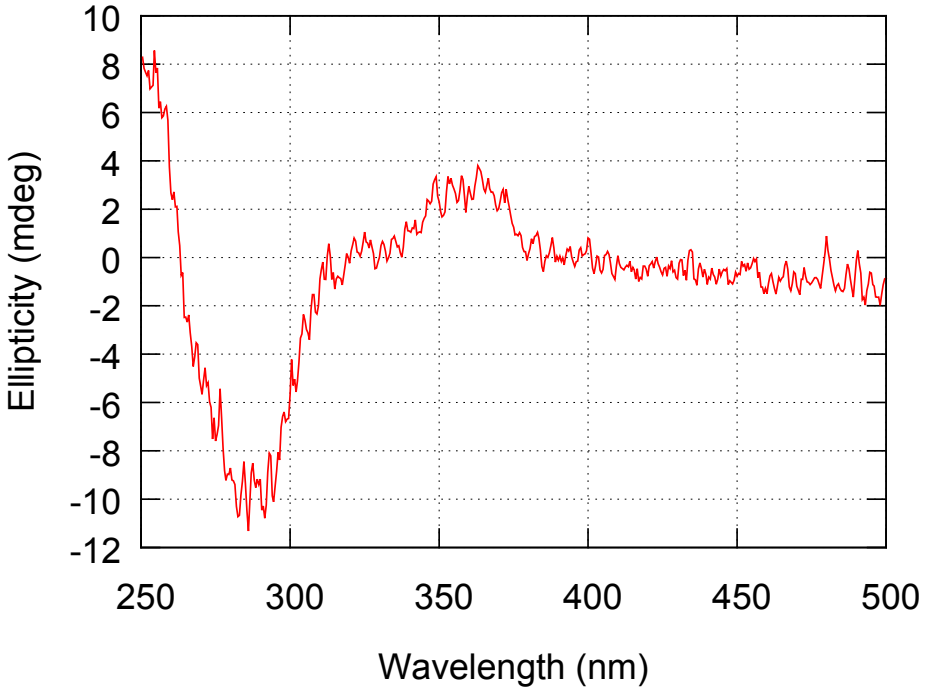

Figure S133. CD spectrum of **3b(5/95)** in *n*-pentane (2.12×10^{-2} g/L, path length = 10 mm).

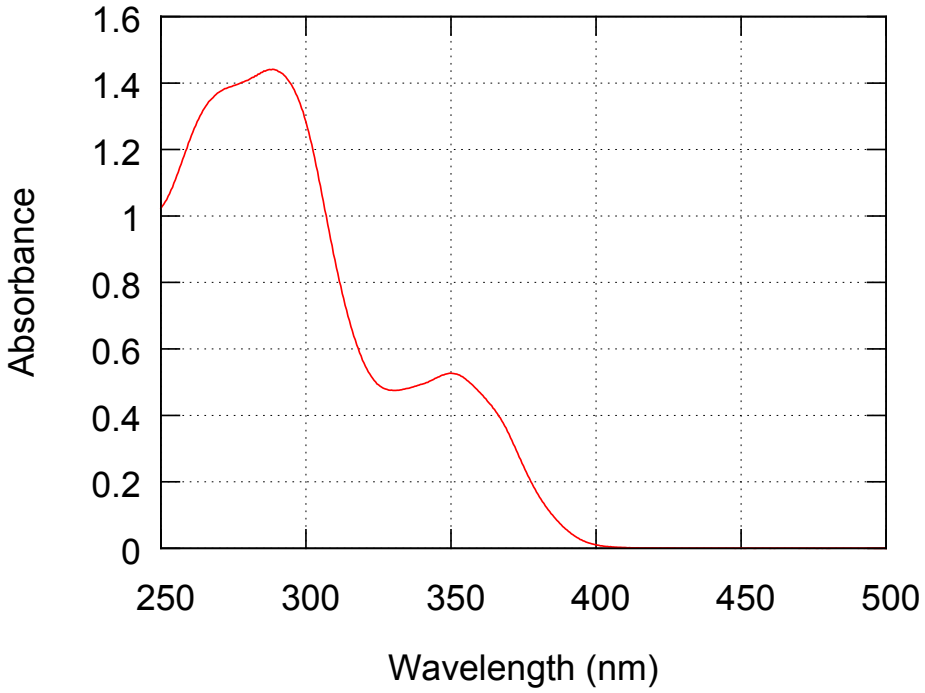

Figure S134. UV-vis absorption spectrum of **3b(5/95)** in *n*-hexane (2.12×10^{-2} g/L, path length = 10 mm).

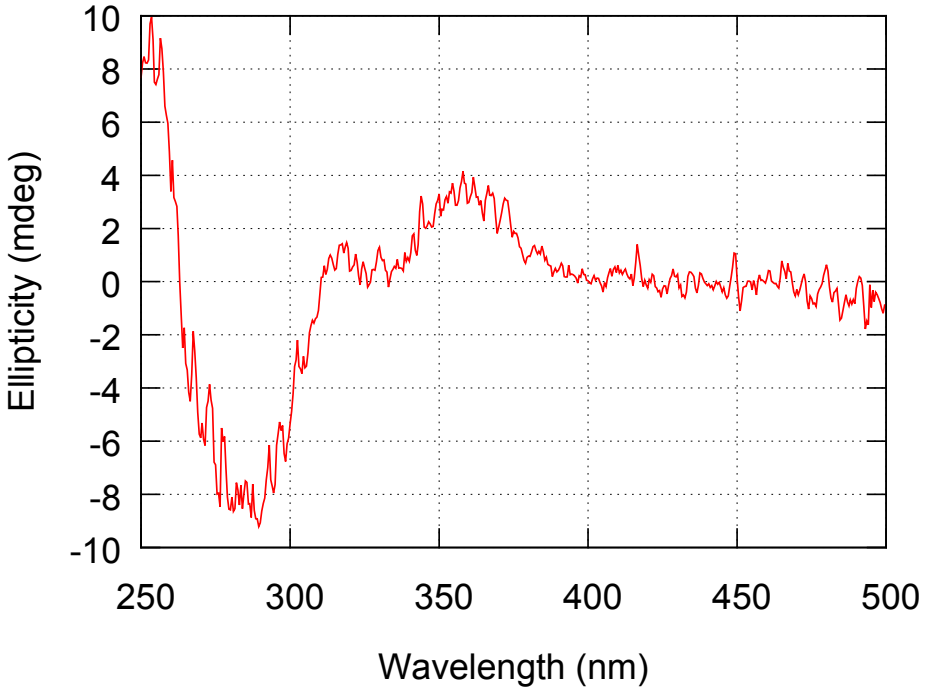

Figure S135. CD spectrum of **3b(5/95)** in *n*-hexane (2.12×10^{-2} g/L, path length = 10 mm).

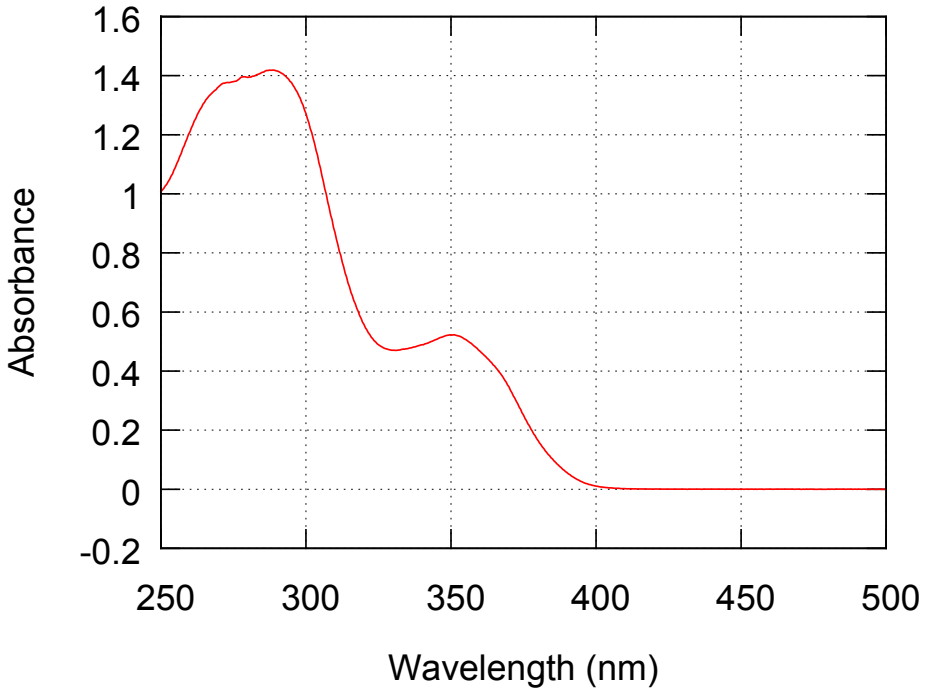

Figure S136. UV-vis absorption spectrum of **3b(5/95)** in *n*-heptane (2.12×10^{-2} g/L, path length = 10 mm).

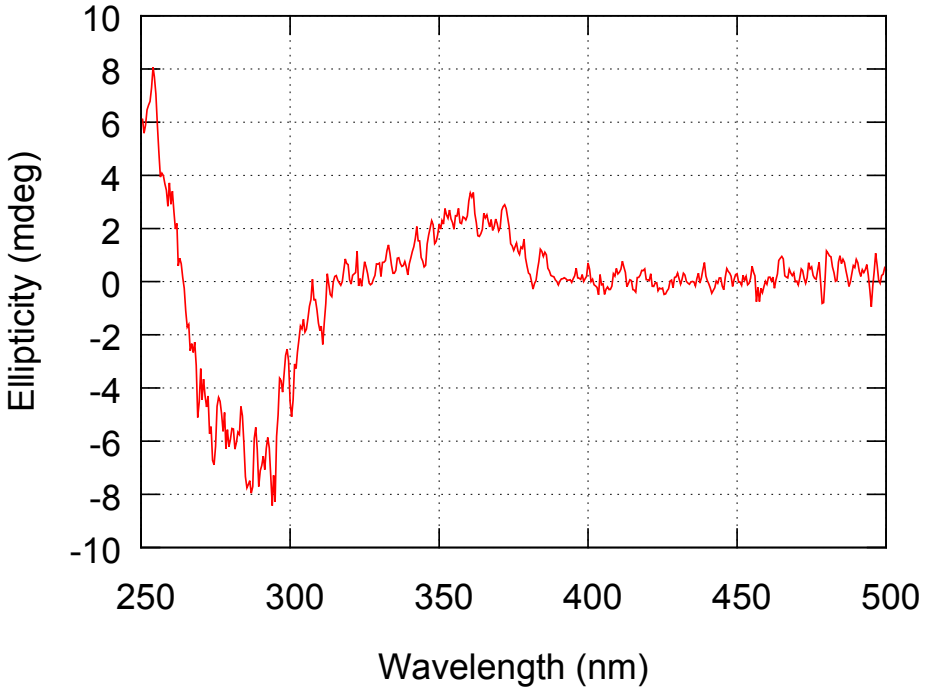

Figure S137. CD spectrum of **3b(5/95)** in *n*-heptane (2.12×10^{-2} g/L, path length = 10 mm).

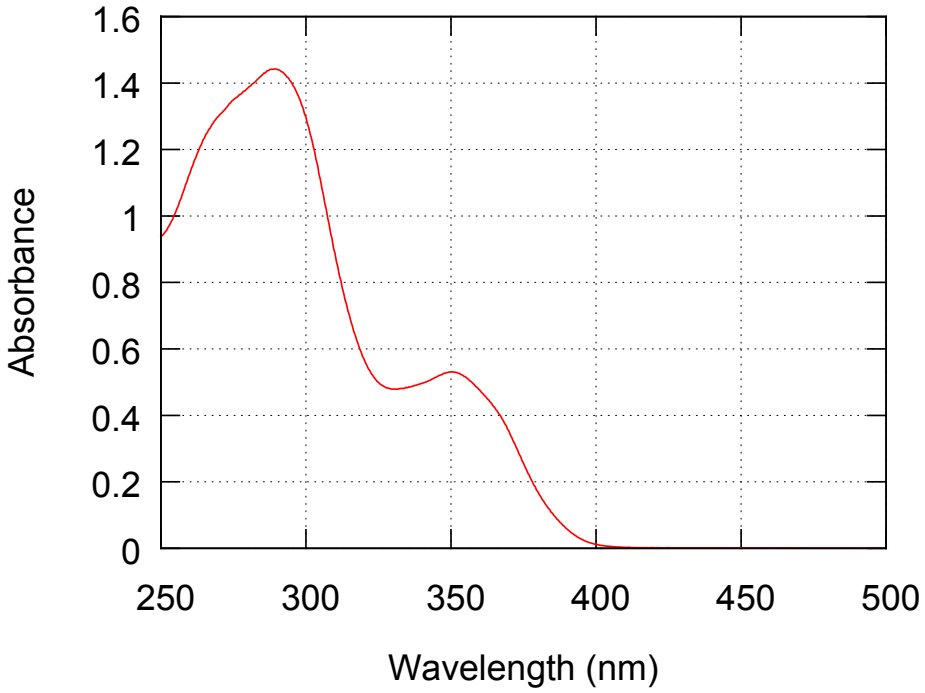

Figure S138. UV-vis absorption spectrum of **3b(5/95)** in *n*-octane (2.12×10^{-2} g/L, path length = 10 mm).

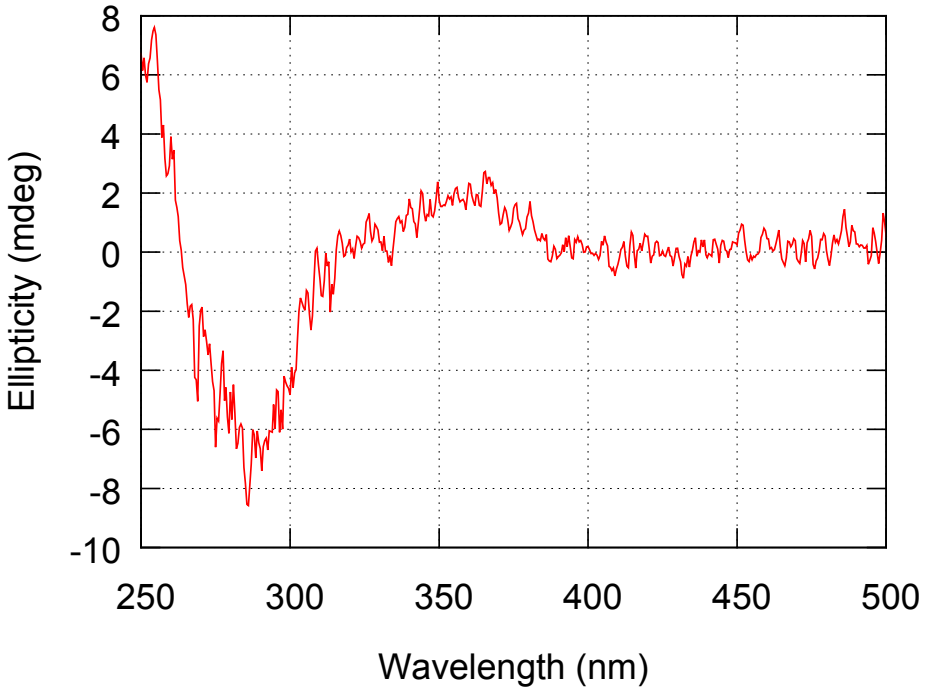

Figure S139. CD spectrum of **3b(5/95)** in *n*-octane (2.12×10^{-2} g/L, path length = 10 mm).

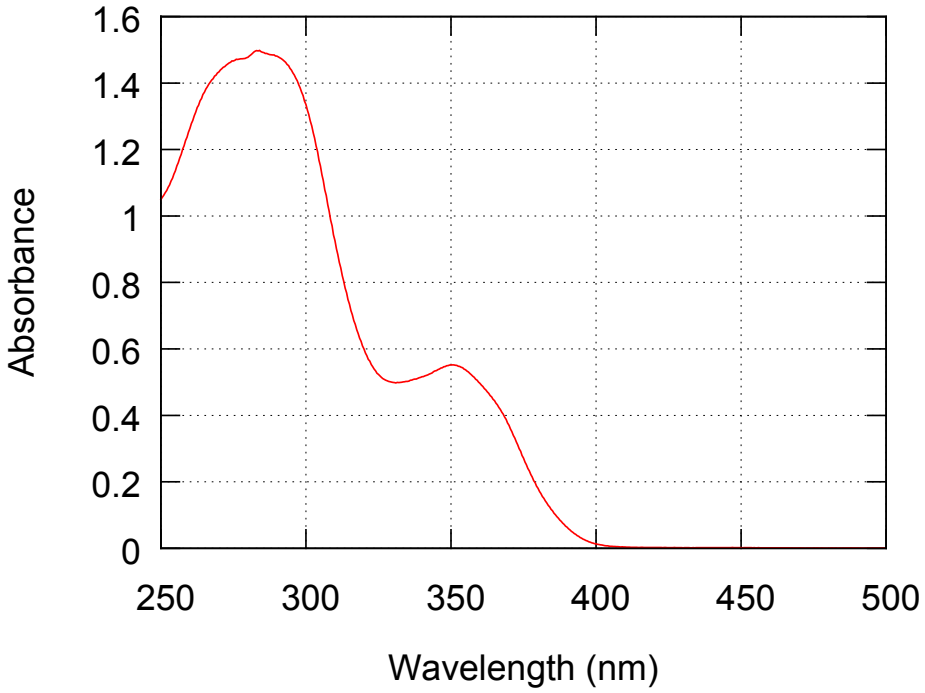

Figure S140. UV-vis absorption spectrum of **3b(5/95)** in *n*-nonane (2.12×10^{-2} g/L, path length = 10 mm).

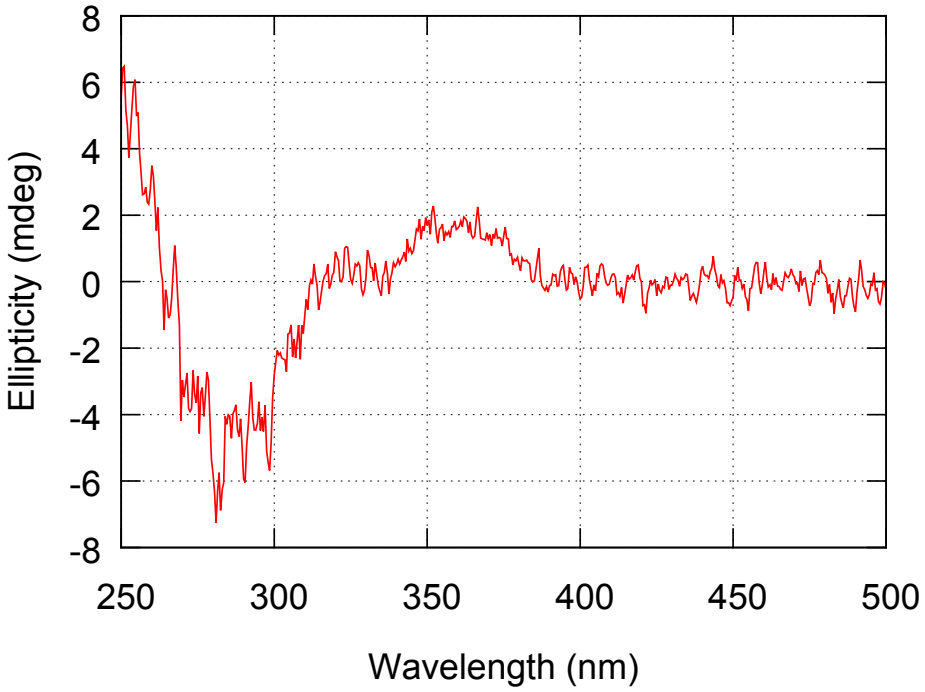

Figure S141. CD spectrum of **3b(5/95)** in *n*-nonane (2.12×10^{-2} g/L, path length = 10 mm).

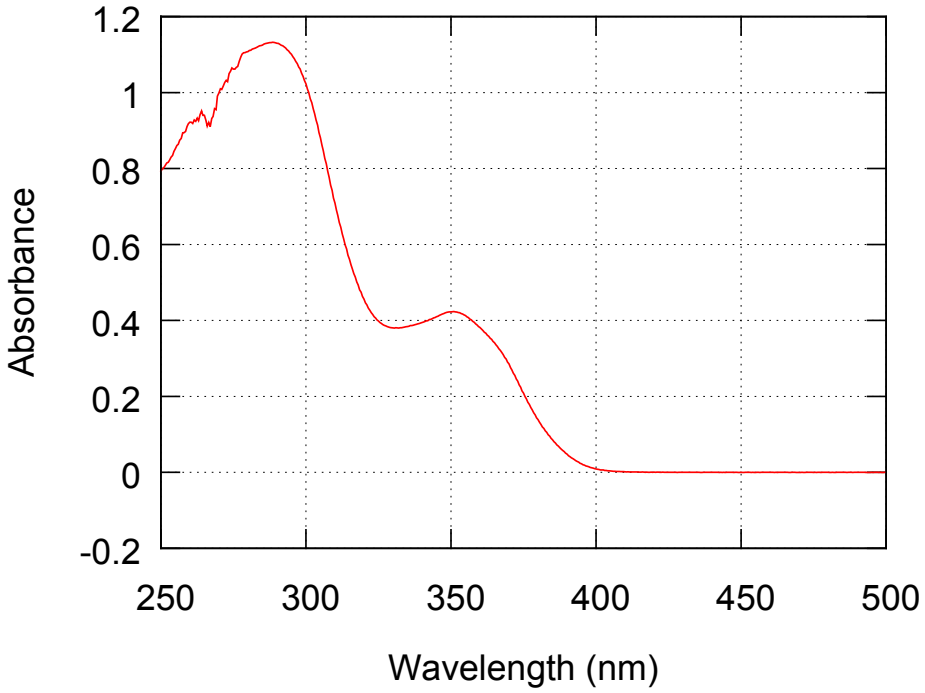

Figure S142. UV-vis absorption spectrum of **3b(5/95)** in *n*-decane (2.12×10^{-2} g/L, path length = 10 mm).

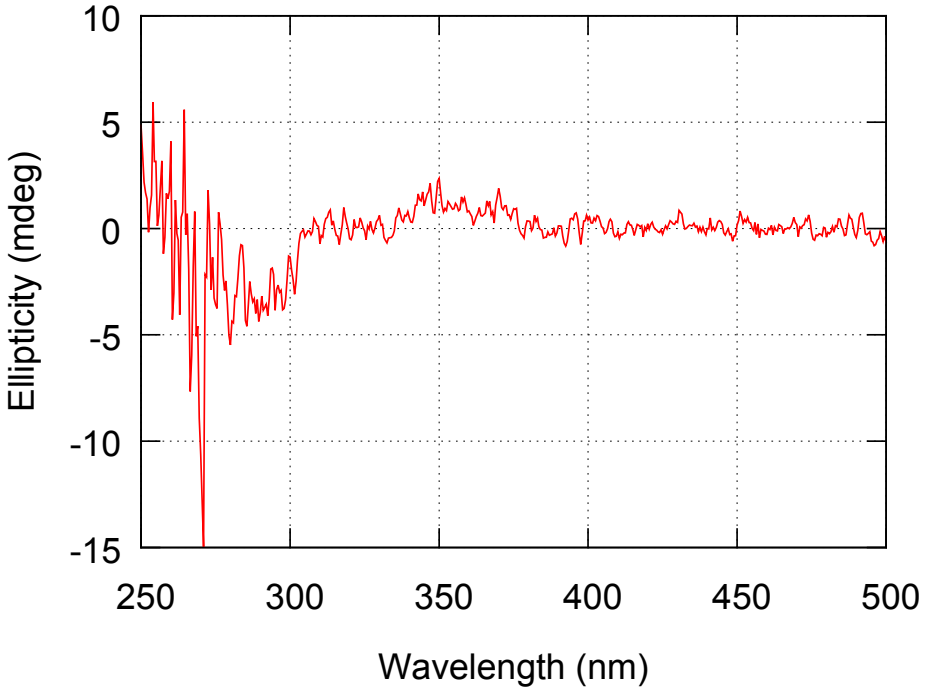

Figure S143. CD spectrum of **3b(5/95)** in *n*-decane (2.12×10^{-2} g/L, path length = 10 mm).

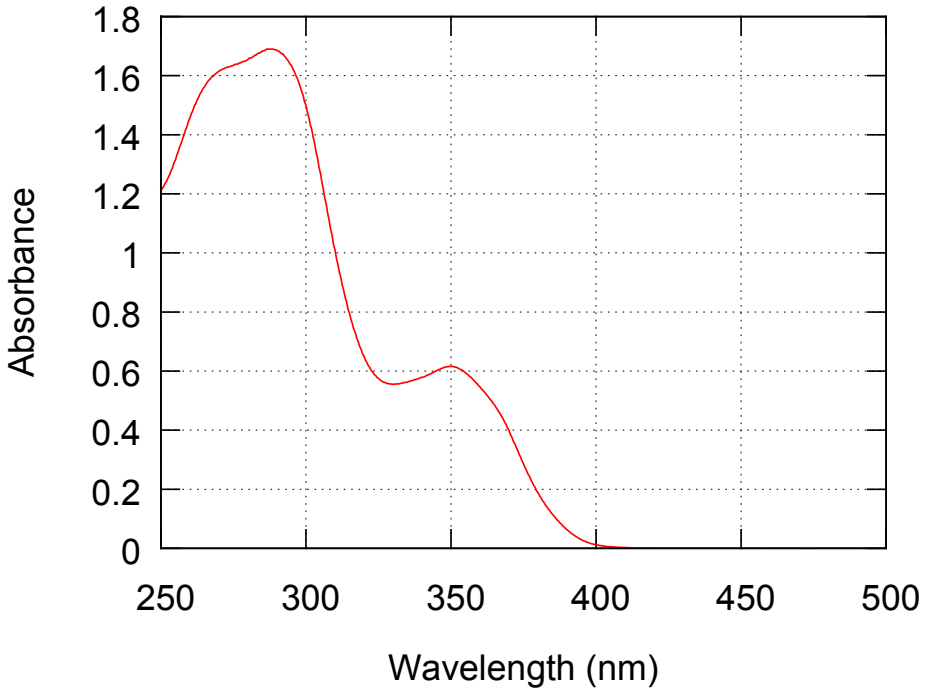

Figure S144. UV-vis absorption spectrum of **3b(7.5/92.5)** in *n*-pentane (2.25×10^{-2} g/L, path length = 10 mm).

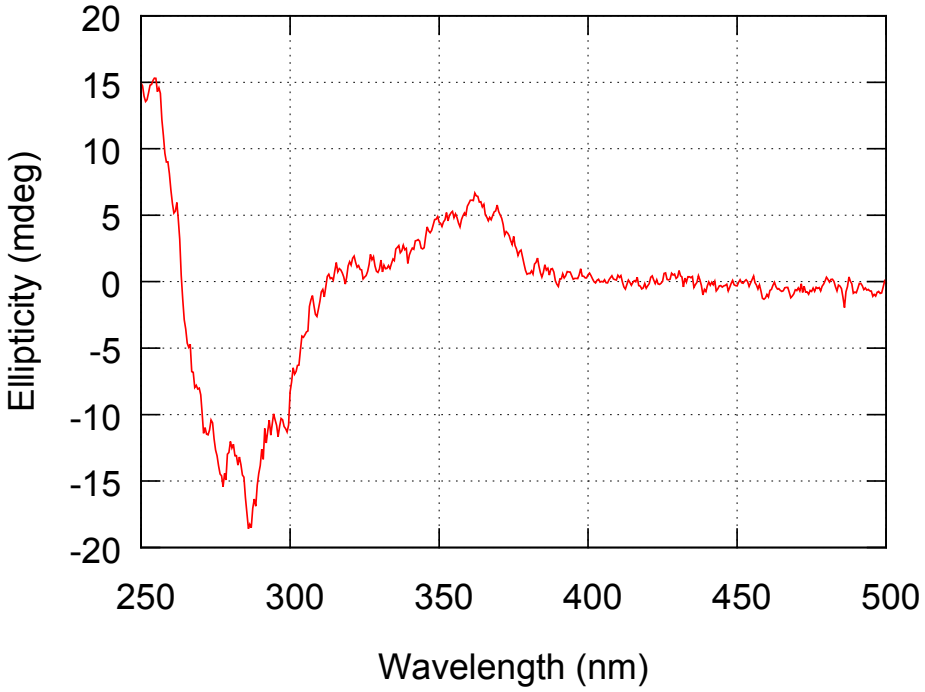

Figure S145. CD spectrum of **3b(7.5/92.5)** in *n*-pentane (2.25×10^{-2} g/L, path length = 10 mm).

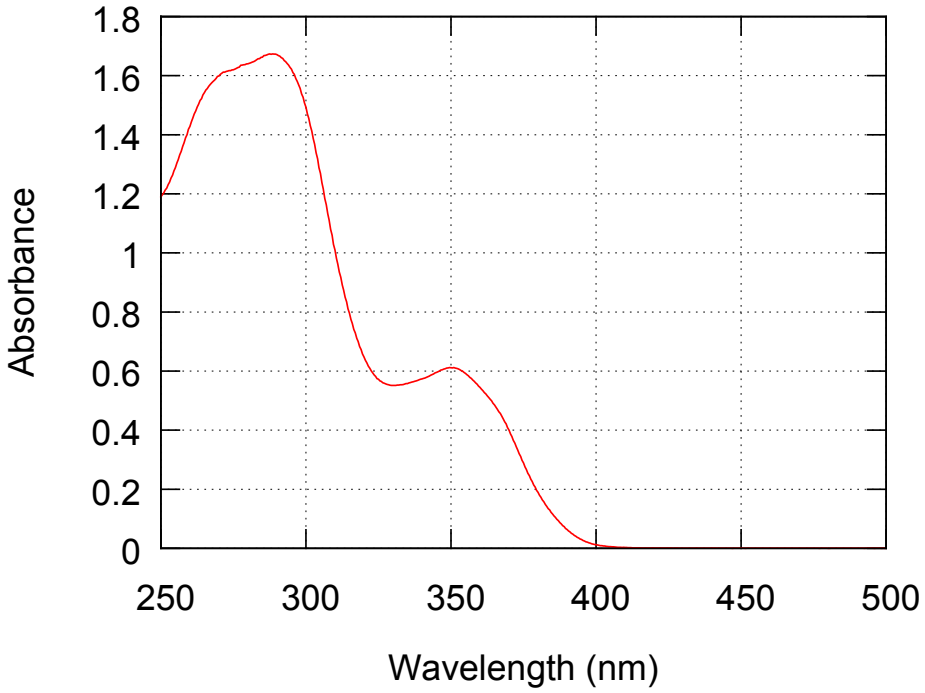

Figure S146. UV-vis absorption spectrum of **3b(7.5/92.5)** in *n*-hexane (2.25×10^{-2} g/L, path length = 10 mm).

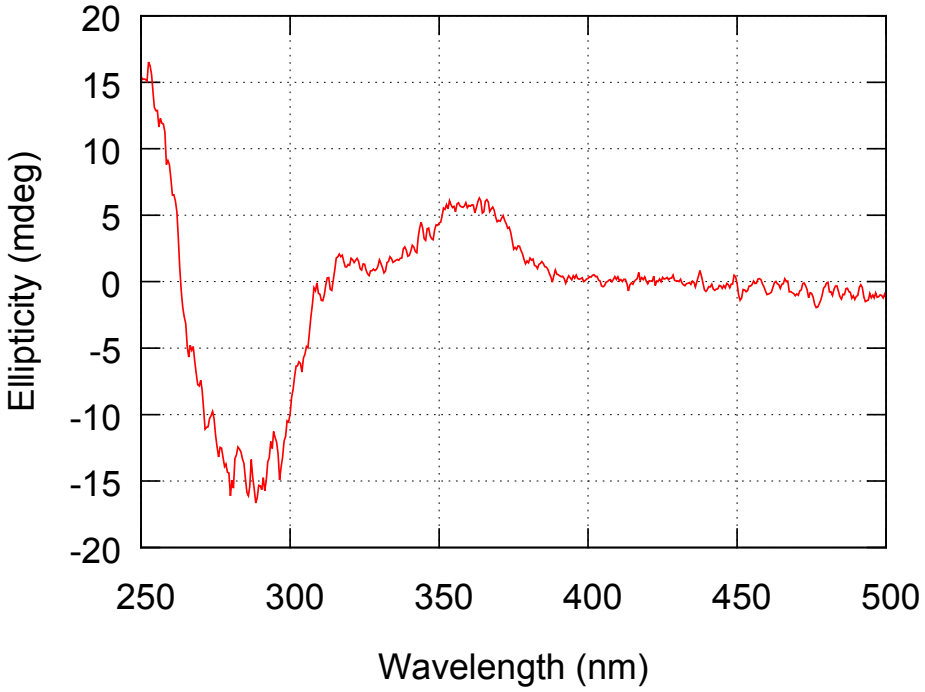

Figure S147. CD spectrum of **3b(7.5/92.5)** in *n*-hexane (2.25×10^{-2} g/L, path length = 10 mm).

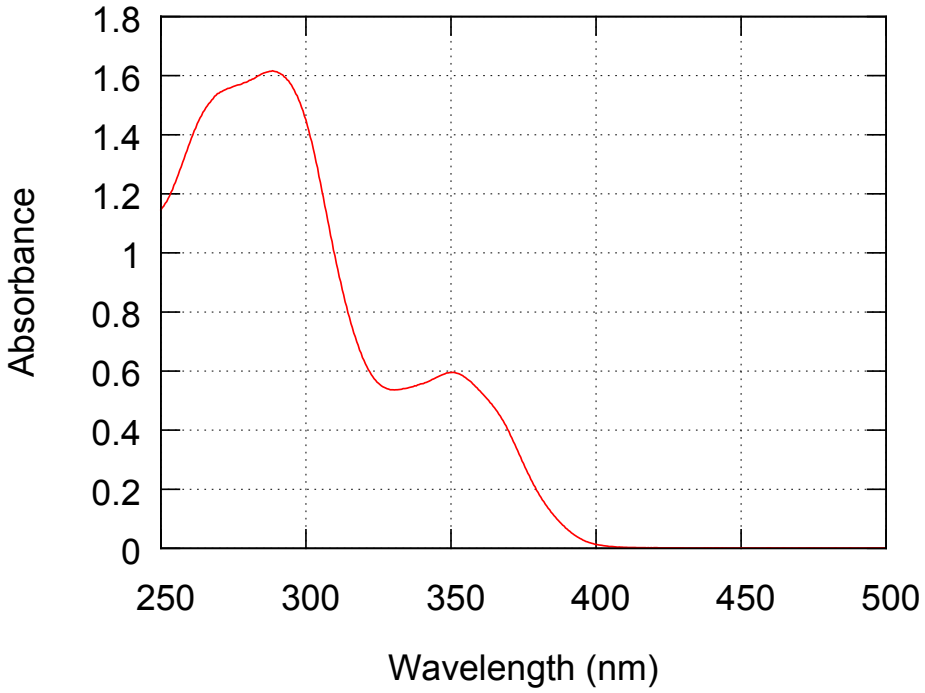

Figure S148. UV-vis absorption spectrum of **3b(7.5/92.5)** in *n*-heptane (2.25×10^{-2} g/L, path length = 10 mm).

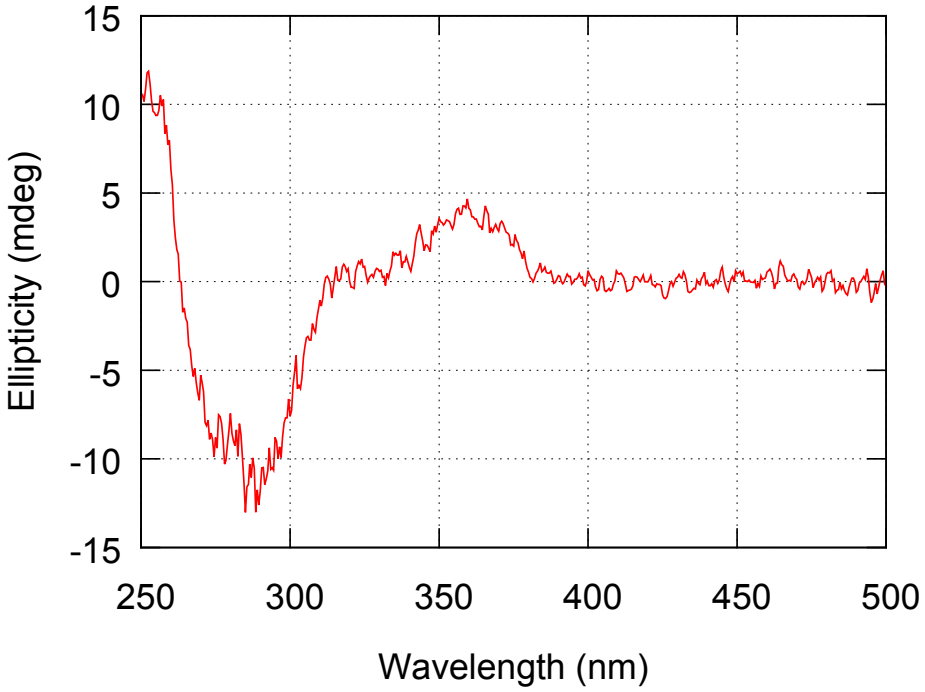

Figure S149. CD spectrum of **3b(7.5/92.5)** in *n*-heptane (2.25×10^{-2} g/L, path length = 10 mm).

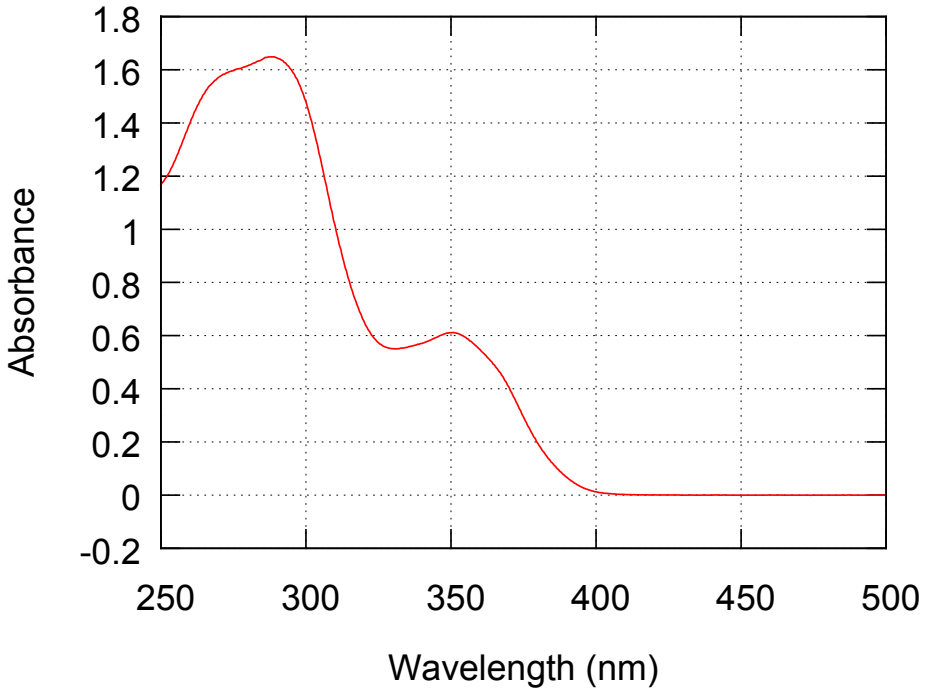

Figure S150. UV-vis absorption spectrum of **3b(7.5/92.5)** in *n*-octane (2.25×10^{-2} g/L, path length = 10 mm).

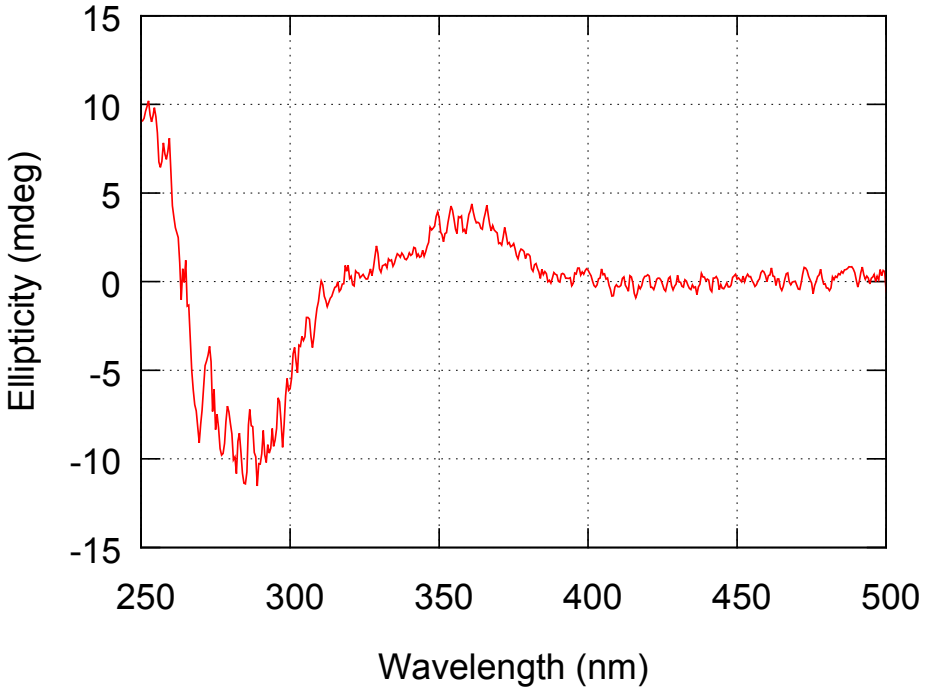

Figure S151. CD spectrum of **3b(7.5/92.5)** in *n*-octane (2.25×10^{-2} g/L, path length = 10 mm).

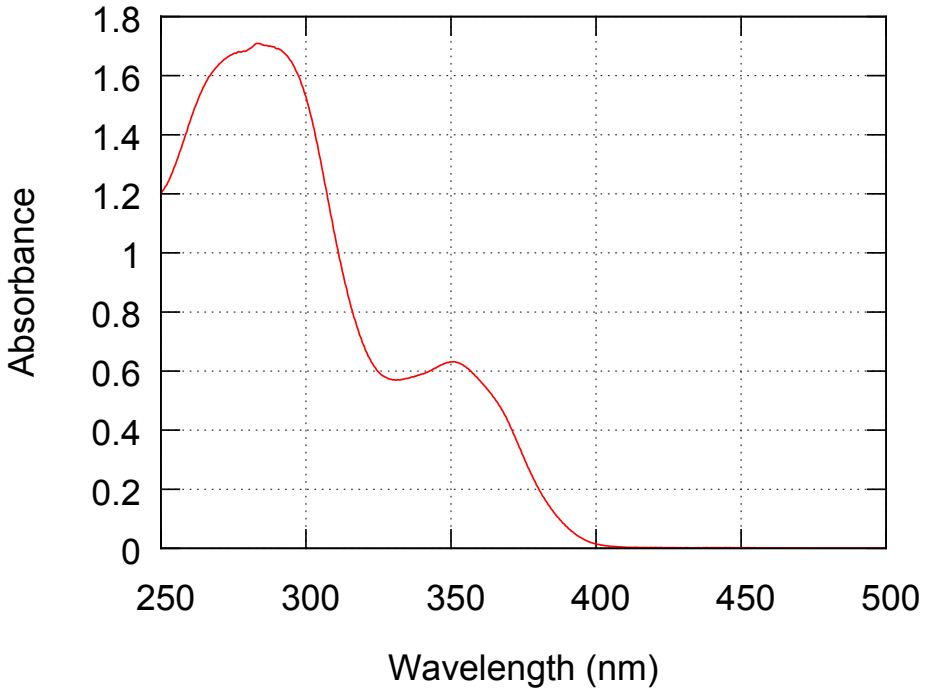

Figure S152. UV-vis absorption spectrum of **3b(7.5/92.5)** in *n*-nonane (2.25×10^{-2} g/L, path length = 10 mm).

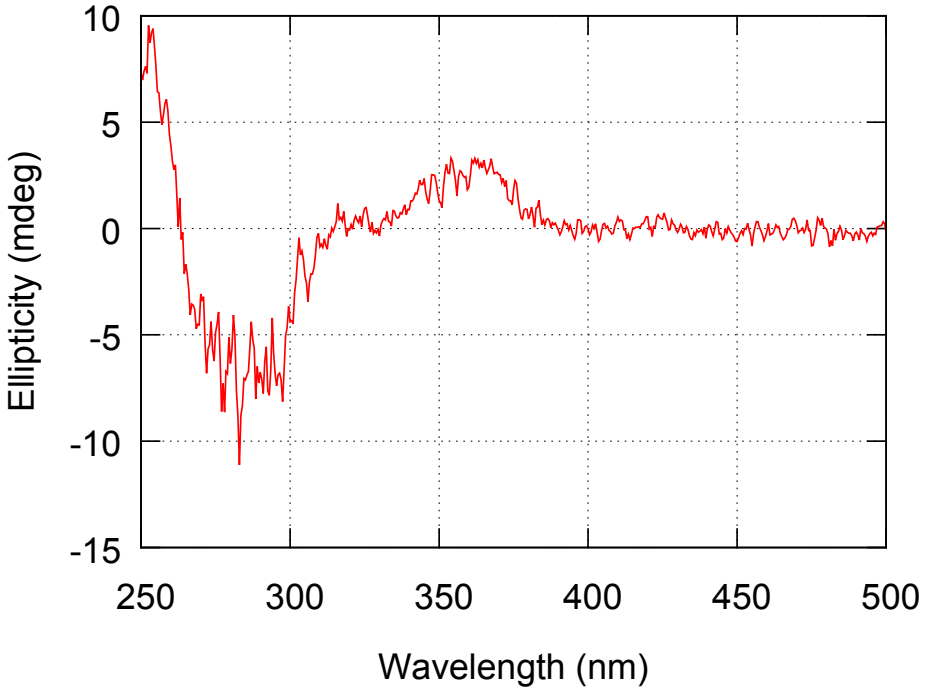

Figure S153. CD spectrum of **3b(7.5/92.5)** in *n*-nonane (2.25×10^{-2} g/L, path length = 10 mm).

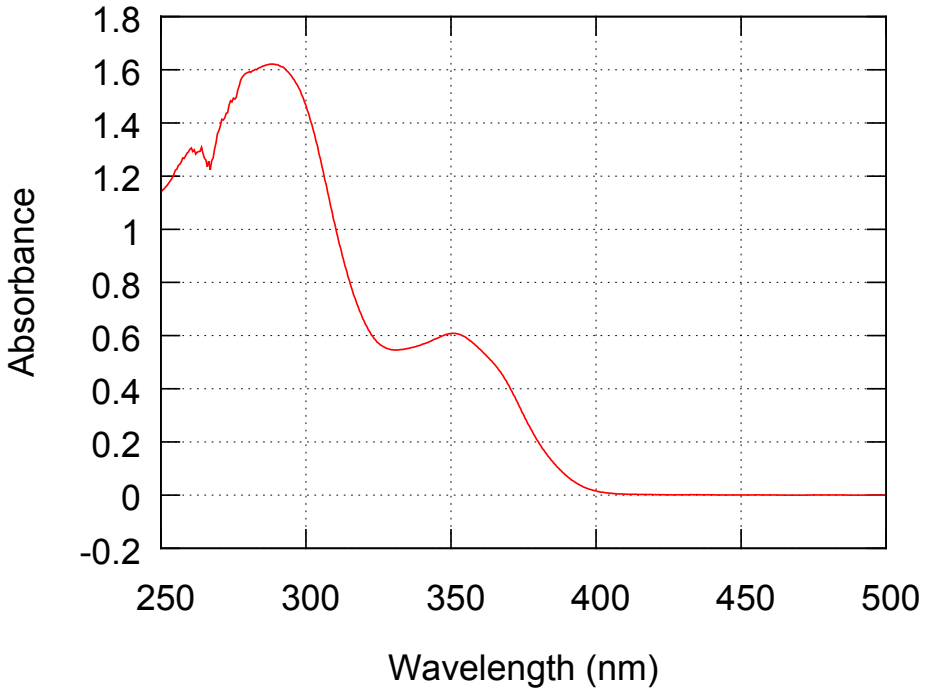

Figure S154. UV-vis absorption spectrum of **3b(7.5/92.5)** in *n*-decane (2.25×10^{-2} g/L, path length = 10 mm).

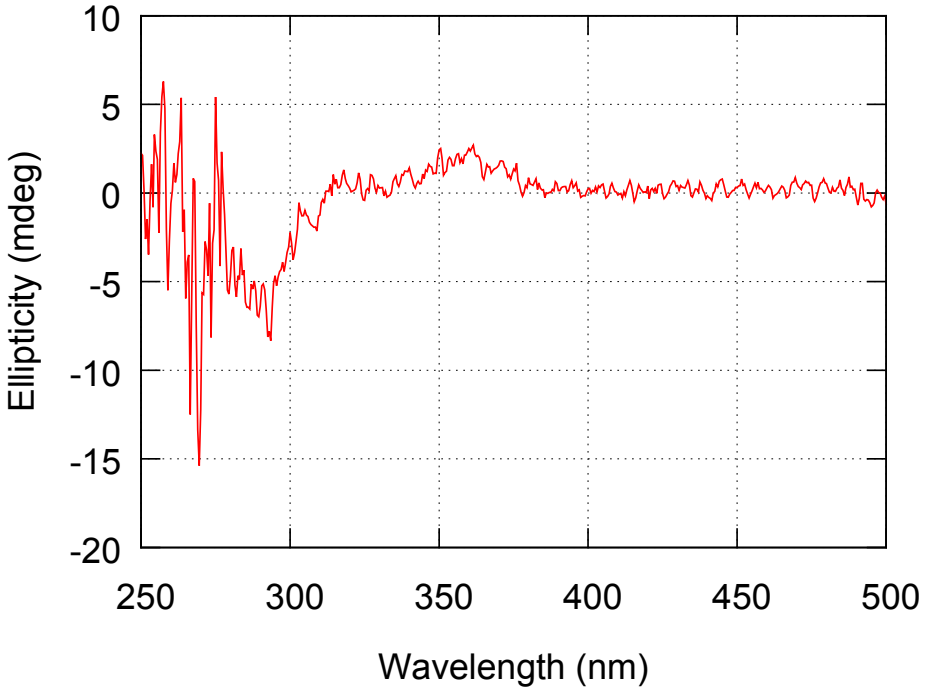

Figure S155. CD spectrum of **3b(7.5/92.5)** in *n*-decane (2.25×10^{-2} g/L, path length = 10 mm).

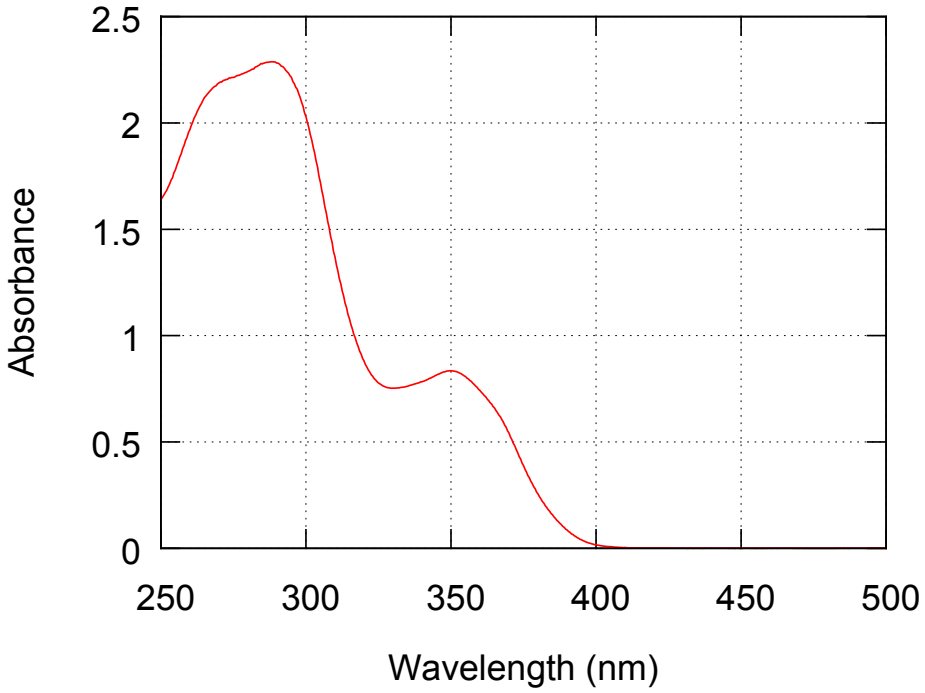

Figure S156. UV-vis absorption spectrum of **3b(10/90)** in *n*-pentane (3.28×10^{-2} g/L, path length = 10 mm).

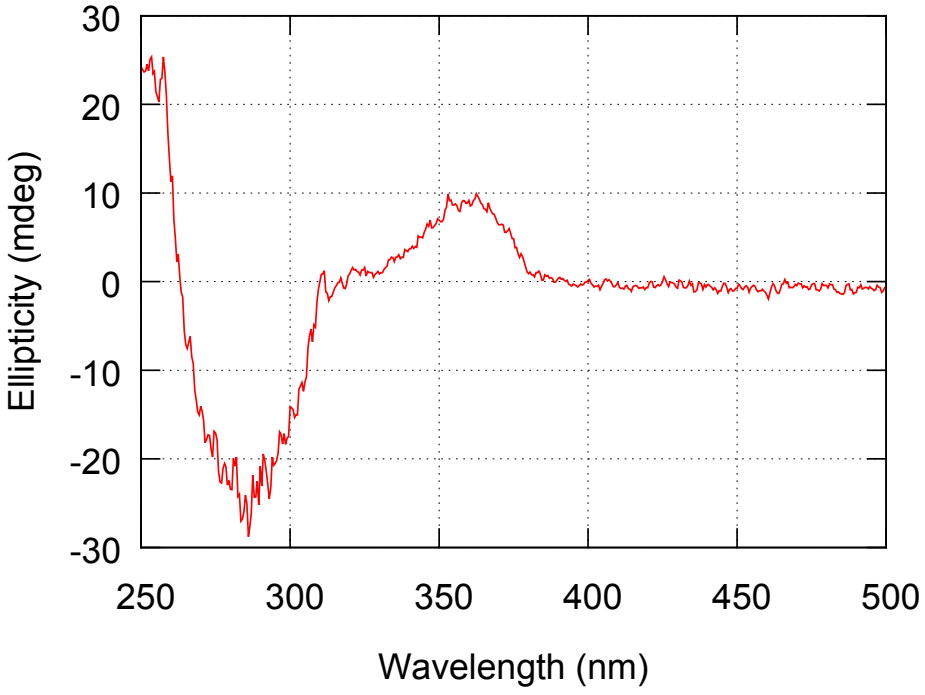

Figure S157. CD spectrum of **3b(10/90)** in *n*-pentane (3.28×10^{-2} g/L, path length = 10 mm).

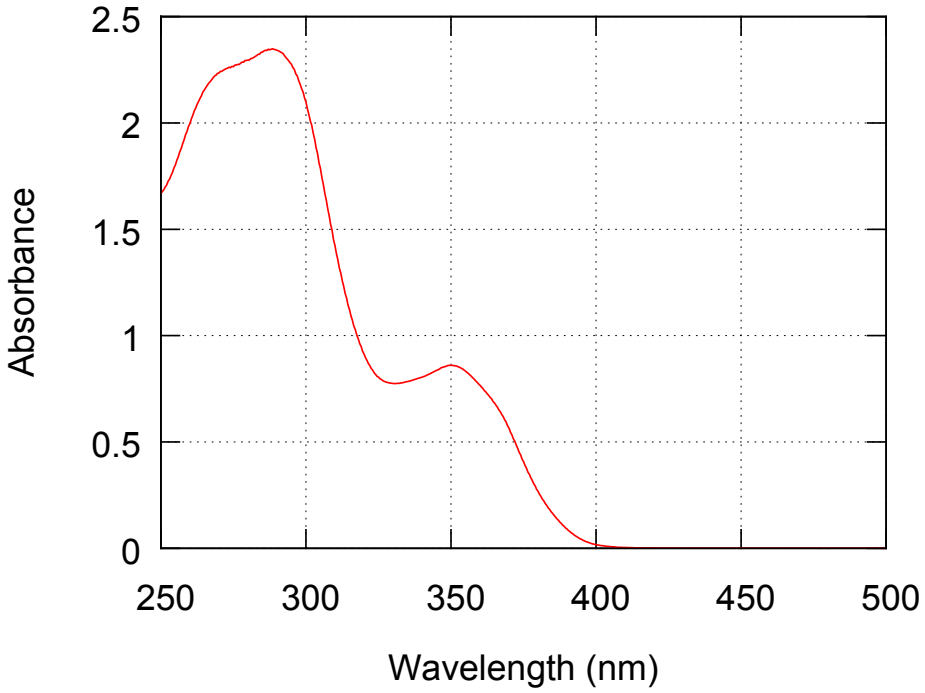

Figure S158. UV-vis absorption spectrum of **3b(10/90)** in *n*-hexane (3.28×10^{-2} g/L, path length = 10 mm).

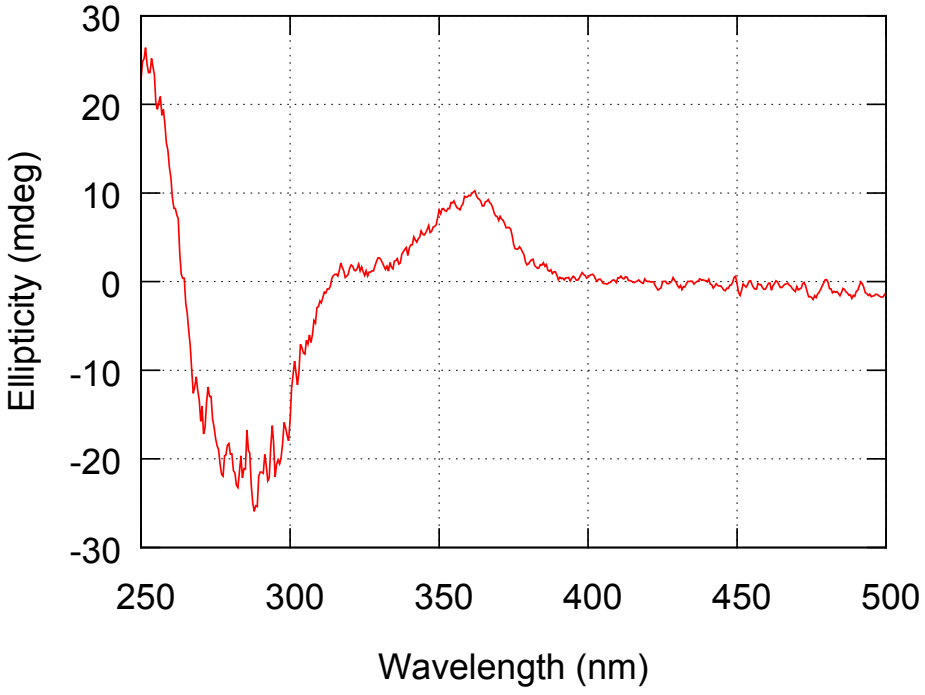

Figure S159. CD spectrum of **3b(10/90)** in *n*-hexane (3.28×10^{-2} g/L, path length = 10 mm).

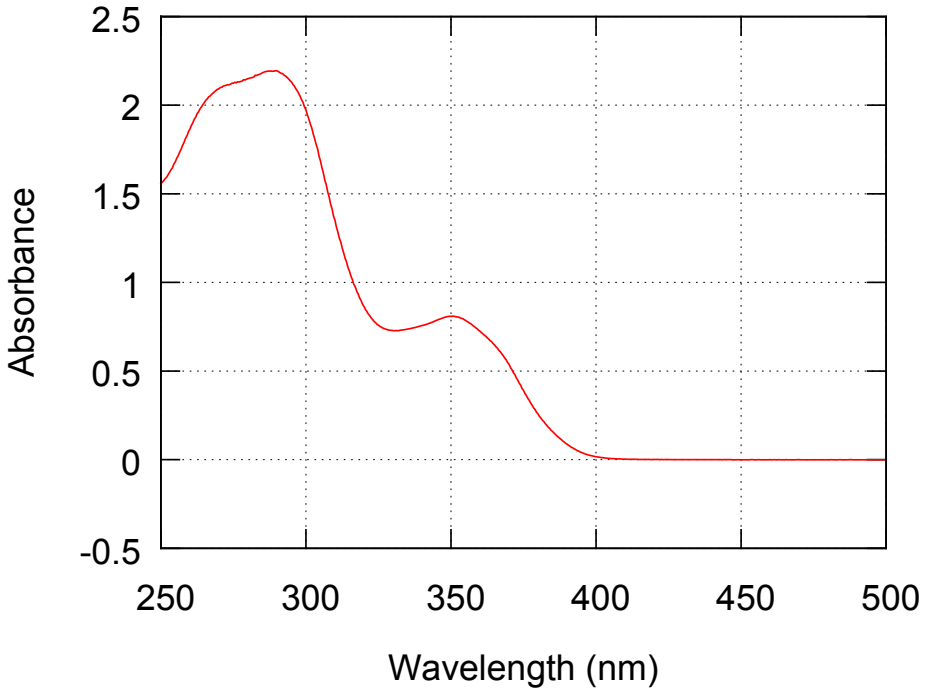

Figure S160. UV-vis absorption spectrum of **3b(10/90)** in *n*-heptane (3.28×10^{-2} g/L, path length = 10 mm).

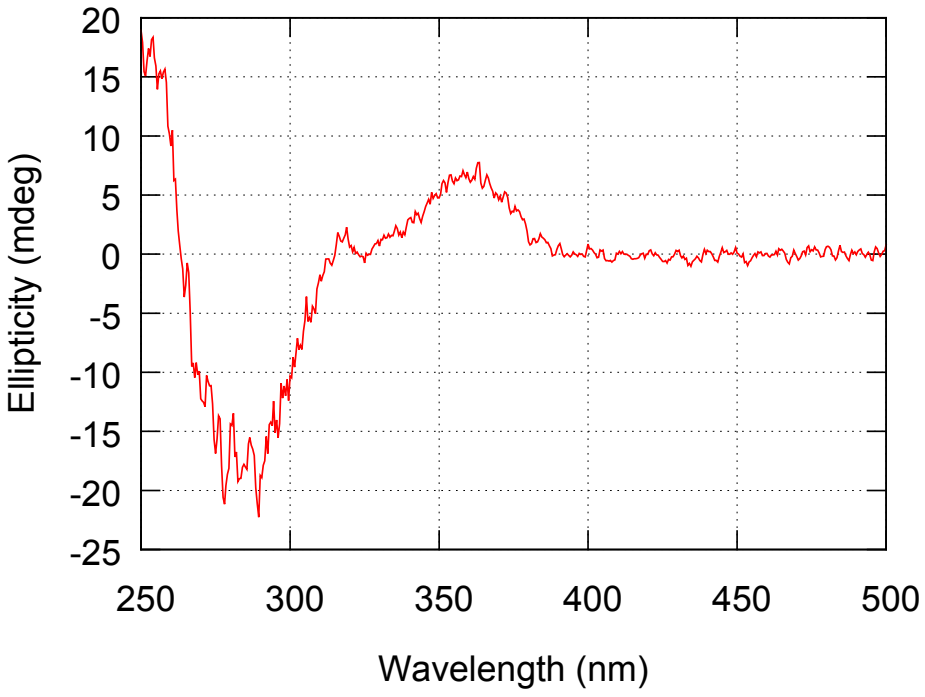

Figure S161. CD spectrum of **3b(10/90)** in *n*-heptane (3.28×10^{-2} g/L, path length = 10 mm).

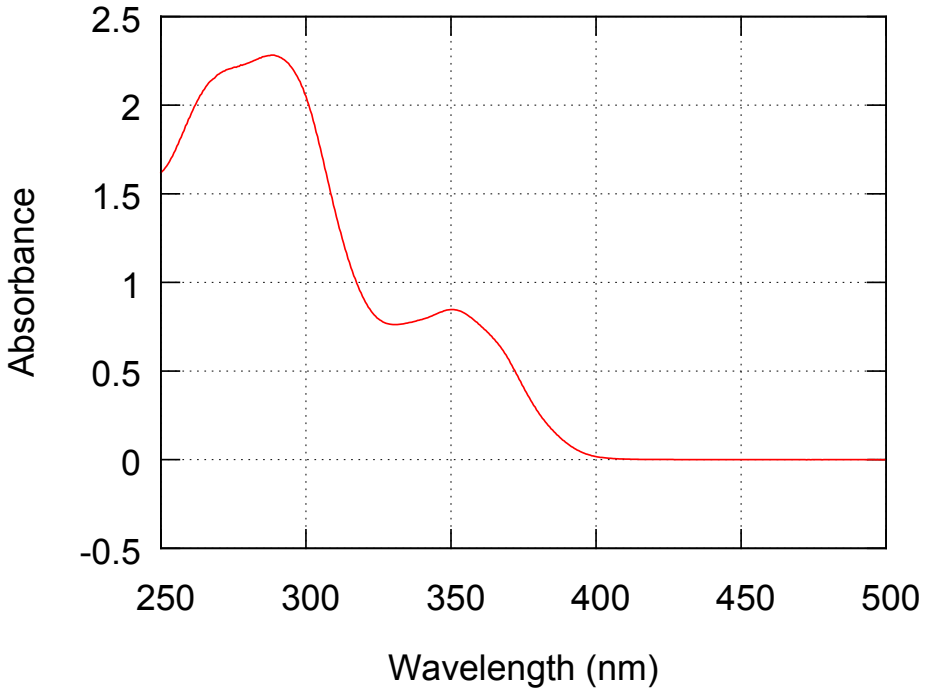

Figure S162. UV-vis absorption spectrum of **3b(10/90)** in *n*-octane (3.28×10^{-2} g/L, path length = 10 mm).

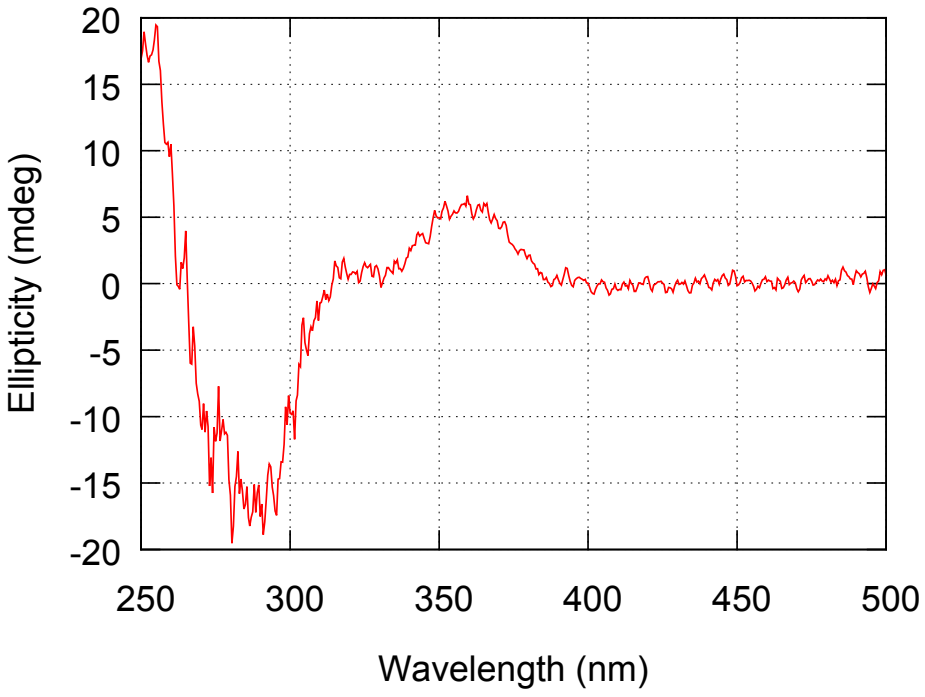

Figure S163. CD spectrum of **3b(10/90)** in *n*-octane (3.28×10^{-2} g/L, path length = 10 mm).

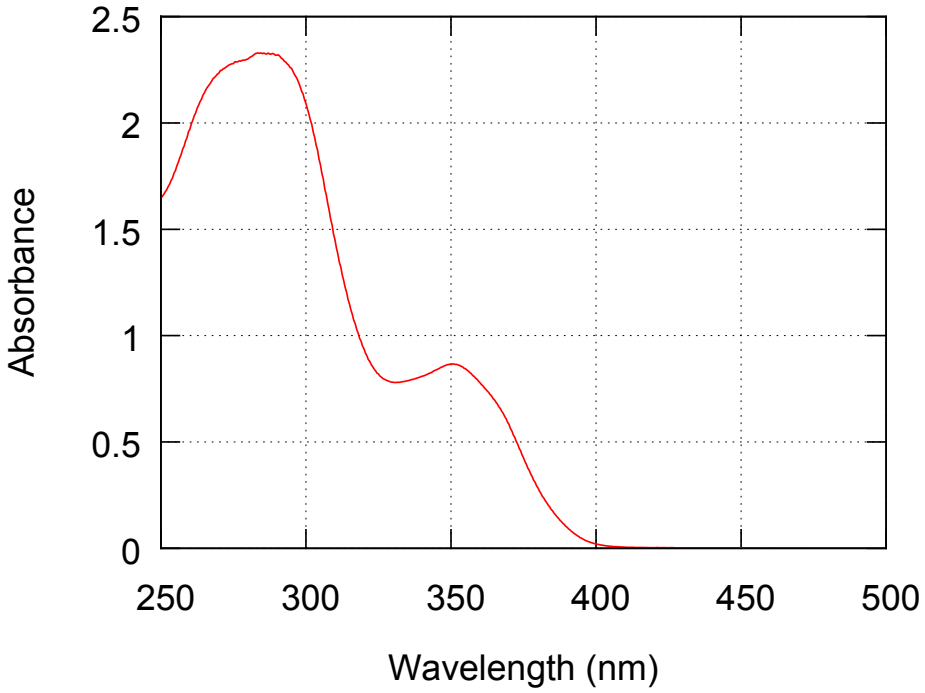

Figure S164. UV-vis absorption spectrum of **3b(10/90)** in *n*-nonane (3.28×10^{-2} g/L, path length = 10 mm).

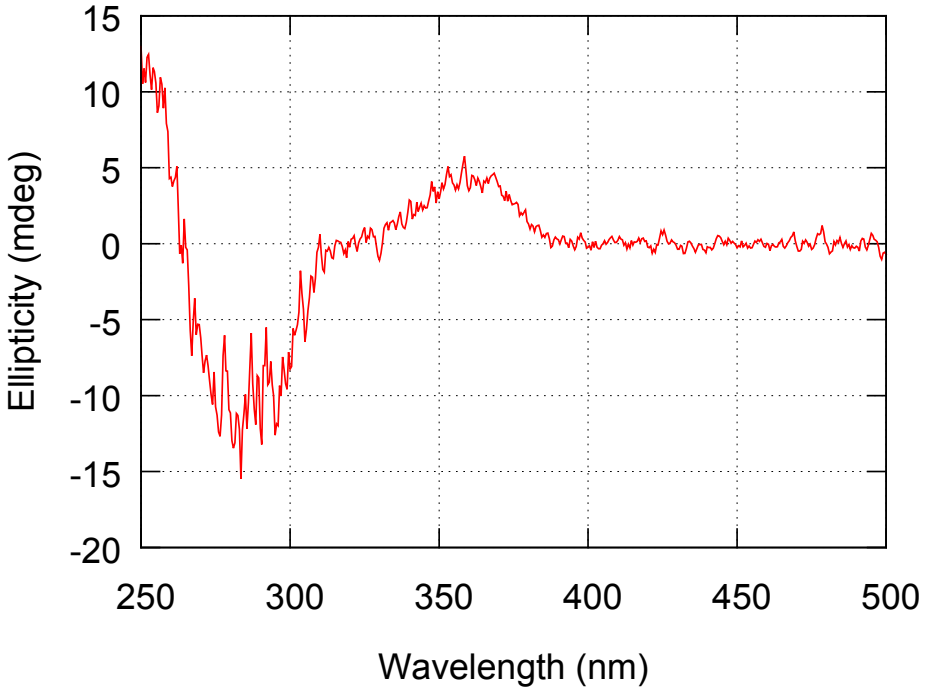

Figure S165. CD spectrum of **3b(10/90)** in *n*-nonane (3.28×10^{-2} g/L, path length = 10 mm).

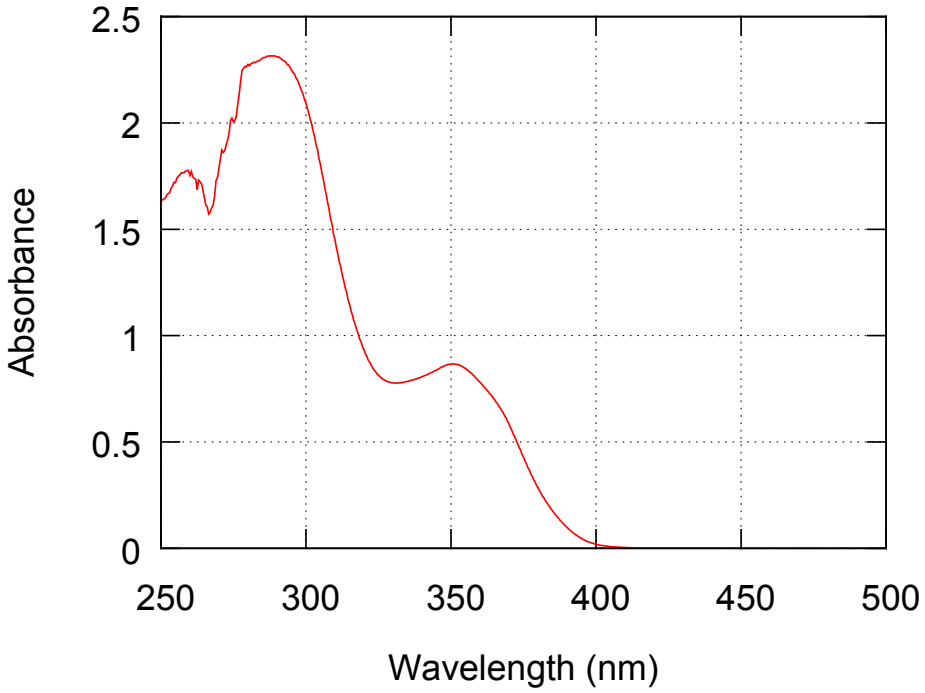

Figure S166. UV-vis absorption spectrum of **3b(10/90)** in *n*-decane (3.28×10^{-2} g/L, path length = 10 mm).

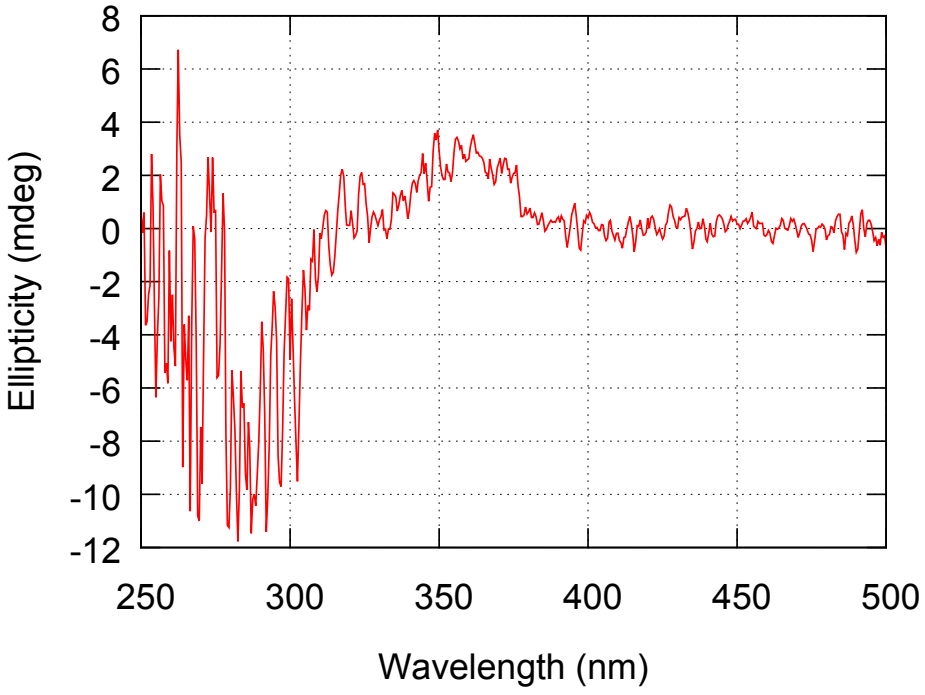

Figure S167. CD spectrum of **3b(10/90)** in *n*-decane (3.28×10^{-2} g/L, path length = 10 mm).

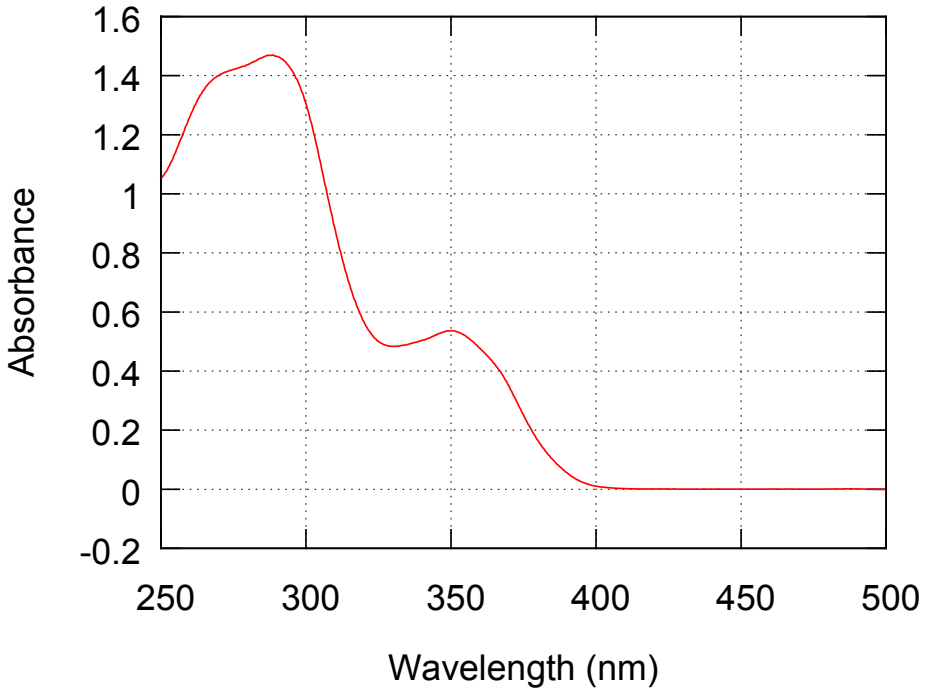

Figure S168. UV-vis absorption spectrum of **3b(15/85)** in *n*-pentane (2.09×10^{-2} g/L, path length = 10 mm).

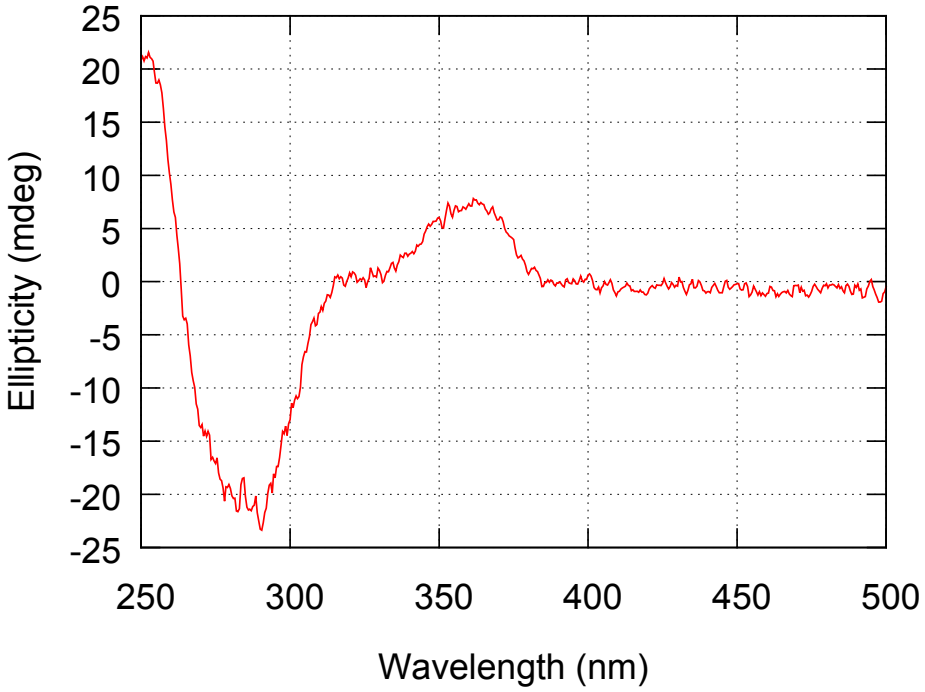

Figure S169. CD spectrum of **3b(15/85)** in *n*-pentane (2.09×10^{-2} g/L, path length = 10 mm).

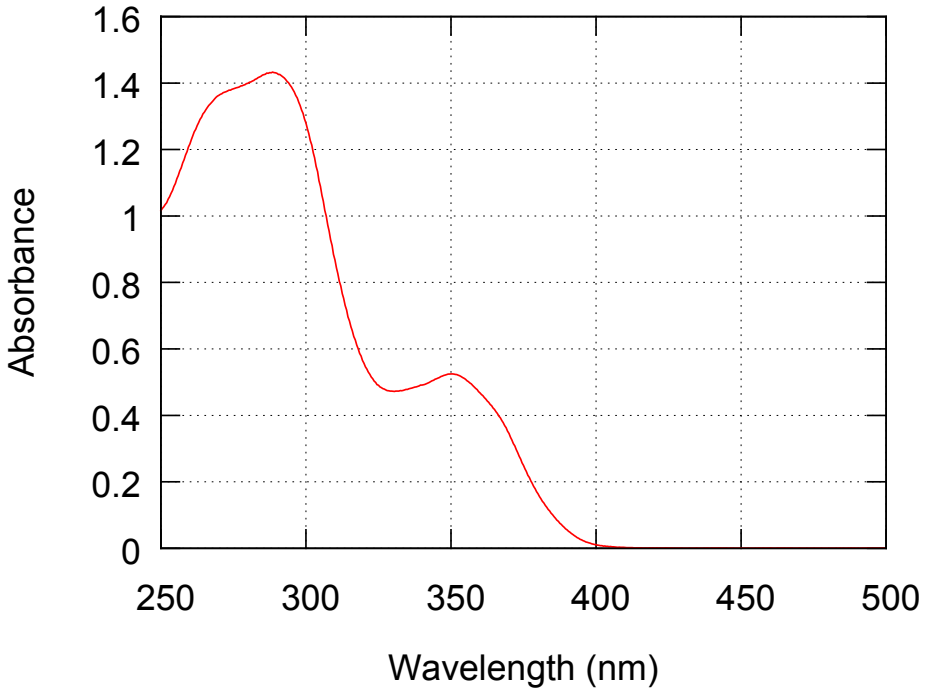

Figure S170. UV-vis absorption spectrum of **3b(15/85)** in *n*-hexane (2.09×10^{-2} g/L, path length = 10 mm).

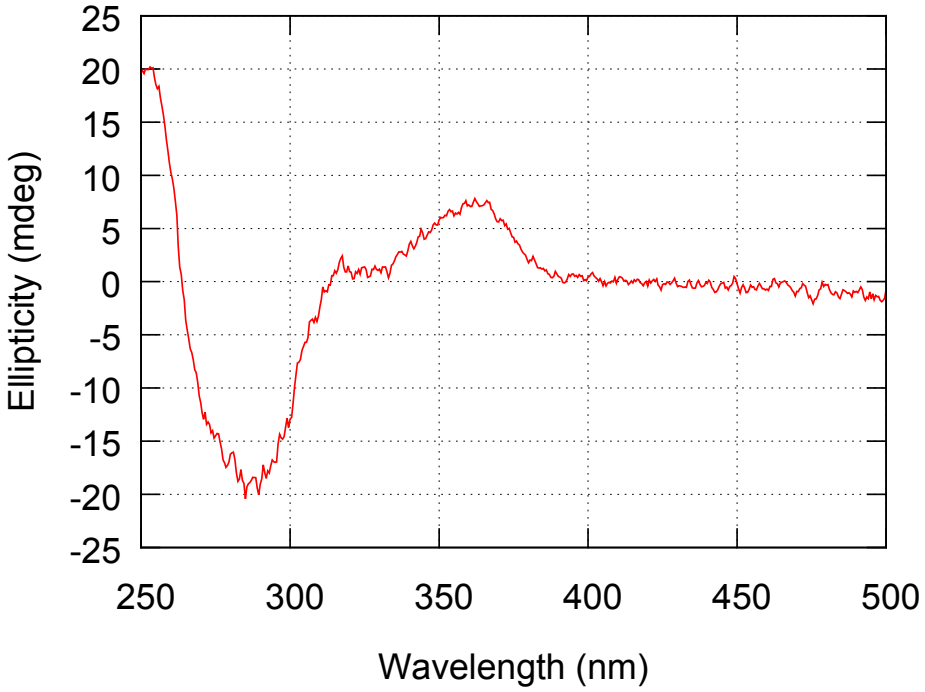

Figure S171. CD spectrum of **3b(15/85)** in *n*-hexane (2.09×10^{-2} g/L, path length = 10 mm).

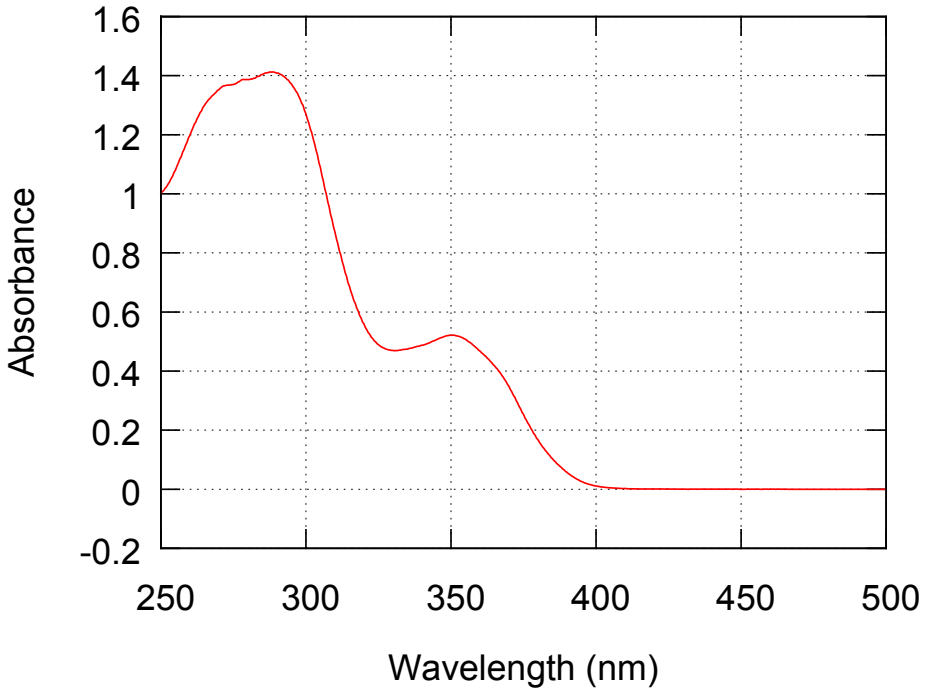

Figure S172. UV-vis absorption spectrum of **3b(15/85)** in *n*-heptane (2.09×10^{-2} g/L, path length = 10 mm).

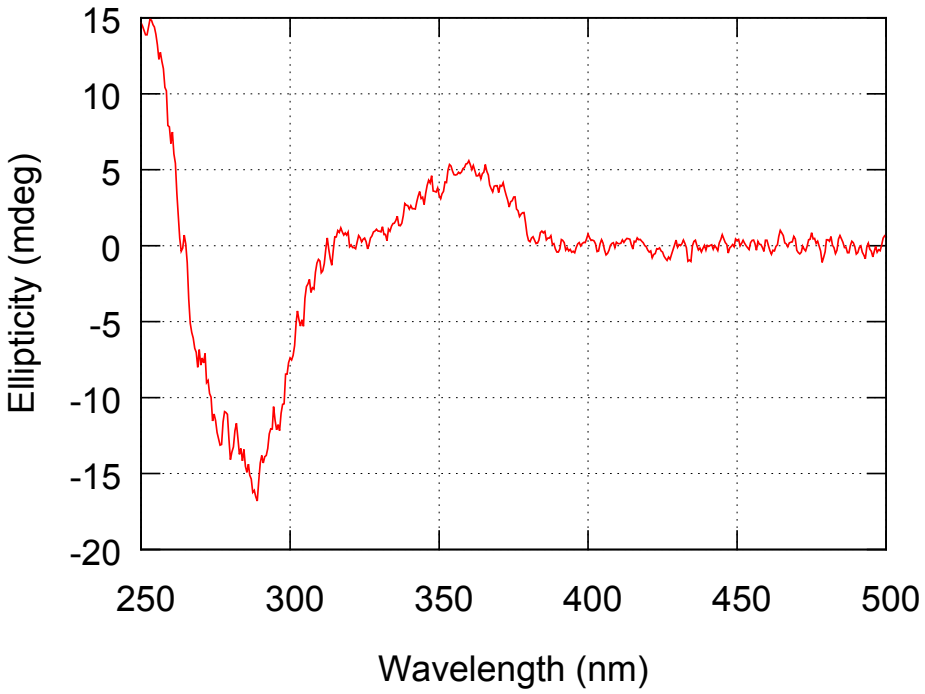

Figure S173. CD spectrum of **3b(15/85)** in *n*-heptane (2.09×10^{-2} g/L, path length = 10 mm).

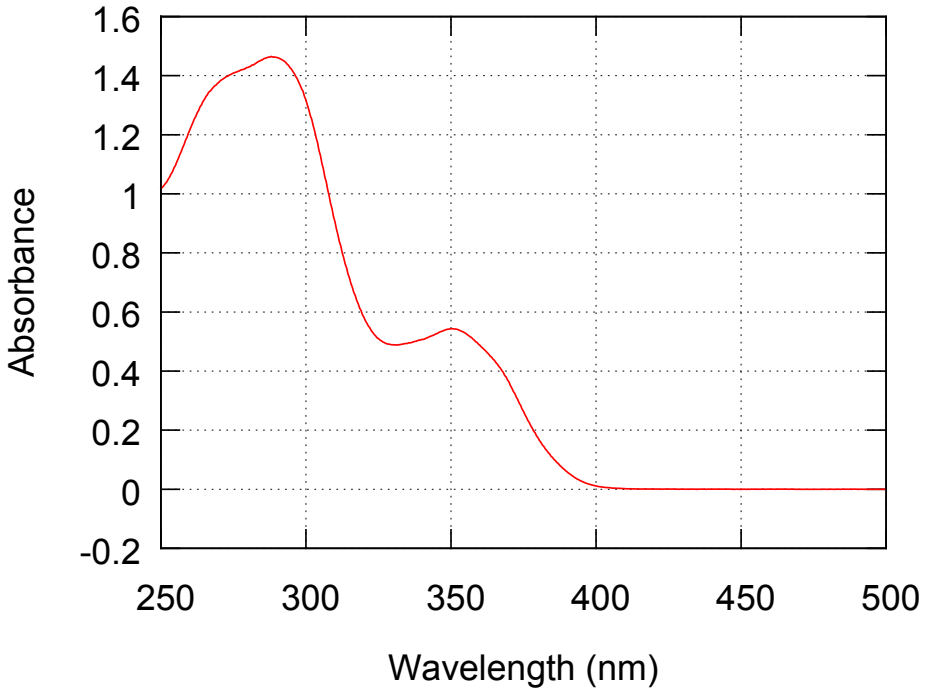

Figure S174. UV-vis absorption spectrum of **3b(15/85)** in *n*-octane (2.09×10^{-2} g/L, path length = 10 mm).

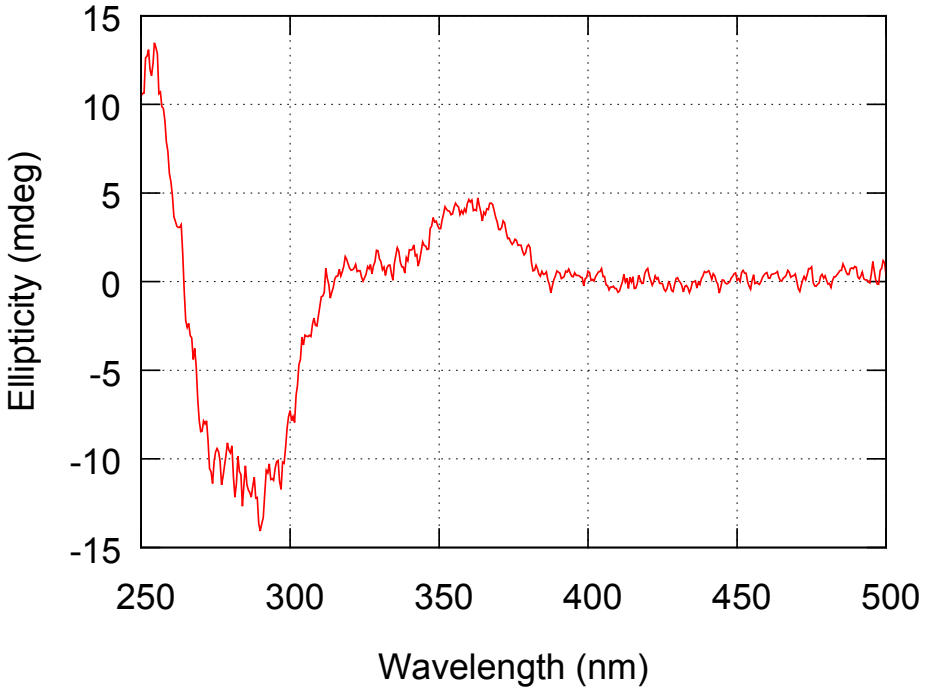

Figure S175. CD spectrum of **3b(15/85)** in *n*-octane (2.09×10^{-2} g/L, path length = 10 mm).

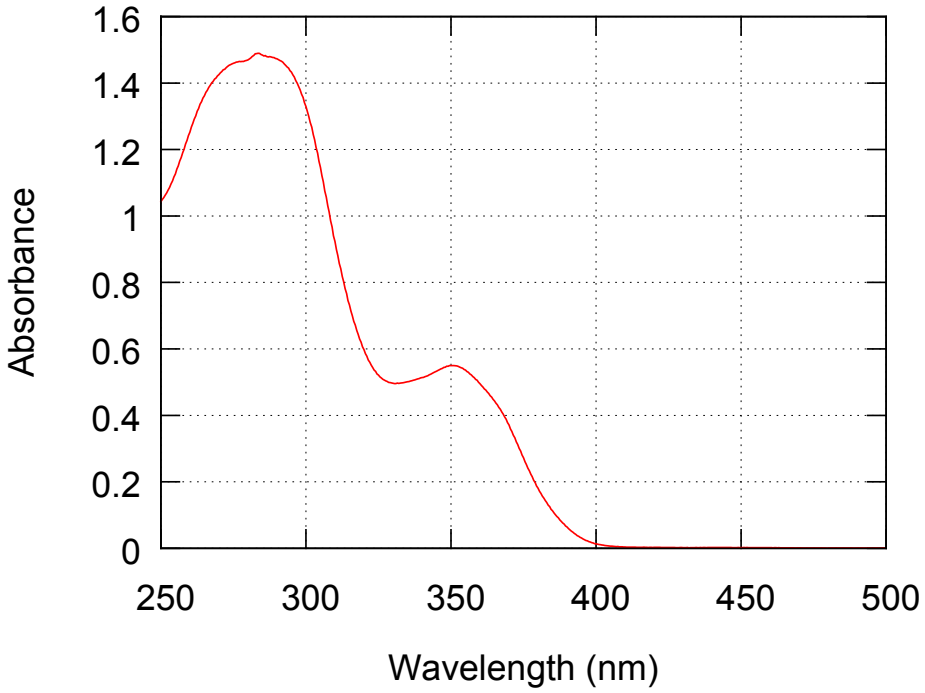

Figure S176. UV-vis absorption spectrum of **3b(15/85)** in *n*-nonane (2.09×10^{-2} g/L, path length = 10 mm).

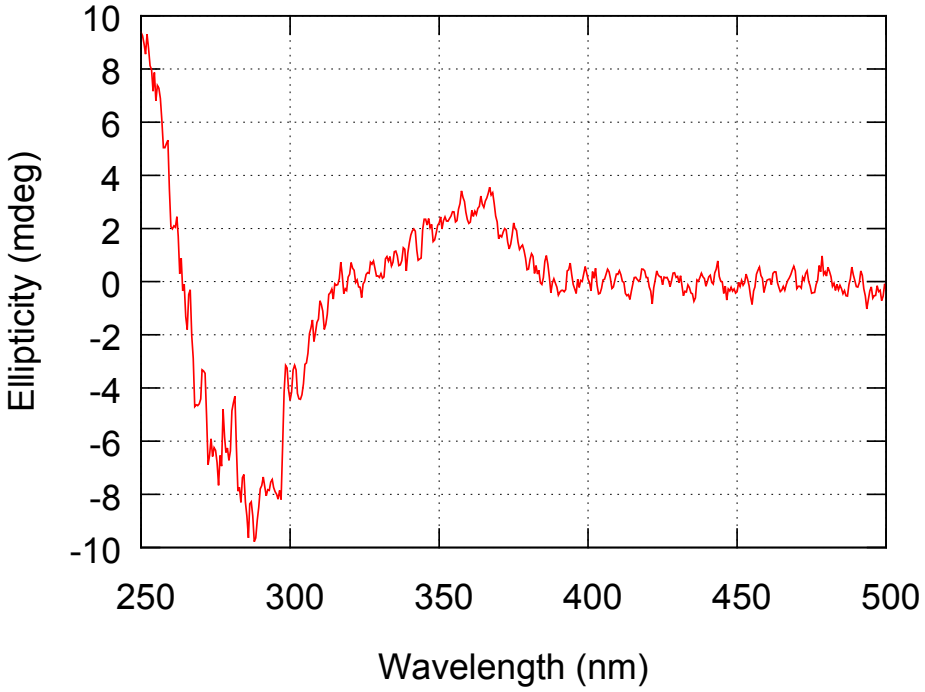

Figure S177. CD spectrum of **3b(15/85)** in *n*-nonane (2.09×10^{-2} g/L, path length = 10 mm).

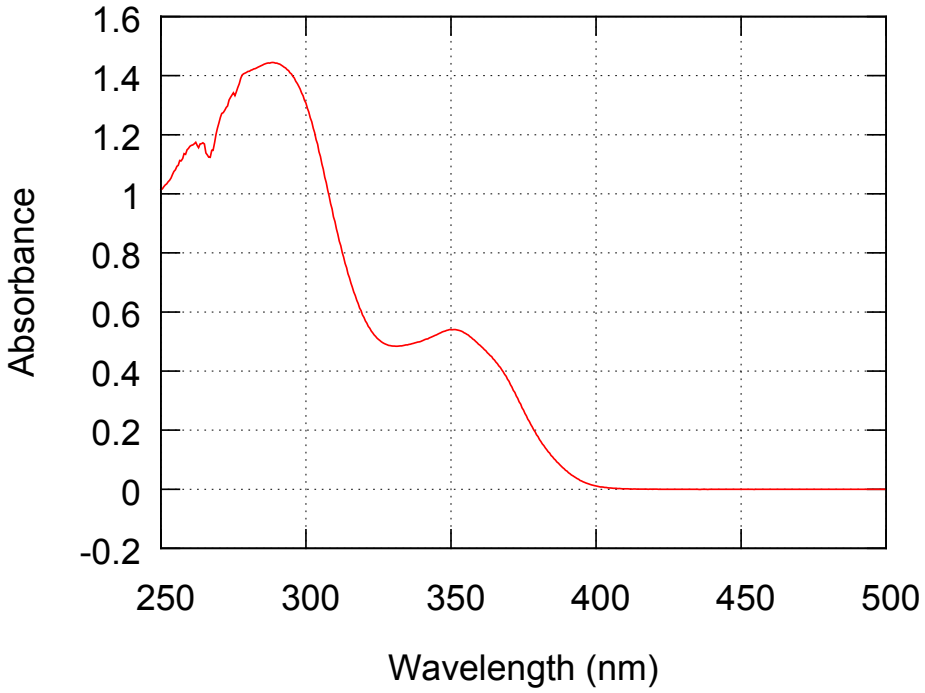

Figure S178. UV-vis absorption spectrum of **3b(15/85)** in *n*-decane (2.09×10^{-2} g/L, path length = 10 mm).

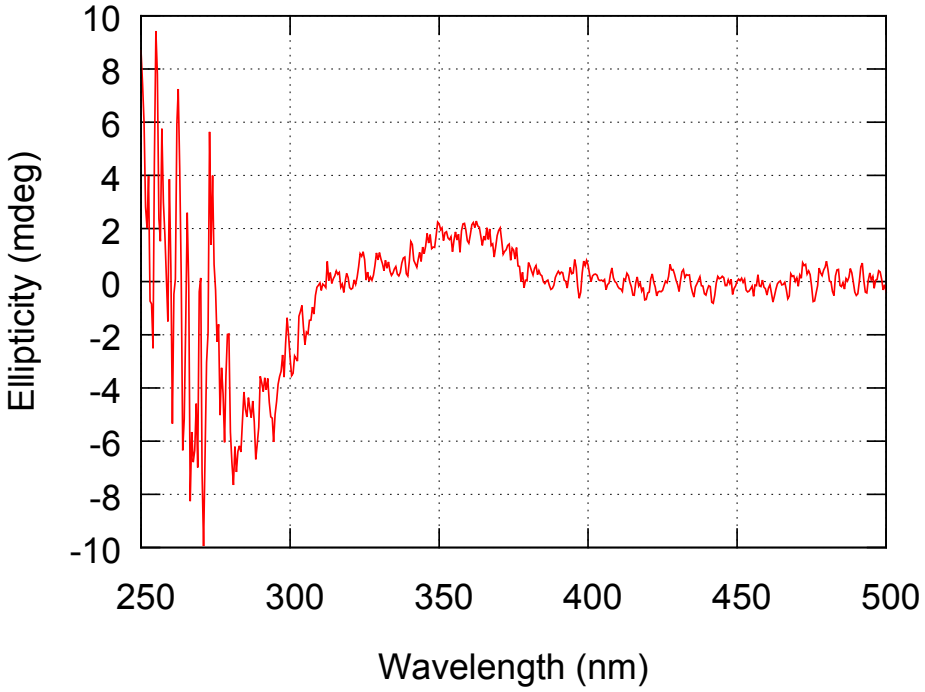

Figure S179. CD spectrum of **3b(15/85)** in *n*-decane (2.09×10^{-2} g/L, path length = 10 mm).

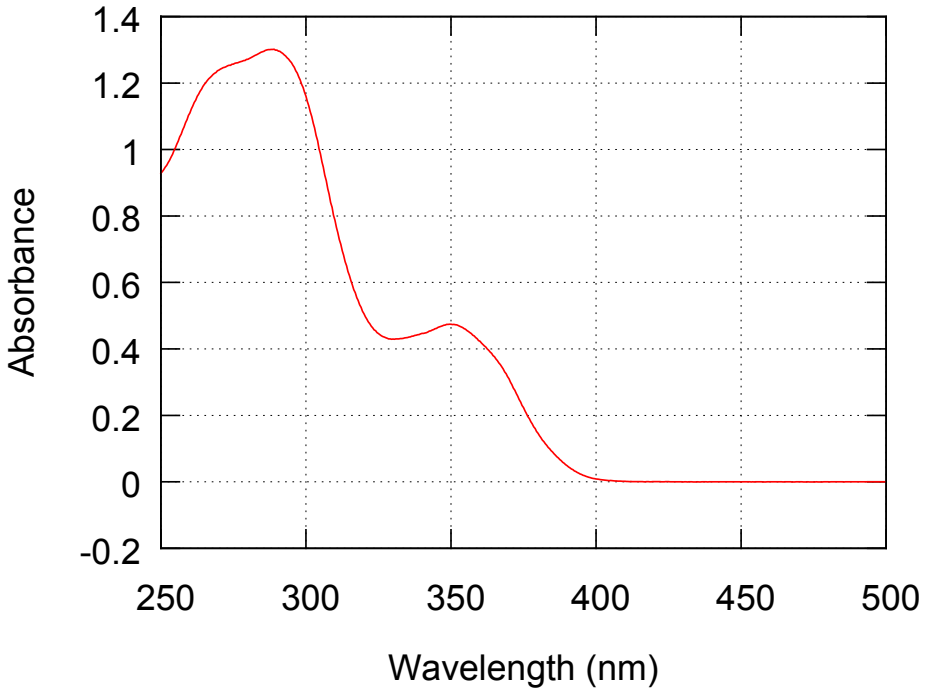

Figure S180. UV-vis absorption spectrum of **3b(20/80)** in *n*-pentane (1.88×10^{-2} g/L, path length = 10 mm).

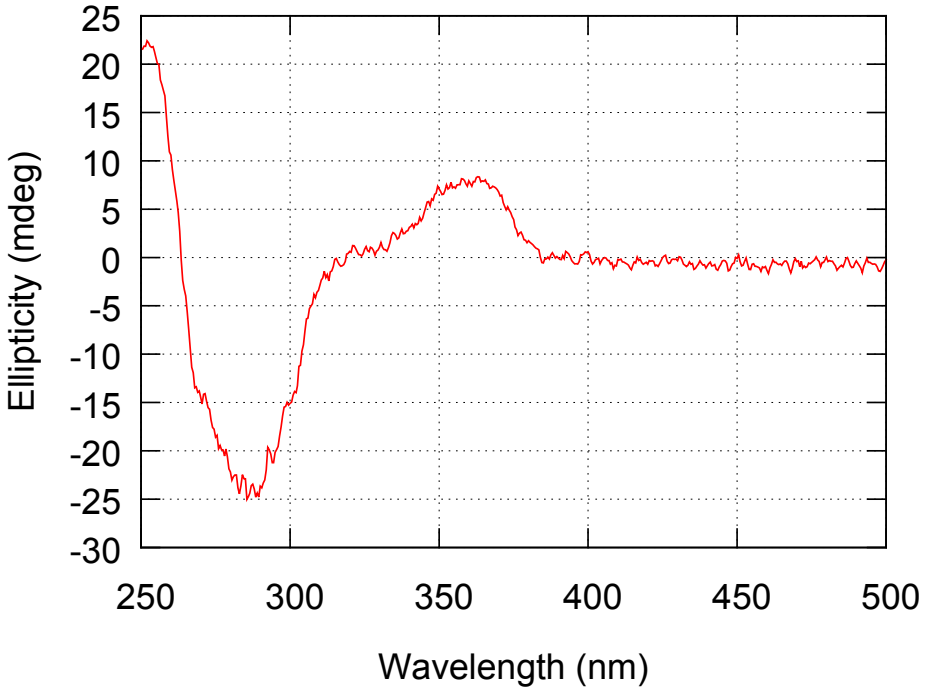

Figure S181. CD spectrum of **3b(20/80)** in *n*-pentane (1.88×10^{-2} g/L, path length = 10 mm).

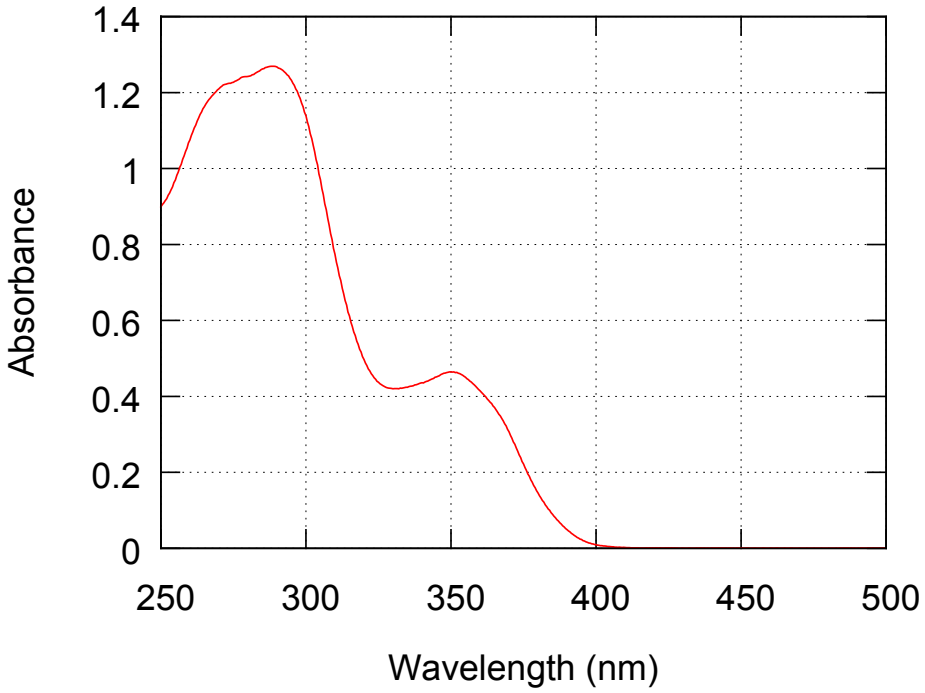

Figure S182. UV-vis absorption spectrum of **3b(20/80)** in *n*-hexane (1.88×10^{-2} g/L, path length = 10 mm).

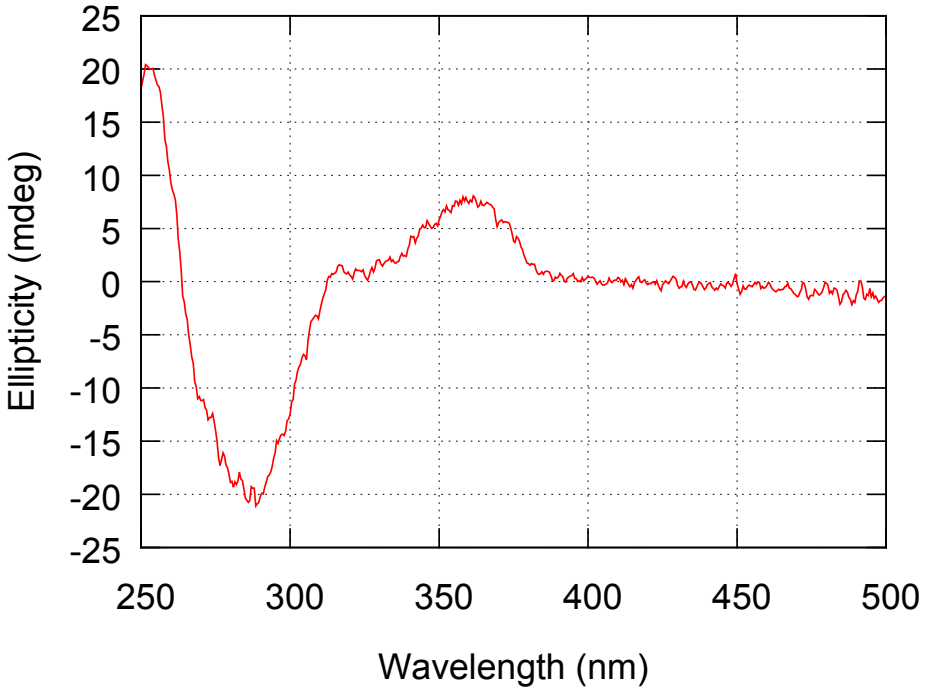

Figure S183. CD spectrum of **3b(20/80)** in *n*-hexane (1.88×10^{-2} g/L, path length = 10 mm).

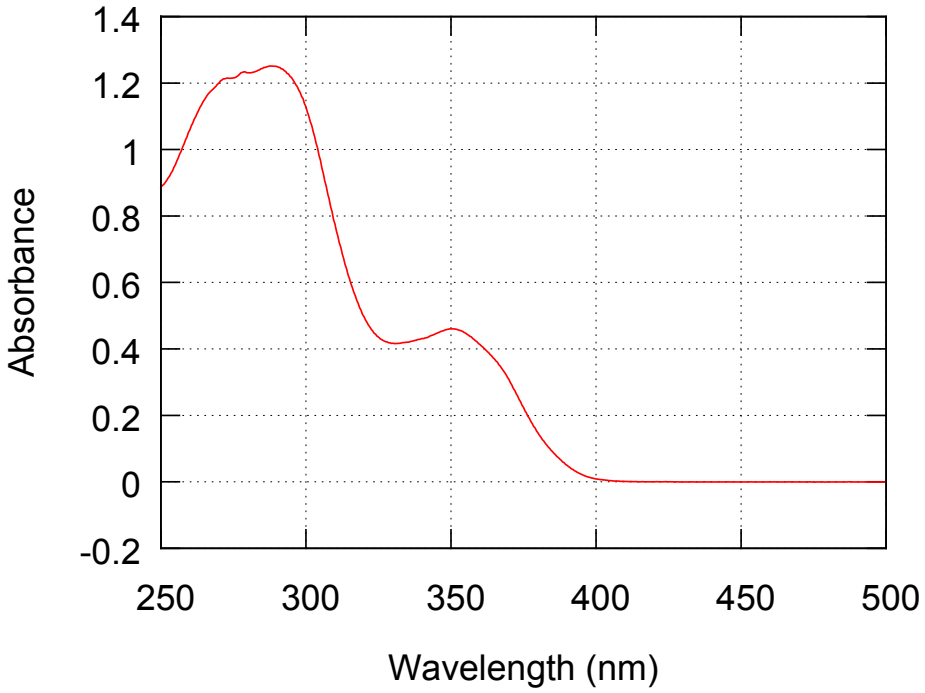

Figure S184. UV-vis absorption spectrum of **3b(20/80)** in *n*-heptane (1.88×10^{-2} g/L, path length = 10 mm).

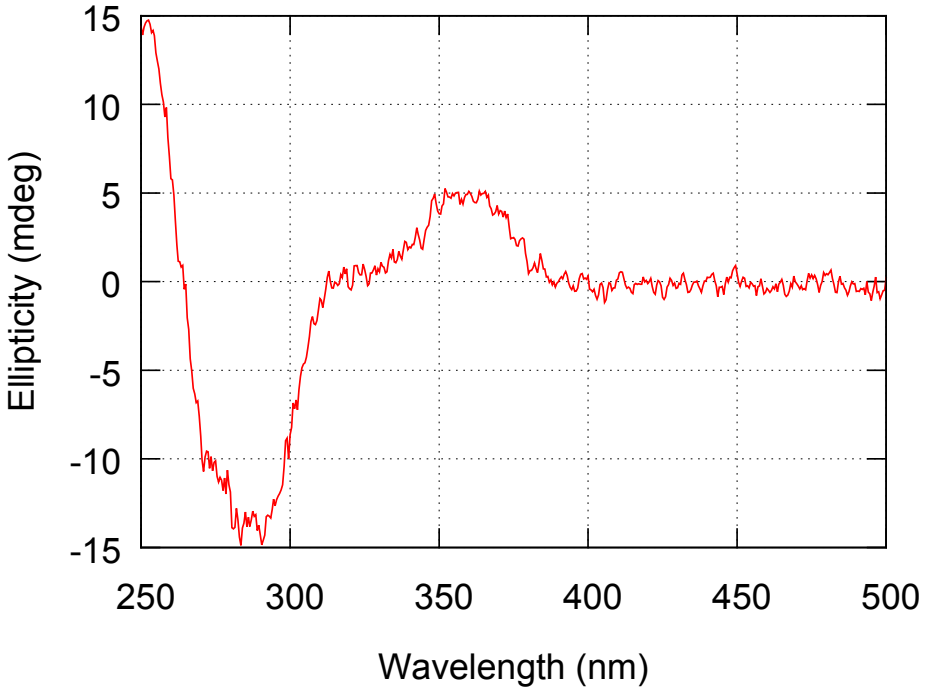

Figure S185. CD spectrum of **3b(20/80)** in *n*-heptane (1.88×10^{-2} g/L, path length = 10 mm).

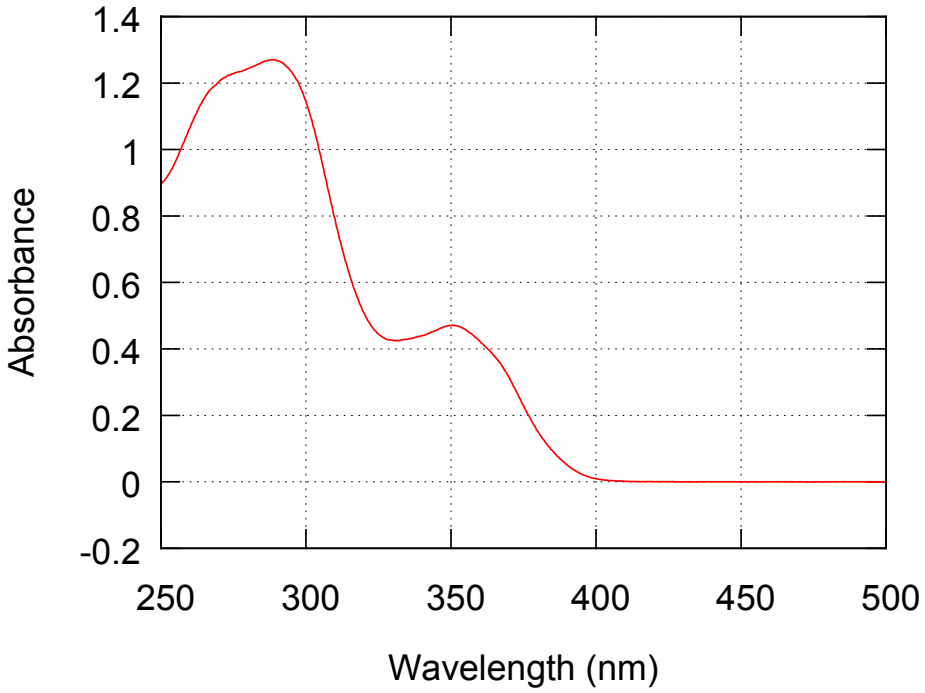

Figure S186. UV-vis absorption spectrum of **3b(20/80)** in *n*-octane (1.88×10^{-2} g/L, path length = 10 mm).

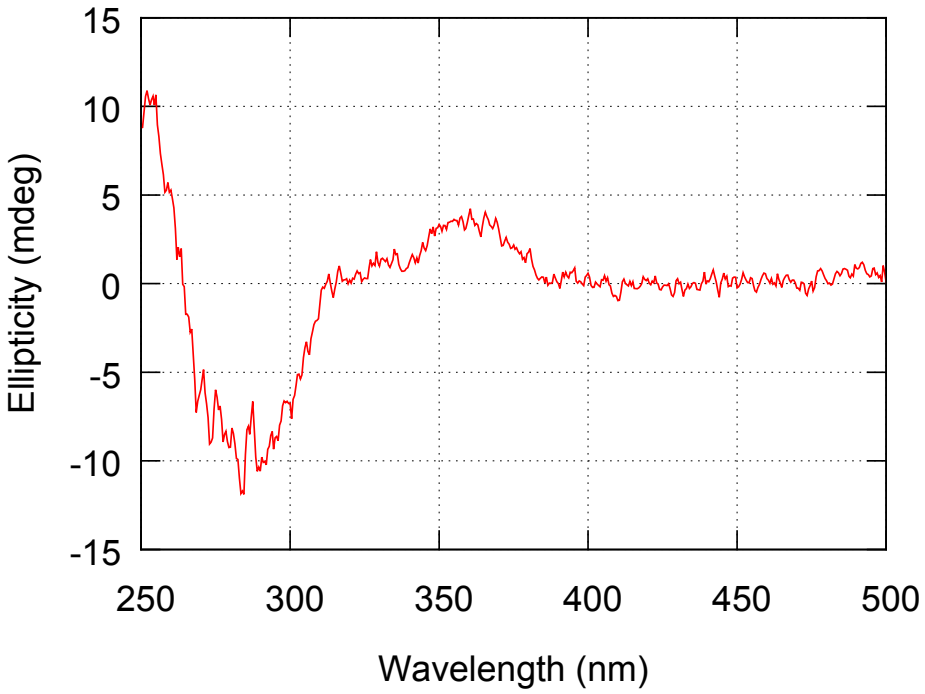

Figure S187. CD spectrum of **3b(20/80)** in *n*-octane (1.88×10^{-2} g/L, path length = 10 mm).

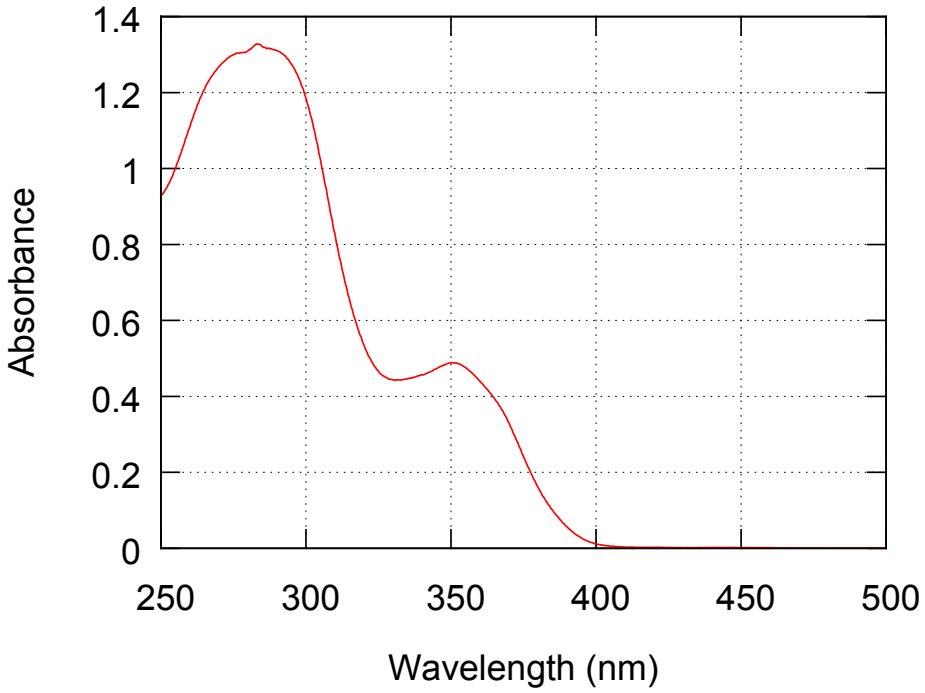

Figure S188. UV-vis absorption spectrum of **3b(20/80)** in *n*-nonane (1.88×10^{-2} g/L, path length = 10 mm).

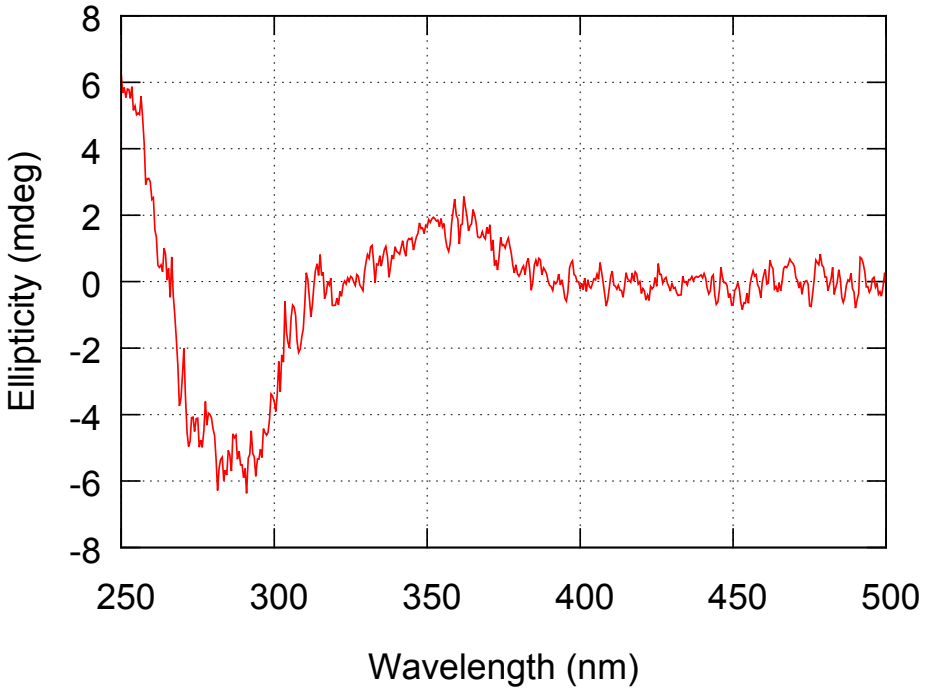

Figure S189. CD spectrum of **3b(20/80)** in *n*-nonane (1.88×10^{-2} g/L, path length = 10 mm).

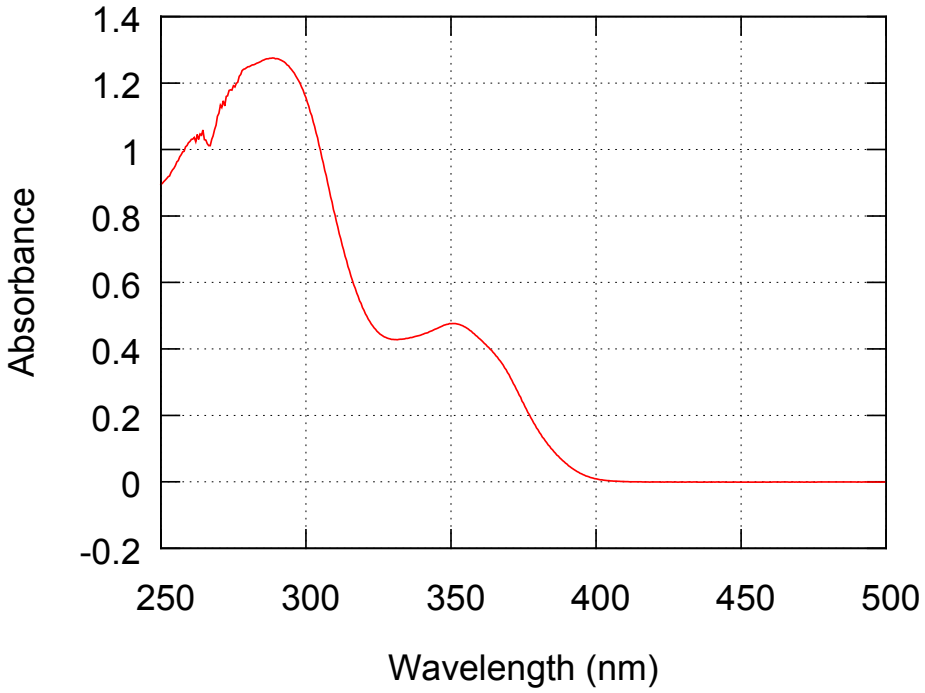

Figure S190. UV-vis absorption spectrum of **3b(20/80)** in *n*-decane (1.88×10^{-2} g/L, path length = 10 mm).

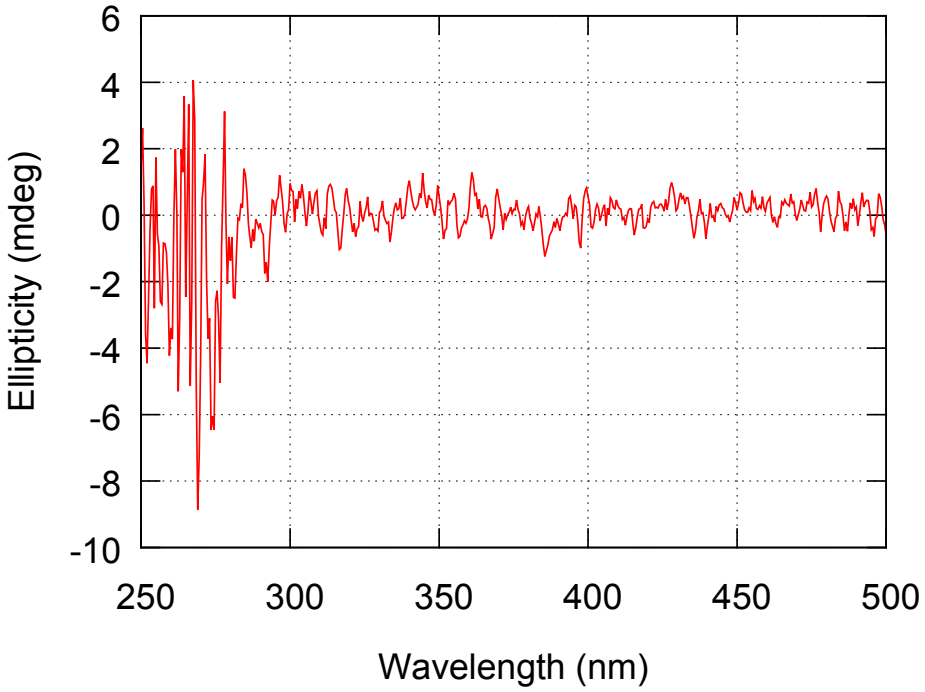

Figure S191. CD spectrum of **3b(20/80)** in *n*-decane (1.88×10^{-2} g/L, path length = 10 mm).

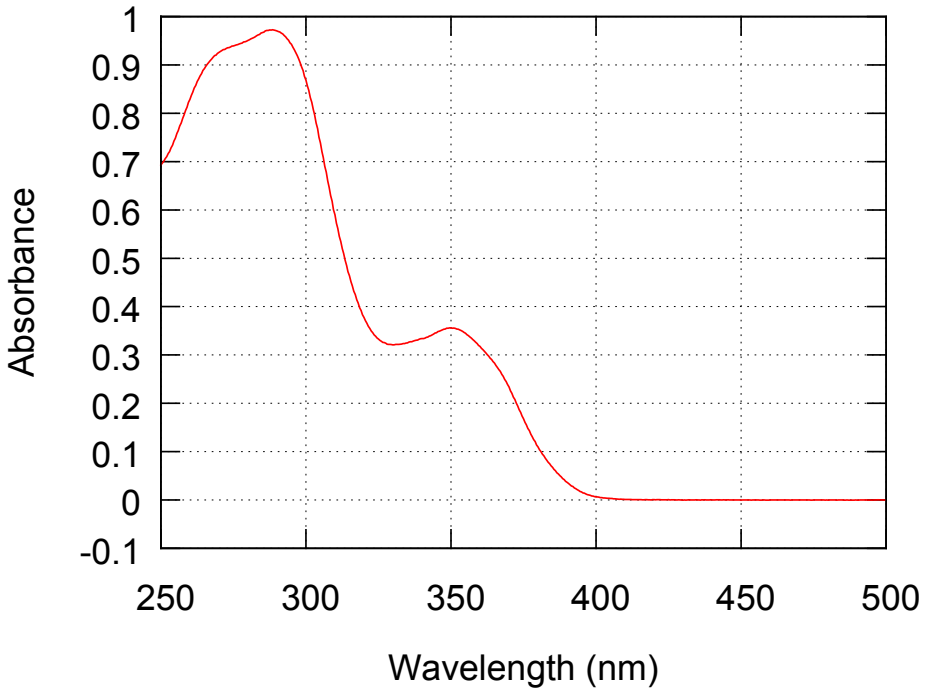

Figure S192. UV-vis absorption spectrum of **3b(30/70)** in *n*-pentane (1.83×10^{-2} g/L, path length = 10 mm).

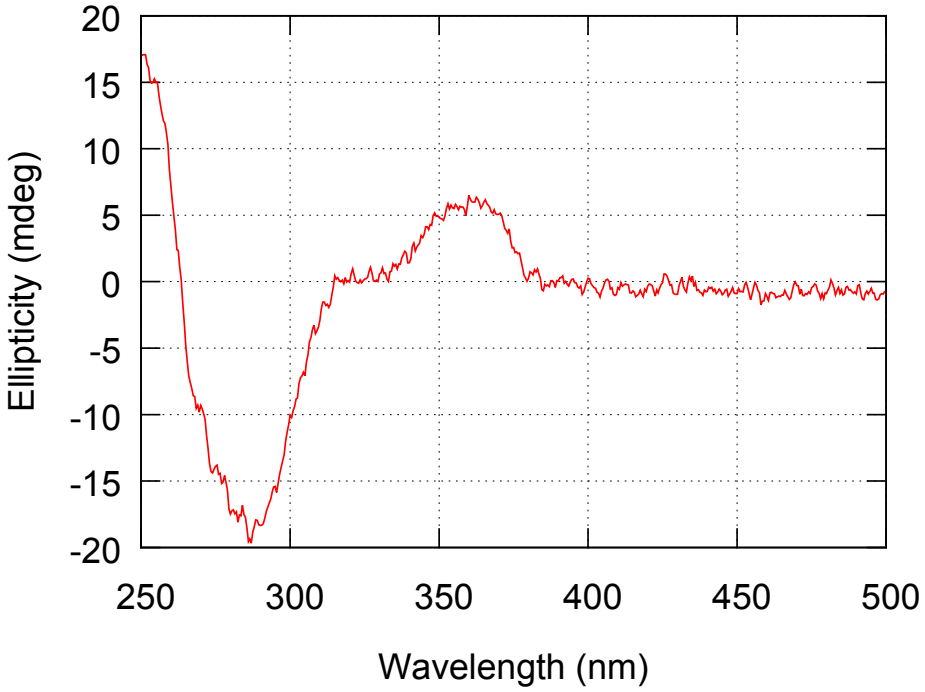

Figure S193. CD spectrum of **3b(30/70)** in *n*-pentane (1.83×10^{-2} g/L, path length = 10 mm).

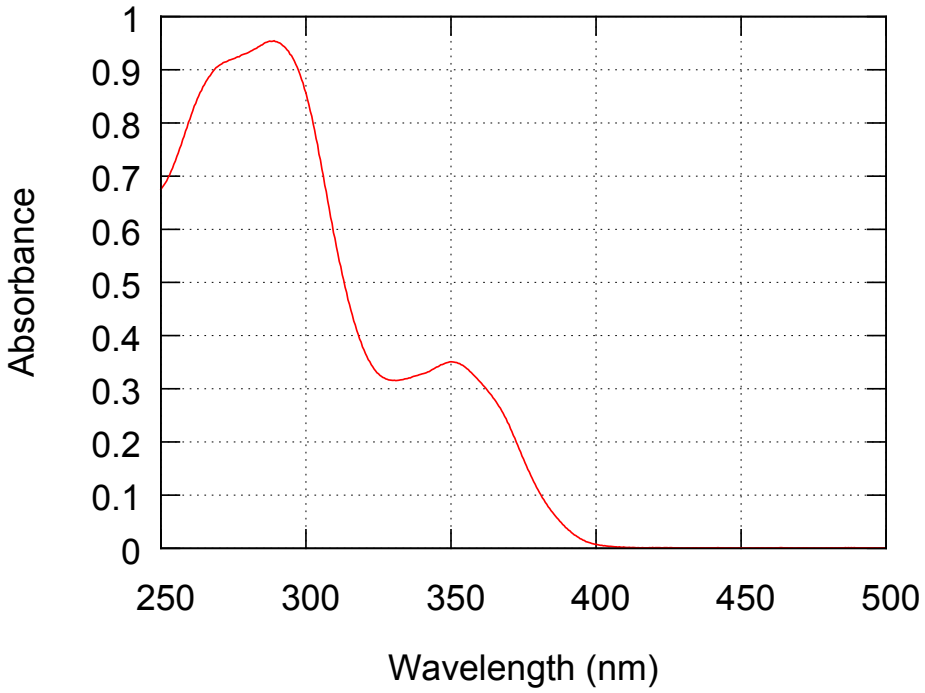

Figure S194. UV-vis absorption spectrum of **3b(30/70)** in *n*-hexane (1.83×10^{-2} g/L, path length = 10 mm).

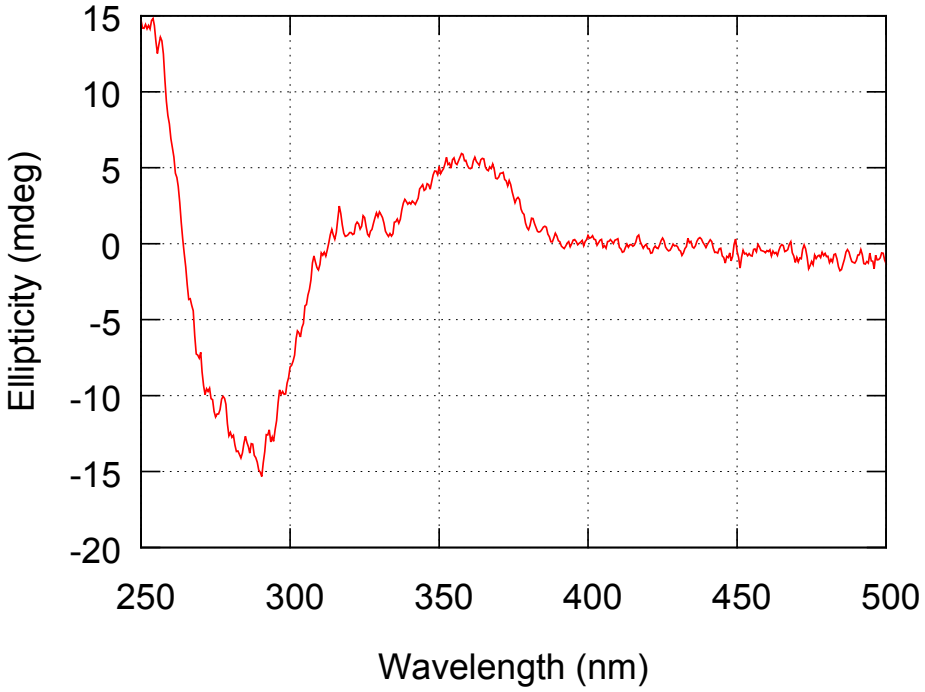

Figure S195. CD spectrum of **3b(30/70)** in *n*-hexane (1.83×10^{-2} g/L, path length = 10 mm).

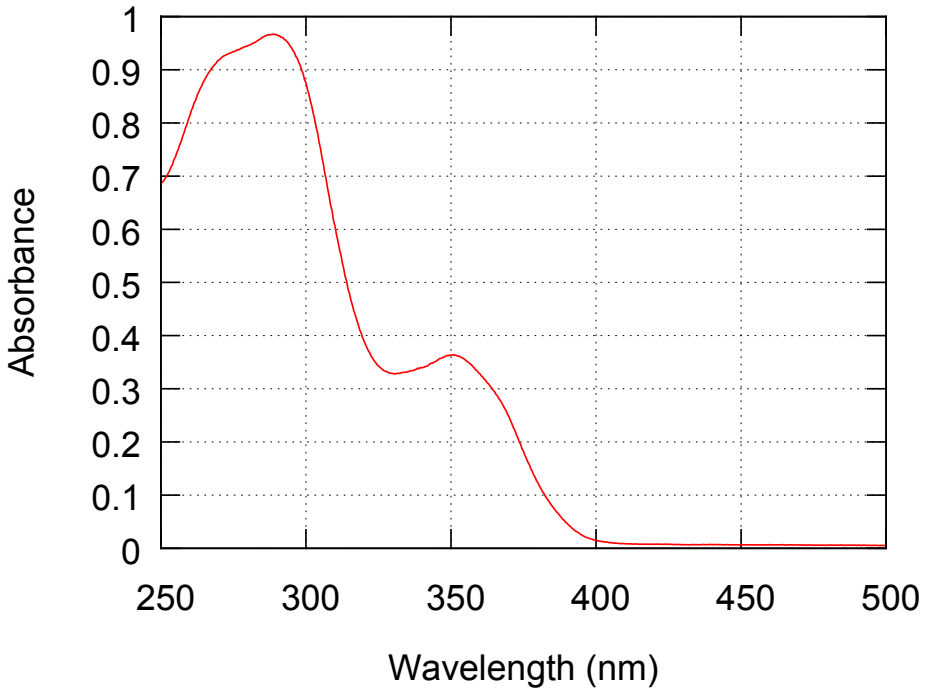

Figure S196. UV-vis absorption spectrum of **3b(30/70)** in *n*-heptane (1.83×10^{-2} g/L, path length = 10 mm).

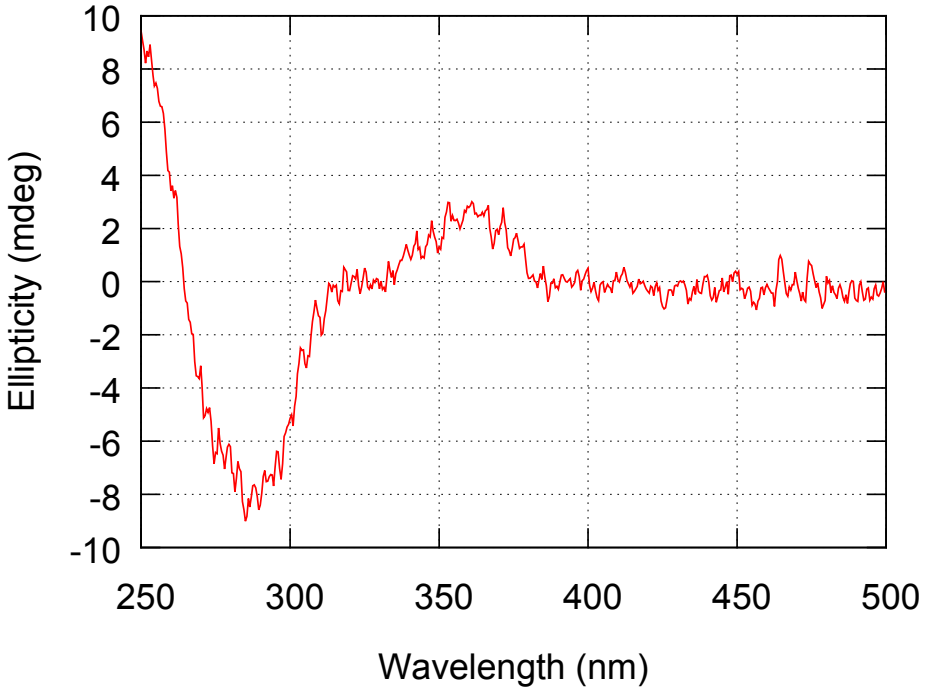

Figure S197. CD spectrum of **3b(30/70)** in *n*-heptane (1.83×10^{-2} g/L, path length = 10 mm).

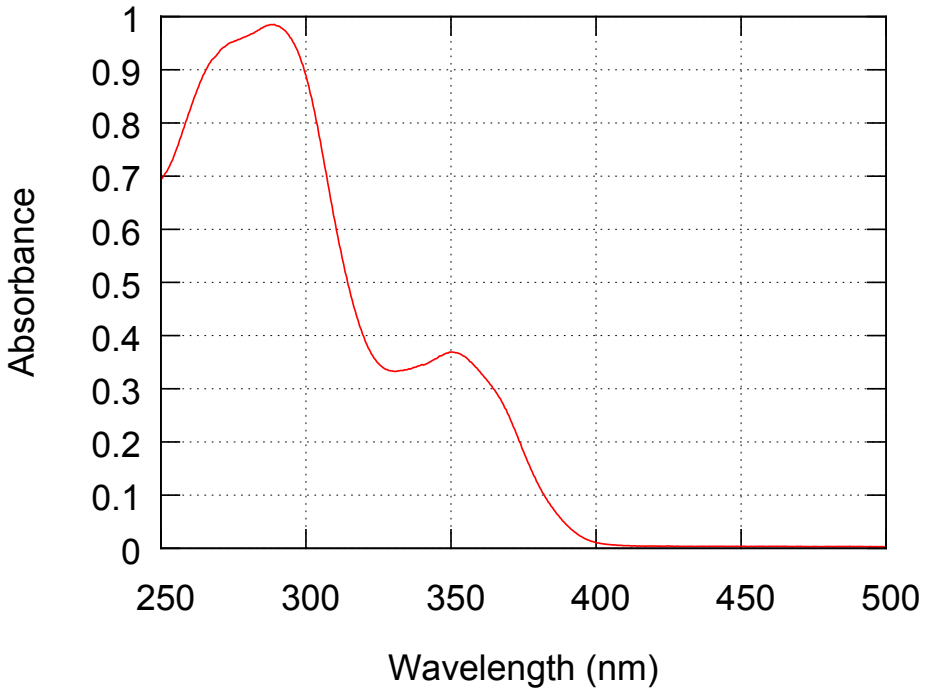

Figure S198. UV-vis absorption spectrum of **3b(30/70)** in *n*-octane (1.83×10^{-2} g/L, path length = 10 mm).

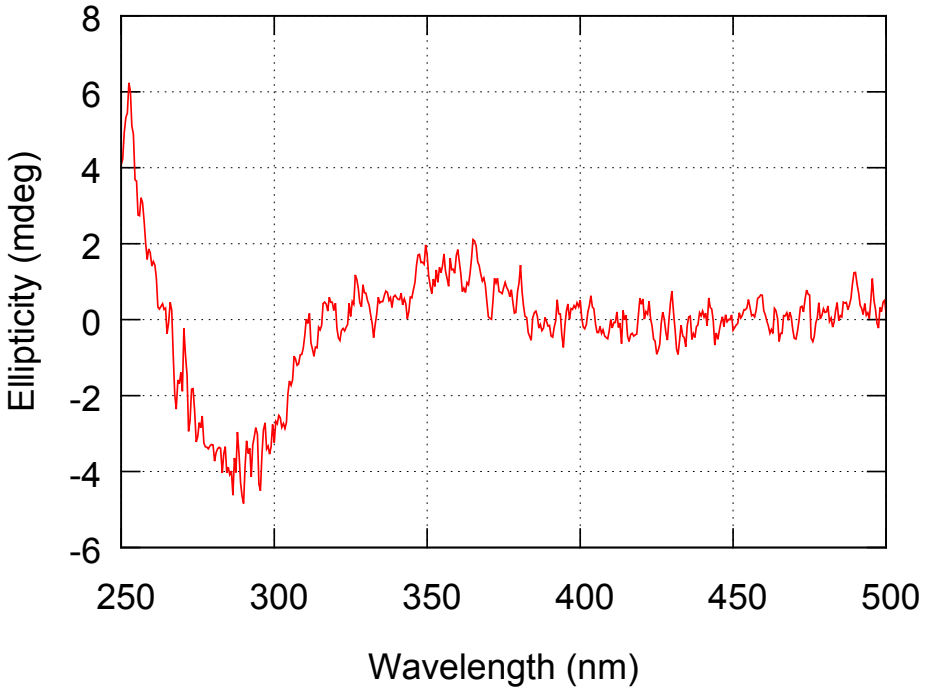

Figure S199. CD spectrum of **3b(30/70)** in *n*-octane (1.83×10^{-2} g/L, path length = 10 mm).

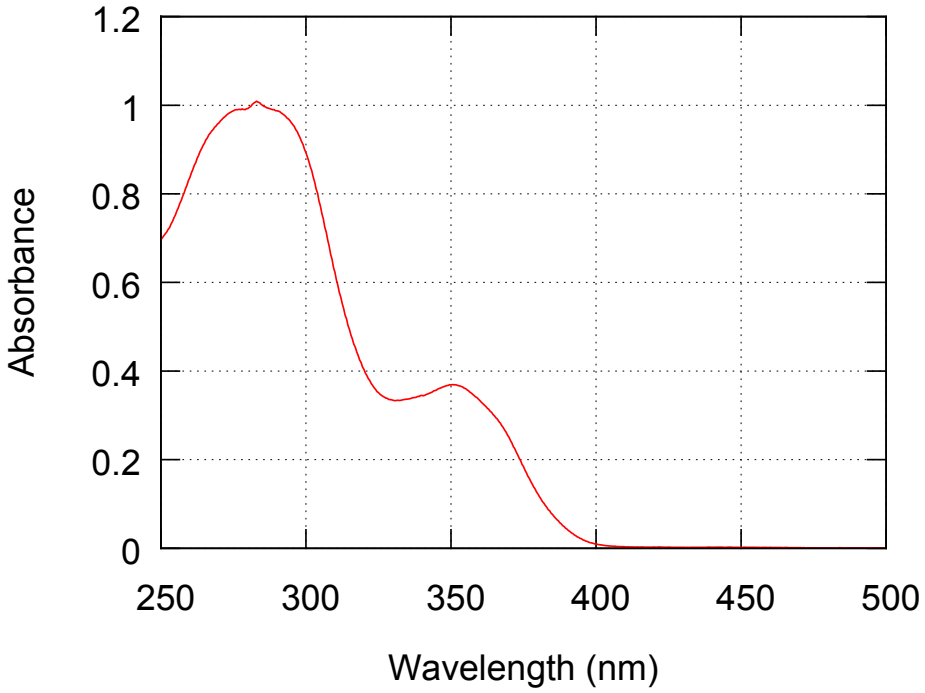

Figure S200. UV-vis absorption spectrum of **3b(30/70)** in *n*-nonane (1.83×10^{-2} g/L, path length = 10 mm).

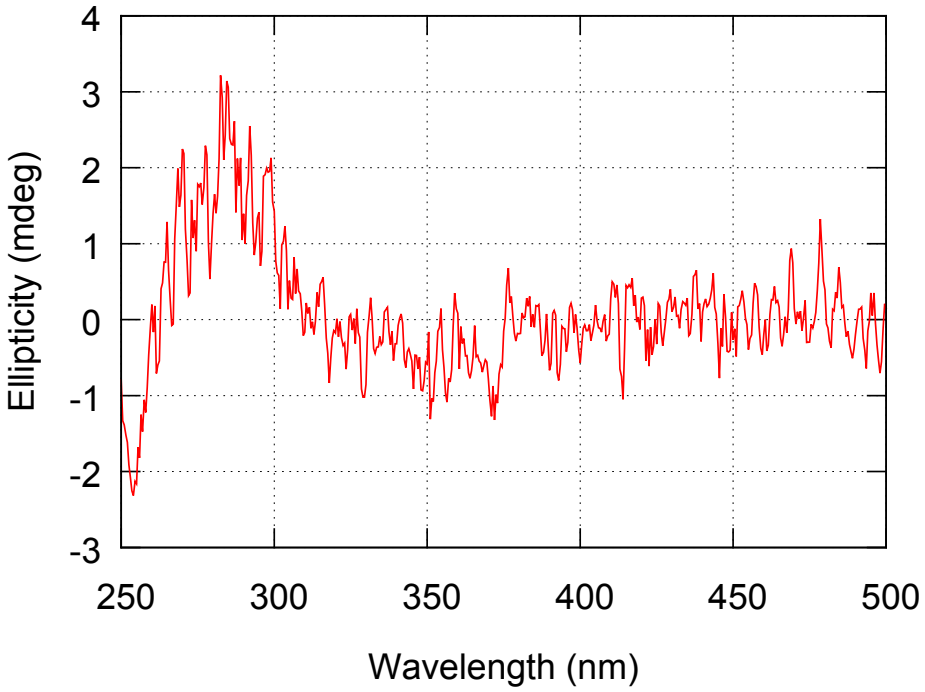

Figure S201. CD spectrum of **3b(30/70)** in *n*-nonane (1.83×10^{-2} g/L, path length = 10 mm).

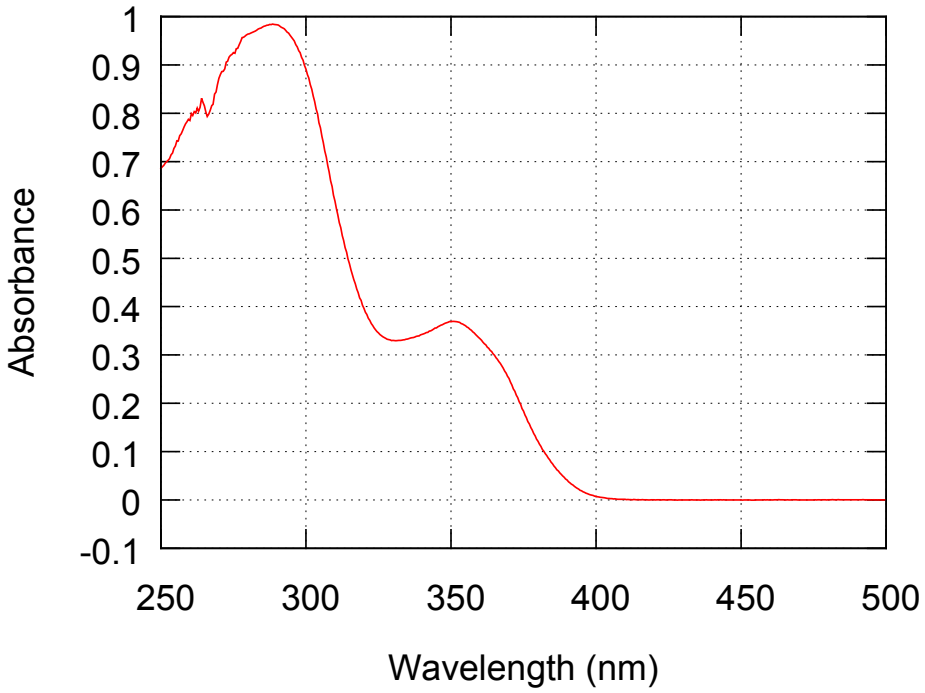

Figure S202. UV-vis absorption spectrum of **3b(30/70)** in *n*-decane (1.83×10^{-2} g/L, path length = 10 mm).

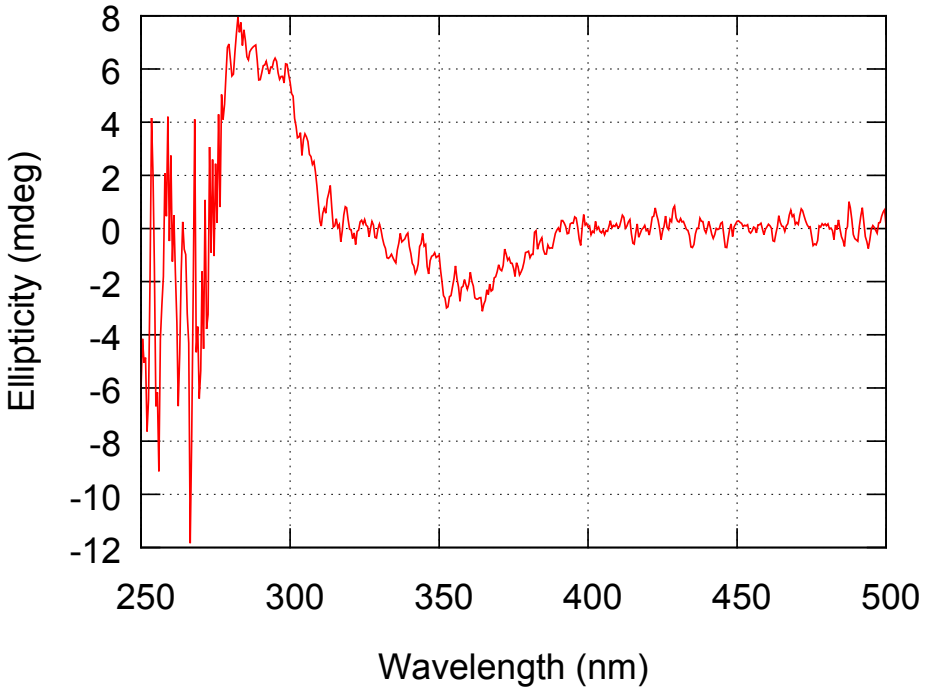

Figure S203. CD spectrum of **3b(30/70)** in *n*-decane (1.83×10^{-2} g/L, path length = 10 mm).

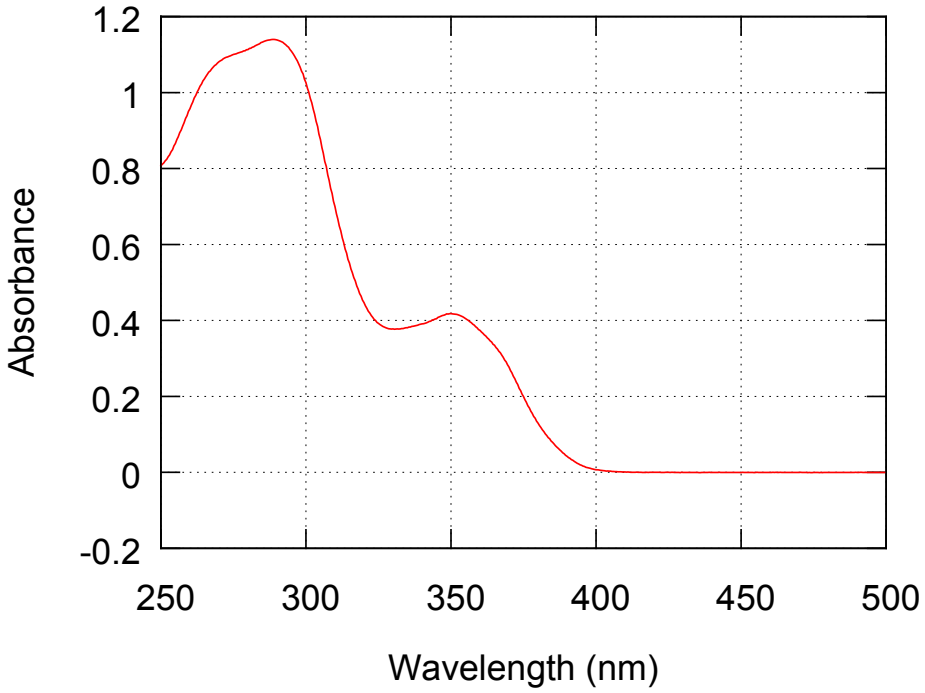

Figure S204. UV-vis absorption spectrum of **3b(60/40)** in *n*-pentane (2.02×10^{-2} g/L, path length = 10 mm).

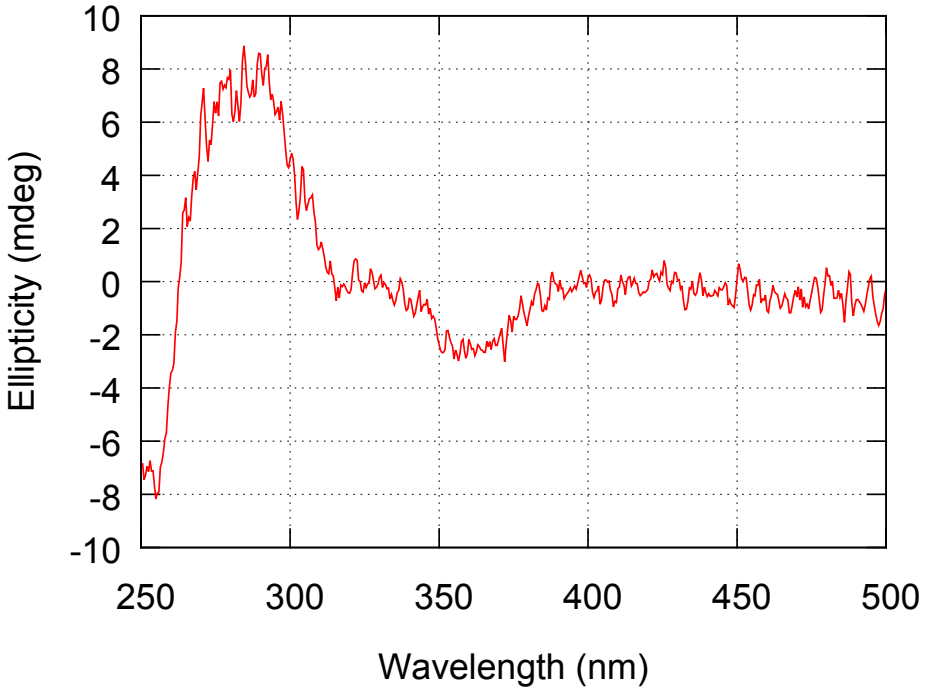

Figure S205. CD spectrum of **3b(60/40)** in *n*-pentane (2.02×10^{-2} g/L, path length = 10 mm).

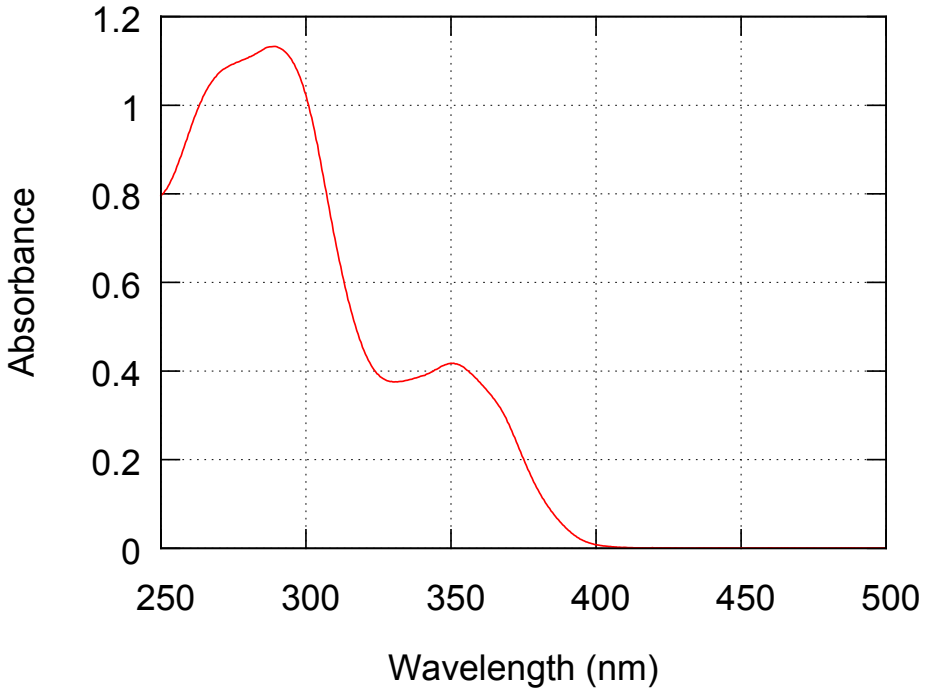

Figure S206. UV-vis absorption spectrum of **3b(60/40)** in *n*-hexane (2.02×10^{-2} g/L, path length = 10 mm).

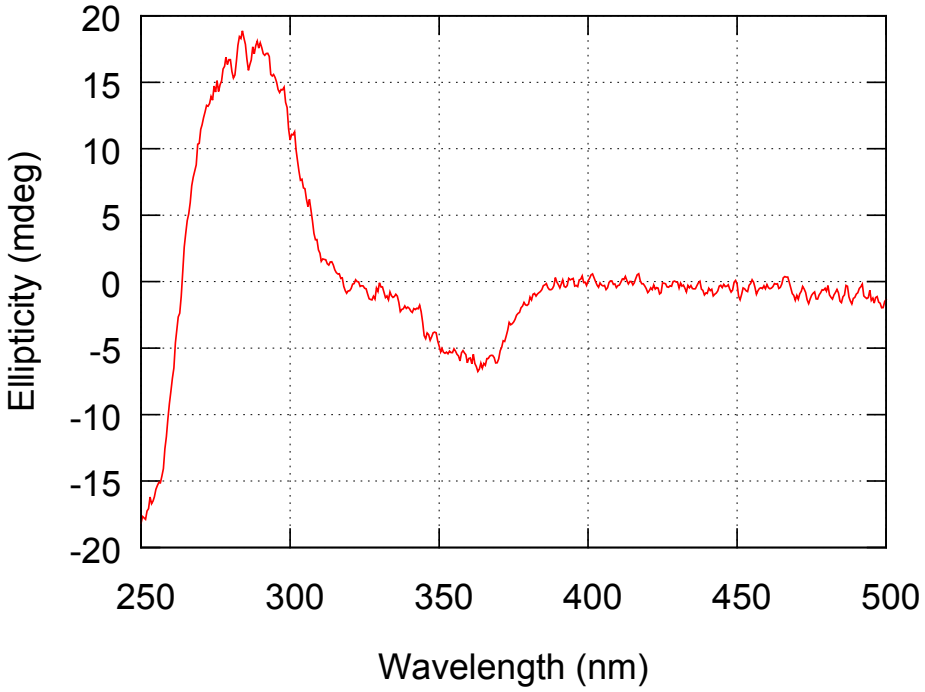

Figure S207. CD spectrum of **3b(60/40)** in *n*-hexane (2.02×10^{-2} g/L, path length = 10 mm).

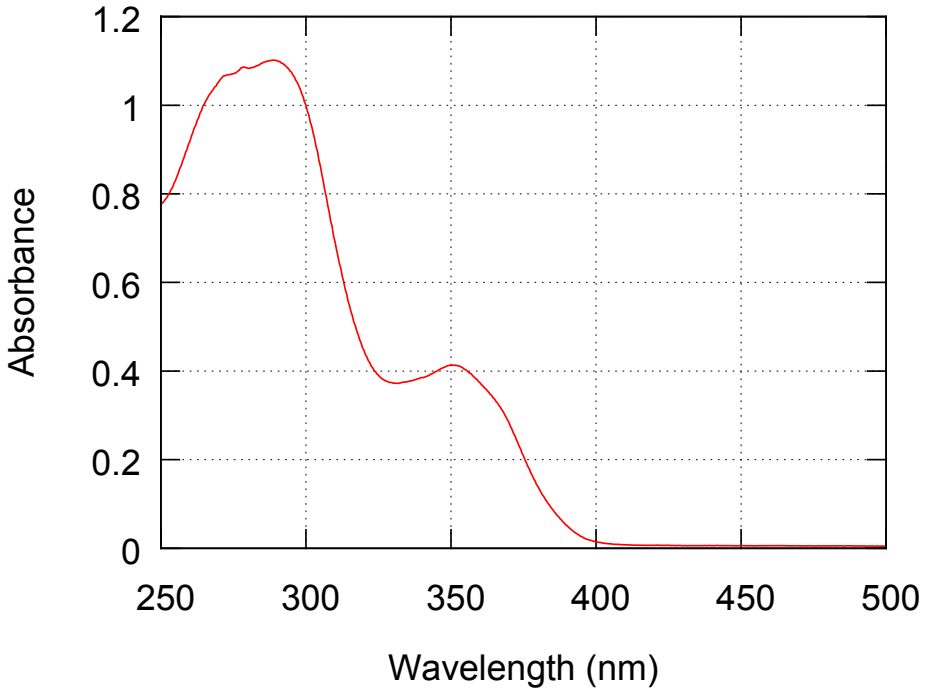

Figure S208. UV-vis absorption spectrum of **3b(60/40)** in *n*-heptane (2.02×10^{-2} g/L, path length = 10 mm).

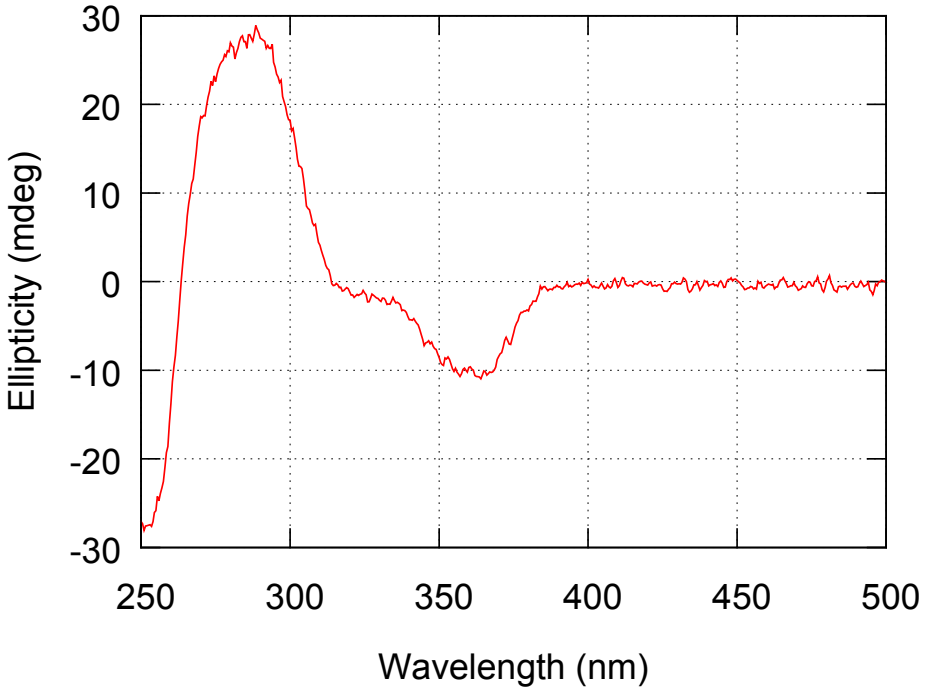

Figure S209. CD spectrum of **3b(60/40)** in *n*-heptane (2.02×10^{-2} g/L, path length = 10 mm).

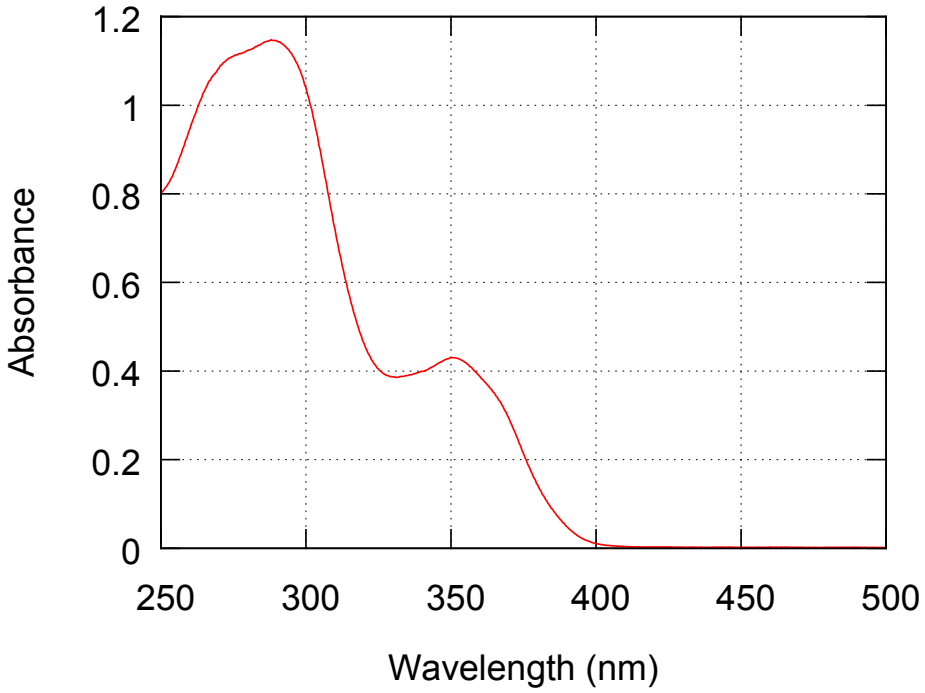

Figure S210. UV-vis absorption spectrum of **3b(60/40)** in *n*-octane (2.02×10^{-2} g/L, path length = 10 mm).

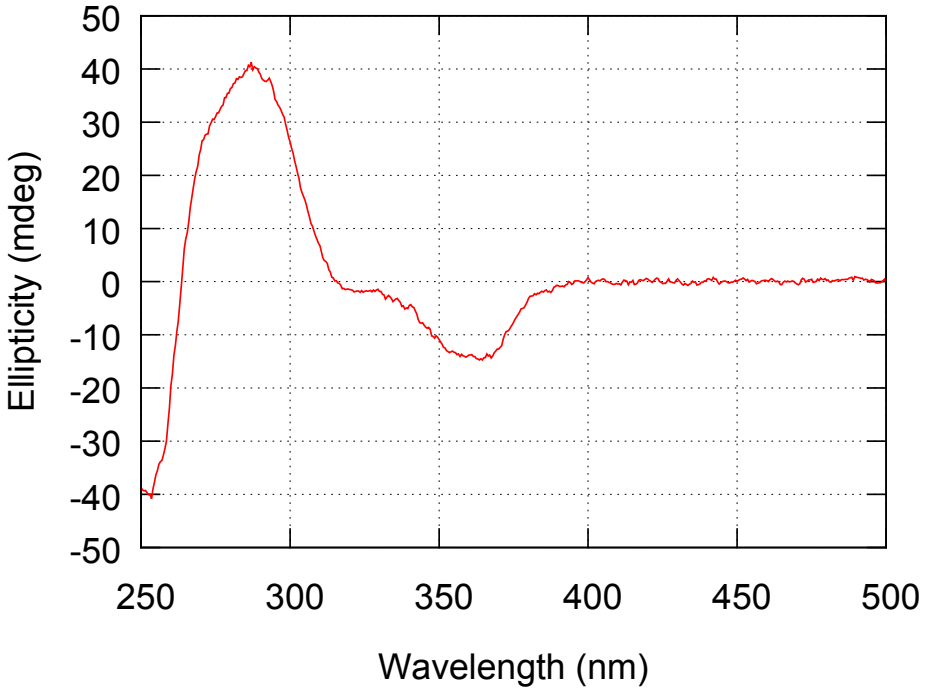

Figure S211. CD spectrum of **3b(60/40)** in *n*-octane (2.02×10^{-2} g/L, path length = 10 mm).

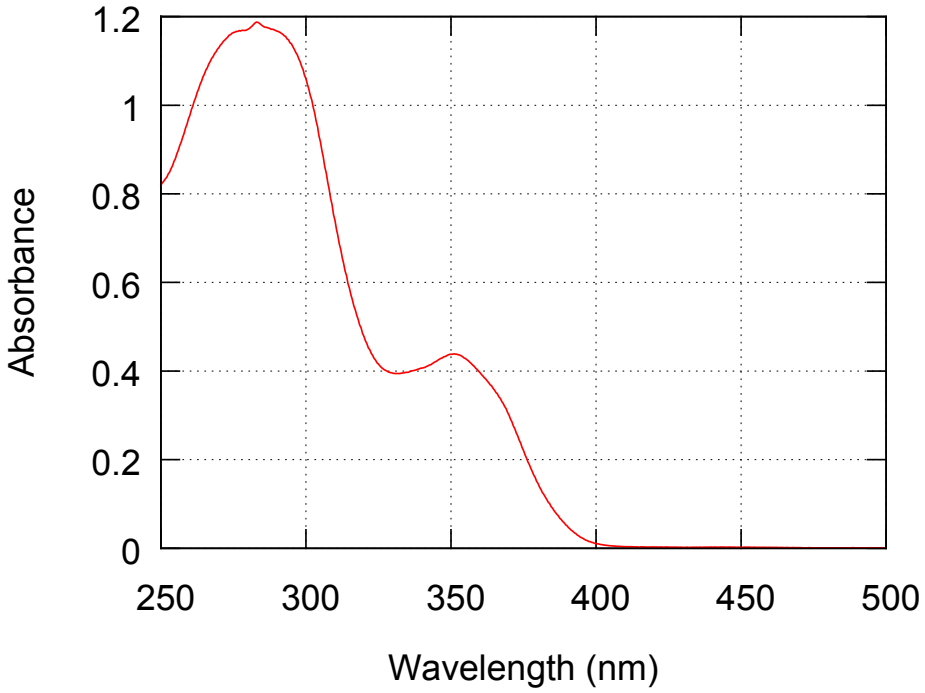

Figure S212. UV-vis absorption spectrum of **3b(60/40)** in *n*-nonane (2.02×10^{-2} g/L, path length = 10 mm).

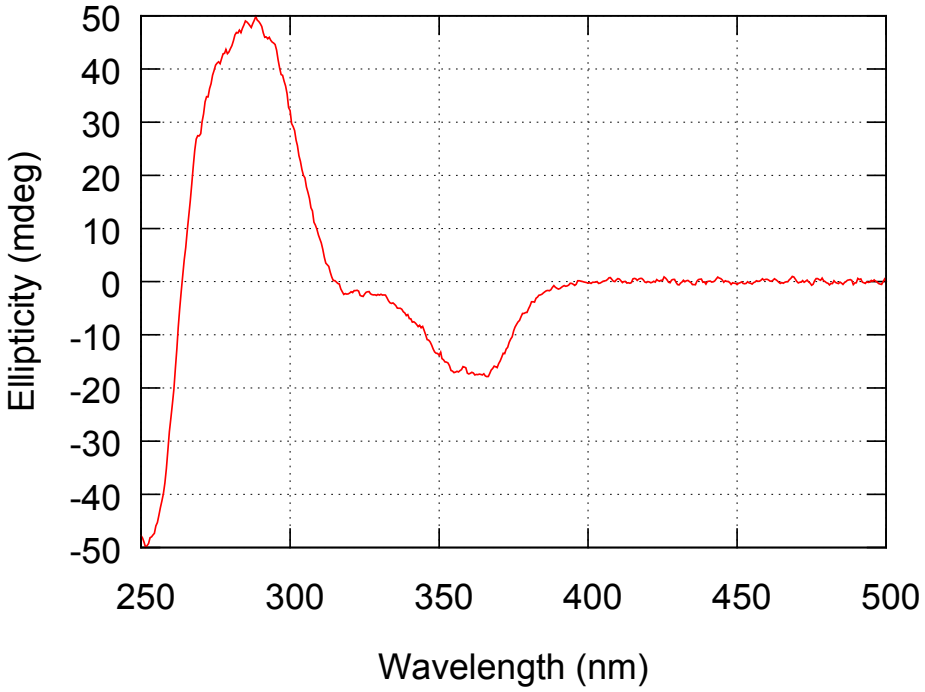

Figure S213. CD spectrum of **3b(60/40)** in *n*-nonane (2.02×10^{-2} g/L, path length = 10 mm).

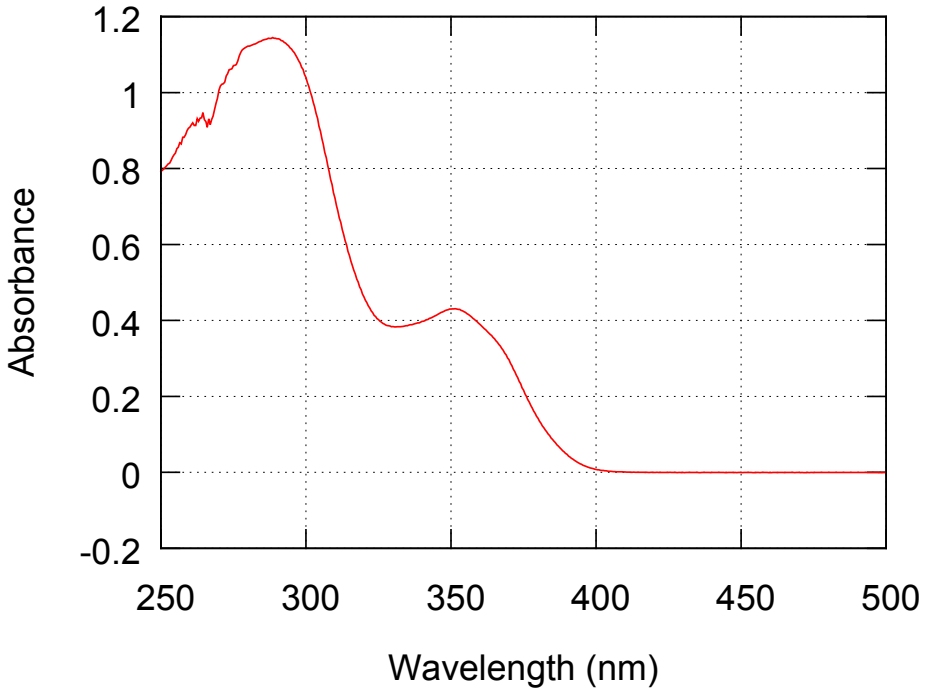

Figure S214. UV-vis absorption spectrum of **3b(60/40)** in *n*-decane (2.02×10^{-2} g/L, path length = 10 mm).

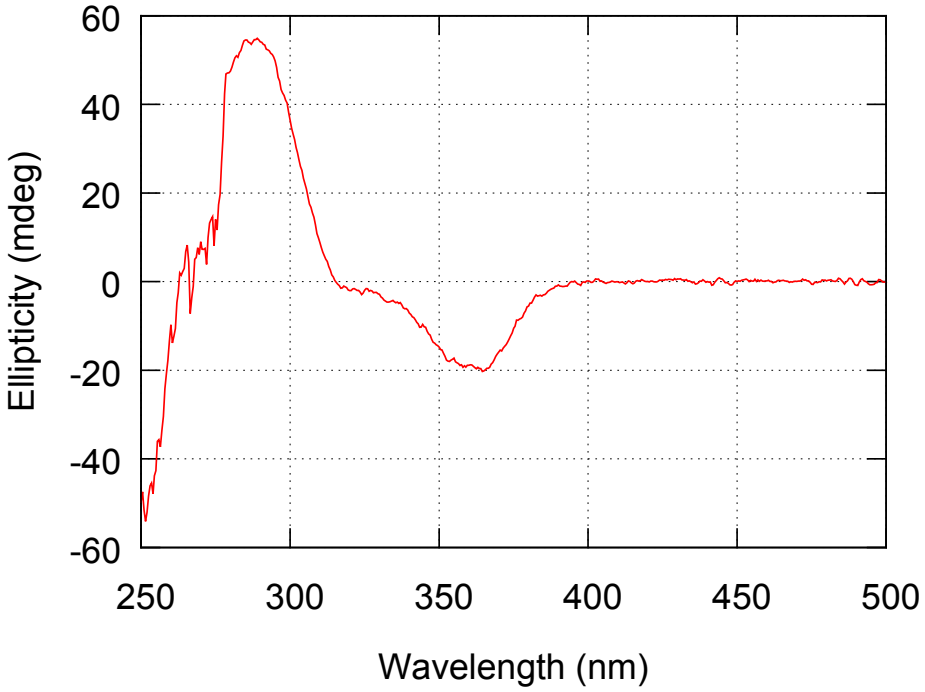

Figure S215. CD spectrum of **3b(60/40)** in *n*-decane (2.02×10^{-2} g/L, path length = 10 mm).

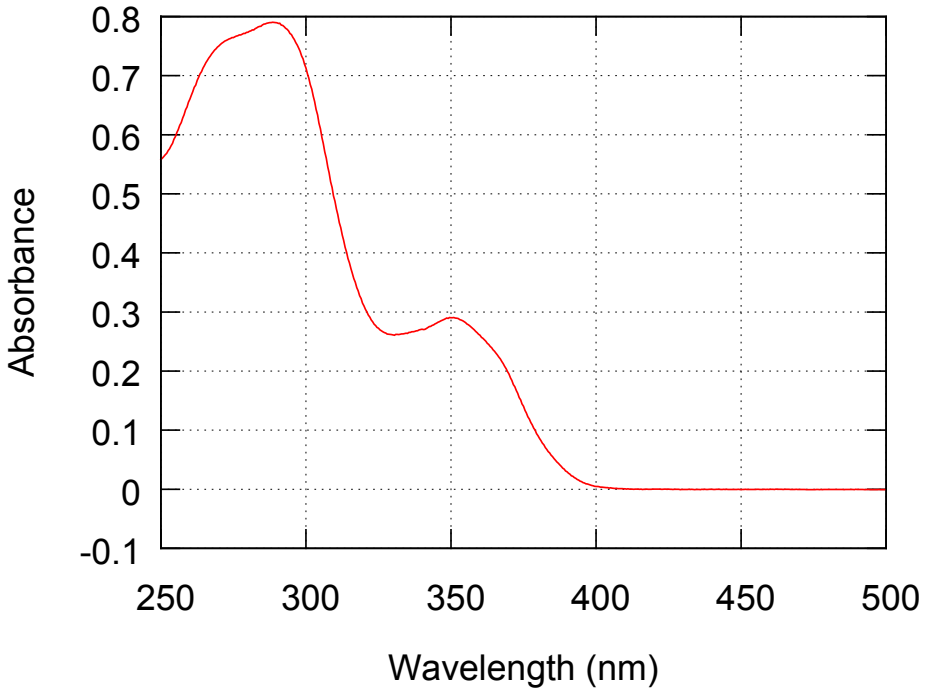

Figure S216. UV-vis absorption spectrum of **3b(80/20)** in *n*-pentane (1.44×10^{-2} g/L, path length = 10 mm).

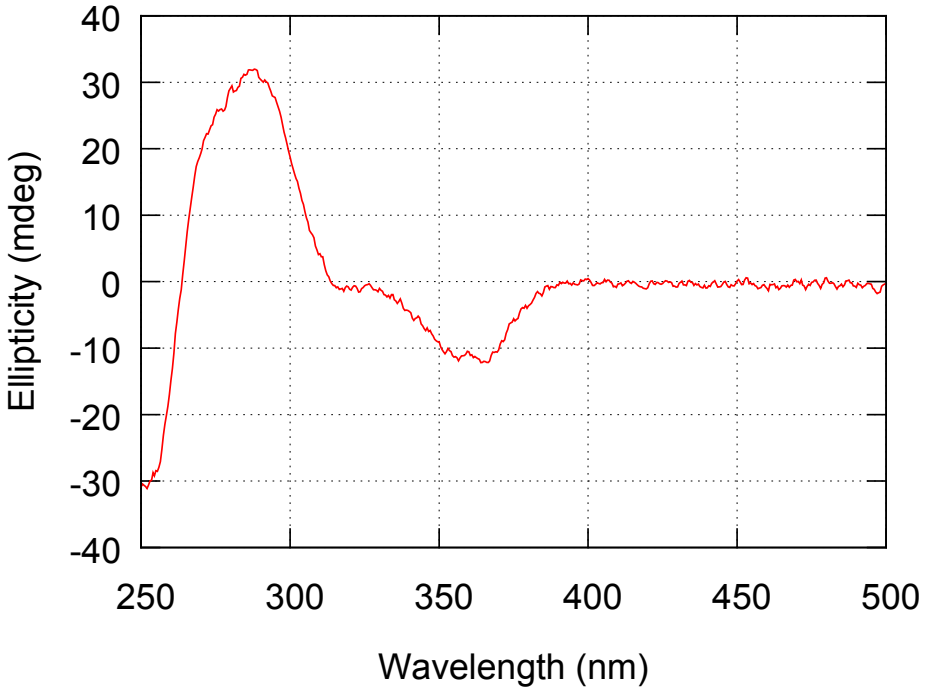

Figure S217. CD spectrum of **3b(80/20)** in *n*-pentane (1.44×10^{-2} g/L, path length = 10 mm).

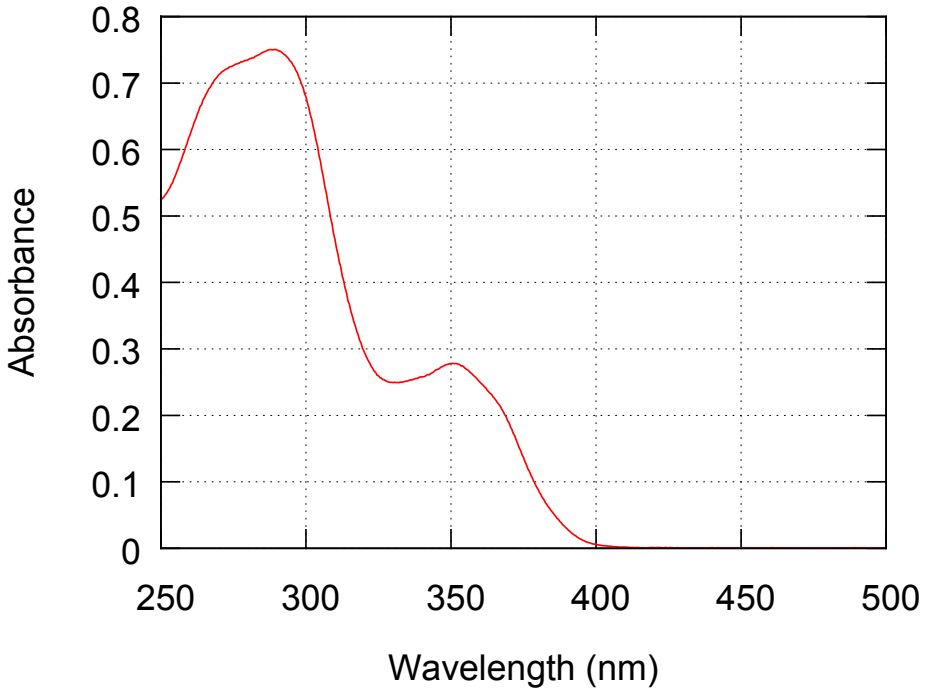

Figure S218. UV-vis absorption spectrum of **3b(80/20)** in *n*-hexane (1.44×10^{-2} g/L, path length = 10 mm).

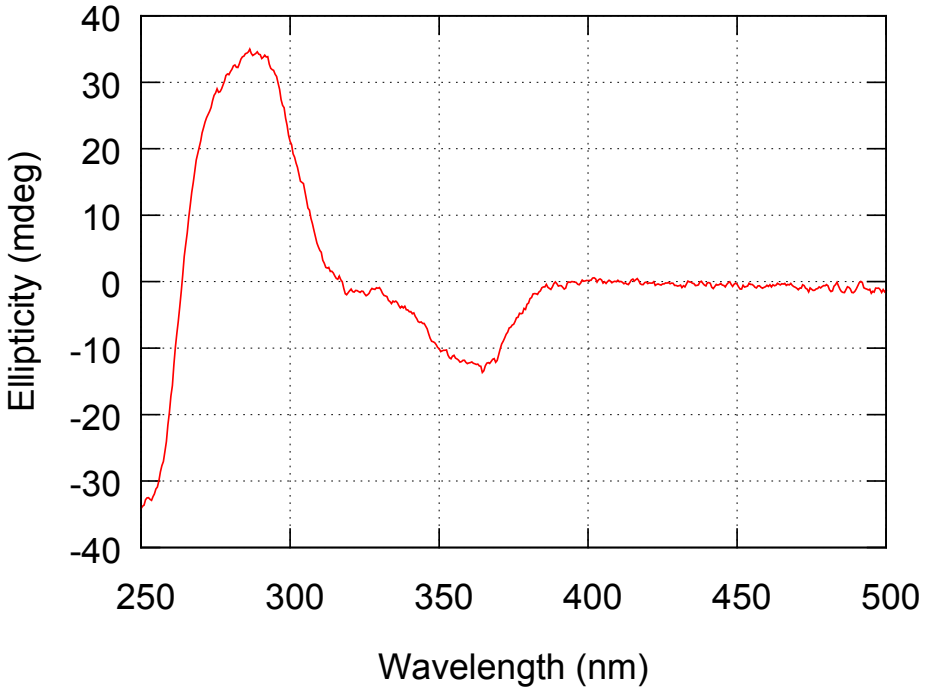

Figure S219. CD spectrum of **3b(80/20)** in *n*-hexane (1.44×10^{-2} g/L, path length = 10 mm).

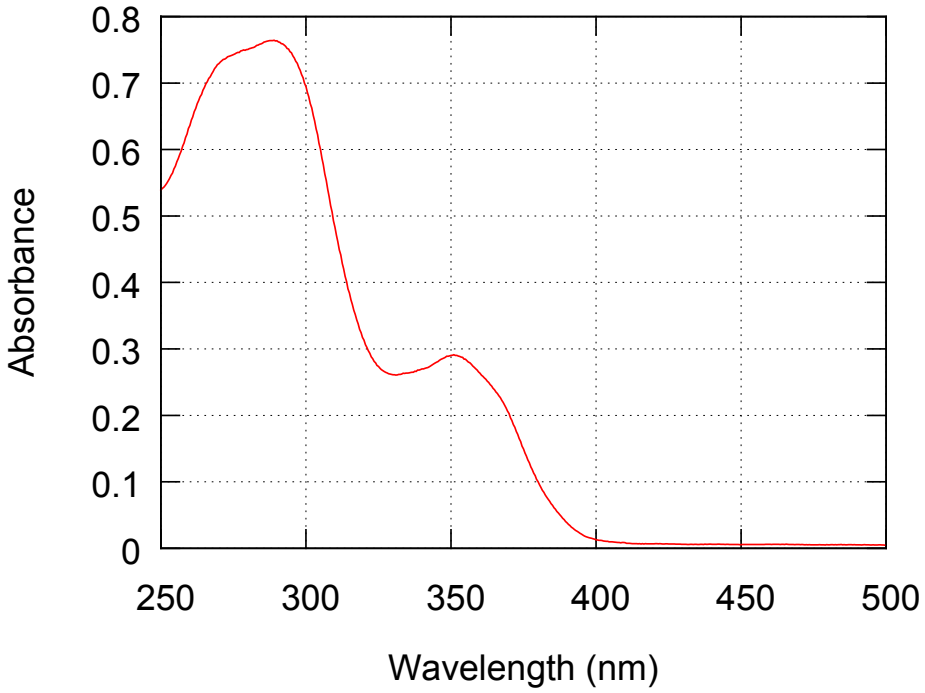

Figure S220. UV-vis absorption spectrum of **3b(80/20)** in *n*-heptane (1.44×10^{-2} g/L, path length = 10 mm).

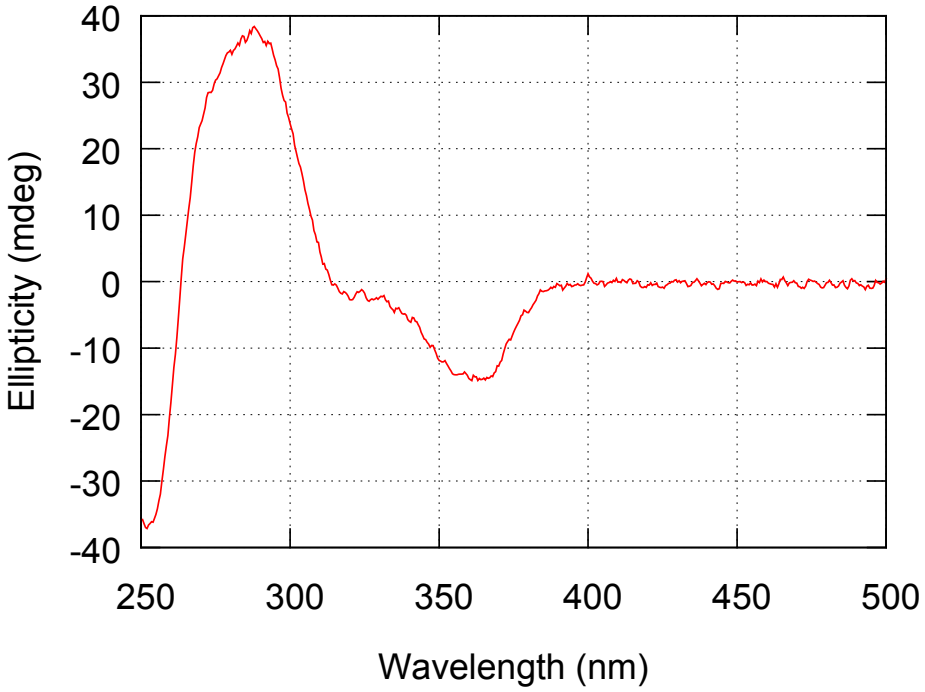

Figure S221. CD spectrum of **3b(80/20)** in *n*-heptane (1.44×10^{-2} g/L, path length = 10 mm).

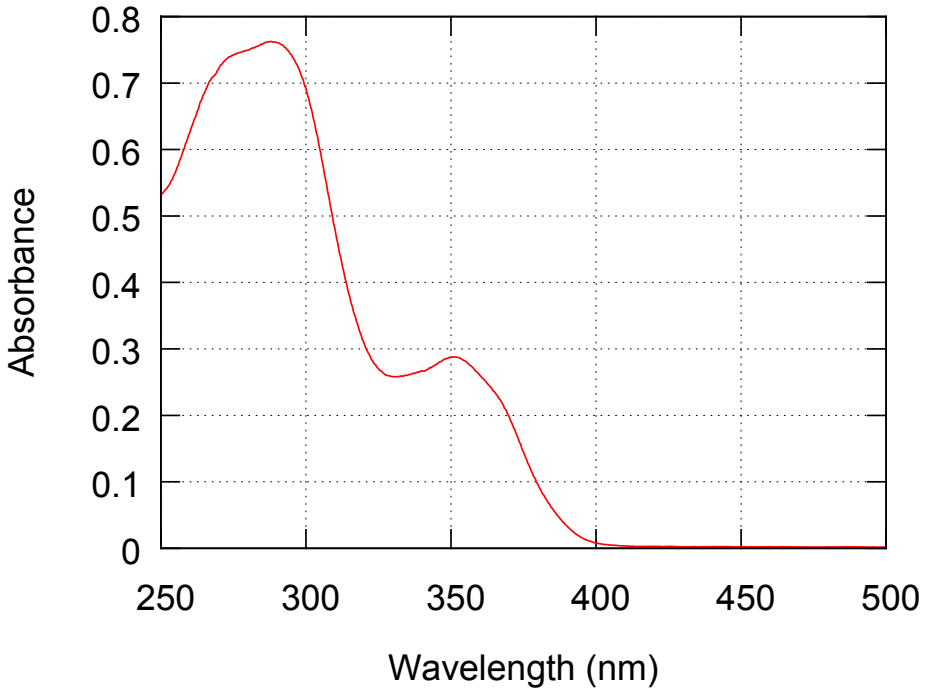

Figure S222. UV-vis absorption spectrum of **3b(80/20)** in *n*-octane (1.44×10^{-2} g/L, path length = 10 mm).

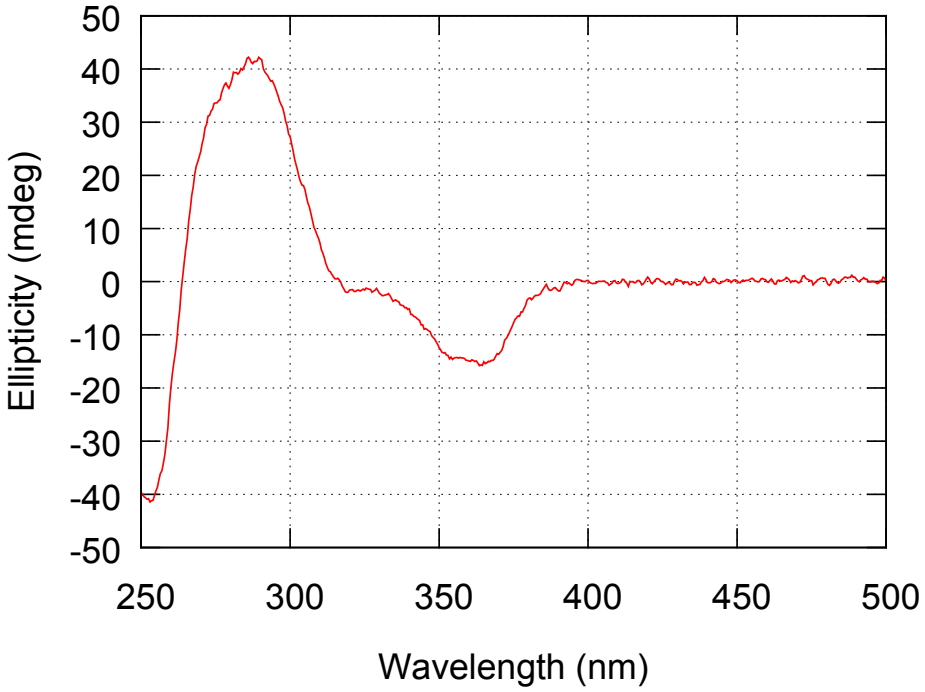

Figure S223. CD spectrum of **3b(80/20)** in *n*-octane (1.44×10^{-2} g/L, path length = 10 mm).

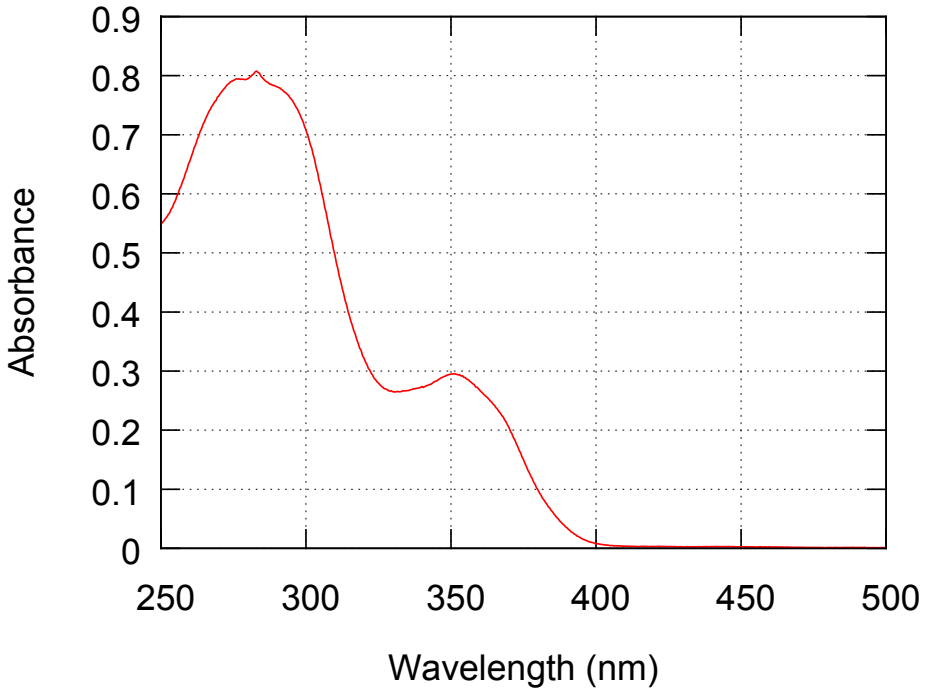

Figure S224. UV-vis absorption spectrum of **3b(80/20)** in *n*-nonane (1.44×10^{-2} g/L, path length = 10 mm).

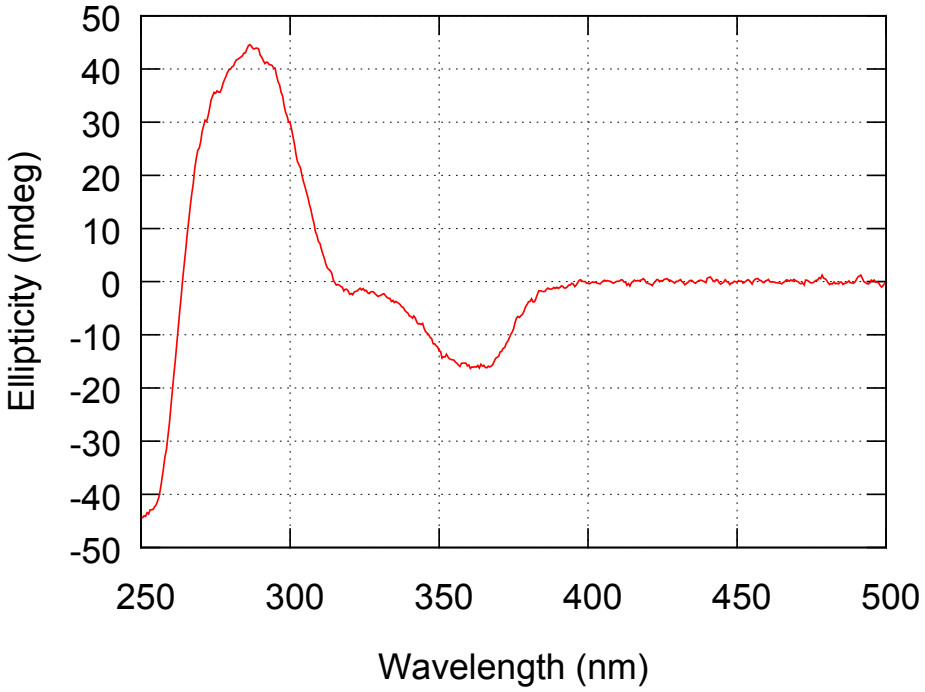

Figure S225. CD spectrum of **3b(80/20)** in *n*-nonane (1.44×10^{-2} g/L, path length = 10 mm).

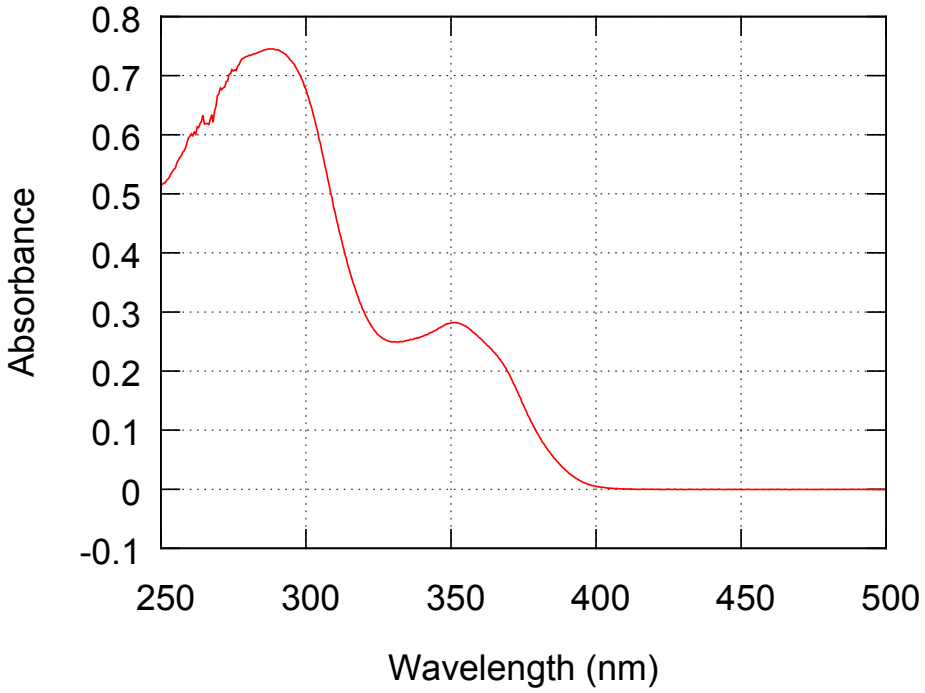

Figure S226. UV-vis absorption spectrum of **3b(80/20)** in *n*-decane (1.44×10^{-2} g/L, path length = 10 mm).

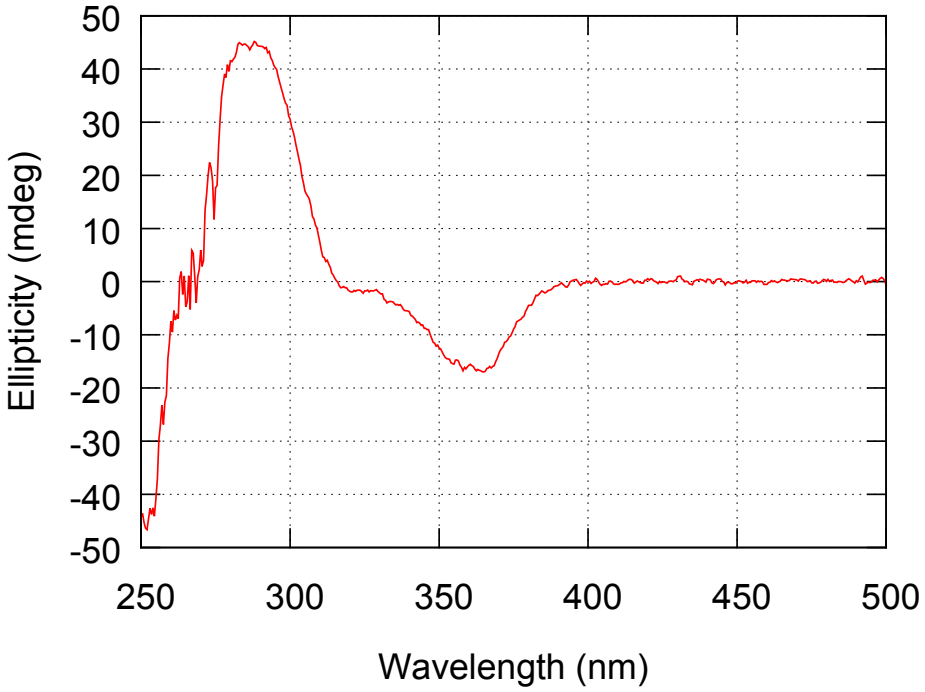

Figure S227. CD spectrum of **3b(80/20)** in *n*-decane (1.44×10^{-2} g/L, path length = 10 mm).

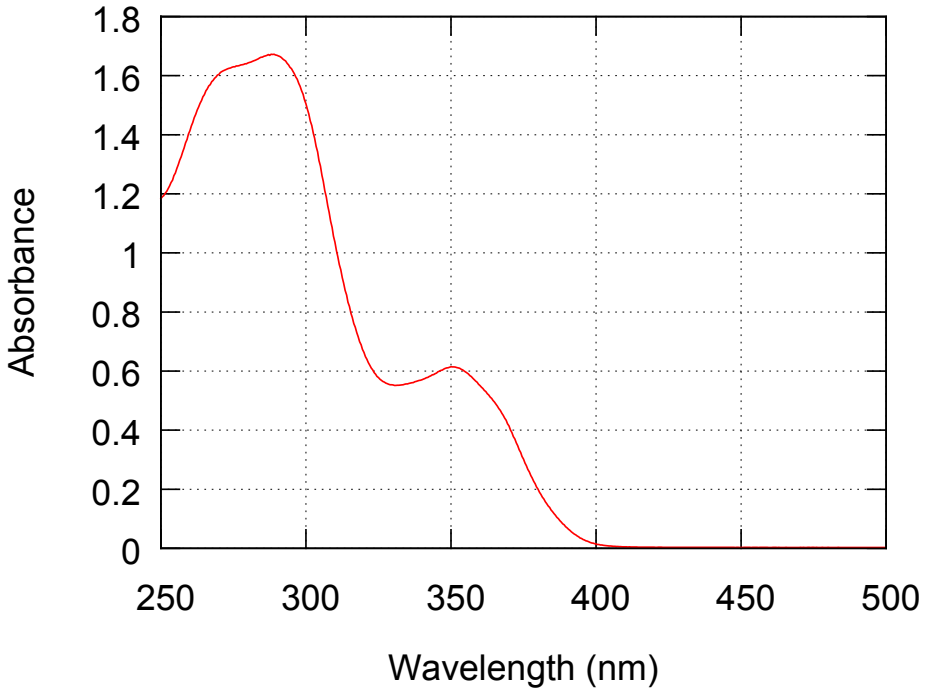

Figure S228. UV-vis absorption spectrum of **3b(350/650)** in *n*-octane (2.65×10^{-2} g/L, path length = 10 mm).

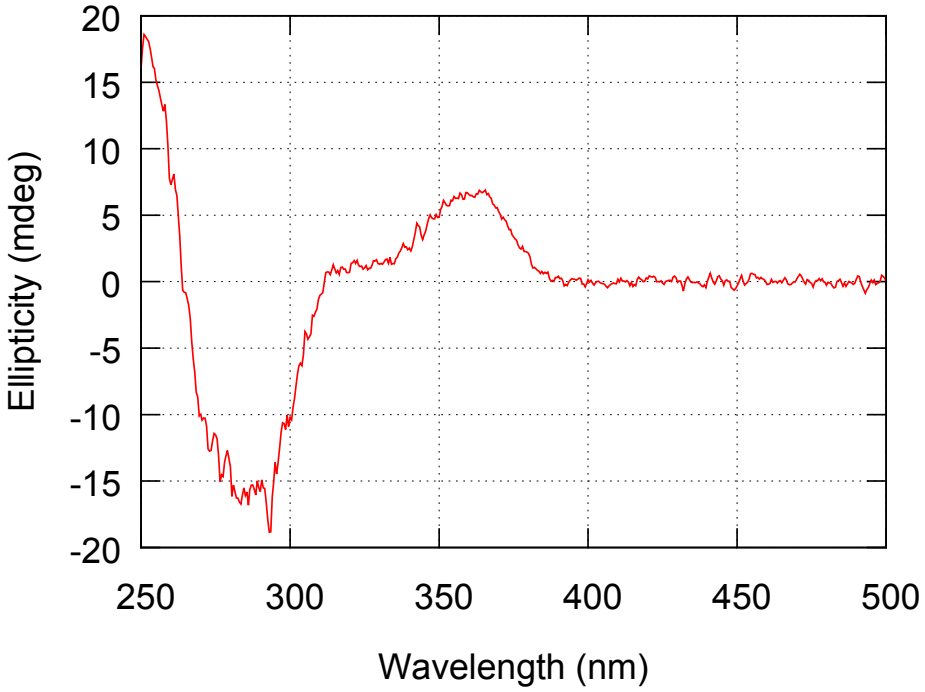

Figure S229. CD spectrum of **3b(350/650)** in *n*-octane (2.65×10^{-2} g/L, path length = 10 mm).

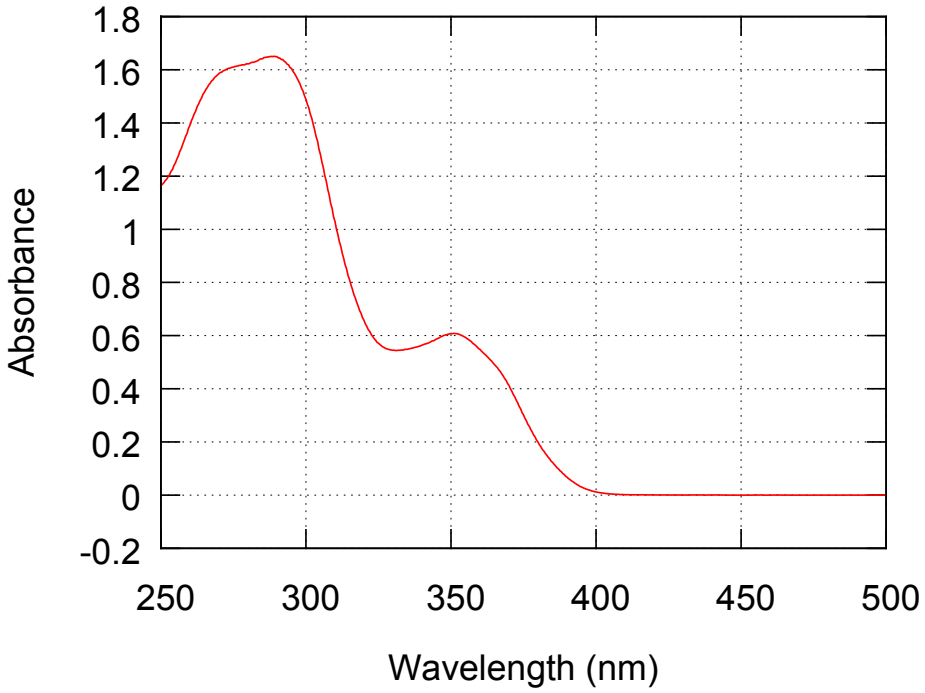

Figure S230. UV-vis absorption spectrum of **3b(350/650)** in *n*-nonane (2.65×10^{-2} g/L, path length = 10 mm).

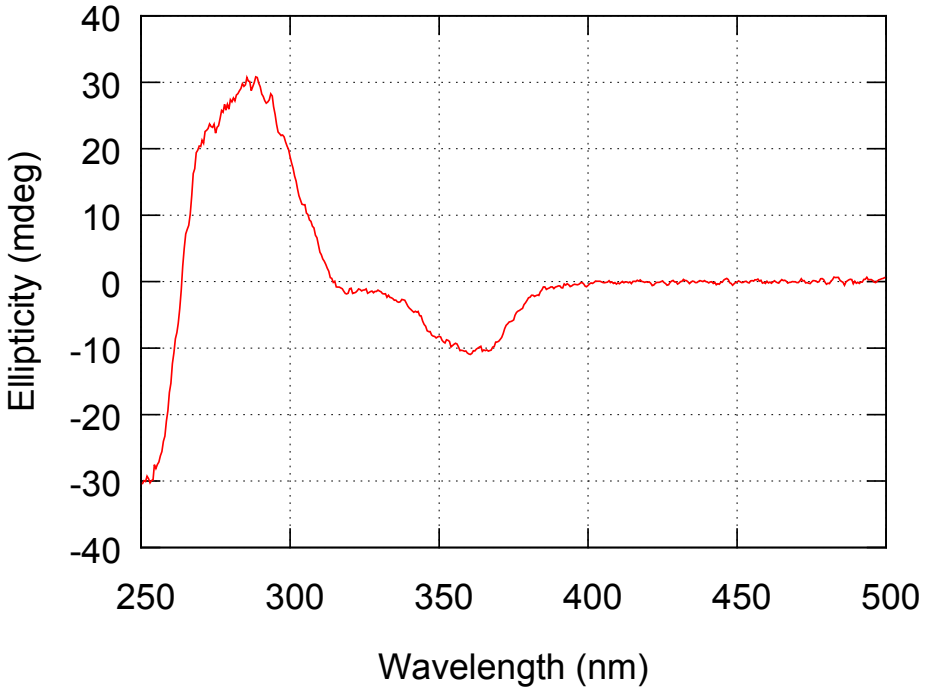

Figure S231. CD spectrum of **3b(350/650)** in *n*-nonane (2.65×10^{-2} g/L, path length = 10 mm).

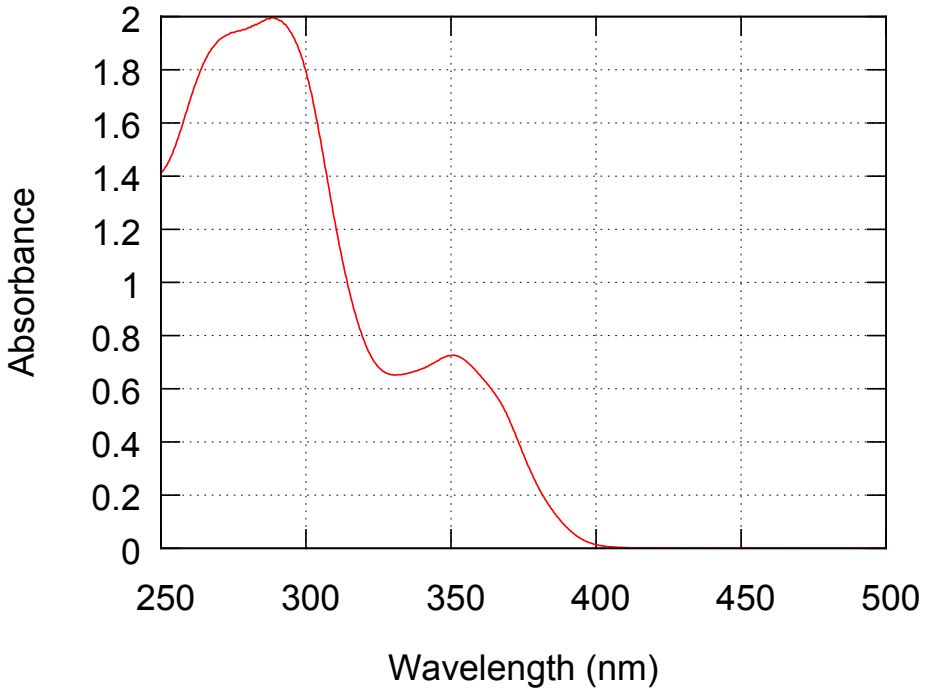

Figure S232. UV-vis absorption spectrum of **3b(400/600)** in *n*-heptane (3.90×10^{-2} g/L, path length = 10 mm).

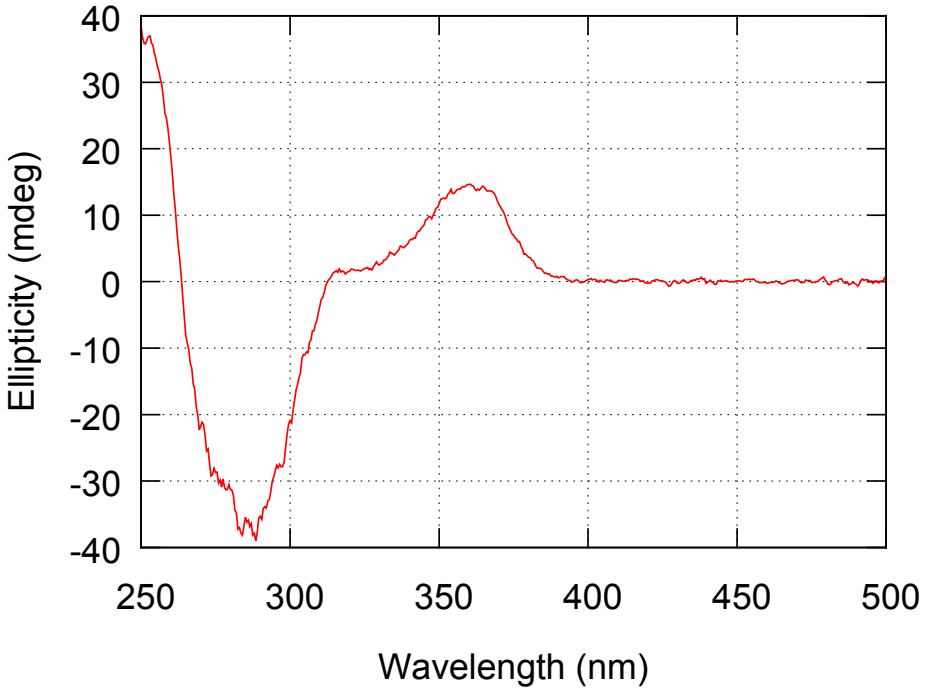

Figure S233. CD spectrum of **3b(400/600)** in *n*-heptane (3.90×10^{-2} g/L, path length = 10 mm).

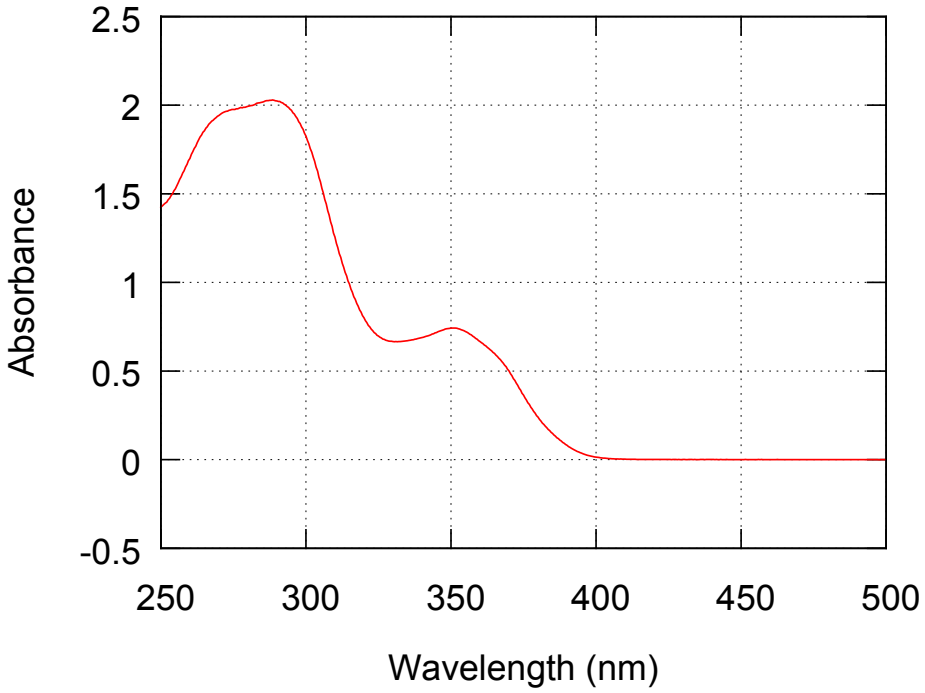

Figure S234. UV-vis absorption spectrum of **3b(400/600)** in *n*-octane (3.90×10^{-2} g/L, path length = 10 mm).

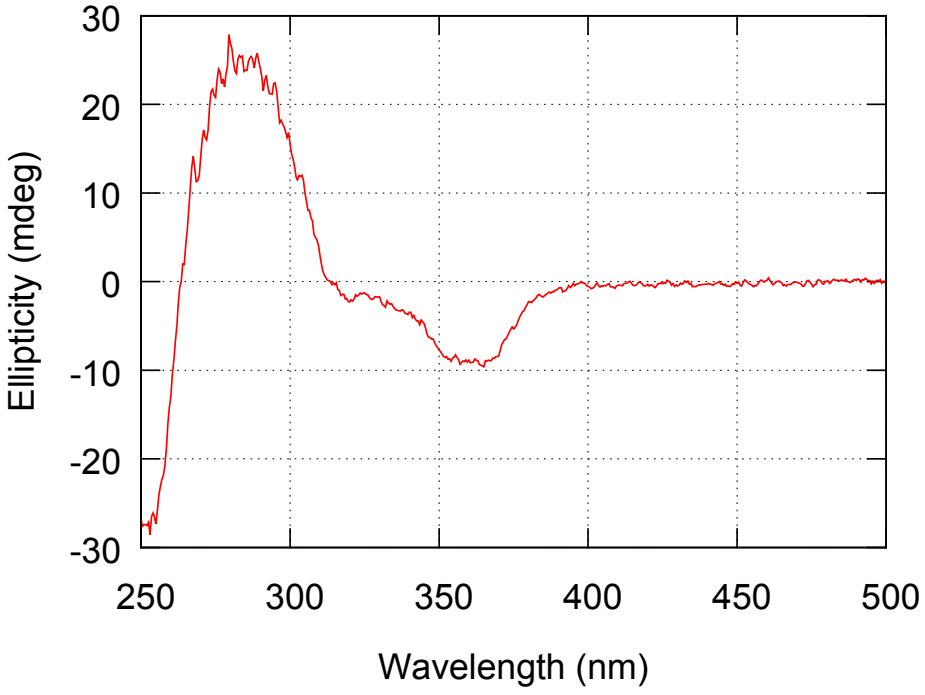

Figure S235. CD spectrum of **3b(400/600)** in *n*-octane (3.90×10^{-2} g/L, path length = 10 mm).

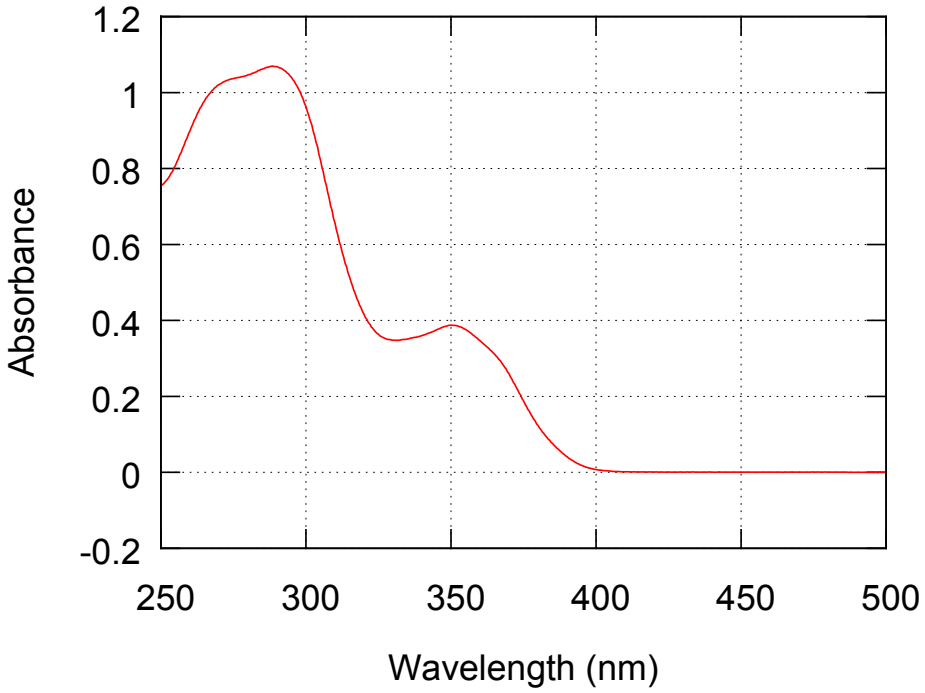

Figure S236. UV-vis absorption spectrum of **3b(500/500)** in *n*-hexane (2.65×10^{-2} g/L, path length = 10 mm).

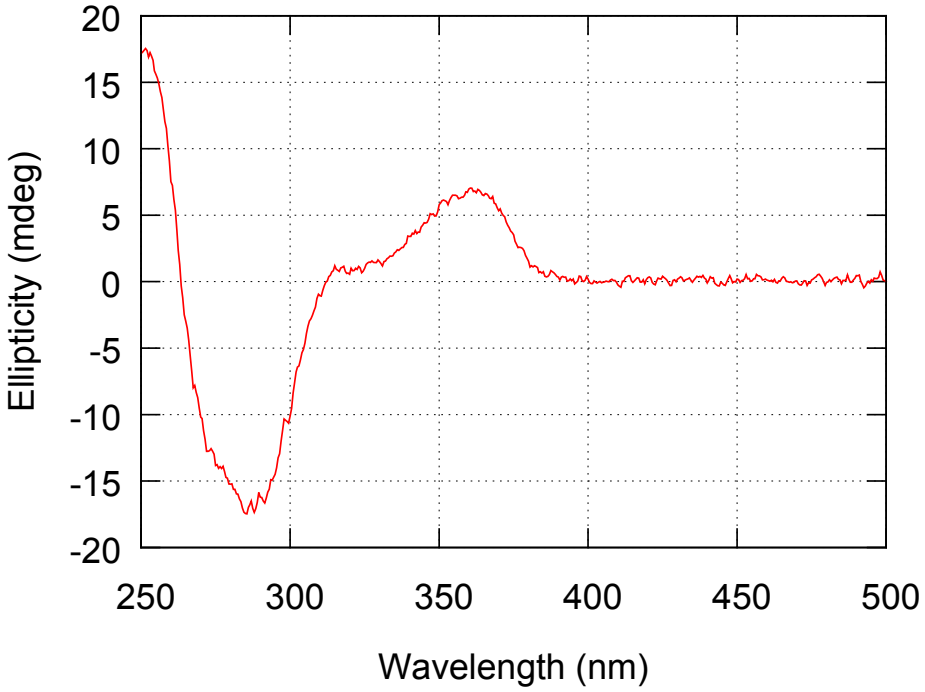

Figure S237. CD spectrum of **3b(500/500)** in *n*-hexane (2.65×10^{-2} g/L, path length = 10 mm).

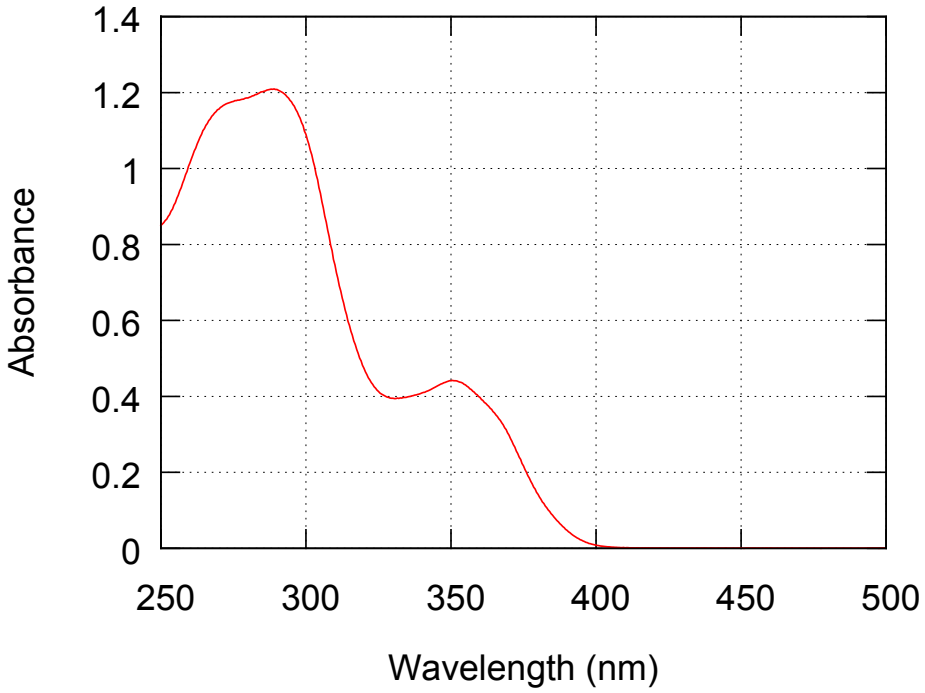

Figure S238. UV-vis absorption spectrum of **3b(500/500)** in *n*-heptane (2.65×10^{-2} g/L, path length = 10 mm).

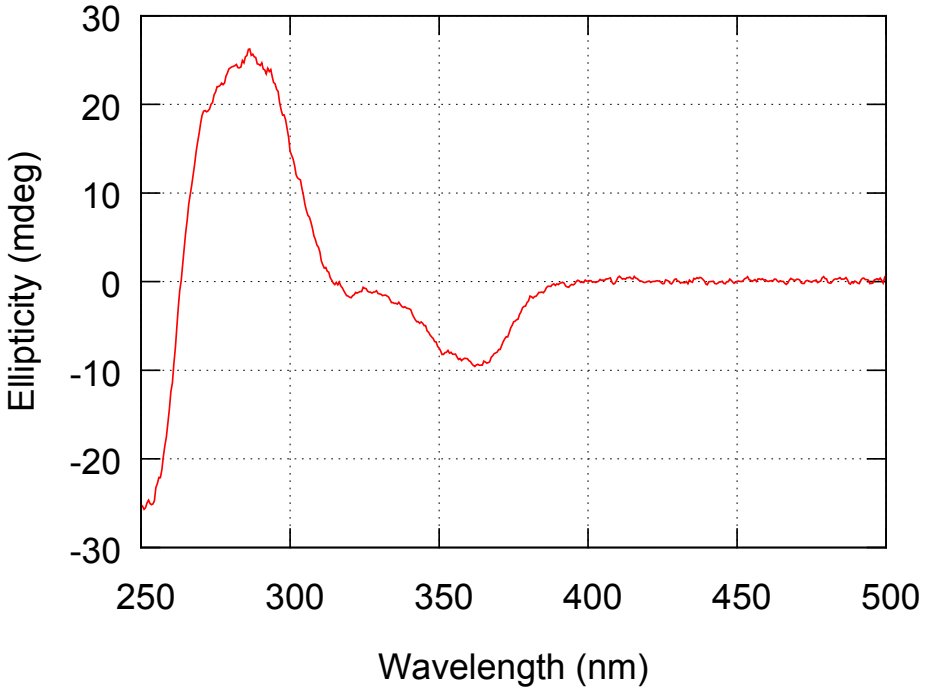

Figure S239. CD spectrum of **3b(500/500)** in *n*-heptane (2.65×10^{-2} g/L, path length = 10 mm).

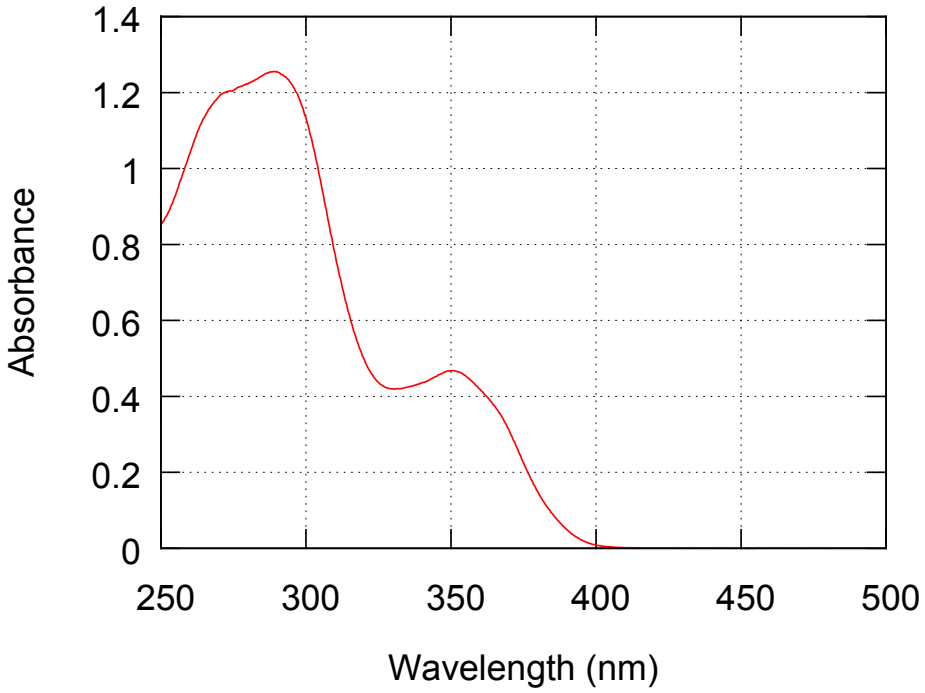

Figure S240. UV-vis absorption spectrum of **3b(400/600/2)** in *n*-heptane (3.32×10^{-2} g/L, path length = 10 mm).

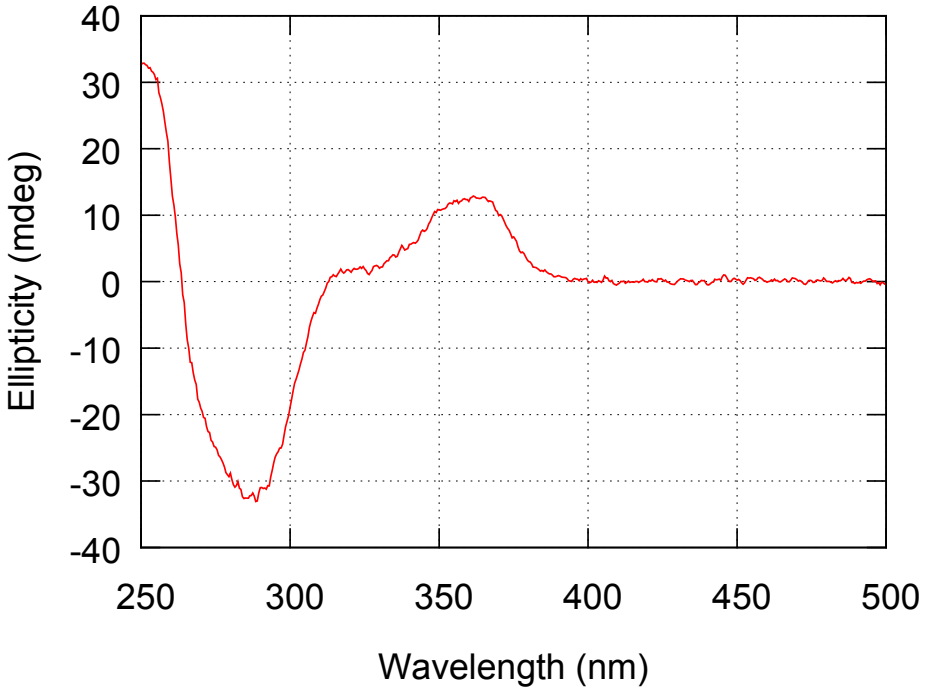

Figure S241. CD spectrum of **3b(400/600/2)** in *n*-heptane (3.32×10^{-2} g/L, path length = 10 mm).

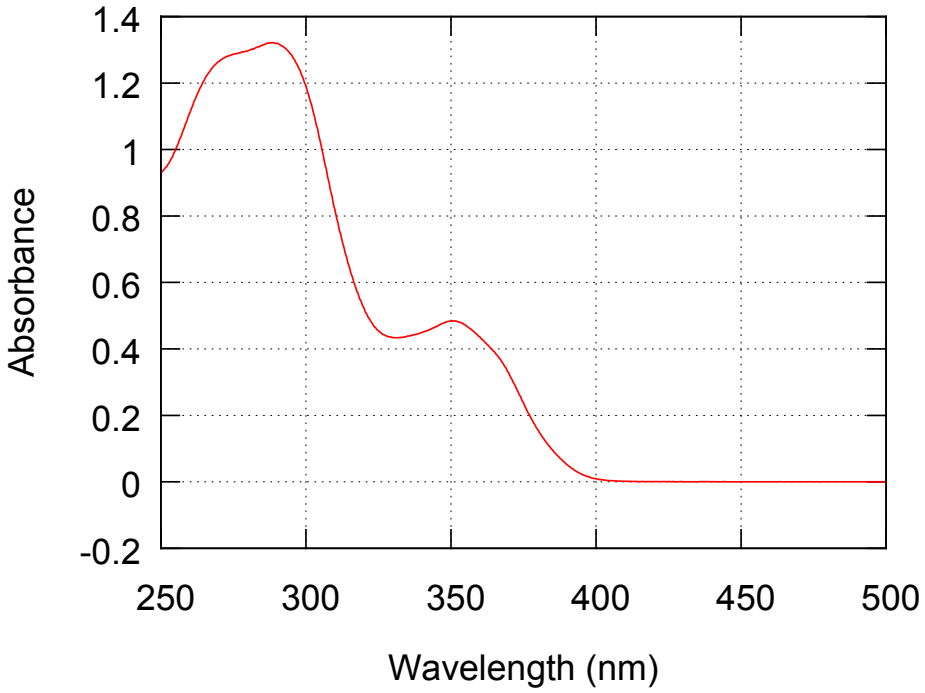

Figure S242. UV-vis absorption spectrum of **3b(400/600/2)** in *n*-octane (3.32×10^{-2} g/L, path length = 10 mm).

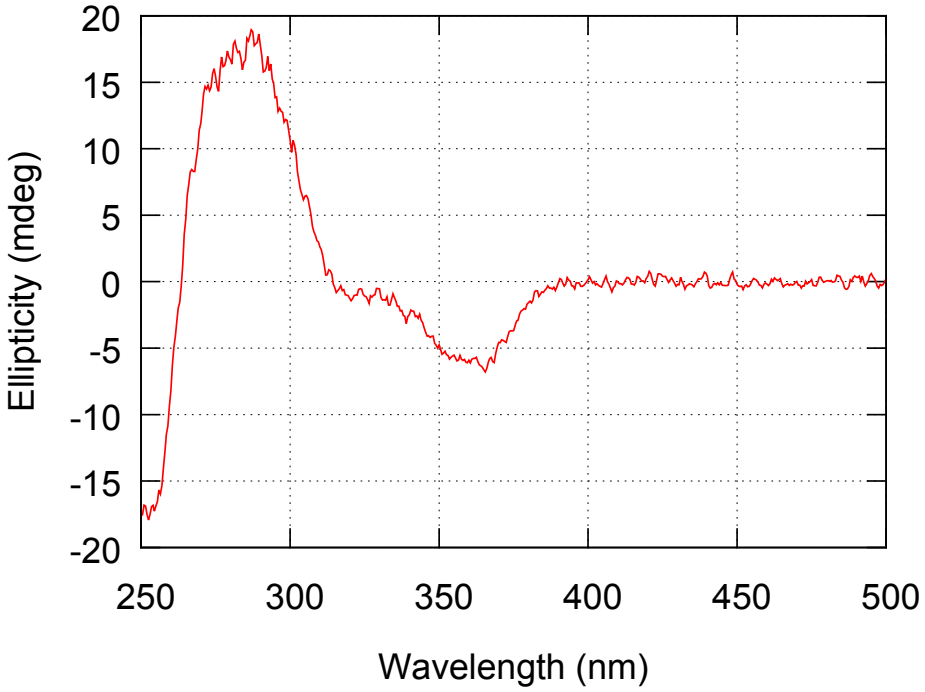

Figure S243. CD spectrum of **3b(400/600/2)** in *n*-octane (3.32×10^{-2} g/L, path length = 10 mm).